



mgr inż. Małgorzata Walewska

Base Adducts of Silylated and Germylated Tetrylenes - Synthesis and Reactivity

DOCTORAL THESIS

to achieve the university degree of
Doktorin der technischen Wissenschaften

submitted to

Graz University of Technology

Supervisor

Ao Univ. Prof. Dipl.-Ing. Dr. Christoph Marschner

Institute of Inorganic Chemistry
Graz University of Technology

AFFIDAVIT

I declare that I have authored this thesis independently, that I have not used other than the declared sources/resources, and that I have explicitly indicated all material which has been quoted either literally or by content from the sources used. The text document uploaded to TUGRAZonline is identical to the present doctoral thesis.

Date

Signature

This work was financed by the Austrian Science Foundation (Fonds zur Förderung der Wissenschaftlichen Forschung) *via* the projects P-22678 and P-26417 and it was carried out from November 2012 to December 2015 at the Institute of Inorganic Chemistry, Graz University of Technology.

*To my Parents, Teresa and Henryk
and my lovely Husband, Łukasz*

Acknowledgments

First of all, I am deeply grateful to my supervisor, Prof. Christoph Marschner not only for giving me an interesting research topic but also for his fruitful advice, help in understanding the results and for giving me a lot of freedom in pursuing my research. It has been a pleasure for me to work in his group.

I would like to acknowledge the valuable input of Dr. Judith Baumgartner, who contributed to many discussions and gave a lot of helpful suggestions. Additionally, she determined structures of all the crystals presented in this work. I am deeply grateful to her for all that.

I would like to thank all my colleagues at the Institute of Inorganic Chemistry, in particular the members of the research group for many exciting discussions about scientific problems I met on my way and for the friendly atmosphere in the Lab. My personal thanks go to Mohammad Aghazadeh Meshgi for notoriously delicious self-made oriental specialties, Dr. Johann Hlina for introducing me to the everyday laboratory practice, Filippo Stella for the foreigner's guide to surviving in Graz and Rainer Zitz for critical reading of a lengthy fragment of this thesis and his support in dealing with the Austrian flavor of the German language.

I wish to express gratitude to my family, Teresa, Henryk, Magdalena and Wojciech, for their constant support and the unshakable belief in my ability to successfully finalize this project.

Last but not least, I am grateful to my husband Łukasz, for his help during my whole stay in Austria. His support and encouragement throughout the course of this research was extremely important to me. I appreciate his patience and understanding, especially during the final stage of my writing and I am grateful for his input into the correction process. He kept me going all the time, accomplishment of this thesis would not be possible without him.

Contents

| | | |
|----------|----------------------------------------------------------------------------|------------|
| 1 | Synthesis of tetrylenes | 10 |
| 1.1 | Introduction | 10 |
| 1.2 | Oligosilylgermylenes and oligogermylgermylenes | 18 |
| 1.2.1 | Synthesis | 18 |
| 1.2.2 | NMR spectroscopy | 23 |
| 1.2.3 | Crystallography | 30 |
| 1.3 | Oligosilastannylenes | 37 |
| 1.3.1 | Synthesis | 37 |
| 1.3.2 | NMR Spectroscopy | 40 |
| 1.3.3 | Crystallography | 42 |
| 1.4 | Conclusions | 47 |
| 2 | Reactivity of tetrylenes | 48 |
| 2.1 | Introduction | 48 |
| 2.1.1 | Addition to unsaturated systems | 48 |
| 2.1.2 | Insertion into σ bonds | 51 |
| 2.2 | Reactions of acyclic germylene adducts with acetylenes | 54 |
| 2.2.1 | Synthesis | 54 |
| 2.2.2 | NMR Spectroscopy | 59 |
| 2.2.3 | Crystallography | 62 |
| 2.3 | Reactions of cyclic germylene adducts with acetylenes | 71 |
| 2.3.1 | Synthesis | 71 |
| 2.3.2 | NMR Spectroscopy | 76 |
| 2.3.3 | Crystallography | 78 |
| 2.4 | Reactions of tetrylene adducts with group 14 halides | 85 |
| 2.4.1 | Synthesis | 85 |
| 2.4.2 | NMR Spectroscopy | 92 |
| 2.4.3 | Crystallography | 94 |
| 2.5 | Reactions of tetrylene adducts with small molecules and carbonyl compounds | 102 |
| 2.5.1 | Synthesis | 102 |
| 2.5.2 | NMR Spectroscopy | 105 |
| 2.5.3 | Crystallography | 106 |
| 2.6 | Conclusions | 113 |
| 3 | Reactions of tetrylenes with transition metal complexes | 114 |
| 3.1 | Introduction | 114 |
| 3.1.1 | Early transition metal complexes | 114 |
| 3.1.2 | Late transition metal complexes | 117 |
| 3.2 | Reaction of germylene with group 4 metal complexes | 121 |
| 3.3 | Reactions of tetrylenes with group 11 metal complexes | 123 |
| 3.3.1 | Synthesis | 123 |

| | | |
|----------|-----------------------------------------------------------------------------------------------------------------------------------------------------------|------------|
| 3.3.2 | NMR spectroscopy | 127 |
| 3.3.3 | Crystallography | 128 |
| 3.4 | Conclusions | 133 |
| 4 | Experimental details | 134 |
| 4.1 | General experimental | 134 |
| 4.1.1 | General remarks | 134 |
| 4.1.2 | Chemical substances | 134 |
| 4.1.3 | Analytical methods | 135 |
| 4.2 | Experimental procedure | 136 |
| 4.2.1 | Bis[tris(trimethylsilyl)silyl]germylene · ^{Me} IiPr (14) | 136 |
| 4.2.2 | Bis[tris(trimethylsilyl)germyl]germylene · ^{Me} IiPr (15) | 137 |
| 4.2.3 | Tris(trimethylsilyl)silyl(bromo)germylene · ^{Me} IiPr (16) | 138 |
| 4.2.4 | Tris(trimethylsilyl)germyltris(trimethylsilyl)silylgermylene · ^{Me} IiPr (17) | 139 |
| 4.2.5 | Bis[tris(trimethylsilyl)silyl]germylene · PMe ₃ (18) | 140 |
| 4.2.6 | Bis[bis(trimethylsilyl)silatranysilyl]germylene · PMe ₃ (20) | 141 |
| 4.2.7 | <i>trans</i> -1,1,2,3-Tetrakis(trimethylsilyl)-2,3-silatranylcyclopropa-1-germa- disilane (21) | 142 |
| 4.2.8 | Bis[bis(trimethylsilyl)silatranysilyl]germylene · IMe ₄ (22) | 143 |
| 4.2.9 | Bis[tris(trimethylsilyl)germyl]germylene · PMe ₃ (23) | 144 |
| 4.2.10 | Bis[tris(trimethylsilyl)silyl]germylene · 2,6-dimethylphenylisocyanide (26) | 145 |
| 4.2.11 | Bis[tris(trimethylsilyl)silyl]germylene · <i>tert</i> -butylisocyanide (27) . . | 146 |
| 4.2.12 | Cyanobis[tris(trimethylsilyl)silyl]germane (28) | 147 |
| 4.2.13 | 1-Germa-2,2,5,5-tetrakis(trimethylsilyl)-3,3,4,4-tetramethylcyclopenta- silan-1-ylidene · PMe ₃ (30) | 148 |
| 4.2.14 | 1-Stanna-2,2,4,4-tetrakis(trimethylsilyl)-3,3-dimethylcyclobutasilan- 1-ylidene · ^{Me} IiPr (31) | 149 |
| 4.2.15 | 1,5-Distanna-2,2,4,4,6,6,8,8-octakis(trimethylsilyl)bicyclo[3.3.0]hexa- silaoct-1,5-ene (32) | 150 |
| 4.2.16 | 1-Stanna-2,2,5,5-tetrakis(trimethylsilyl)-3,3,4,4-tetramethylcyclopenta- silan-1-ylidene · IMe ₄ (33) | 151 |
| 4.2.17 | Bis[tris(trimethylsilyl)silyl]stannylene · IMe ₄ (34) | 152 |
| 4.2.18 | Bis[tris(trimethylsilyl)silyl]stannylene · PMe ₃ (35) | 153 |
| 4.2.19 | 1,1-Bis[tris(trimethylsilyl)silyl]-2,3-diphenyl-1-germacyclopropene (36) | 154 |
| 4.2.20 | [<i>Z</i> -1-Phenyl-2-(tris(trimethylsilyl)silyl)vinyl]tris(trimethylsilyl)silyl]- germylene · PMe ₃ (37) | 155 |
| 4.2.21 | Bis[<i>Z</i> -1-phenyl-2-(tris(trimethylsilyl)silyl)vinyl]germylene · PMe ₃ (38) | 156 |
| 4.2.22 | (<i>Z</i>)-1-(2-(tris(trimethylsilyl)silyl)-1-phenylvinyl)-4-phenyl-1,2,2-tris- (trimethylsilyl)-1,2-dihydro-1,2-silagermete (39) | 157 |
| 4.2.23 | Bis[<i>Z</i> -1-Phenyl-2-tris(trimethylsilyl)silylvinyl]germylene · IMe ₄ (40) | 158 |
| 4.2.24 | 1-[Tris(trimethylsilyl)silyl]-4-phenyl-1,2,2-tris(trimethylsilyl)-1,2-dihydro- 1,2-silagermete (41) | 159 |

| | | |
|--------|-------------------------------------------------------------------------------------------------------------------------------------------------------------|-----|
| 4.2.25 | [<i>Z</i> -1-phenyl-2-tris(trimethylsilyl)silylvinyl]tris(trimethylsilyl)silylgermylene · IMe ₄ (42) | 160 |
| 4.2.26 | [<i>Z</i> -1-Trimethylsilyl-2-(tris(trimethylsilyl)silyl)vinyl]tris(trimethylsilyl)silyl]germylene · PMe ₃ (43) | 161 |
| 4.2.27 | [<i>Z</i> -1-Trimethylsilyl-2-(tris(trimethylsilyl)silyl)vinyl]tris(trimethylsilyl)silyl]germylene · IMe ₄ (44) | 162 |
| 4.2.28 | 2,3-Diethyl-1,1-bis[tris(trimethylsilyl)silyl]-1-germacyclopropene (47) | 163 |
| 4.2.29 | [<i>Z</i> -1-Butyl-2-(tris(trimethylsilyl)silyl)vinyl]tris(trimethylsilyl)silylgermylene · PMe ₃ (48) | 164 |
| 4.2.30 | 3,4-Diethyl-1-[tris(trimethylsilyl)silyl]-1,2,2-tris(trimethylsilyl)-1,2-dehydro-2-silagermete (49) | 165 |
| 4.2.31 | 1-[Tris(trimethylsilyl)silyl]-3,4-diphenyl-1,2,2-tris(trimethylsilyl)-1,2-dehydro-2-silagermete (50) | 166 |
| 4.2.32 | 5-Germa-1,3,3,6,8,8-hexakis(trimethylsilyl)-4,4,9,9-tetramethylspiro[4.4]-3,4,7,8-tetrasilanon-1,6-diene (51) | 167 |
| 4.2.33 | 52 and 53 | 168 |
| 4.2.34 | 3,4,7-Trigerma-3,3,6,6-tetrakis(trimethylsilyl)-8,9-dimethyl-1,5-diphenylspiro[3.5]-8,9-disilanon-1,5-diene (55) | 169 |
| 4.2.35 | 3-Germa-4,4,7,7-tetrakis(trimethylsilyl)-5,5,6,6-tetramethyl-1,2-diphenylspiro[2.4]-4,5,6,7-tetrasilahaept-1-ene (56) | 170 |
| 4.2.36 | 3,4,7-Trigerma-4,4,7,7-tetrakis(trimethylsilyl)-5,5,6,6-tetramethyl-1,2-diphenylspiro[2.4]-5,6-disilahept-1-ene (57) | 171 |
| 4.2.37 | 4-Germa-5,5,6,6-tetrakis(trimethylsilyl)-3,3,5,5-tetramethyl-1,2-diphenylspiro[3.3]-3,5,6,7-tetrasilahaept-1-ene (58) | 172 |
| 4.2.38 | 4,5,6-Trigerma-5,5,6,6-tetrakis(trimethylsilyl)-3,3,5,5-tetramethyl-1,2-diphenylspiro[3.3]-3,7-disilahept-1-ene (59) | 173 |
| 4.2.39 | 60 and 61 | 174 |
| 4.2.40 | {Dichloro[tris(trimethylsilyl)silyl]germyl}[tris(trimethylsilyl)silyl]germylene · PMe ₃ (62) | 175 |
| 4.2.41 | {Dichloro[tris(trimethylsilyl)silyl]germyl}[tris(trimethylsilyl)silyl]germylene · IMe ₄ (63) | 176 |
| 4.2.42 | Bis{dichloro[tris(trimethylsilyl)silyl]germyl}germylene · PMe ₃ (64) . | 177 |
| 4.2.43 | 65 and 66 | 178 |
| 4.2.44 | 67 and 68 | 179 |
| 4.2.45 | 2-Chloro-2-tris(trimethylsilyl)silyl-5,5-bis(trimethylsilyl)-3-phenyl-1,2-digerma-5-silacyclopent-3-en-1-ylidene · PMe ₃ (69) | 180 |
| 4.2.46 | Germanium dichloride · bis[<i>Z</i> -1-phenyl-2-tris(trimethylsilyl)silylvinyl]germylene · IMe ₄ (72) | 181 |
| 4.2.47 | 1-Bromo-1-ethylgerma-2,2,5,5-tetrakis(trimethylsilyl)tetramethylcyclopentasilane (73) | 182 |
| 4.2.48 | 1-Hydroxy-1-germa-2,2,5,5-tetrakis(trimethylsilyl)-3,3,4,4-tetramethylcyclopentasilane (74) | 183 |

| | | |
|--------------------------------------|--------------------------------------------------------------------------------------------------------------------------------------------------------------------------------|------------|
| 4.2.49 | 1-Aminogermana-2,2,5,5-tetrakis(trimethylsilyl)-3,3,4,4-tetramethylcyclopentasilane (75) | 184 |
| 4.2.50 | Amino[tris(trimethylsilyl)silyl][bis(trimethylsilyl)silyl]germane (76) | 185 |
| 4.2.51 | 5,7-Digerma-6,13-disulfo-1,1,4,4,8,8,11,11-octakis(trimethylsilyl)octamethyldispiro[4.1.4.1]dodecasilane (77) | 186 |
| 4.2.52 | 1,2,2,5-Tetrakis(trimethylsilyl)-7,7-diphenyl-bicyclo[3.2.0]-7-carba-1-germa-6-oxa-heptasilane (79) | 187 |
| 4.2.53 | 2,3,7,7,8,8-Hexamethyl-6,6,9,9-tetrakis[tris(trimethylsilylsilyl)-spiro[4.4]-5-germa-1,4-dioxa-6,7,8,9-tetrasilanon-2-ene (81) | 188 |
| 4.2.54 | Trimethylsilyl[tris(trimethylsilyl)silyl]germylene–hafnocene · PMe ₃ complex (84) | 189 |
| 4.2.55 | Cyano[bis(trimethylsilyl)]silyl{bis[tris(trimethylsilyl)silyl]germylene · IMe ₄ }silver(I) · B(C ₆ F ₅) ₃ (85) | 190 |
| 4.2.56 | Tris(trimethylsilyl)silyl{bis[tris(trimethylsilyl)silyl]stannylene · IMe ₄ }gold(I) (86) | 191 |
| 4.2.57 | 87 | 192 |
| 4.2.58 | 88 | 193 |
| Abbreviations | | 194 |
| X-ray Crystallographic Tables | | 195 |
| Curriculum Vitae | | 252 |

1 Synthesis of tetrylenes

1.1 Introduction

Metallylenes (also called tetrylenes) are heavy carbene analogs, in which the central carbon atom is substituted with Si (silylenes), Ge (germylenes), Sn (stannylenes) or Pb (plumbylenes). The general formula of these reactive compounds can be summarized as R_2E , where $E = Si, Ge, Sn, Pb$. In contrast to the parent carbenes, the central atom of metallylenes has low propensity to form a hybrid orbital. This results in two electrons being located at the ns orbital and forming a singlet pair. The ground state of H_2E : ($E = Si, Ge, Sn, Pb$) is a singlet, in contrast to $H_2C:$, where the ground state is a triplet [1]. In metallylenes the central atom is surrounded by six electrons and a vacant p-orbital. This dictates an extremely high reactivity. To resolve the electron deficiency, carbenes and their analogs react in a characteristic manner. They can insert into σ bonds, add to unsaturated bonds, form adducts with Lewis acids and Lewis bases, and react with transition metals to give stable complexes (Figure 1). In the absence of reactive partners dimerization and polymerization can occur.

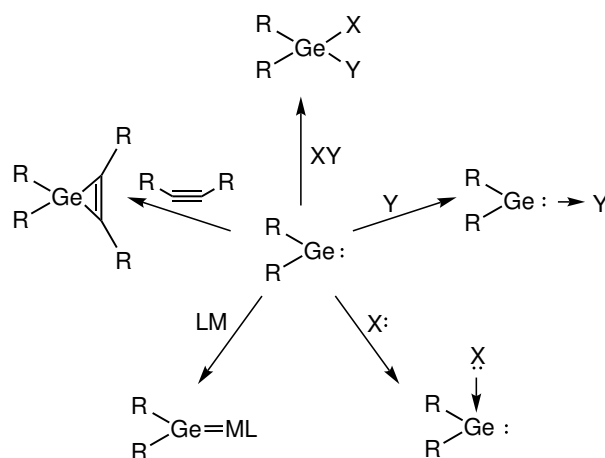


Figure 1: Characteristic reactions of metallylenes for the case of germylene.

There are two main synthesis routes to tetrylenes: i) the reduction of an E^{IV} precursor, or ii) the substitution reaction of an E^{II} halide with a nucleophile, such as RLi or RK (Figure 2). The method of choice depends mainly on the availability of starting materials. In the case of plumbylenes and stannylenes, which are the most stable of all metallylenes, starting halides ($PbBr_2$, $PbCl_2$ and $SnCl_2$) are easily available from chemical suppliers. Germylenes, which are far less stable than Pb- and Sn-based low valent compounds, can be obtained using the dioxane complex of germanium dichloride [1, 2] – a agent that can be prepared with moderate effort. The least stable metallylenes, the silylenes, could be stabilized by even stronger and more bulky Lewis base such as N-heterocyclic carbene [3], on the expense of their limited reactivity in further reactions. Thus, a different approach is required and the majority of silylenes is obtained by the reduction of silanes. There are

several ways of reducing R_4E to R_2E : species: the photochemical reductive elimination of disilene from $R_2E(SiR'_3)_2$, the thermal or photochemical reductive elimination of an olefin or an alkyne from a three membered ring system, and the reduction of the corresponding dihalide R_2EX_2 ($X = Cl, Br, I$). It should also be noted, that bases e. g. N-heterocyclic carbene were used as a dehydrochlorinating agent in the preparation of germylenes [4].

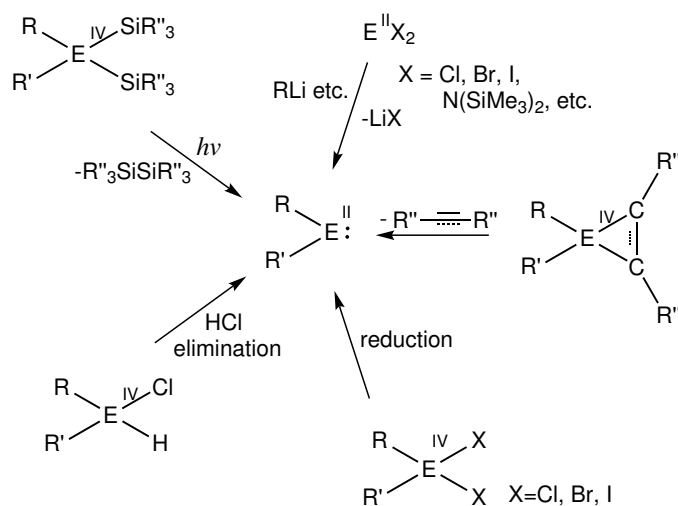


Figure 2: Synthetic methods for tetrylenes.

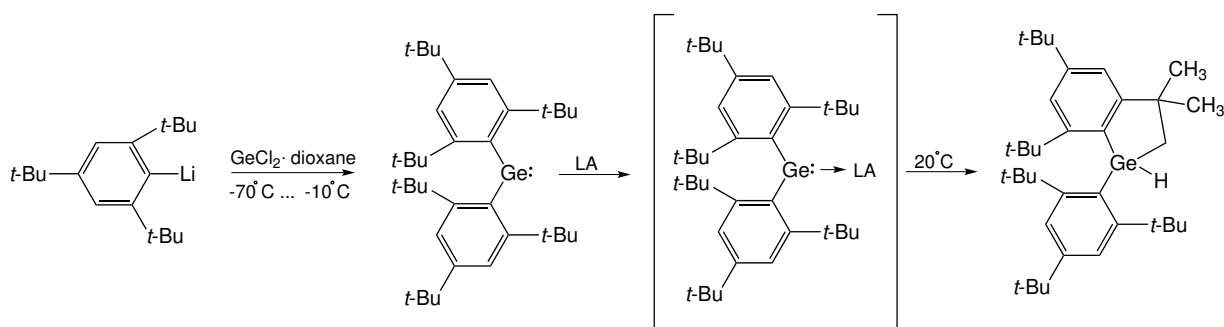
The choice of ligand bonded to the low valent group 14 element species determines the formation and isolability of tetrylenes. Germylenes with small and non-functionalized substituents dimerize or polymerize rapidly [5]. In order to prevent the formation of such an aggregate product, thermodynamic or kinetic stabilization can be utilized. The former can be achieved by donating electrons to the vacant p-orbital of the germanium center using donor ligands (e. g. Cp^* [6, 7], NR_2 [8–11], PR_2 [12], OR [11, 13], SR [14–16], etc). The latter, which follows the steric hindrance of an electron deficient center, can be implemented by introducing a bulky ligand.

The first stable germylene was obtained by Lappert and co-workers in 1976 [17, 18]. This bis[bis(trimethylsilyl)methyl]germylene occurs as a monomer in solution, however, in solid state it exhibits dimeric structure of a digermene [19]. Fifteen years later the first isolable, asymmetrically substituted dialkylgermylene was synthesized by Jutzi and coworkers [20]. The authors obtained $(Me_3Si)_3CGeCH(SiMe_3)_2$ in the reaction of nucleophilic substitution of $Me_5C_5GeCH(SiMe_3)_2$ with $LiC(SiMe_3)_3$. Replacing of one of bis(trimethylsilyl)methyl groups in the Lappert's germylene with the more bulky tris(trimethylsilyl)methyl group prevented the dimerization and enabled the isolation of a $(Me_3Si)_3CGeCH(SiMe_3)_2$ monomer in solid state.

In the case of stable diaryl substituted germylenes, Ar_2Ge , the substituent dictates whether the compound appears as a monomer or as a dimer in the solid state. According to Weidenbruch *et al.* the 2-*t*-Bu-4,5,6- Me_3C_6H ligand is not sufficient to stabilize a monomer and a dimer is formed upon crystallization, although in the liquid phase the monomer is

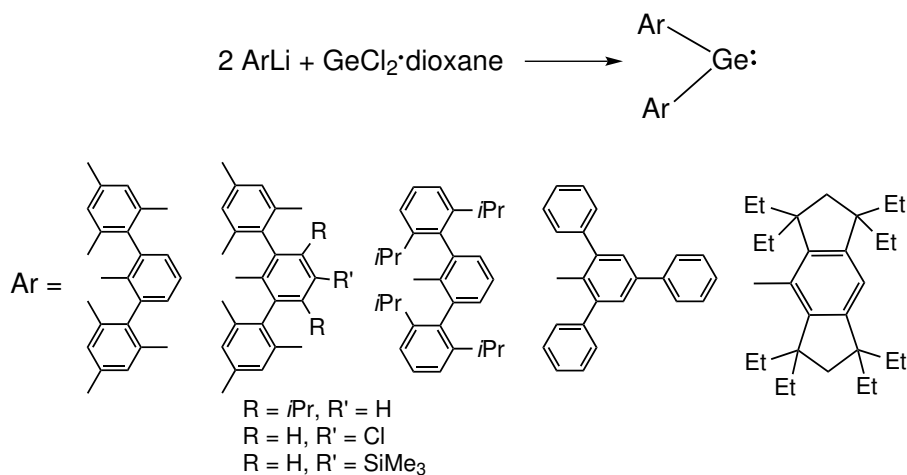
preferred [21].

Bis(2,4,6-tri-*t*-butylphenyl)germylene was synthesized in the reaction of 2,4,6-tri-*t*-butylphenyllithium with $\text{GeCl}_2 \cdot \text{dioxane}$ [22, 23]. It crystallizes as a monomer at -10°C and can be stored at -30°C for months, however, at room temperature it decomposes to 1,3,5-tri-*tert*-butylbenzene after several weeks. When stored in solution at room temperature in the presence of a Lewis acid, such as germanium dichloride, the divalent center gets inserted into the C–H bond of a *tert*-butyl group, which results in the formation of a germaindane (Scheme 1).

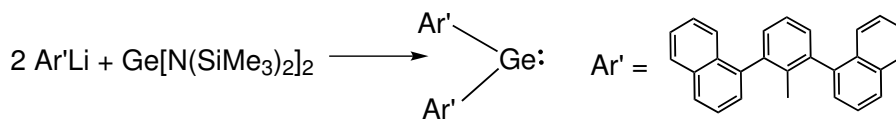


Scheme 1: Synthesis of bis(2,4,6-tri-*t*-butylphenyl)germylene and its rearrangement at ambient temperature in the presence of Lewis acid.

Germylenes with even more bulky aryl-substituents can occur as monomers in solid state, as exemplified by 2,6-bis(2,4,6-trimethylphenyl)phenyl (terphenyl) and its derivatives, 2,4,6-triphenylphenyl, 2,6-bis(1-naphthyl)phenyl and alike [1, 24–28], which were obtained in the substitution reaction (Scheme 2 and 3).



Scheme 2: Synthesis of stable diarylgermylenes starting from dioxan complex of germanium dichloride.

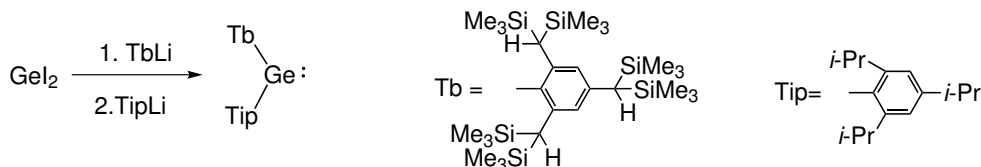


Scheme 3: Synthesis of stable diarylgermylene starting from $\text{Ge}[\text{N}(\text{SiMe}_3)_2]_2$.

Since the C–E–C angle of tetrylenes dictates how much the two unpaired electrons (:) are exposed to other reagents, it is reasonable to expect, that this angle correlates with their reactivity, as already suggested by some authors [26]. It is thus interesting to discuss structural and electronic effects in sterically encumbered divalent group 14 derivatives. Substitution of a terphenyl ligand in the *meta* position with a bulky isopropyl group pushes the mesityl groups towards the core of a molecule. The increased sterical crowding around the M^{II} center enhances the C–Ge–C angle in such isopropyl-substituted bis(terphenyl)germylene to $124.46(11)^\circ$ [26] as compared to $114.4(1)^\circ$ in the non-substituted bis(terphenyl)germylene [24]. The electron-releasing group ($-\text{SiMe}_3$) has similar but smaller effect: when attached in the *para* position, the C–Ge–C angle increases to $116.3(2)^\circ$. On the other hand, the electronegative substituent ($-\text{Cl}$) attached in the *para* position of the central ring results in the reduction of the C–Ge–C angle to $112.63(7)^\circ$ [26].

The fluoroarylgermylene bis[2,4,6-tris(trifluoromethyl)phenyl]germylene was obtained in the reaction of the dioxane complex of germanium dichloride with two equivalents of [2,4,6-tris(trifluoromethyl)phenyl]lithium in 41 % yield [29]. The authors used strong electron-withdrawing groups on the aryl rings and demonstrated that ligands attached to the germanium center do not need to be strong donors. However, the germanium center is stabilized by weak interaction between germanium and four fluorines of the *ortho*-trifluoromethyl groups.

The aryl substituted germylenes discussed so far were all symmetric in the sense that both Ar substituents were identical. However, there is at least one published example of an asymmetric compound, in which the two aryl groups are different. This interesting compound has been first synthesized by Tokitoh and co-workers [30] by adding 2,4,6-tris[bis(trimethylsilyl)methyl]phenyllithium to the suspension of germanium(II) iodide at -78°C in the presence of hexamethylphosphoramide (HMPA), followed by the addition of 2,4,6-tris(*isopropyl*phenyl)lithium (Scheme 4).



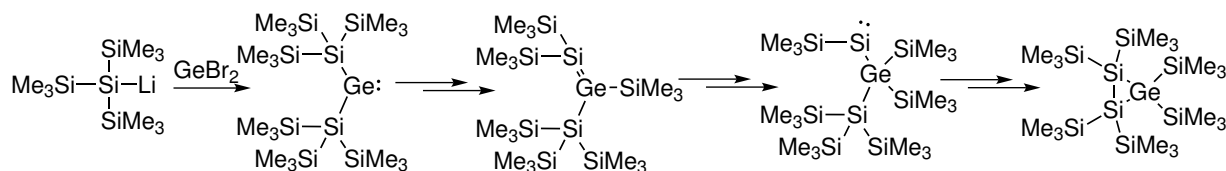
Scheme 4: Synthesis of a stable asymmetric diarylgermylene starting from GeI_2 .

The silylated tetrylenes are an important class of compounds. They are very reactive towards dimerization because of the σ -electron donating character of the silyl group. However, addition of a suitable Lewis base leads to the stabilization of the electron deficient center and allows for isolation, characterization and further reactivity study.

The first stable silylated tetrylenes were obtained by treatment of 2 equivalents of $(\text{Me}_3\text{Si})_3\text{SiK}$ with $\text{E}[\text{N}((\text{SiMe}_3)_3)_2]_2$ ($\text{E} = \text{Sn}, \text{Pb}$) [31, 32]. The bis[tris(trimethylsilyl)silyl]stannylene is monomeric in solution and forms a dimer in solid state in contrast to bis[tris(trimethylsilyl)silyl]plumbylene which is monomeric not only in solution but also in solid state.

To stabilize monomeric bis[tris(trimethylsilyl)silyl]stannylene also in solid state an N-heterocyclic carbene was used and adduct $[(\text{Me}_3\text{Si})_3\text{Si}]_2\text{Sn} \cdot ^\text{Me}\text{IIPr}$ was formed [33].

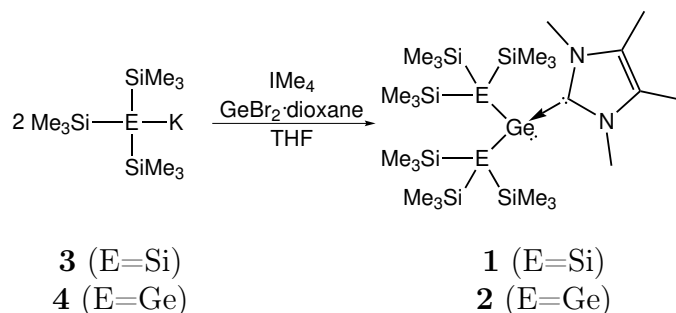
An attempt to obtain bis[tris(trimethylsilyl)silyl]germylene in the reaction of $(\text{Me}_3\text{Si})_3\text{SiLi}$ with GeBr_2 was unsuccessful [34]. The transient germylene rearranged to a three-membered ring germirane *via* 1,2-trimethylsilyl shifts to germanium [35] (Scheme 5).



Scheme 5: Formation of bis[tris(trimethylsilyl)silyl]germylene and mechanistic explanation of its rearrangement to disilagermirane.

The analogous three-membered ring, hexakis(trimethylsilyl)cyclotrigermane $[\text{Ge}(\text{SiMe}_3)_2]_3$, was formed in the reaction of $(\text{Me}_3\text{Si})_3\text{GeLi}$ with GeBr_2 [36], suggesting that bis[tris(trimethylsilyl)germyl]germylene was present in the reaction mixture, however, similar to the disilylated germylene, rearrangement to the more stable product occurred.

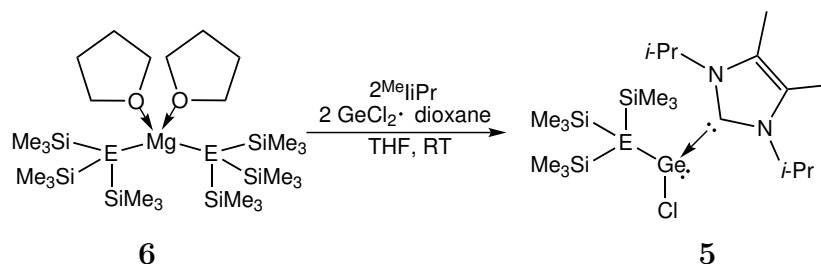
Trapping of the germylenes described above was possible using a strong Lewis base such as N-heterocyclic carbene. The preparation of 1,3,4,5-tetramethylimidazol-2-ylidene adduct of acyclic disilylated or digermylated germylenes (**1** and **2** respectively, Scheme 6) was achieved by the reaction of tris(trimethylsilyl)silyl potassium (**3**) or tris(trimethylsilyl)-



Scheme 6: Synthesis of acyclic germylenes **1** and **2**.

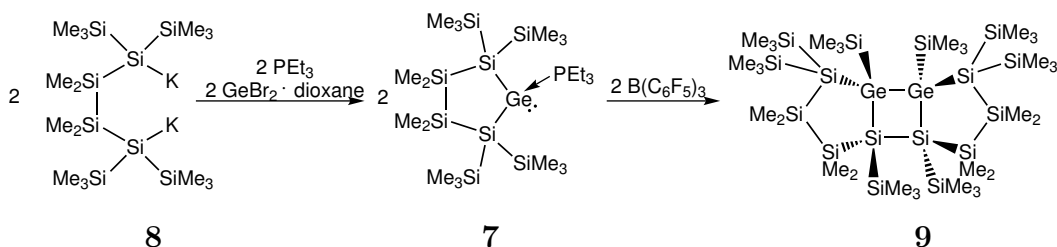
germyl potassium (**4**) with $\text{GeBr}_2 \cdot \text{dioxane}$ in the presence of carbene [37].

The first donor-stabilized tris(trimethylsilyl)silyl(chloro)germylene (**5**) was obtained in 2011 by Katir *et al.* [33], which opened new possibilities in the synthesis of germylenes. Synthesis of **5** was enabled by employing less reactive bis[tris(trimethylsilyl)silyl]magnesium \cdot 2 THF (**6**) instead of previously used potassium anion (Scheme 7). In the similar procedure authors obtained also N-heterocyclic adducts of tris(trimethylsilyl)germyl(chloro)germylene, $[(\text{Me}_3\text{Si})_3\text{Ge}](\text{Cl})\text{Ge} \cdot {}^{\text{Me}}\text{IiPr}$.



Scheme 7: Synthesis of tris(trimethylsilyl)silyl(chloro)germylene **5**.

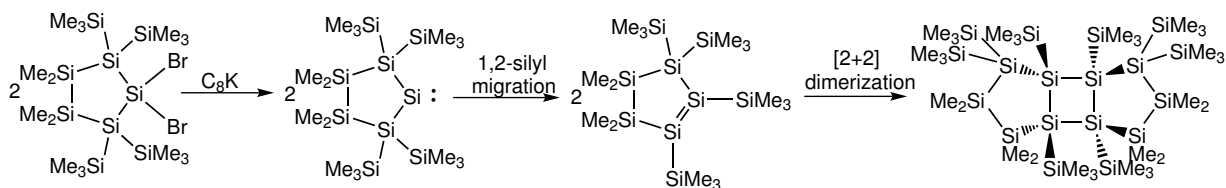
Triethylphosphine adduct of a cyclic disilylated germylene **7** was synthesized in the reaction of 1,4-dipotassio-1,1,4,4-tetrakis(trimethylsilyl)tetramethyltetrasilane (**8**) with dioxane complex of germanium dibromide and PEt_3 . Abstraction of phosphine with $\text{B}(\text{C}_6\text{F}_5)_3$ led to the formation of base-free germylene followed by 1,2-silyl migration to the dimerized product **9** [38] (Scheme 8).



Scheme 8: Formation of triethylphosphine adduct of cyclic germylene (**7**) and its dimerization after extraction of PEt_3 .

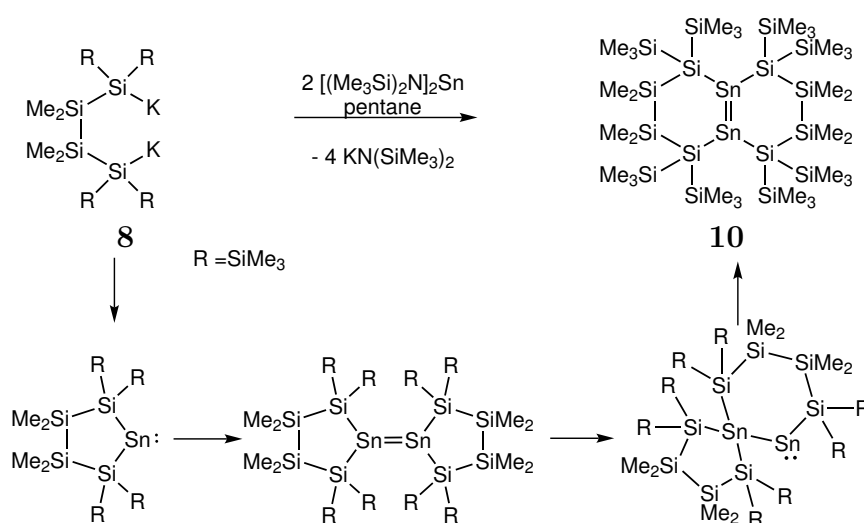
A similar dimerization path was observed for a five-membered ring silylene [39]. Reduction of the 1,1-dibromocyclopentasilane with potassium graphite led to the formation of a [2+2] cycloaddition product *via* 1,2-silyl shift (analogous to **9**, Scheme 9). Authors investigated theoretically the mechanism of the silagermane formation and reported, that the trimethylsilyl group is bulky enough to protect the silylene from dimerization, however, it is not a good protecting group for hindering the 1,2-silyl migration, which was observed also before [40, 41].

A different reaction path of dimerization was observed for a five-membered ring stanylene. The reaction of **8** with $[(\text{Me}_3\text{Si})_2\text{N}]_2\text{Sn}$ led to the formation of a transient stanylene, which rearranged to the endocyclic distannene **10** via stannylstanylene intermediate (Scheme 10). The formation of stannylstanylene was observed before by Power and



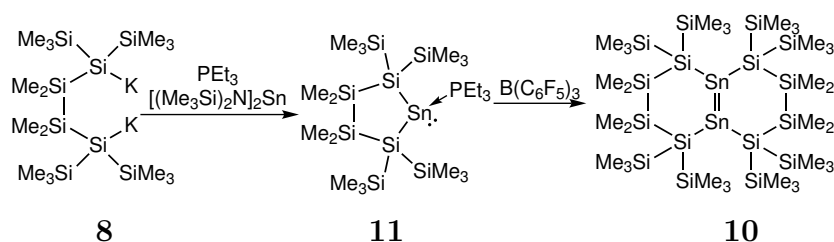
Scheme 9: Mechanistic explanation of the formation head-to-head dimer.

co-workers [42]. After treatment of Ar^*SnCl ($\text{Ar}^* = \text{C}_6\text{H}_3\text{-2,6-Trip}_2$; $\text{Trip} = \text{C}_6\text{H}_2\text{-2,4,6-}i\text{-Pr}_3$) with LiPh the reversible equilibrium between $\text{Ar}^*\text{SnSnPh}_2\text{Ar}^*$ and Ar^*SnPh was established.



Scheme 10: Mechanistic explanation of the formation distannene **10**.

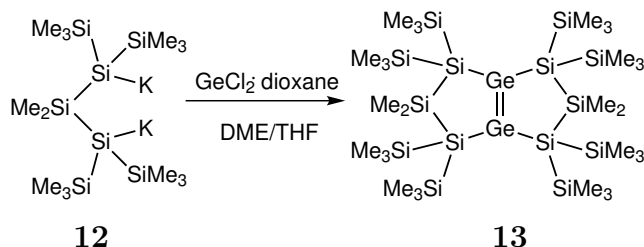
To obtain the triethylphosphine adduct of a cyclic stannylene **11** the reaction of **8** with $[(\text{Me}_3\text{Si})_2\text{N}]_2\text{Sn}$ was carried out in the presence of PEt_3 [43]. Addition of $\text{B}(\text{C}_6\text{F}_5)_3$ to **11** led to the formation of endocyclic distannene **10** (Scheme 11).



Scheme 11: Formation of triethylphosphine adduct of a cyclic stannylene **11** and distannene **10**.

Reaction of 1,3-dipotassio-1,1,3,3-tetrakis(trimethylsilyl)dimethyltrisilane (**12**) with germanium dichloride led to the formation of an endocyclic digermene (Scheme 12) [44]. Reaction carried out in the presence of PMe_3 proceeded to the formation of germylene-phosphine

adduct, which was not enough stable to be isolated in the solid state. Using N-heterocyclic carbene (IMe₄) as a Lewis base allowed for crystallization of the germylene-NHC carbene adduct.



Scheme 12: Formation of endocyclic digermene **13**.

It is advantageous to use a silyl substituent on the tetrylene center. Although tetrylenes that carry amine ligand are very popular, their reactivity is limited due to the strong stabilization by electron donation from the lone pair of nitrogen into the empty p orbital. In the most abundant N-heterocyclic systems, such stabilization is additionally reinforced by the chelating effect of the ring. Thus these compounds react less easily with nucleophiles than related non-cyclic tetrylenes. Both arylated and alkylated tetrylenes are much more reactive than the aminated ones, due to the lack of intramolecular π -stabilization. Using a silyl group, which is more σ -donating in character than a carbonyl one results in increased reactivity. Therefore arylated, alkylated and silylated tetrylenes need to be kinetically stabilized by bulky substituents.

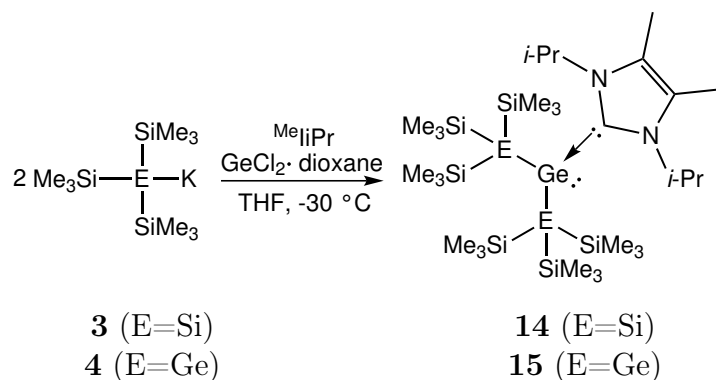
Theoretical study showed that electronic and steric effects due to the substituent have influence on the singlet (¹A₁)–triplet (³B₁) energy separation [45]. In contrast to electronegative groups, which increase the S–T energy gap, the electropositive group, such as a silyl one, reduces this gap. As suggested by Grev *et al.*, the combination of an electropositive substituent and a large R–Si–R angle should be employed for the design of the triplet ground state silylenes [46]. Increase of the bond angle at a divalent silicon atom is accompanied by the increase of the p-character of the singlet electron pair orbital. For symmetry reasons the 180° case is degenerate and – according to the Hund’s rule – its ground state should be a triplet. In practical terms, the R–Si–R angle exceeding 120° is already assumed to result in the triplet ground state [46, 47]. As it was demonstrated, the production of the dialkylsilylene in the triplet ground state would be significantly more difficult than for disilylated silylene [46]. This theoretical prediction has been confirmed experimentally. Bis(*tri-iso*-propylsilyl)silylene [48] and bis(*tri-tert*-butylsilyl)silylene [49] possess triplet ground state, which was confirmed by EPR spectroscopy in the case of the latter compound.

The preparation of the triplet ground stage silylene has been one of the most challenging issues in the modern silicon chemistry. Until now, a bulky silyl substituent on divalent silicon atom is the only possibility to solve it.

1.2 Oligosilylgermylenes and oligogermylgermylenes

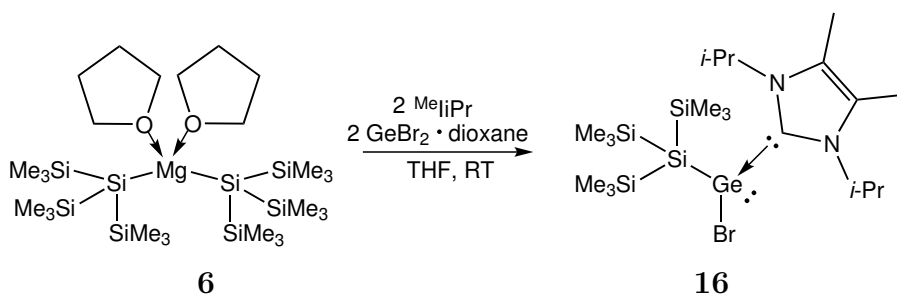
1.2.1 Synthesis

Reaction of tris(trimethylsilyl)silyl potassium (**3**) or tris(trimethylsilyl)germyl potassium (**4**) with germanium dichloride·dioxane in the presence of 1,3-diisopropyl-4,5-dimethylimidazol-2-ylidene (^{Me}IiPr) at $-30\text{ }^{\circ}\text{C}$ led to the formation of the corresponding germylenes: bis[tris(trimethylsilyl)silyl]germylene · ^{Me}IiPr (**14**) and bis[tris(trimethylsilyl)germyl]germylene · ^{Me}IiPr (**15**) (Scheme 13) in high yields (77% and 88%, respectively). The corresponding monoanion (**3** and **4**, respectively) should be dropped very slowly to the vigorously stirring solution of $\text{GeCl}_2 \cdot \text{NHC}$ complex in THF. Too fast dropping results in the formation of tetrakis(trimethylsilyl)silane as a side product. Both N-heterocyclic carbene adducts of germylene (**14** and **15**) are sensitive to moisture and oxygen, however, they are relatively stable at room temperature: after 1 year of storage under inert atmosphere neither of the two compounds showed signs of decomposition.



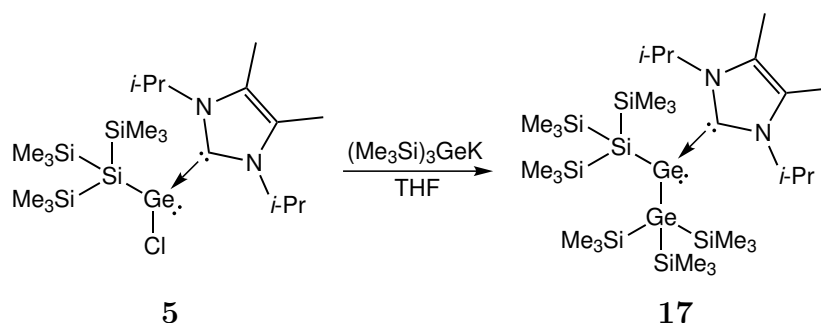
Scheme 13: Synthesis of **14** and **15**.

Formation of the monosubstituted tris(trimethylsilyl)silyl(bromo)germylene stabilized by N-heterocyclic carbene (**16**) in the reaction of tris(trimethylsilyl)silyl potassium (**3**) with germanium dibromide in the ratio 1:1 carried out at low temperature ($-30\text{ }^{\circ}\text{C}$ as well as $-60\text{ }^{\circ}\text{C}$) in the presence of ^{Me}IiPr was not observed. It was necessary to use less reactive bis[tris(trimethylsilyl)]silylmagnesium · 2 THF (**6**) instead of tris(trimethylsilyl)silyl potassium (**3**) in the reaction with two equivalents of germanium dibromide · dioxane and two equivalents of N-heterocyclic carbene, which finally led to the formation of **16** (Scheme 14). Repetition of this reaction with germanium dibromide and PMe_3 as a Lewis base at $-30\text{ }^{\circ}\text{C}$ revealed that formation of germylene did not occur and tris(trimethylsilyl)silylbromide was obtained instead.



Scheme 14: Synthesis of monosubstituted germylene **16**.

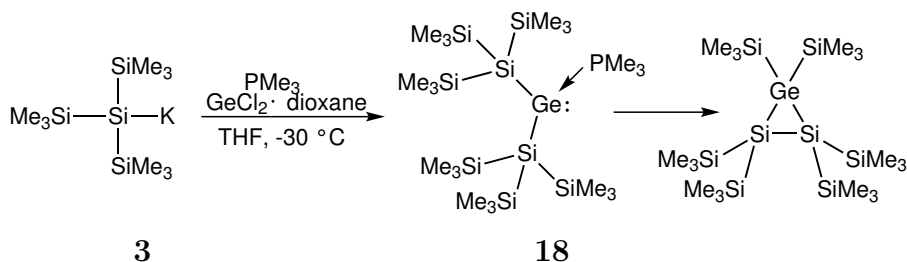
An asymmetric adduct of 1,3-diisopropyl-4,5-dimethylimidazol-2-ylidene with one tris(trimethylsilyl)germyl group and one tris(trimethylsilyl)silyl group attached to the central germanium atom (**17**) was obtained at room temperature in the reaction of tris(trimethylsilyl)silyl(chloro)germylene stabilized by NHC-carbene **5** with tris(trimethylsilyl)germyl potassium (Scheme 15).



Scheme 15: Synthesis of **17**.

Reaction of two equivalents of tris(trimethylsilyl)silyl potassium (**3**) with dioxane complex of germanium dichloride in the presence of pyridine showed that pyridine is not able to stabilize the germylene and during this reaction several different products were formed. Attempt to stabilize bis[tris(trimethylsilyl)silyl]germylene with triethylphosphine was also unsuccessful, i.e. hexakis(trimethylsilyl)disilagermirane was obtained instead of expected germylene. Repetition of the reaction with a smaller phosphine, i.e. PMe_3 , led to the formation of the expected germylene adduct **18**. However, using trimethylphosphine instead of N-heterocyclic carbene results in the destabilization of the acyclic germylene and its rapid conversion into disilagermirane (Scheme 16). Due to this fact, isolation of **18** is not possible in solid state, thus **18** should be prepared freshly prior to its use.

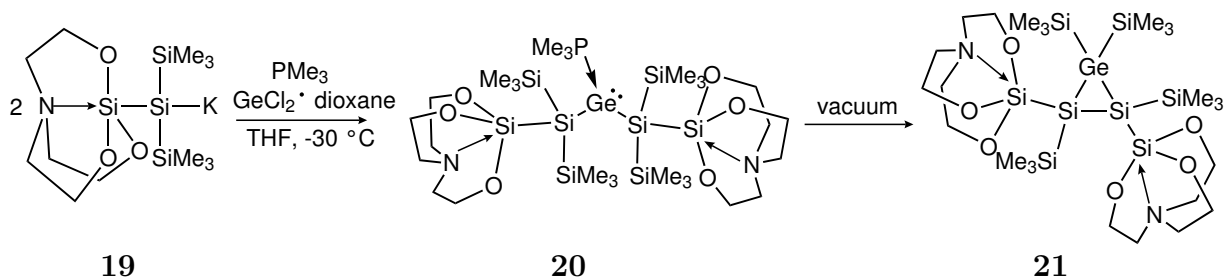
Comparison of the SiMe_3 ^1H NMR signal of **18** to that of Me_3SiOtBu , which is present in the solution resulting from the formation of tris(trimethylsilyl)silyl potassium, revealed an approximate yield of 60%. The prominent feature in the electron paramagnetic resonance spectrum provided evidence that the germanium radicals were created in the reaction described above, however, poor quality of the recorded spectrum did not allow for its assignment to any molecule. Trimethylphosphine adduct of bis[tris(trimethylsilyl)silyl]germylene



Scheme 16: Synthesis of **18** and fast conversion into disilagermirane.

could be also obtained in the reaction of tris(trimethylsilyl)silyl potassium (**3**) with dioxane complex of germanium dibromide in the presence of PMe_3 at $-30\text{ }^\circ\text{C}$. However, changing the solvent from THF to benzene or applying lower temperature ($-60\text{ }^\circ\text{C}$) did not lead to a clean formation of **18**.

Attempts to use less bulky groups bonded to the germanium atom in germylene and its stabilization with trimethylphosphine were unsuccessful. Reaction of 2-ethyl-1,1,1,3,3,3-hexamethyltrisilan-2-yl potassium or 2-phenyl-1,1,1,3,3,3-hexamethyltrisilan-2-yl potassium with dioxane complex of germanium dichloride in the presence of PMe_3 at $-30\text{ }^\circ\text{C}$ led mainly to the formation of radicals invisible in the NMR spectra. Replacement of one of the tris(trimethylsilyl)silyl groups with a chloride did not lead to the stabilization of germylene either. Using more bulky monoanion, such as $[(\text{SiMe}_3)_2\text{TIPSSi}]\text{K}$, did not result in the formation of a germylene, however, using $[(\text{SiMe}_3)_2\text{Sa}]\text{K}$ (**19**) (Sa=silatranlyl) proceeded to the stabilization of an electron deficient center and the formation of germylene **20** (Scheme 17). **20** is slightly more stable than trimethylphosphine adduct of bis[tris(tri-

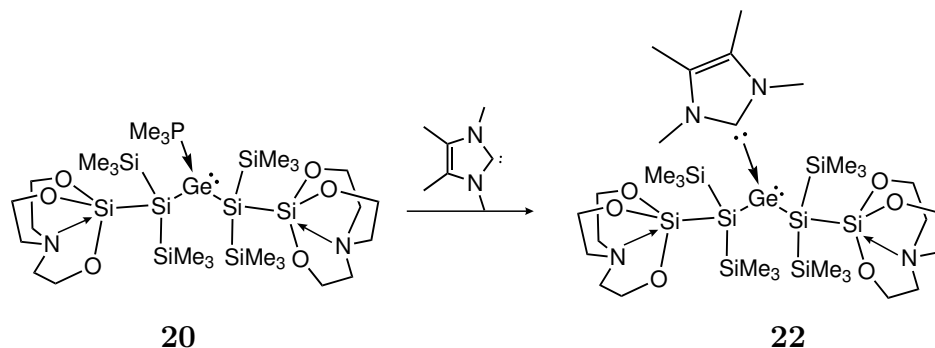


Scheme 17: Synthesis of **20** and its rearrangement upon loss of PMe_3 .

methylsilyl)silyl]germylene and precipitates very well from pentane, toluene at $-30\text{ }^\circ\text{C}$, and also from pentane - ether mixture (1:1) at room temperature. None of these pale yellow crystals were suitable to X-ray study. Applying vacuum led to the extraction of the phosphine and the rearrangement of a germylene into disilagermirane **21**. Based on ^1H NMR spectrum only the isomer *trans* was formed. A possible explanation for this effect may be found when the steric demand of silatranlyl groups is taken into account. The silatranlyl groups are too bulky to have enough space to exist at the same side of the ring, thus only isomer *trans* can be formed.

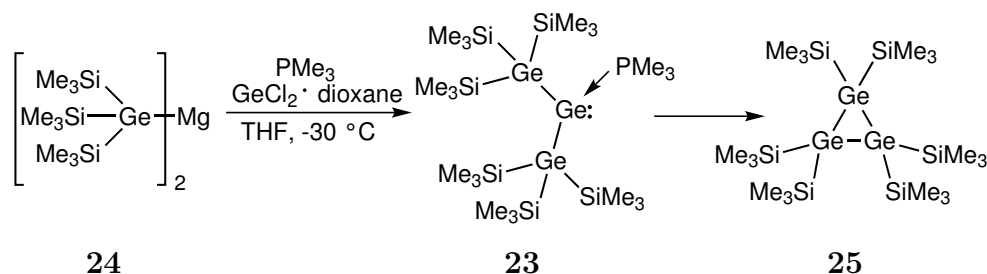
Addition of N-heterocyclic carbene (IME_4) into the stirring solution of **20** in THF at

room temperature led to the replacement of PMe_3 with carbene and formation of **22**. N-heterocyclocarbene-stabilized germylene **22** is stable and does not rearrange to **21**.



Scheme 18: Synthesis of **22**.

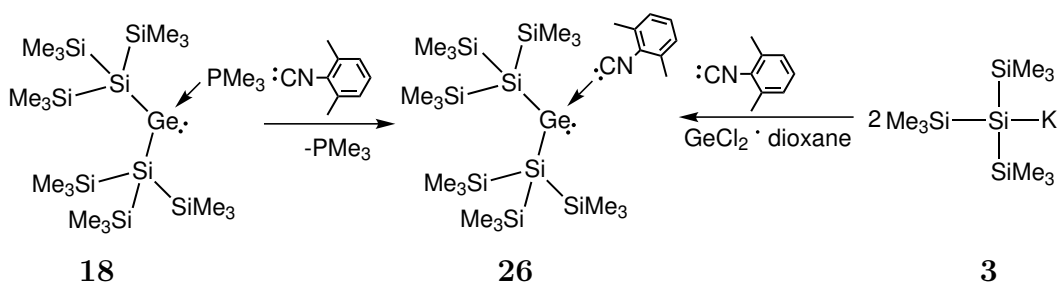
Attempt to synthesize a digermylated germylene stabilized with trimethylphosphine (**23**) using tris(trimethylsilyl)germyl potassium was unsuccessful. It was merely the use of less reactive magnesium anion **24** that eventually gave the expected results and digermylated germylene **23** was synthesized at $-35\text{ }^\circ\text{C}$ (Scheme 19). However, the ^{29}Si NMR spectrum indicated not only **23**, but also the product of its rearrangement e. i. trigermirane **25**. The lack of success in obtaining clean digermylated germylene suggests that the phosphine adduct of digermylated germylene **23** is less stable than its disilylated analog **18**.



Scheme 19: Synthesis of **23** and its conversion into trigermirane **25**.

Reaction of phosphine adduct of bis[tris(trimethylsilyl)silyl]germylene with 2,6-dimethylphenylisocyanide carried out at low temperature ($-30\text{ }^\circ\text{C}$) led to substitution of PMe_3 and the formation of isocyanide adduct of germylene **26** (left reaction in Scheme 20). Isocyanide adduct of an acyclic germylene **26** could also be obtained in the reaction of potassium monoanion **3** with dioxane complex of germanium dichloride in the presence of 2,6-dimethylphenylisocyanide at $-30\text{ }^\circ\text{C}$ (right reaction in Scheme 20). Compound **26** is quite stable and can be stored at room temperature for months, heating up to $260\text{ }^\circ\text{C}$ does not lead to its decomposition.

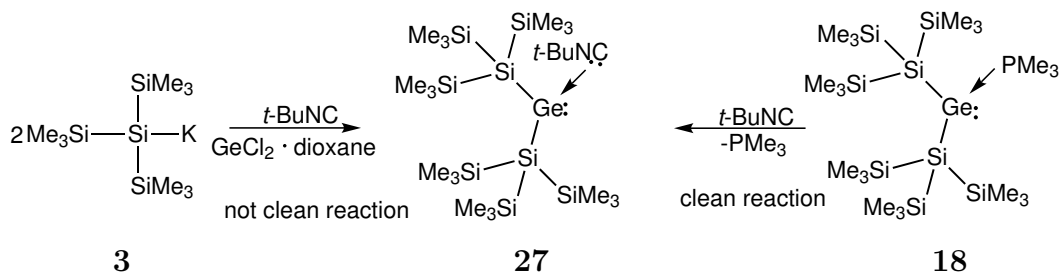
In contrast to Ar^*SnPh ($\text{Ar}^* = \text{C}_6\text{H}_3\text{-2,6-Trip}_2$; $\text{Trip} = \text{C}_6\text{H}_2\text{-2,4,6-Pr}_3^i$) [50], isocyanide adduct of bis[tris(trimethylsilyl)silyl]germylene (**26**) did not react with phenyllithium at



Scheme 20: Stepwise (left) and direct (right) formation of bis[tris(trimethylsilyl)silyl]germylene isocyanide adduct **26**.

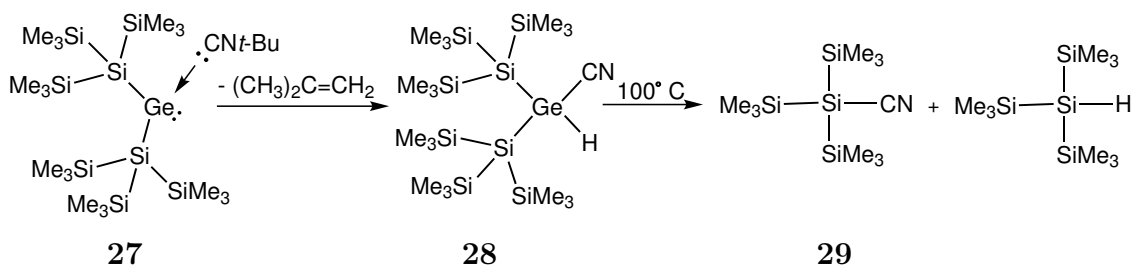
room temperature. The reaction of bis[tris(trimethylsilyl)silyl]germylene PMe_3 adduct (**18**) with PhLi did not proceed either and disilagermirane resulting from decomposition of germylene **18** was detected in the reaction mixture.

In the reaction of tris(trimethylsilyl)silyl potassium **3** with dioxane complex of germanium dichloride in the presence of a smaller isocyanide, $t\text{-BuNC}$, carried out at low temperature (-30°C), tetrakis(trimethylsilyl)silyl was formed in addition to the expected germylene adduct **27**. Addition of *tert*-butylisocyanide to the stirring solution of phosphine adduct of bis[tris(trimethylsilyl)silyl]germylene prevented the formation of side product, tetrakis(trimethylsilyl)silyl, thus clean isocyanide adduct of germylene (**27**) was formed (Scheme 21).



Scheme 21: Stepwise and direct formation of bis[tris(trimethylsilyl)silyl]germylene isocyanide adduct **27**.

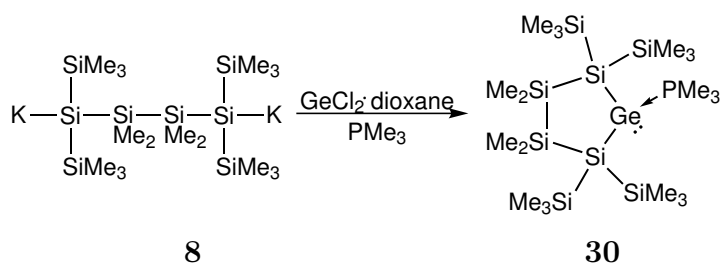
Surprisingly, as a product of the crystallization of **27**, tris(trimethylsilyl)silyl cyanide was found. Analysis of the mother liquor by ^{29}Si NMR spectroscopy proved the rearrangement of the germylene adduct **27**. The main product presented in the solution exhibit chemical shifts of -107.2 and -8.5 ppm, as a one of the compound present in low concentration tris(trimethylsilyl)silyl cyanide was found. It was figured out, that the *tert*-butylisocyanide adduct of bis[tris(trimethylsilyl)silyl]germylene **27** is not stable, and follow-up chemistry took place in the solution of pentane. **27** rearranged to the [bis(trimethylsilyl)silyl]germylcyanide **28**, which slowly decomposed to tris(trimethylsilyl)silylcyanide (**29**) (Scheme 22). Heating up **28** to 100°C led to faster formation of tris(trimethylsilyl)silylcyanide (**29**), as a second compound tris(trimethylsilyl)silane was found according to the ^{29}Si NMR and ^1H NMR spectra. The mechanism of the formation of **28**



Scheme 22: Rearrangement of **27**.

as well as its rearrangement to the silylcyano and silane remains unknown, however the presence of **28** and tris(trimethylsilyl)silylcyano (**29**) in the rearrangement path of **27** was confirmed by X-ray studies.

Cyclic disilylated germylene stabilized with trimethylphosphine (**30**) was obtained in the reaction of one equivalent of dianion **8** with dioxane complex of germanium dichloride in the presence of PMe_3 (Scheme 23).



Scheme 23: Synthesis of **30**.

1.2.2 NMR spectroscopy

The ^{29}Si NMR chemical shifts for the quaternary (SiSiMe_3) and the TMS (SiMe_3) silicon nuclei for acyclic germylenes are compiled in the first and the second column of Table 1, respectively. The most up-field shifted signal for N-heterocyclic carbene adduct of bis[tris(trimethylsilyl)silyl]germylene related to the quaternary silicon atom, -125.5 ppm, is associated with the bis[tris(trimethylsilyl)silyl]germylene featuring the IME_4 carbene [37]. The resonance of $-\text{SiMe}_3$ group is observed at -8.6 ppm. The corresponding spectra for the digermylated germylene **2** and **15** show single resonances at -4.1 ppm. The ^{29}Si NMR spectrum of an asymmetric germylene $[(\text{Me}_3\text{Si})_3\text{Si}][(\text{Me}_3\text{Si})_3\text{Ge}]\text{Ge} \cdot \text{MeLiPr}$ (**17**) shows three resonances at -4.2 , -8.7 and -123.3 ppm, which lie very close to the corresponding signals in the symmetric $[(\text{Me}_3\text{Si})_3\text{Si}]_2\text{Ge} \cdot \text{MeLiPr}$ compound (**14**) (-8.8 and -122.9 ppm). The chemical shift difference between SiMe_3 group attached to the germanium and the silicon atom in **17** is typical [51] and yields 4.5 ppm in the presented case.

The ^1H NMR spectrum of **15** shows two singlets at 1.56 and 1.62 ppm (3 H each), which correspond to the two CH_3 groups attached to the imidazole ring. The two multiplets at 5.64 and 6.45 ppm (1 H each) and two doublets at 1.10 and 1.31 ppm (6 H each) are

Table 1: ^{29}Si NMR data for base adducts of acyclic germylenes.

| Compound | Group | | |
|-----------------------------------------------------------------------------------------------------------------------|---------------------------|-------------------------|-----------|
| | <i>SiSiMe₃</i> | <i>SiMe₃</i> | Sa |
| $[(\text{Me}_3\text{Si})_3\text{Si}]_2\text{Ge} \cdot \text{IMe}_4^a$ (1) | -125.5 (s) | -8.6 (s) | n/a |
| $[(\text{Me}_3\text{Si})_3\text{Ge}]_2\text{Ge} \cdot \text{IMe}_4^a$ (2) | n/a | -4.1 (s) | n/a |
| $[(\text{Me}_3\text{Si})_3\text{Si}] (\text{Cl}) \text{Ge} \cdot \text{MeLiPr}^b$ (5) | -119.12 (s) | -7.53 (s) | n/a |
| $[(\text{Me}_3\text{Si})_3\text{Si}] (\text{Br}) \text{Ge} \cdot \text{MeLiPr}$ (16) | -121.2 (s) | -7.2 (s) | n/a |
| $[(\text{Me}_3\text{Si})_3\text{Si}]_2\text{Ge} \cdot \text{MeLiPr}$ (14) | -122.9 (s) | -8.8 (s) | n/a |
| $[(\text{Me}_3\text{Si})_3\text{Ge}]_2\text{Ge} \cdot \text{MeLiPr}$ (15) | n/a | -4.1 (s) | n/a |
| $[(\text{Me}_3\text{Si})_3\text{Si}] [(\text{Me}_3\text{Si})_3\text{Ge}] \text{Ge} \cdot \text{MeLiPr}$ (17) | -123.3 (s) | -4.2 (s) -8.7 (s) | n/a |
| $[(\text{Me}_3\text{Si})_3\text{Si}]_2\text{Ge} \cdot \text{PMe}_3$ (18) | -119.9 (d) | -8.9 (d) | n/a |
| $[(\text{Me}_3\text{Si})_2\text{SaSi}]_2\text{Ge} \cdot \text{PMe}_3$ (20) | -125.7 (d) | -8.1 (d) -8.4 (s) | -43.7 (d) |
| $[(\text{Me}_3\text{Si})_3\text{Ge}]_2\text{Ge} \cdot \text{PMe}_3$ (23) | n/a | -5.3 (d) | n/a |
| $[(\text{Me}_3\text{Si})_3\text{Si}]_2\text{Ge} \cdot \text{CN}(2,6\text{-MePh})$ (26) | -115.7 (s) | -8.3 (s) | n/a |
| $[(\text{Me}_3\text{Si})_3\text{Si}]_2\text{Ge} \cdot \text{CN}(t\text{-Bu})$ (27) | -118.8 (s) | -8.0 (s) | n/a |

^a data taken from [37], ^b data taken from [33]

assigned to the protons of the isopropyl groups. These spectral features provide evidence for hindering of NHC-carbene rotation. This interpretation was confirmed by ^{13}C NMR spectrum, which showed the following 10 resonances. The signal at 5.1 ppm is assigned to the trimethylsilyl group. Further peaks at 9.7, 10.1, 52.0 and 54.7 ppm correspond to the carbon atoms of the isopropyl group. The signals at 126.2 and 126.5 ppm are assigned to the carbon nuclei in the imidazole ring and the resonances at 21.6 and 22.7 ppm to the methyl group attached to the imidazole ring. The signal at 174.8 ppm corresponds to the N-C-N carbon.

The peak broadening in the ^1H NMR spectrum of **14** suggests a dynamic process, which takes place at room temperature (upper panel in Figure 3). The interpretation of the ^{13}C NMR spectrum supports this conjecture. The three resonances, located at 4.7, 126.5 and 173.2 ppm (assigned to the trimethylsilyl group, C-CH₃ and N-C-N, respectively) are sharp, whereas the remaining signals are broadened. The resonance observed at 10.0 ppm is assigned to the methyl groups attached to the imidazole ring, the two signals at 21.7 and 22.7 ppm result from the methyl groups of the isopropyl substituent, the peaks at 52.3 and 54.7 ppm characterize the C-H group. Lowering the temperature to -30 °C led to the separation of the resonances in the ^1H NMR spectrum and allowed for the assignment of the resonances to the corresponding atoms (lower panel in Figure 3). The singlet at 0.37 ppm is assigned to the trimethylsilyl group. Two doublets at 1.02 and 1.22 ppm (6 H each) and two multiplets at 5.57 and 6.55 ppm (1 H each) originate from the isopropyl groups, the two singlets at 1.43 and 1.51 ppm represent the methyl groups attached to the imidazole ring. These features confirm the hindering of the N-heterocyclic carbene rotation at -30 °C.

The chloro-substituted germylene (**5**) is characterized by the chemical shifts of -119.12 and -7.53 ppm [33], which can be compared to the chemical shifts of -121.2 and -7.2 ppm recorded for the bromo-substituted compound (**16**). The signal corresponding to the central silicon atom of **16** is shifted by about 2.1 ppm high-field compared to the chloride derivative (**5**).

The ^1H NMR spectrum of monosilylated germylene (**16**) reveals the carbene and tris(trimethylsilyl)silyl moieties to be in a 1:1 ratio. The most intensive resonance, located at 0.49 ppm, is assigned to the trimethylsilyl group. The two doublets at 1.11 and 1.26 ppm (6 H each) suggest that the methyls of the isopropyl group are not equivalent. The proton bonded to the central carbon atom of the isopropyl group is characterized by the septet located at 5.59 ppm. The singlet at 1.45 ppm is assigned to the methyl groups attached to the imidazole ring.

The presence of six resonances in the ^{13}C NMR spectrum confirms the free rotation of the N-heterocyclic carbene. The signal at 3.5 ppm results from the carbon atom of the trimethylsilyl group, the peaks at 21.7 and 53.0 ppm are assigned to the isopropyl group (CH₃ and CH, respectively). The methyl group attached to the imidazole ring is characterized by chemical shift of 9.6 ppm. The resonance of the N-C-N carbon (170.0 ppm) is slightly up-field shifted compared to the corresponding carbon of the disilylated and digermlylated N-heterocyclic carbene adducts of germylene.

The most down-field shifted $S\text{iSiMe}_3$ signal at -115.7 ppm is assigned to the 2,6-

Table 2: ^1H NMR chemical shifts of N–heterocyclic carbene adducts of germylene.

| Compound | Group | | | | |
|---------------------------------------------------------------------------------------------------------------------|--------------|--------------|--------------|------------------------|----------------------|
| | Si Me_3 | C Me | N Me | C H Me | C H Me |
| $[(\text{Me}_3\text{Si})_3\text{Si}]_2\text{Ge} \cdot \text{MeIiPr}$ (14) | 0.41 | 1.55 | n/a | 5.73 (br) 6.56 (br) | 1.30 (br) |
| $[(\text{Me}_3\text{Si})_3\text{Ge}]_2\text{Ge} \cdot \text{MeIiPr}$ (15) | 0.42 | 1.56 1.62 | n/a | 5.64 6.45 | 1.10 (d) 1.31 (d) |
| $[(\text{Me}_3\text{Si})_3\text{Si}]_2\text{Ge} \cdot \text{IMe}_4$ (1) | 0.35 | 1.34 1.44 | 3.52 3.67 | n/a | n/a |
| $[(\text{Me}_3\text{Si})_3\text{Ge}]_2\text{Ge} \cdot \text{IMe}_4$ (2) | 0.40 | 1.32 1.43 | 3.48 3.68 | n/a | n/a |
| $[(\text{Me}_3\text{Si})_3\text{Si}](\text{Cl})\text{Ge} \cdot \text{MeIiPr}$ (5) | 0.51 | 1.49 | n/a | 5.48 | 1.15 (d) 1.30 (d) |
| $[(\text{Me}_3\text{Si})_3\text{Si}](\text{Br})\text{Ge} \cdot \text{MeIiPr}$ (16) | 0.49 | 1.45 | n/a | 5.59 | 1.11 (d) 1.26 (d) |
| $[(\text{Me}_3\text{Si})_3\text{Si}][(\text{Me}_3\text{Si})_3\text{Ge}]\text{Ge} \cdot \text{MeIiPr}$ (17) | 0.41 0.43 | 1.53 1.59 | n/a | 5.66 (m) 6.52 (m) | 1.33 (br) |

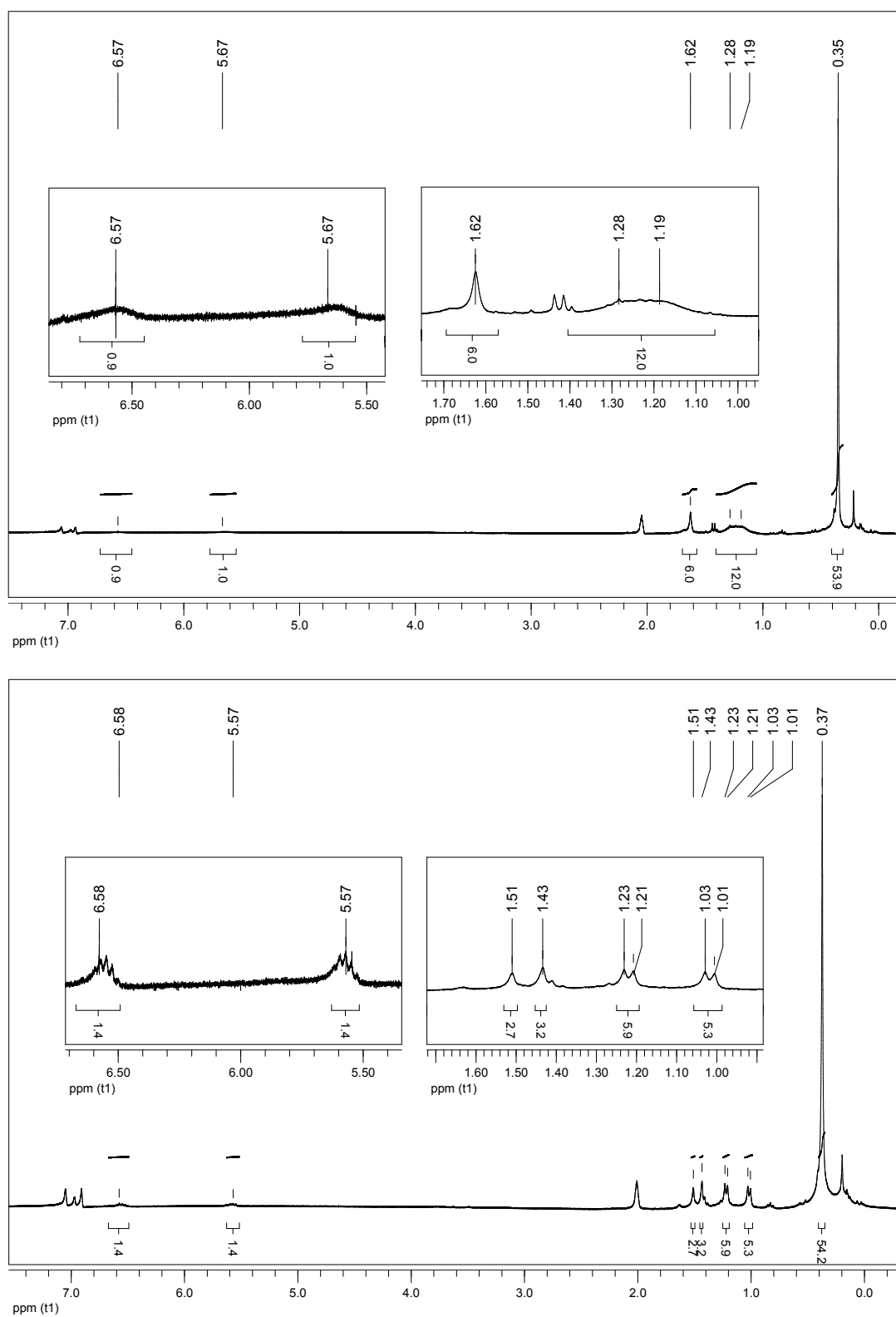


Figure 3: ^1H NMR Spectrum of **14** in toluene- d_8 at room temperature (upper panel) and at $-30\text{ }^\circ\text{C}$ (lower panel).

dimethylphenylisocyanide-stabilized germylene (**26**), which could be easily explained by the influence of the phenyl ring. The resonance of the $-\text{SiMe}_3$ group of **26** is observed at -8.3 ppm. The corresponding spectra for the *tert*-butylisocyanide stabilized germylene (**27**) shows resonances at -118.8 and -8.0 ppm. The ^{13}C NMR resonances for the NC carbon in **26** is highly deshielded (165.0 ppm) compared to the free 2,6-dimethylphenylisocyanide (142.1 ppm) [52]. The ^{29}Si NMR resonances of the trimethylphosphine adduct of bis[tris(trimethylsilyl)silyl]germylene (**18**) are observed as doublets at: -119.9 ($^2J_{\text{Si-P}}=15$ Hz) and -8.9 ($^3J_{\text{Si-P}}=11$ Hz) ppm (Figure 4). The ^{31}P NMR signal of **18** is located at -20.1 ppm.

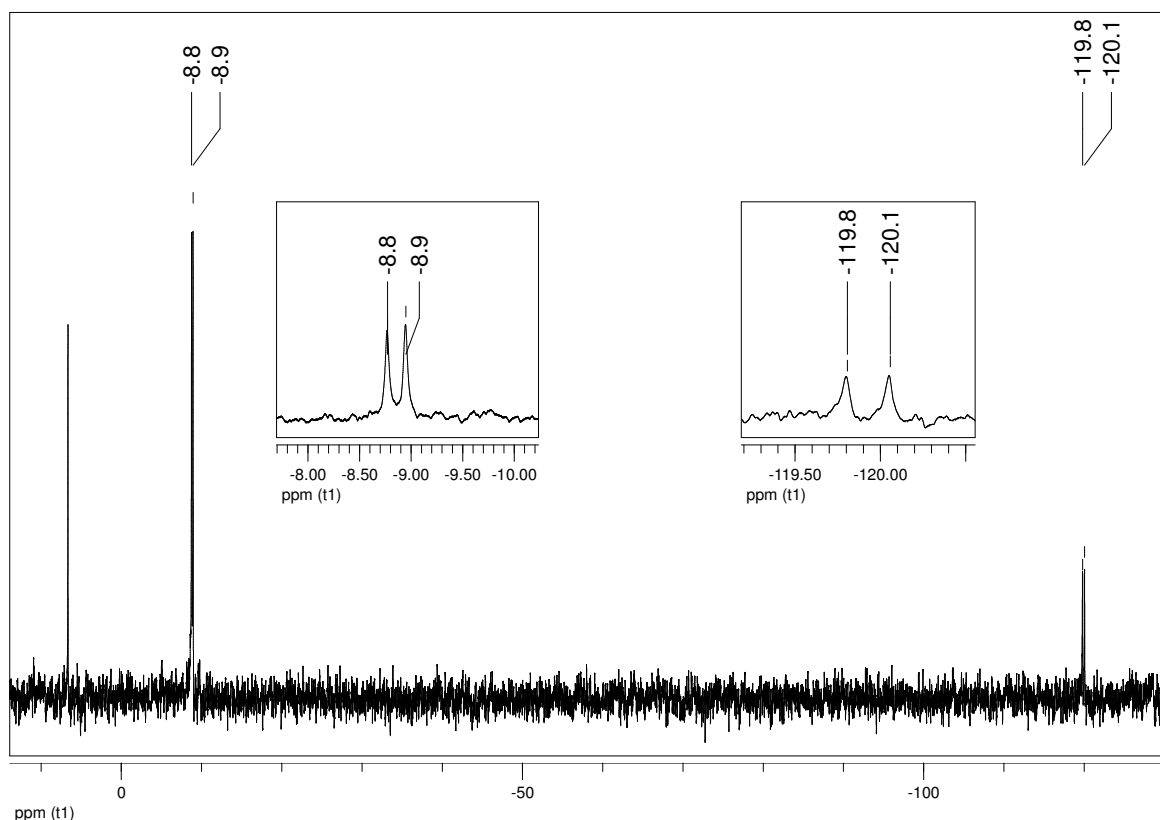


Figure 4: ^{29}Si NMR spectrum of **18**.

The slightly more deshielded ^{31}P NMR resonance of **20** (-18.2 ppm) compared to **18** (-20.1 ppm) suggests stronger interaction between the phosphine and the germanium atom in **20** than in **18**. Compound **20** shows four resonances in ^{29}Si NMR (INEPT pulse sequence) spectrum. The doublet at -125.7 ppm is assigned to the central silicon atom. Two non-equivalent trimethylsilyl groups are characterized by the doublet at -8.1 ppm and the singlet at -8.4 ppm. The doublet with very low intensity at -43.7 ppm could be assigned to the silicon atom of the silatranyl group. To confirm the location of this signal the ^{29}Si NMR s2pul pulse sequence was acquired. In the ^1H NMR spectrum all trimethylsilyl groups give one signal located at 0.64 ppm (36 H), which results from the overlapping resonances of the non-equivalent trimethylsilyl groups. The ^{13}C NMR spectrum features

two resonances originating from the TMS groups located roughly at 3.8 ppm. The differences in chemical shifts is relatively small, which supports the notion of overlapping signals in the ^1H NMR spectrum.

The product of the rearrangement of bis[bis(trimethylsilyl)silatranyl]germylene, **21**, is characterized by four singlets: resonances at -0.6 and -6.5 ppm are assigned to the trimethylsilyl group bonded to germanium and silicon atoms, respectively, the peak -53.1 ppm belongs to the silicon atom within silatranyl group and the signal at -168.6 corresponds to silicon atoms in the three-membered ring. The chemical shifts described above are similar to the resonances of hexakis(trimethylsilyl)disilagermirane (0.0 , -7.0 , -160.1 ppm), which is expected, given the similar structure of the two compounds. The presence of the two singlets (0.66 and 0.73 ppm) in the ^1H NMR spectral range, in which the protons of the trimethylsilyl group are usually observed, suggests the formation of only one isomer of **21**, i. e. the *trans* isomer. The *cis* form would give rise to two resonances corresponding to the two trimethylsilyl groups bonded to the germanium atom, which are chemically non-equivalent in this isomer. This observation is also supported by the ^{29}Si NMR spectrum, which shows only one singlet (at -0.6 ppm) for the trimethylsilyl group attached to the germanium atom. The triplets at 1.93 and 3.38 ppm result from the proton of the silatranyl group (NCH_2 and OCH_2 , respectively).

The ^{29}Si NMR resonances of the trimethylphosphine adduct of bis[tris(trimethylsilyl)germyl]germylene (**23**) is observed as doublet at -5.3 ppm. The ^{31}P NMR signal of **23** is located at -17.5 ppm.

The ^{29}Si NMR spectrum of the cyclic germylene **30** shows four resonances: two broad signals at -4.3 and -8.5 ppm represent trimethylsilyl groups, a doublet at -22.3 ppm originates from the SiMe_2 group and a doublet at -126.0 ppm is assigned to the quaternary silicon. The ^{31}P resonance of **30** is observed at -20.0 ppm.

1.2.3 Crystallography

Orange crystals of 1,3-diisopropyl-4,5-dimethylimidazol-2-ylidene adduct of bis[tris(trimethylsilyl)silyl]germylene (**14**), which precipitated from toluene solution at $-35\text{ }^{\circ}\text{C}$ were subjected to X-ray diffraction analysis (Figure 5, Table 3).

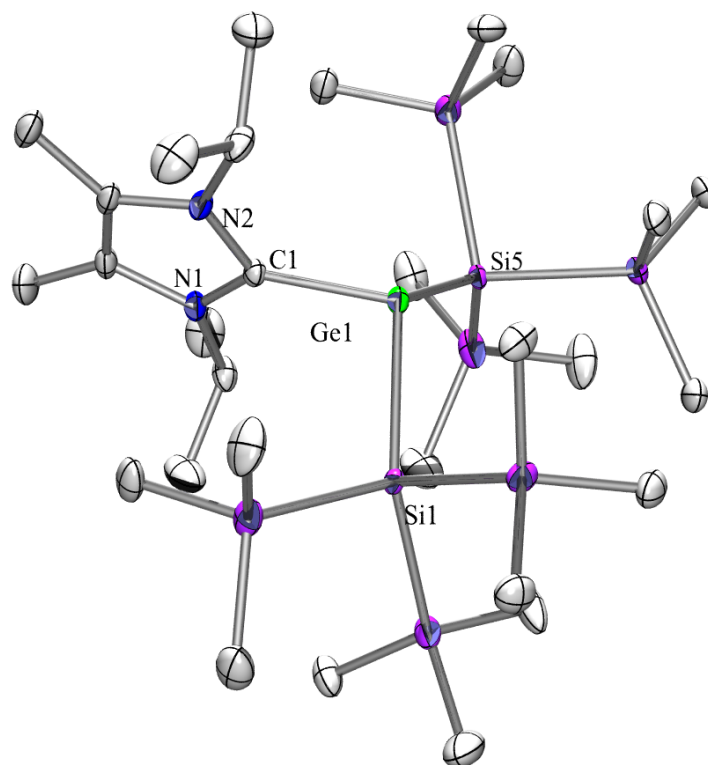


Figure 5: Crystal structure of **14**.

Table 3: Selected bond lengths and angles of **14**.

| Bond | Length [Å] | Bonds | Angle [°] |
|-------------|--------------|-------------------|-------------|
| Ge(1)–Si(1) | 2.5023(9) | Si(1)–Ge(1)–Si(5) | 117.39(2) |
| Ge(1)–Si(5) | 2.4834(8) | Si(1)–Ge(1)–C(1) | 102.36(7) |
| Ge(1)–C(1) | 2.089(2) | Si(5)–Ge(1)–C(1) | 104.69(7) |
| C(1)–N(1) | 1.357(3) | N(1)–C(1)–N(2) | 104.7(2) |
| C(1)–N(2) | 1.365(3) | N(1)–C(1)–Ge(1) | 135.66(17) |
| | | N(2)–C(1)–Ge(1) | 119.63(17) |

Compound **1**, which is analogous to **14**, was obtained earlier [37] but its structure has not been determined. The present study enables the comparison of **1** (Figure 6, Table 4) and **14** (Figure 5, Table 3) in terms of their crystal structure.

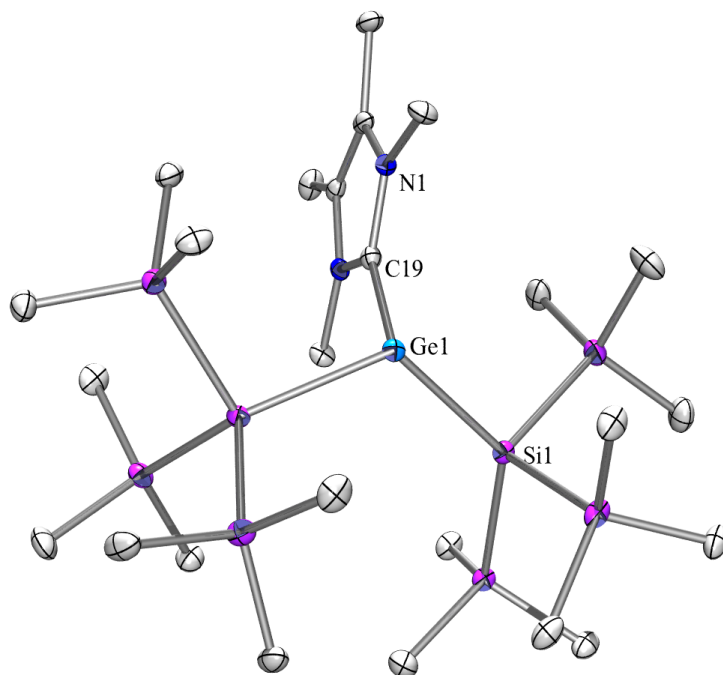


Figure 6: Crystal structure of **1**.

Table 4: Selected bond lengths and angles of **1**.

| Bond | Length [Å] | Bonds | Angle [°] |
|-------------|--------------|-------------------|-------------|
| Ge(1)–Si(1) | 2.4861(11) | C(19)–Ge(1)–Si(5) | 98.98(10) |
| Ge(1)–Si(5) | 2.4707(11) | C(19)–Ge(1)–Si(1) | 99.03(10) |
| Ge(1)–C(19) | 2.052(4) | Si(5)–Ge(1)–Si(1) | 116.61(4) |
| C(1)–N(1) | 1.355(5) | Ge(1)–C(19)–N(1) | 122.7(3) |
| C(1)–N(2) | 1.391(5) | Ge(1)–C(19)–N(2) | 133.4(3) |
| | | N(1)–C(19)–N(2) | 103.8(3) |

Due to different solvents used for crystallization, the crystal structures of the two compounds (**1** and **14**) do not belong to the same symmetry space group. **14** belongs to the monoclinic space group $P2(1)/n$, whereas **1** forms crystals of the orthorhombic space group $Pca2(1)$. In addition to two molecules of **1**, two molecules of benzene were found in the asymmetric unit. Despite these differences the corresponding bond lengths in **1** and **14** are very similar (see Table 3 and 4, respectively). Both compounds exhibit flattened pyramidal geometry at the three-coordinated germanium atom and almost planar environment around the carbene carbon atoms (sum of angles ca. 359°). The lengths of Ge(1)–C_{carbene} bonds of 2.052(4) Å in **1** and 2.089(2) Å in **14** compare well with those of Mes₂Ge·^{Me}IiPr [53] and Cl₂Ge·^{Me}IiPr [54] (2.078(3) and 2.106(3) Å, respectively).

Dark red crystals of 2,6-dimethylphenylisocyanide adduct of bis[tris(trimethylsilyl)silyl]germylene (**26**) precipitated from pentane solution within 18 hours. Crystals suitable for X-ray measurement crystallized in triclinic space group $P\bar{1}$ (Figure 7, Table 5). The distance between germanium and carbon atoms yields 1.9676(17) Å and between carbon and nitrogen yields 1.166(2) Å. The lengths of germanium–silicon bonds are a little bit shorter than in N-heterocyclic carbene analogous and amounted 2.4631(9) and 2.4527(8) Å. The angle between Si–Ge–Si atoms yields 116.61(4)° is approximately 4° bigger than in the N-heterocyclic adducts **1** and **14**.

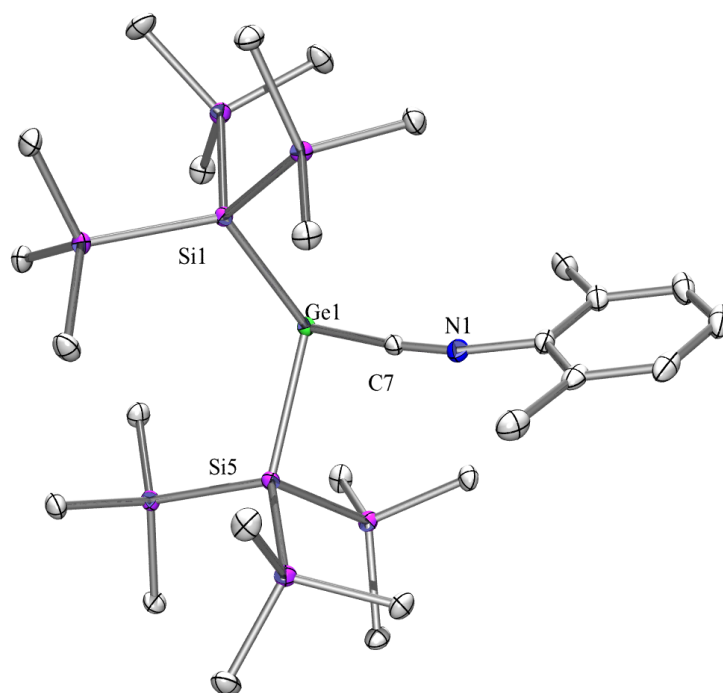


Figure 7: Crystal structure of **26**.

Table 5: Selected bond lengths and angles of **26**.

| Bond | Length [Å] | Bonds | Angle [°] |
|-------------|--------------|-------------------|-------------|
| Ge(1)–Si(1) | 2.4631(9) | Si(1)–Ge(1)–Si(5) | 121.94(3) |
| Ge(1)–Si(5) | 2.4527(8) | Si(1)–Ge(1)–C(7) | 96.83(5) |
| Ge(1)–C(7) | 1.9676(17) | Si(5)–Ge(1)–C(7) | 92.43(5) |
| C(7)–N(1) | 1.166(2) | Ge(1)–C(7)–N(2) | 167.76(14) |

The *tert*-butylisocyanide adduct of bis[tris(trimethylsilyl)silyl]germylene (**27**) forms orange crystals, which belong to the monoclinic space group P2(1)/n (Figure 8, Table 6). The silicon - germanium bonds are slightly longer than in the 2,6-dimethylphenylisocyanide adduct **26** and yield 2.4739(11) and 2.4504(11) Å. The angle Si–Ge–Si yields 119.31(4)°. The length of Ge–C bond is slightly longer than in **26** (2.006 Å in **27**, 1.9676(17) Å in **26**), however the C–N bond is shorter compared to corresponding bond in **26** (2.149(4) Å in **27**, 1.166(2) Å in **26**).

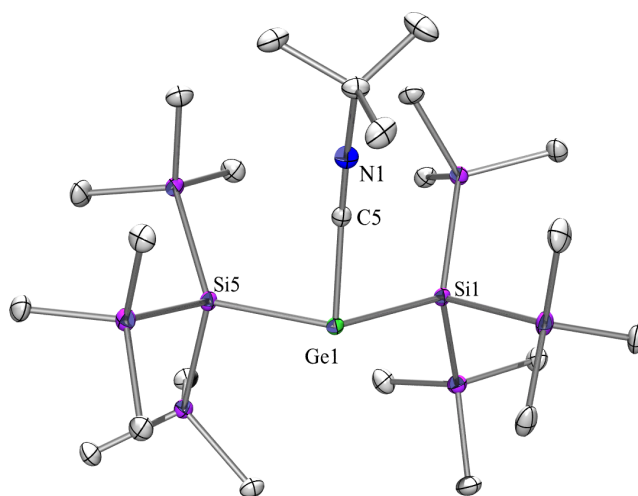


Figure 8: Crystal structure of **27**.

Table 6: Selected bond lengths and angles of **27**.

| Bond | Length [Å] | Bonds | Angle [°] |
|-------------|--------------|-------------------|-------------|
| Ge(1)–Si(1) | 2.4739(11) | Si(1)–Ge(1)–Si(5) | 119.31(4) |
| Ge(1)–Si(5) | 2.4504(11) | Si(1)–Ge(1)–C(5) | 93.78(8) |
| Ge(1)–C(5) | 2.006(3) | Si(5)–Ge(1)–C(5) | 93.78(8) |
| C(5)–N(1) | 1.149(4) | Ge(1)–C(5)–N(2) | 169.9(3) |

28 crystallized in the monoclinic space group P2(1). The Ge–Si bonds are slightly shorter than for a silylated germynes, what is characteristic for tetracoordinated germanium atom. The Si–Ge–Si angle (137.59(6) Å) is much larger than for the germynes described above (116.61(4)–121.94(3) Å). The distance between Ge and CN group (2.021(8) Å) is the longest of all known Ge–CN bond lengths in tetracoordinated germanium compounds (1.94(2) and 1.98(2) Å in (CH₃)₂Ge(CN)₂ [55]; 1.975 and 1.944 Å in Mes₂(CN)₂ [56]; 1.947 Å in diarylgermanium hydride/cyanide species Ar₂GeH CN; Ar = C₆H₃-2,6-(C₆H₂-2,4,6-(CH₃)₃)₂ [57]).

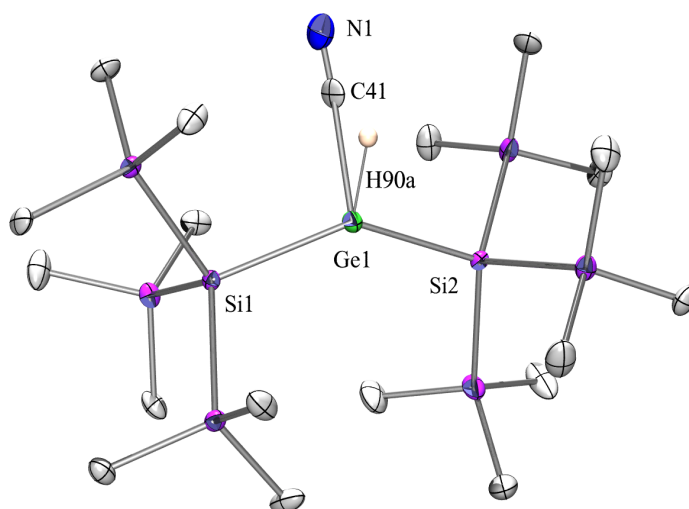


Figure 9: Crystal structure of **28**.

Table 7: Selected bond lengths and angles of **28**.

| Bond | Length [Å] | Bonds | Angle [°] |
|-------------|--------------|-------------------|-------------|
| Ge(1)–Si(1) | 2.4048(17) | Si(1)–Ge(1)–Si(2) | 137.59(6) |
| Ge(1)–Si(2) | 2.4231(18) | C(41)–Ge(1)–Si(1) | 102.6(2) |
| Ge(1)–C(41) | 2.021(8) | C(41)–Ge(1)–Si(2) | 105.46(18) |
| C(41)–N(1) | 1.029(9) | Ge(1)–C(41)–N(1) | 174.8(8) |

29 crystallized in the cubic space group $Pa\bar{3}$ (Figure 10, Table 8). The length of Si–CN bond (1.885(2) Å) is within expected ranges (1.873–1.905 Å) [55, 58, 59]

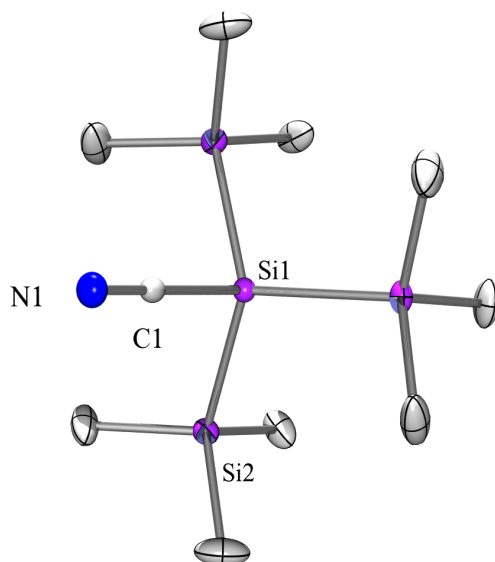


Figure 10: Crystal structure of **29**.

Table 8: Selected bond lengths and angles of **29**.

| Bond | Length [Å] | Bonds | Angle [°] |
|------------|--------------|-----------------|-------------|
| Si(1)–C(1) | 1.885(2) | Si(1)–C(1)–N(1) | 180.0(3) |
| C(1)–N(1) | 1.143(3) | | |

Crystalline **30** (Figure 11, Table 9) has the symmetry of the monoclinic space group $C2/c$. The structure of **30** features the five-membered ring in an envelope conformation with one of the $\text{Si}(\text{SiMe}_3)_2$ unit on the flap. The distance between the germanium (Ge1) and the phosphorus atom (P1) is similar to the analogous distance in **7** and yields approximately 2.35 Å.

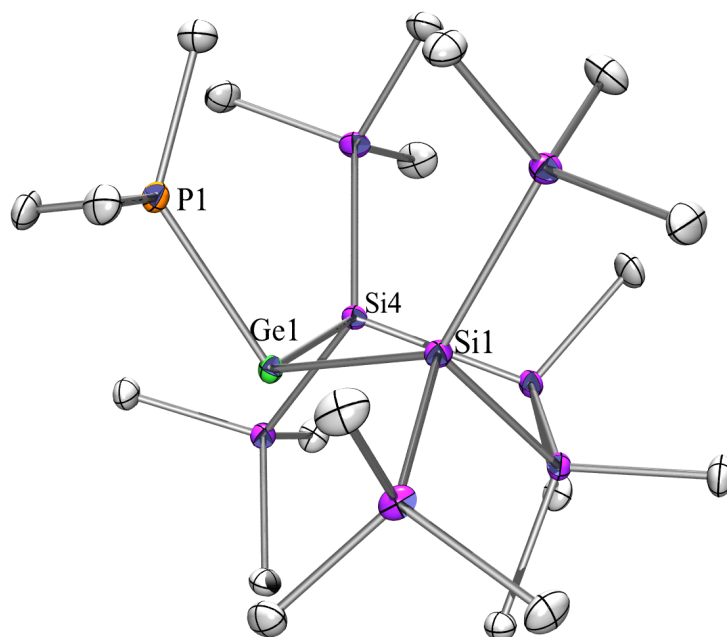


Figure 11: Crystal structure of **30**.

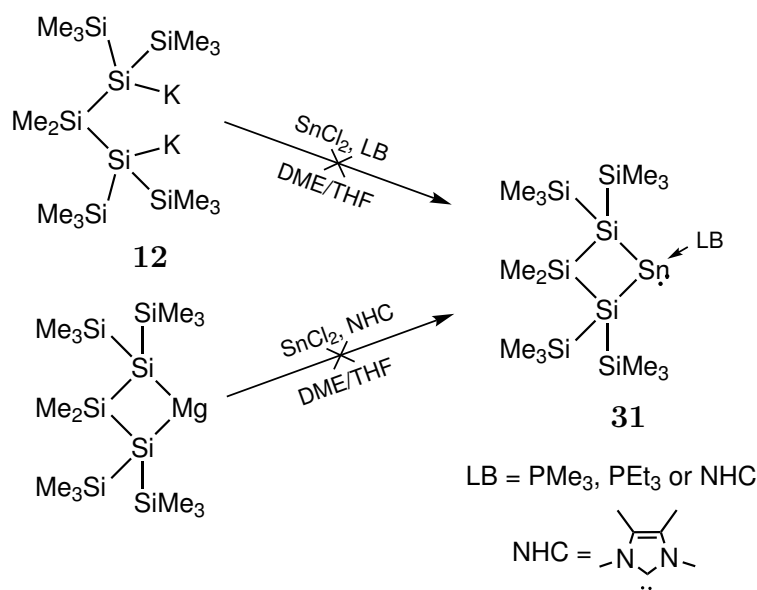
Table 9: Selected bond lengths and angles of **30**.

| Bond | Length [Å] | Bonds | Angle [°] |
|-------------|--------------|-------------------|-------------|
| Ge(1)–Si(1) | 2.4533(6) | Si(1)–Ge(1)–Si(4) | 102.70(2) |
| Ge(1)–Si(4) | 2.4589(5) | Si(1)–Ge(1)–P(1) | 102.163(19) |
| Ge(1)–P(1) | 2.3484(6) | Si(4)–Ge(1)–P(1) | 105.239(18) |
| Si(1)–Si(2) | 2.3504(6) | Ge(1)–Si(1)–Si(2) | 94.89(2) |
| Si(2)–Si(3) | 2.3421(6) | Si(3)–Si(4)–Ge(1) | 103.49(2) |
| Si(3)–Si(4) | 2.3605(7) | Si(1)–Si(2)–Si(3) | 107.26(2) |
| | | Si(2)–Si(3)–Si(4) | 104.88(2) |

1.3 Oligosilastannylenes

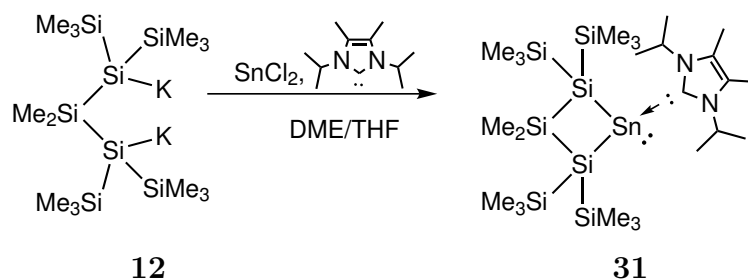
1.3.1 Synthesis

Reaction of 1,3-dipotassio-1,1,3,3-tetrakis(trimethylsilyl)dimethyltrisilane (**12**) with SnCl_2 in the presence of various Lewis bases (trimethylphosphine, triethylphosphine and 1,3,4,5-tetramethylimidazol-2-ylidene) was attempted, but did not lead to the formation of the expected stannylene (**31**). Moreover, replacing potassium with magnesium in the anionic reactant and using mild reaction conditions (slow dropping of the reactant into stirred solution of the substrate at $-35\text{ }^\circ\text{C}$) did not lead to the expected result either (Scheme 24).



Scheme 24: Unsuccessful attempts to synthesize **31**.

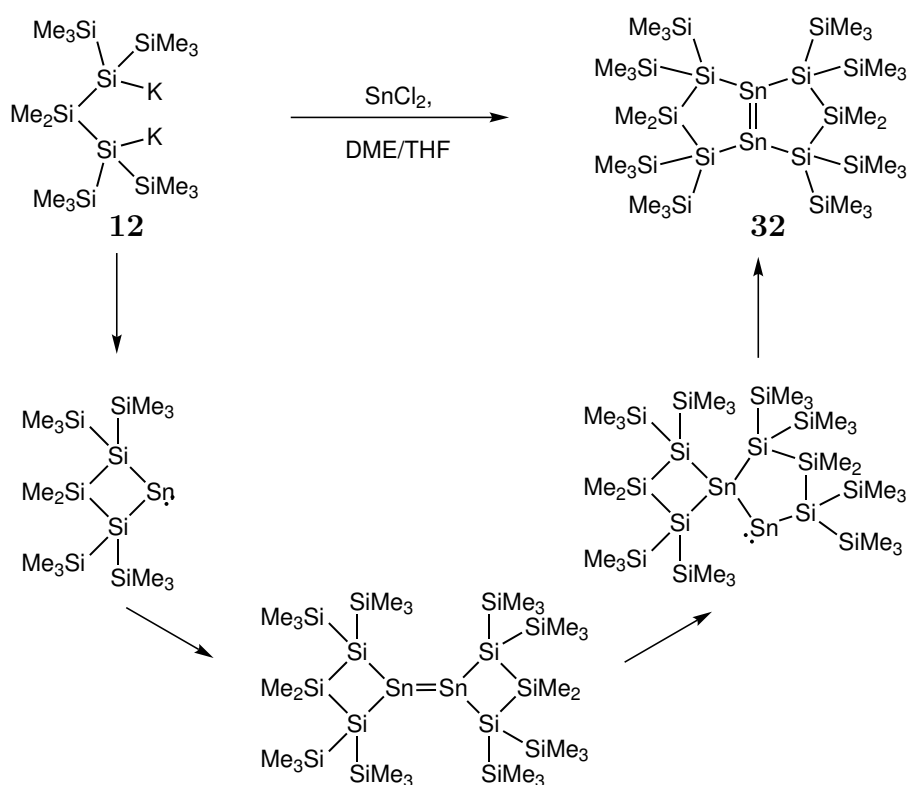
It was merely the use of 1,3-diisopropyl-4,5-dimethylimidazol-2-ylidene as a Lewis base that eventually worked and stannylene **31** was synthesized at $-35\text{ }^\circ\text{C}$ with almost 85 % yield (Scheme 25).



Scheme 25: Successful attempt to synthesize **31**.

Distannene **32** was obtained in the reaction of 1,3-dipotassio-1,1,3,3-tetrakis(trimethylsilyl)dimethyltrisilane (**12**) with tin dichloride in the presence of triethylphosphine and was

crystallized from pentane. **32** was also synthesized in the reaction of **12** with tin chloride at room temperature without phosphine. It suggests that the Lewis base did not contribute to the formation of distannene **32**. UV adsorption spectrum of **32** exhibit hypsochromic shift at 558 nm compared to the shifts of larger distannene **10** of 626 nm [43] and Sekiguchi's distannene (*t*Bu₂ Me Si)₂Sn Sn(Si Me *t*Bu₂) of 670 nm.

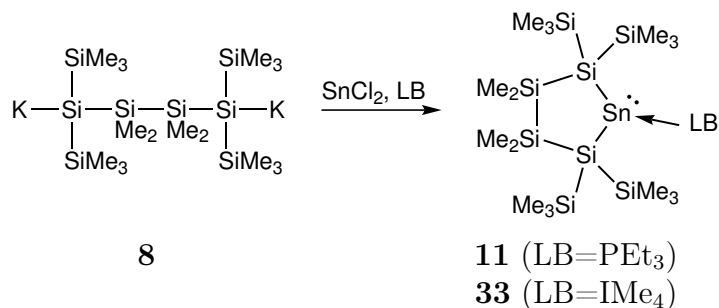


Scheme 26: Proposed mechanism of the formation of **32**.

The mechanism of formation of distannene **32** was proposed based on the dimerization of an analogous molecule [43] (Scheme 26). The first step of the reaction is the formation of a stannylene, which dimerizes and rearranges *via* stannylstannylene to the endocyclic distannene **32**. A similar dimerization process *via* double 1,2-silyl migration, which resulted in the formation of a bicyclic disilene, was reported by Kira and coworkers in 2005 [60].

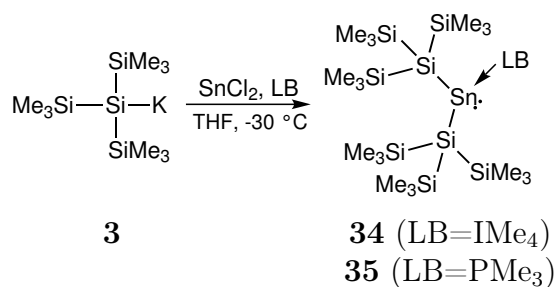
As mentioned before, the four-membered ring stannylene can be stabilized only with a bulky N-heterocyclic carbene. In contrast, the five-membered ring stannylene can be stabilized by both phosphine and N-heterocyclic carbene (Scheme 27). Triethylphosphine adduct of cyclic stannylene **11** was synthesized before by Arp *et al.* [43]. An N-heterocyclic carbene adduct (**33**) was synthesized in this work in the reaction of **8** with tin chloride in the presence of 1,3,4,5-tetramethylimidazol-2-ylidene (Scheme 27). In the ²⁹Si NMR spectrum of **33** two different resonances for SiMe₃ group were observed (−7.1 and −5.1 ppm), what indicates configurational stability at tin center. A similar feature was observed for the PEt₃ adduct of five-membered ring stannylene **11** [43], however in corresponding

germylene phosphine adducts (**7** [38] and **30**) as well as N-heterocyclic carbene adduct [38] configurational stability of the germanium center was not observed.



Scheme 27: Synthesis of five-membered ring cyclic stannylene base adduct **11** [43] and **33**.

Reaction of tris(trimethylsilyl)silyl potassium (**3**) with tin dichloride in the presence of a Lewis base such as 1,3,4,5-tetramethylimidazol-2-ylidene or trimethylphosphine led to the formation of stannylenes **34** and **35** respectively (Scheme 28).



Scheme 28: Synthesis of acyclic stannylene base adducts **34** and **35**.

1.3.2 NMR Spectroscopy

The ^{29}Si NMR spectrum of the four-membered ring NHC-carbene adduct **31** shows four resonances. In the spectrum of four-membered ring stannylene **31** two signals originating from trimethylsilyl groups are observed at -6.5 and -10.3 ppm, what suggests configurational stability of the tin center, in contrast to the corresponding four-membered ring germylene [61]. The resonance of a quaternary silicon (-121.3 ppm) is about 17 ppm up-field shifted contrary to the corresponding signal of four-membered ring germylene (-103.5 ppm). The peak originated from SiMe_2 group within the four-membered ring is located at -15.0 ppm, what is typical for this group. The tin atom is represented in ^{119}Sn NMR spectrum by a resonance at -272.9 ppm.

Distannene **32** exhibits the ^{119}Sn NMR shift of 730.7 ppm, which is down-field shifted compared to the various distannenes [43, 62]. All three signals at -93.6 , -8.4 and -2.0 ppm in the ^{29}Si NMR spectrum of **32** are in the expected spectral region according to the corresponding **13** [44] and fit perfectly to distannene **32**.

The ^{29}Si NMR spectrum of N-heterocyclic carbene adduct of five-membered ring stannylene **33** shows four resonances located at -5.1 , -7.1 , -15.9 and -136.5 ppm. Similar to the case of four-membered ring stannylene **31** the hindering of the Sn-carbene bond rotation can be ruled out based on ^1H NMR and ^{13}C NMR spectra.

The ^{29}Si NMR spectrum of **34** shows two resonances located at -7.2 and -136.5 ppm. The signal of the quaternary silicon of the tris(trimethylsilyl)silyl group in the trimethylphosphine adduct of the acyclic stannylene **35** is down-field shifted by about 10 ppm with respect to NHC analog **34** and yields -126.8 ppm. The silicon atoms involved in the TMS groups of **35** are represented in the ^{29}Si NMR spectrum by the signal at -7.4 ppm. The resonances of the trimethylphosphine adduct **35** are very similar to these reported by Arp *et al.* for triethylphosphine adduct which yield -7.0 and -127.6 ppm [63]. Similar to the NHC adducts of germylene **1** and **2**, the NHC-carbene of **34** does not rotate based on ^1H NMR and ^{13}C NMR spectra. The ^{31}P NMR spectrum of **35** shows a broad peak located at -61.7 ppm, which suggests a very weak interaction between phosphorus and tin atoms (the chemical shift of a non-bonded phosphine yields -62 ppm). The ^{119}Sn NMR reveals unusually up-field shifted broaden doublet located at -43.5 ppm with huge $^1J_{\text{Sn-P}}$ coupling constant of 2060 Hz. In the ^{119}Sn NMR spectrum acquired at -30°C with toluene- d_8 as a deuterated solvent the tin resonances is observed at -89.9 ppm (upper panel on Scheme 12). The huge coupling constants were also observed in the ^{31}P NMR spectrum recorded at low temperature, in which the broaden $^{117/119}\text{Sn}$ satellite signals are observed (lower panel on Scheme 12) with very large $^1J_{\text{P-117/119Sn}}$ coupling of 1980/1896 Hz.

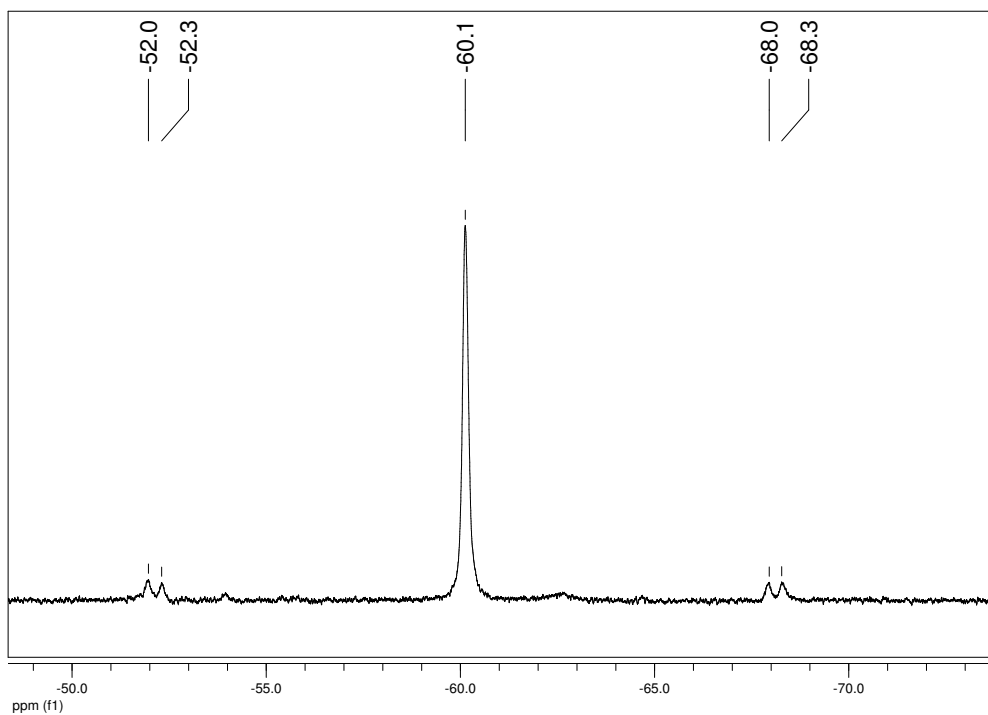
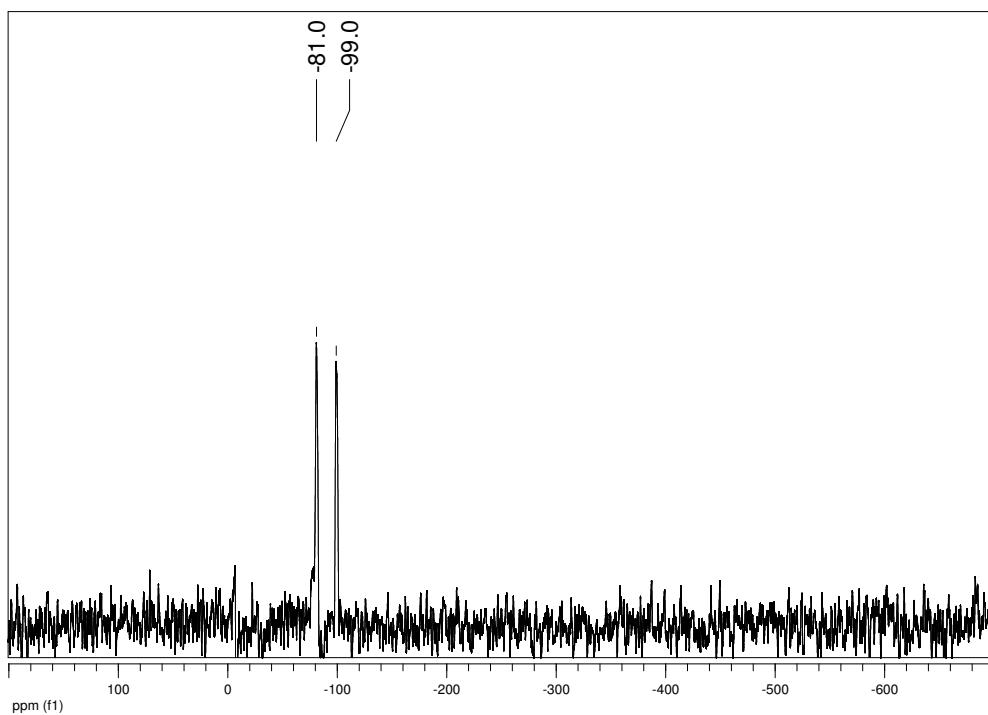


Figure 12: The ^{119}Sn NMR (upper panel) and ^{31}P NMR (lower panel) spectra of PMe_3 adduct of bis[tris(trimethylsilyl)silyl]stannylene (**35**) acquired at $-30\text{ }^\circ\text{C}$.

1.3.3 Crystallography

Crystal structure analysis of **31** reveals disordering of the silyl group attached to the Si(1) atom. Compound **31** crystallized in monoclinic space group P2(1)/n (Figure 13, Table 10). The Si–Sn–Si angle of $80.97(11)^\circ$ is smaller than for the corresponding germylene with angle of $86.88(2)^\circ$ [37]. The endocyclic Si–Si–Si angle is considerably larger ($95.42(17)^\circ$) than Si–Sn–Si angle, and the Sn–Si–Si angle are almost equal to 90° ($89.99(14)^\circ$ and $90.58(16)^\circ$), compared to the regular square. It goes along with Sn–Si bond distances of $2.669(4)$ and $2.680(4)$ Å, compared to the silicon–silicon bond length within the ring of $2.340(5)$ and $2.355(5)$ Å.

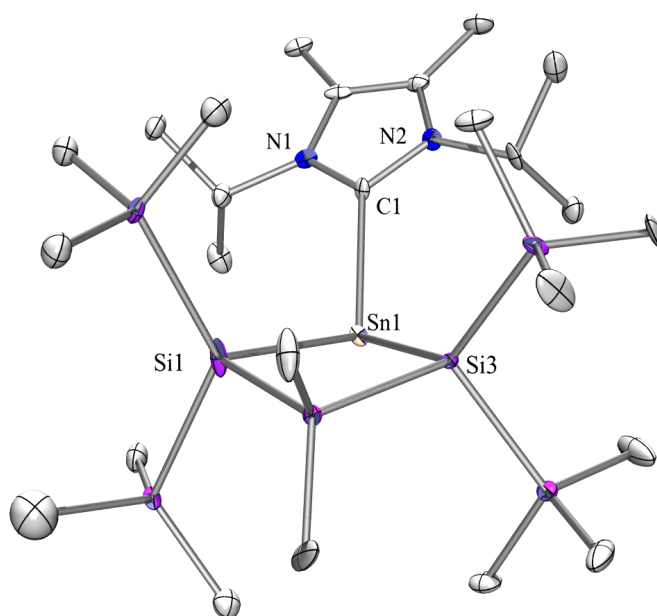


Figure 13: Crystal structure of **31**.

Table 10: Selected bond lengths and angles of **31**.

| Bond | Length [Å] | Bonds | Angle [°] |
|-------------|--------------|-------------------|-------------|
| Sn(1)–Si(1) | 2.669(4) | Si(1)–Sn(1)–Si(3) | 80.97(11) |
| Si(3)–Sn(1) | 2.680(4) | Si(1)–Sn(1)–C(1) | 109.0(3) |
| Sn(1)–C(1) | 2.295(13) | Si(3)–Sn(1)–C(1) | 112.7(3) |
| Si(1)–Si(2) | 2.340(5) | Si(1)–Si(2)–Si(3) | 95.42(17) |
| Si(2)–Si(3) | 2.355(5) | | |

A dark violet crystal of **32** was measured using X-ray technique. Crystalline **32** has the symmetry of monoclinic space group P2(1)/n. It features slightly shorter tin–tin bond of 2.6171(14) Å compared to 2.69 Å observed for distannene **10** [43] and 2.67 Å for Sekiguchi’s acyclic tetrasilylated distannene (*t*Bu₂MeSi)₂=Sn(Si*t*Bu₂Me)₂ [64, 65]. The tin–silicon bond **32** (2.564(2) Å) is shorter than in **31** (2.669(4) and 2.680(4)Å). The sum of bond angles around the tricoordinated tin atom (352.66°) indicates a pyramidalization of the Sn center.

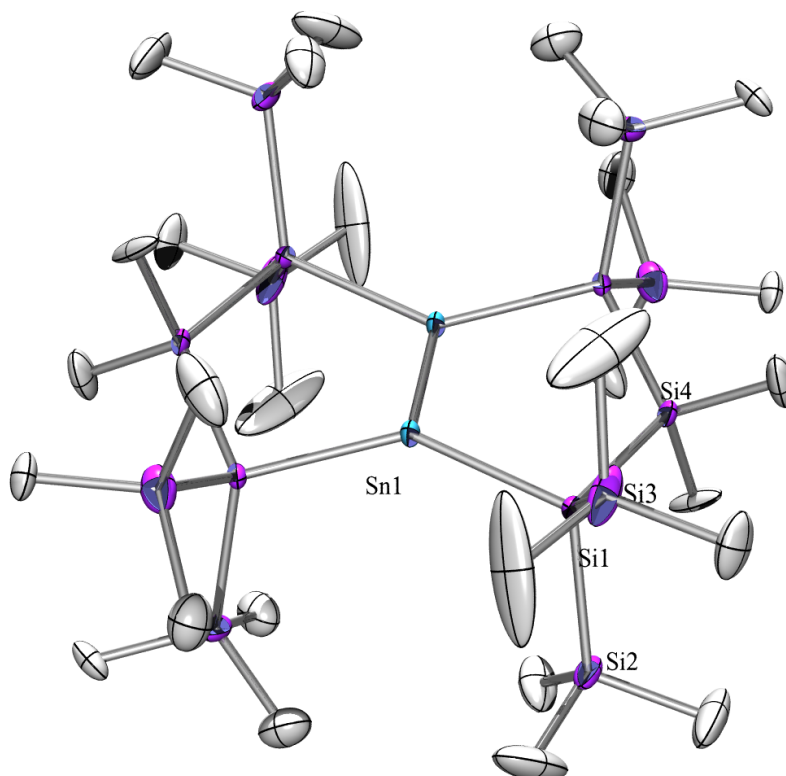


Figure 14: Crystal structure of **32**.

Table 11: Selected bond lengths and angles of **32**.

| Bond | Length [Å] | Bonds | Angle [°] |
|---------------|--------------|-------------------|-------------|
| Sn(1)–Si(1) | 2.564(2) | Sn(1)–Si(1)–Si(2) | 113.90(12) |
| Si(1)–Si(2) | 2.346(4) | Sn(1)–Si(1)–Si(3) | 107.65(13) |
| Si(1)–Si(3) | 2.318(4) | Sn(1)–Si(1)–Si(4) | 102.01(12) |
| Si(1)–Si(4) | 2.441(4) | Si(2)–Si(1)–Si(3) | 110.63(17) |
| Sn(1)–Sn(1)#1 | 2.6171(14) | Si(3)–Si(1)–Si(4) | 117.77(18) |
| | | Si(2)–Si(1)–Si(4) | 104.83(16) |

An orange crystal of **33** was subjected to X-ray diffraction analysis (Figure 15, Table 12). Crystalline **33** has the symmetry of monoclinic space group $P2(1)/c$. The length of the Sn–C bond is roughly equal to such bond in the corresponding NHC adduct of four-membered ring stannylene **31** and yields 2.295(13) Å. Stannylene **33** as well as stannylene **31** exhibit slightly elongated Sn–Si bond contrary to distannene **32**, however the difference is much smaller than for the corresponding germylene and digermene [37, 44].

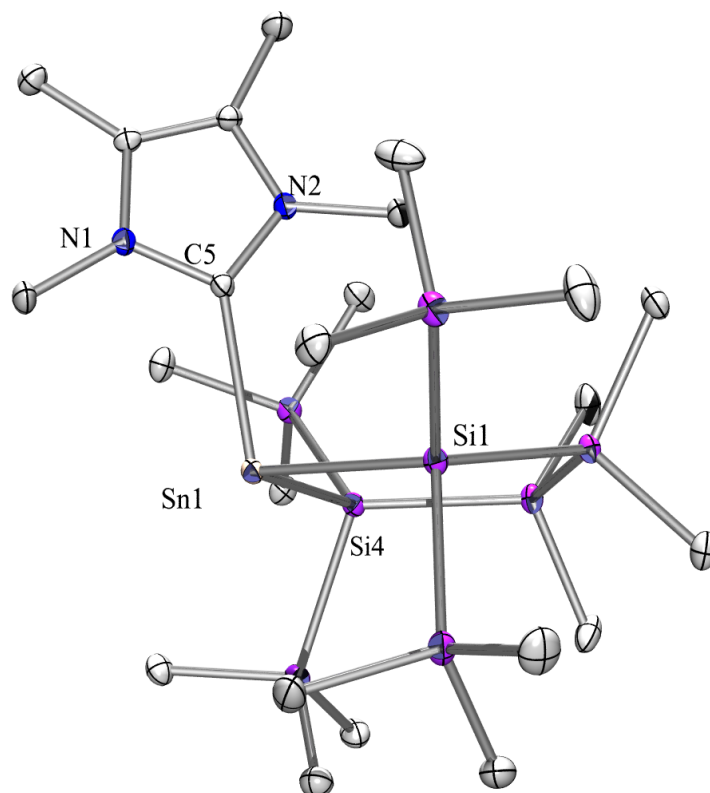


Figure 15: Crystal structure of **33**.

Table 12: Selected bond lengths and angles of **33**.

| Bond | Length [Å] | Bonds | Angle [°] |
|-------------|--------------|-------------------|-------------|
| Sn(1)–Si(1) | 2.6639(9) | Si(1)–Sn(1)–Si(4) | 94.14(3) |
| Si(4)–Sn(1) | 2.6639(9) | Si(4)–Sn(1)–C(5) | 93.39(7) |
| Sn(1)–C(5) | 2.295(2) | Si(1)–Sn(1)–C(5) | 102.09(7) |

Yellow crystals of **34** and **35** were subjected to X-ray study (Figure 16, Table 13 and Figure 17, Table 14, respectively). The distance between Sn and C atoms in **34** yields 2.287 Å and is almost the same like in the NHC adducts of cyclic stannylene **31** (2.295(13) Å) and **33** (2.295(2) Å). The Si–Sn–Si angle of **34** and **35** (115.92(3)° and 117.53(6)°) is slightly smaller than analogous angle of bis(trimethylsilyl) distannene (120.46(4)°)[31].

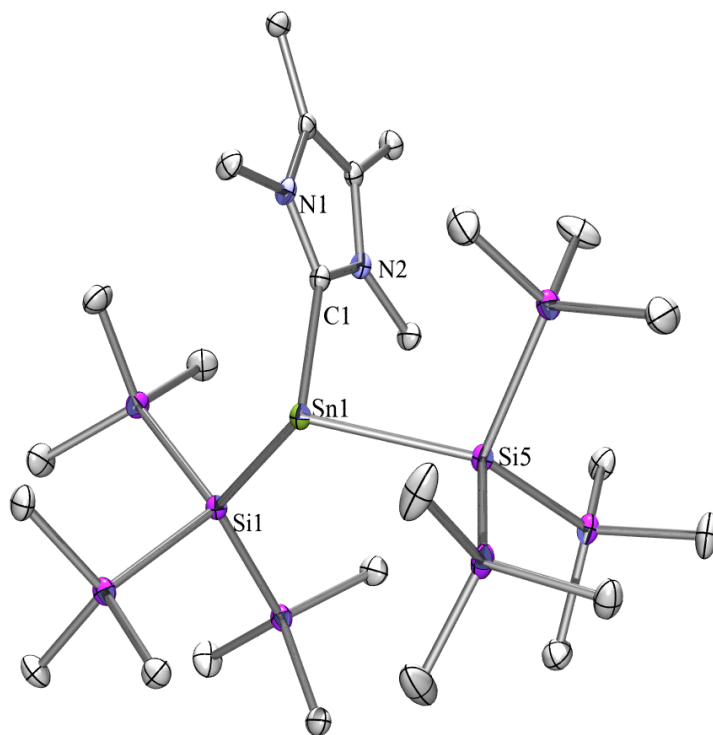


Figure 16: Crystal structure of **34**.

Table 13: Selected bond lengths and angles of **34**.

| Bond | Length [Å] | Bonds | Angle [°] |
|-------------|--------------|-------------------|-------------|
| Sn(1)–C(1) | 2.287(3) | C(1)–Sn(1)–Si(1) | 94.68(9) |
| Sn(1)–Si(1) | 2.6796(11) | C(1)–Sn(1)–Si(5) | 96.04(9) |
| Sn(1)–Si(5) | 2.6918(11) | Si(1)–Sn(1)–Si(5) | 115.92(3) |

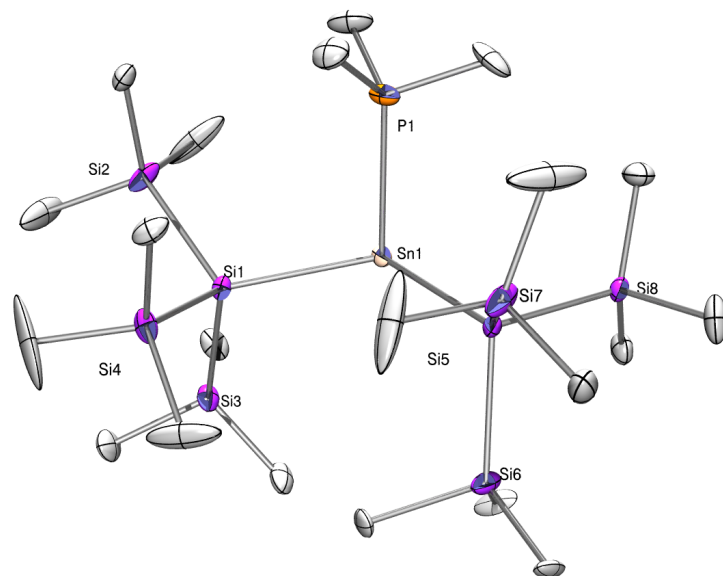


Figure 17: Crystal structure of **35**.

Table 14: Selected bond lengths and angles of **35**.

| Bond | Length [Å] | Bonds | Angle [°] |
|-------------|--------------|-------------------|-------------|
| Sn(1)–C(1) | 2.618(2) | P(1)–Sn(1)–Si(1) | 97.51(7) |
| Sn(1)–Si(1) | 2.6864(17) | P(1)–Sn(1)–Si(5) | 95.86(7) |
| Sn(1)–Si(5) | 2.698(2) | Si(1)–Sn(1)–Si(5) | 117.53(6) |

1.4 Conclusions

Base adducts of disilylated germylenes and stannylenes were obtained in reactions of the corresponding oligosilanyl anions with halogermynes or halostannylenes ($\text{GeCl}_2 \cdot \text{dioxane}$, $\text{GeBr}_2 \cdot \text{dioxane}$ or SnCl_2) in the presence of suitable Lewis bases. Coordination strength of the Lewis base and steric hindrance of the low valent germanium center have influence on the stability of the tetrylene adduct. However, the formation of a strong donor–acceptor complex does not allow for the use of this adduct in further reactions. The phosphine adduct of tris(trimethylsilyl)silyl germylene (**18**) was found to be well suited for investigations into the chemical reactivity of silylated germylenes, due to the very facile interaction between the phosphine and the germylene. Such an interaction enables the release of a free germylene under mild conditions. Relatively short life time of **18** (hours) compared to that of NHC analogs (years) does not allow for its storage and enforces the preparation *in situ*, which is feasible because the formation of the germylene PMe_3 adduct is very clean and **18** can be used without purification. The trimethylphosphine adduct of germylene substituted with two bis(trimethylsilyl)silatranyl groups (**20**) is more stable than the bis(trimethylsilyl)silyl substituted analog (**18**), however, after applying vacuum **20** lost the PMe_3 group and rearranged to disilagermyrane **21**. For the stabilization of bis[(trimethylsilyl)silyl]stannylene PMe_3 is sufficient.

All synthesized compounds were characterized using multinuclear NMR spectroscopy. The ^{29}Si NMR, ^1H NMR, ^{13}C NMR, ^{31}P NMR and ^{119}Sn NMR chemical shifts of base adducts of germylene and stannylene were found within the expected spectral ranges of this type of compound. The ^{13}C NMR spectra of the N-heterocyclic carbene stabilized germylenes and stannylenes exhibit significantly upfield-shifted resonances for carbenic carbons (170–175 ppm) in comparison to that of the free carbene (205.89 ppm for $^{\text{Me}}\text{LiPr}$ and 212.70 ppm for IMe_4) [66], which is indicative of carbene coordination [53] as well as Lewis acidity of tetrylenes. The ^{31}P NMR spectra of the phosphine-stabilized tetrylenes show resonances that are down-field shifted by about 40 ppm relative to the free phosphine, with the exception of PMe_3 adduct of bis[(trimethylsilyl)silyl]stannylene (**35**) where PMe_3 resonance is broadened and has almost the same chemical shift as the free germylene. This feature suggests weak interaction between the stannylene and the phosphine in this case. The hindering of the NHC-carbene rotation is not observed in monosilylated compounds **5** [33] and **16**, however, disilylated germylenes **1** and **2** show such hindering. For stannylenes, the rotation hindering in the solution is observed for bis[(trimethylsilyl)silyl]stannylene \cdot NHC **34**, whereas in cyclic stannylenes **31** and **33** such hindering is not observed.

Crystal structures were determined for most of the obtained compounds. Synthesized products exhibit typical bond lengths and angles. Our crystallographic data is in good agreement with the previous results of Baines [67] as well as Castel [33], which demonstrate that substitution of the chloride atom with the $\text{E}((\text{Me}_3\text{Si})_3)_3$ group has negligible influence on the length of $\text{M}^{\text{II}}\text{-C}_{\text{carbene}}$ bonds, despite the very different electronic effect.

2 Reactivity of tetrylenes

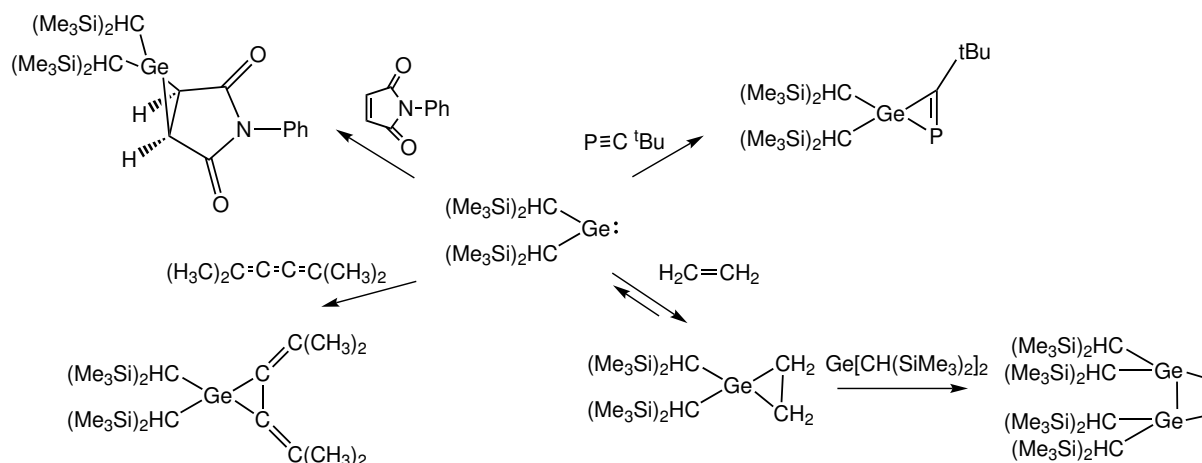
2.1 Introduction

As mentioned above heavy tetrylenes are very reactive species. Due to the large variety of available ligands they can form very unique systems. However, not only the substituents influence their reactivity. Germylenes and stannylenes in general are less reactive than silylenes due to the larger energy gap between s- and p-orbitals of germanium and tin, respectively. Despite of this fact, they are able to dimerize or polymerize, activate small molecules, insert into the σ bond of organic and inorganic compounds, add to unsaturated systems such as alkenes, alkynes, conjugated dienes, etc, participate in redox chemistry, form donor-acceptor Lewis adducts and react with transition metal complexes. The examples of the latter type of reactions will be presented in Section 3. Due to the large number of known germylene and stannylene reactions they will be discussed mainly using Lappert's germylene. Historically, $\text{Ge}[\text{CH}(\text{SiMe}_3)_2]_2$ is the first stable germylene ever obtained. It occurs in solution as a monomer, and since its discovery in 1976 a lot of research was devoted to the chemistry of this important compound. Its structure is pretty simple and contains neither extremely bulky substituents nor heteroatoms, which could be involved in the stabilization of intermediates. There is no systematic study of the reactivity of disilylated germylenes available, thus Lappert's germylene seems to be the closest structural analog of the compounds discussed in this work.

2.1.1 Addition to unsaturated systems

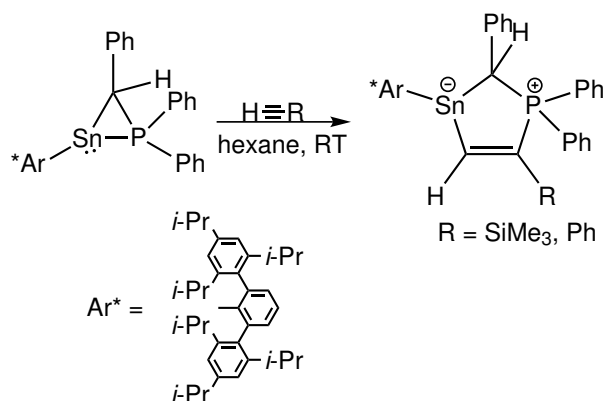
The reaction of tetrylenes with unsaturated organic compounds, such as alkenes and alkynes, results in the [1+2] cycloaddition and the formation of metalliranes and metallirenes (Scheme 29). For example, treatment of $\text{Ge}[\text{CH}(\text{SiMe}_3)_2]_2$ with N-phenylmaleimide and 2,5-dimethyl-2,3,4-hexatriene led to the formation of the [1+2]-cycloadducts [68]. This reaction proceeded not only with typical alkenes and alkynes, but also with phosphalkyne derivatives. On the early stage of investigations, $\text{Ge}[\text{CH}(\text{SiMe}_3)_2]_2$ was reacted with ${}^t\text{BuC}\equiv\text{P}$ and formed the first phosphagermyrene [69] (Scheme 29). However, the addition of alkene/alkyne can result in high energy products, which will react further to form more stable products. Good example illustrating this type of reaction is the treatment of Lappert's germylene with ethylene, which resulted in the formation of colorless crystals of 1,2-digermacyclobutane [70]. The first step was the formation of germacyclopropane, a typical product of this reaction, which was in this case in equilibrium with starting materials. Then, the insertion of the second molecule of $\text{Ge}[\text{CH}(\text{SiMe}_3)_2]_2$ germylene into Ge-C bond of germacyclopropane occurred.

More complex systems, which contain heteroatoms, are able to react with alkynes in a different way. A stannylene containing the three-membered ring composed of Sn, P and C atoms, treated with phenylacetylene or trimethylsilylacetylene formed phosphastannacyclopentenes [71] (Scheme 30). This reaction was repeated for diarylstannylene containing four- and five-membered rings (Sn-P-C-C and Sn-P-C-C-C , respectively) [72]. The four-



Scheme 29: Addition of Lappert's germylene to unsaturated systems.

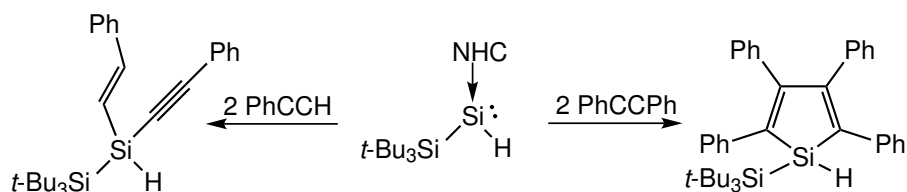
membered ring diarylstannylene reacted regioselectively with phenylacetylene at room temperature within 13 days to give six-membered ring, whereas five-membered ring did not react with PhCCH at all.



Scheme 30: Formation of phosphastannacyclopentenes.

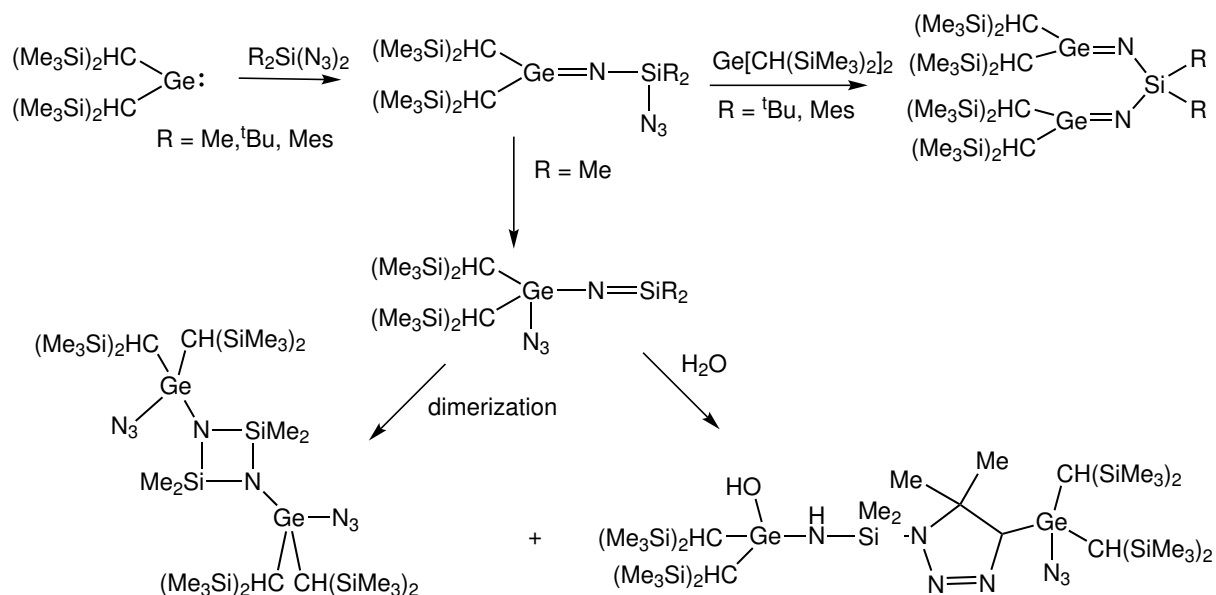
In the case of the reaction of terminal acetylenes not only cycloaddition is possible. Most recently Inoue and coworkers studied experimentally and theoretically the reactivity of the N-heterocyclic carbene stabilized silylene monohydride with acetylenes [73]. The reaction pathway depends on the alkyne species. Treatment of silylene $t\text{Bu}_3\text{Si}(\text{H})\text{Si} \leftarrow \text{NHC}$ with diphenylacetylene gave a silole in a [2+2+1] cycloaddition (Scheme 31). In contrast, the reaction of the same silylene with phenylacetylene yielded 1-alkenyl-1-alkynylsilane $t\text{Bu}_3\text{Si}(\text{H})\text{Si}(\text{CH}=\text{CHPh})(\text{C}\equiv\text{CPh})$. Theoretical calculations showed that N-heterocyclic carbene plays major role in the formation of intermediates and transition states.

Reaction of $\text{Ge}[\text{CH}(\text{SiMe}_3)_2]_2$ with diazidosilanes led to the formation of N-(azidosilyl)-germanimine, which subsequently reacted with the second equivalent of Lappert's germy-



Scheme 31: Reaction of silylene $t\text{Bu}_3\text{Si}(\text{H})\text{Si}\leftarrow\text{NHC}$ with acetylenes (NHC = 1,3,4,5-tetramethylimidazol-2-ylidene).

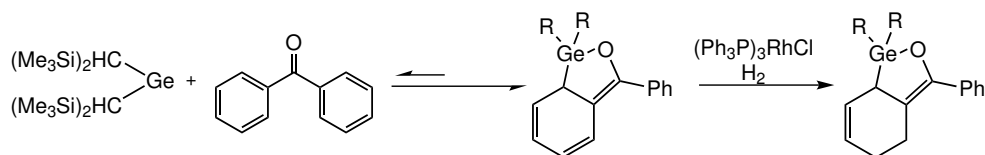
lene and gave bis(germanimines) (Scheme 32) [74, 75]. However, for the less bulky methyl substituent on diazosilane this reaction resulted in cyclosilazane and siladihydrotetrazole derivative [75, 76]. The former was formed *via* rearrangement of N-(azidosilyl)germanine to N-(azidogermly)silaimine and the subsequent dimerization, whereas the latter was synthesized by [3+2] cycloaddition of N-(azidosilyl)germanine to N-(azidogermly)silaimine followed by the hydrolysis in air.



Scheme 32: Addition of Lappert's germylene to diazidosilanes.

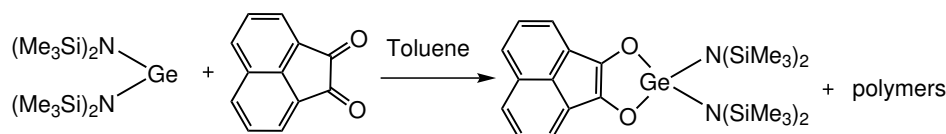
An interesting reactivity of tetrylene towards ketone systems can be observed. For instance, $\text{Ge}[\text{CH}(\text{SiMe}_3)_2]_2$ reacted with phenones to give conjugated trienes [77]. The double bond of the conjugated triene resulting from the reaction of the Lappert's germylene with benzophenone was hydrogenated using Wilkinson's catalyst, $\text{RH}(\text{PPh}_3)_3\text{Cl}$ [78] (Scheme 33).

The reaction of a germylene with a α -dicarbonyl compound was the subject of interest of Rivi re and coworkers [79]. The authors showed that Lappert's germylene $[(\text{Me}_3\text{Si})_2\text{N}]_2\text{Ge}$ reacted with acenaphthene quinone and formed a cycloadduct and a polymer at -78°C



Scheme 33: Activation of benzophenone to form conjugated triene followed by catalytic hydrogenation of one of the double bonds.

(Scheme 34). When the reaction was carried out at 20 °C only a polymer was formed.



Scheme 34: Reaction of Lappert's germylene with quinone.

2.1.2 Insertion into σ bonds

Tetrylenes insert into variety of single bonds i. e. $\text{Si}-\text{H}$, $\text{Si}-\text{Si}$, $\text{Si}-\text{X}$ ($\text{X} = \text{Cl}$, Br , I), $\text{C}-\text{O}$, $\text{H}-\text{O}$, $\text{H}-\text{N}$, $\text{B}-\text{H}$, $\text{B}-\text{B}$ [1, 80]. Due to the lone pair of tetrylenes being relatively inert when acting as a nucleophile, the reaction is initiated by the electrophilic interaction of an empty tetrylene orbital with a halogen or oxygen lone pair, which leads to the formation of the intermediate zwitterionic donor-acceptor complex $\text{R}_2\text{E}^{\delta-}-\text{X}^{\delta+}-\text{R}'$. This coordination results in the enhancement of the nucleophilic character of the tetrylene, thus the nucleophilic attack of tetrylene's lone pair towards R' moiety occurs (left panel in Figure 18). Insertion reactions of tetrylene into $\text{B}-\text{H}$, $\text{B}-\text{B}$, $\text{Si}-\text{H}$, $\text{Si}-\text{Si}$ can be explained by initial interaction of vacant p orbital of tetrylene and the high energy orbital of the $\text{X}-\text{Y}$ bond (right panel in Figure 18).

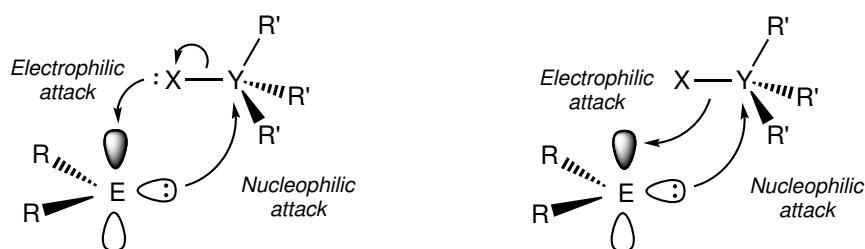
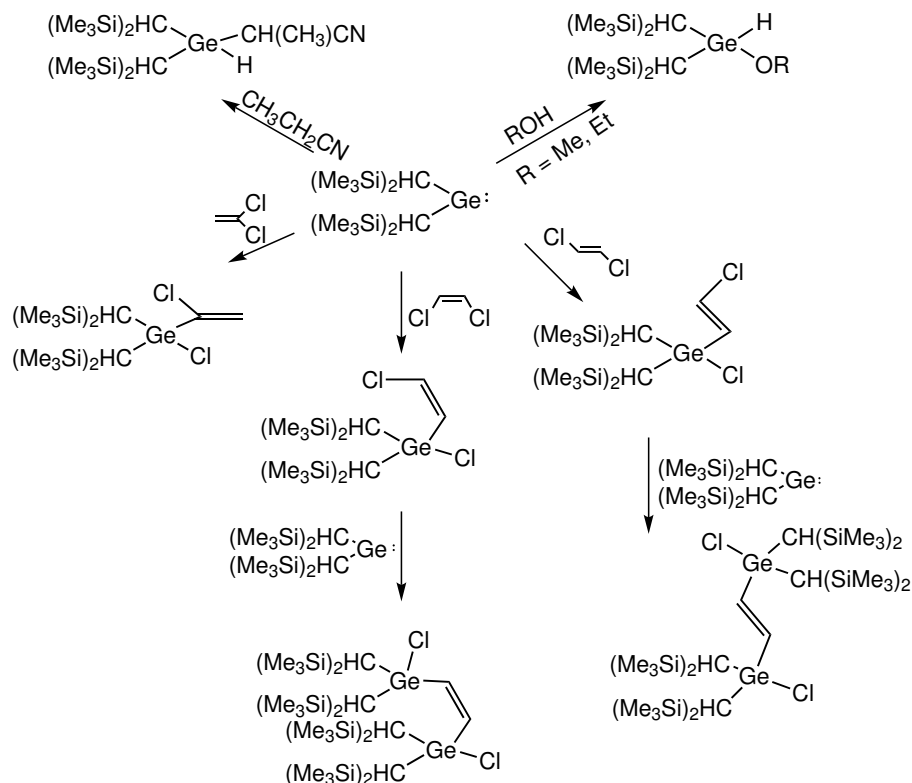


Figure 18: Orbital interaction in the insertion of tetrylenes into $\text{X}-\text{Y}$ σ -bond taken from [80].

$\text{Ge}[\text{CH}(\text{SiMe}_3)_2]_2$ was found to insert into σ -bond of alcohols [81] (Scheme 35) as well as into the $\text{C}-\text{Cl}$ bond of vinyl chlorides such as *trans*-1,2-dichloroethylene, *cis*-1,2-dichloroethylene and 1,1-dichloroethylene. The stereochemistry of the starting material

was retained in the product (Scheme 35), which showed that the insertion reaction proceeded stereospecifically. Although germylenes are known to insert into variety of bonds



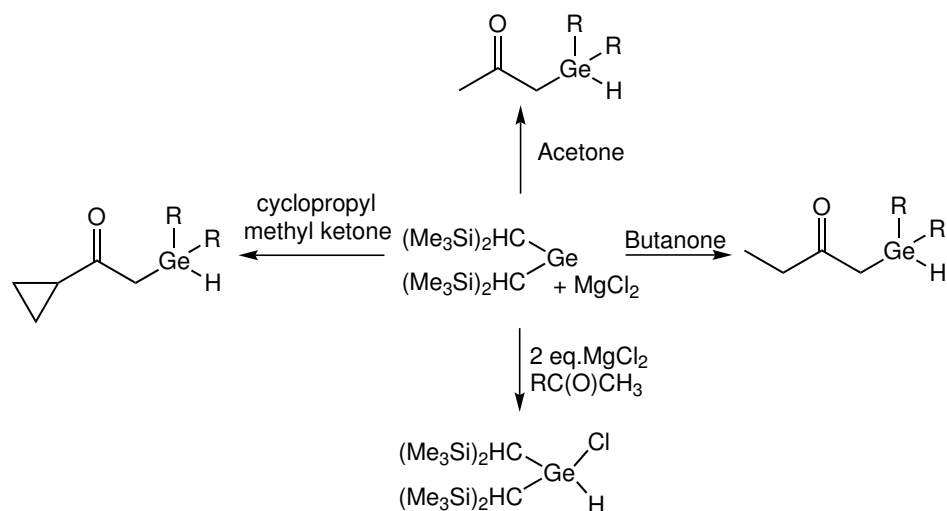
Scheme 35: Insertion reactions of Lappert's germylene into σ bond.

(including Si-H, Ge-H, C-X) both C-C and C-H bonds are generally less reactive towards germylenes. However, $\text{Ge}[\text{CH}(\text{SiMe}_3)_2]_2$ inserts into α -C-H bond of nitrile such as acetonitrile, propionitrile, phenylacetonitrile, and succinonitrile [82]. These insertions are very sensitive to the conditions at which the reaction is carried out – the THF solvent and the presence of a salt (one of LiCl, MgCl, or LiBr) is required.

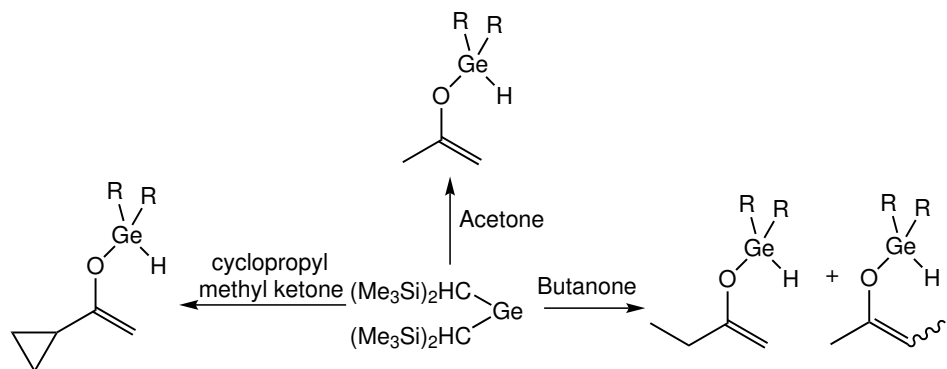
Kampf and coworkers investigated the reaction of $\text{Ge}[\text{CH}(\text{SiMe}_3)_2]_2$ with acetyl-containing ketones in the presence as well as absence of MgCl_2 [83]. The reaction carried out in the presence of magnesium chloride resulted in the insertion of a germylene into the C-H bond (Scheme 36), whereas in the absence of magnesium chloride a germyl vinyl ether was formed (Scheme 37).

Germylenes and stannylenes react with ammonia and hydrogen. As demonstrated by Power [84] the treatment of germylene $\text{GeAr}^\#_2$ ($\text{Ar}^\# = \text{C}_6\text{H}_3-2,6-(\text{C}_6\text{H}_2-2,4,6-\text{Me}_3)_2$) with ammonia or hydrogen led to the tetravalent product $\text{Ar}^\#_2\text{Ge}(\text{H})\text{NH}_2$ or $\text{Ar}^\#_2\text{GeH}_2$. Reaction of more bulky GeAr'_2 ($\text{Ar}' = \text{C}_6\text{H}_3-2,6-(\text{C}_6\text{H}_3-2,6-\text{Pr}_2)_2$) with NH_3 proceeded to tetravalent amine, however, the treatment with H_2 resulted in the $\text{Ar}'\text{H}$ elimination and the formation of $\text{Ar}'\text{GeH}_3$.

Reaction of IPrGeCl_2 with one equivalent of $\text{GeCl}_2 \cdot \text{dioxane}$ in toluene led to the for-

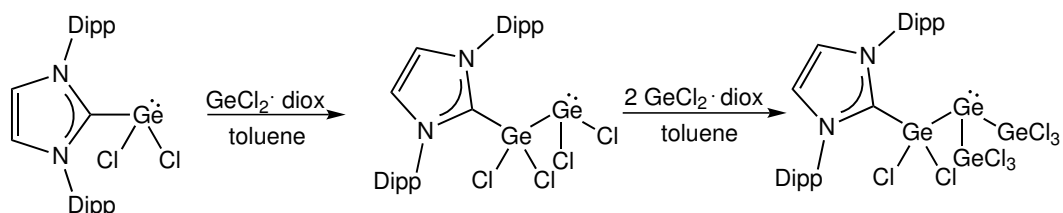


Scheme 36: Insertion of a germylene into C-H bonds in the presence of MgCl_2 .



Scheme 37: Insertion of a germylene into O-H bonds in the absence of MgCl_2 .

mation of a linear N-heterocyclic carbene adduct of tetrachlorodigermene [85] (Scheme 38). An attempt to add either one or two equivalent of GeCl_2 -dioxane gave the branched Ge_4 adduct, $\text{IPr}\cdot\text{GeCl}_2\text{Ge}(\text{GeCl}_3)_2$.



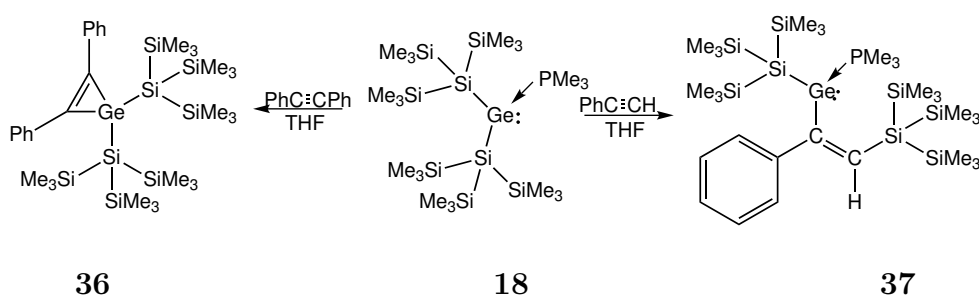
Scheme 38: Formation of a N-heterocyclic carbene adduct of tetrachlorodigermene.

The selected examples of tetrylene reactivity presented above demonstrate a wide diversity of their possible products. The following sections present original results obtained by the author for disilylated germylenes, which have not been investigated so far.

2.2 Reactions of acyclic germylene adducts with acetylenes

2.2.1 Synthesis

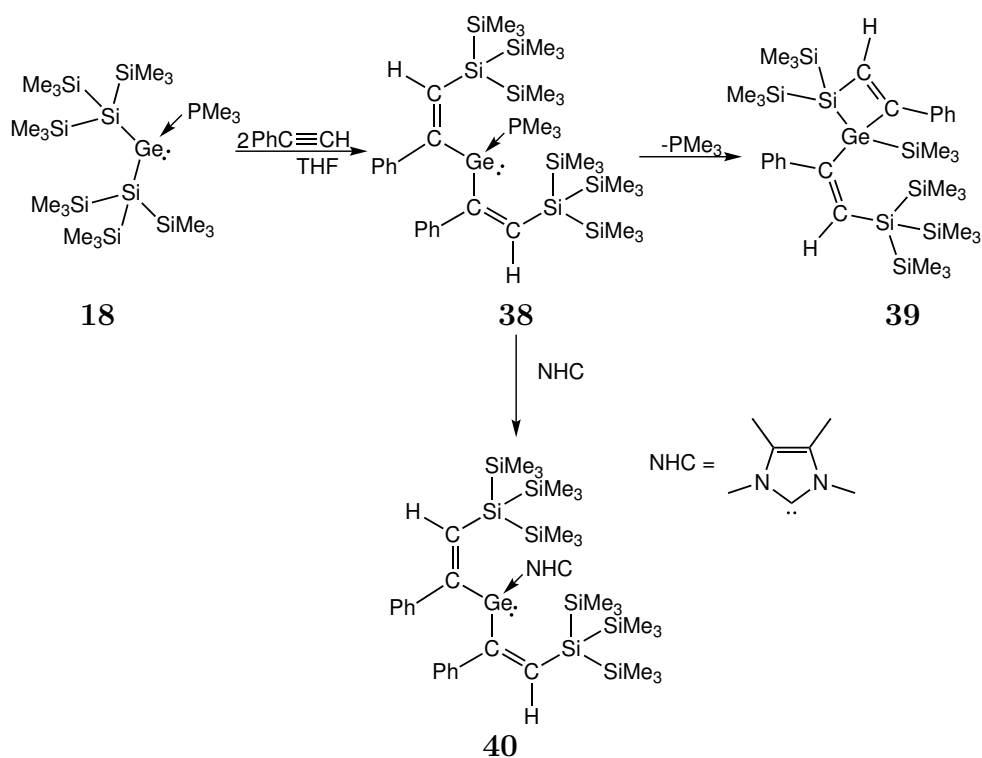
Knowing how to synthesize bis[tris(trimethylsilyl)silyl]germylene \cdot PMe_3 (**18**) it was possible to check its reactivity towards acetylene derivatives. Surprisingly, the products depended on the type of acetylene species. The reaction of germylene with diphenylacetylene led to the formation of a well known germacyclopropene-type compound **36** [48, 86–89]. However, using phenylacetylene under identical conditions resulted in an unexpected product of the regio- and stereoselective insertion of the alkyne into the germanium-silicon bond (**37**) (Scheme 39). Crystal structures of both compounds **36** and **37** were determined by X-ray study. The yellow crystals suitable for measurement precipitated from pentane at -35 °C. It is important to notice that compound **37** is the first known example of a vinylgermylene. Related vinylcarbenes are known to be intermediates, which rearrange to cyclopropenes [90, 91]. Related insertion of acetylenes into borylsubstituted germylene and stannylene systems has been reported very recently [92].



Scheme 39: Reaction of **18** with acetylenes.

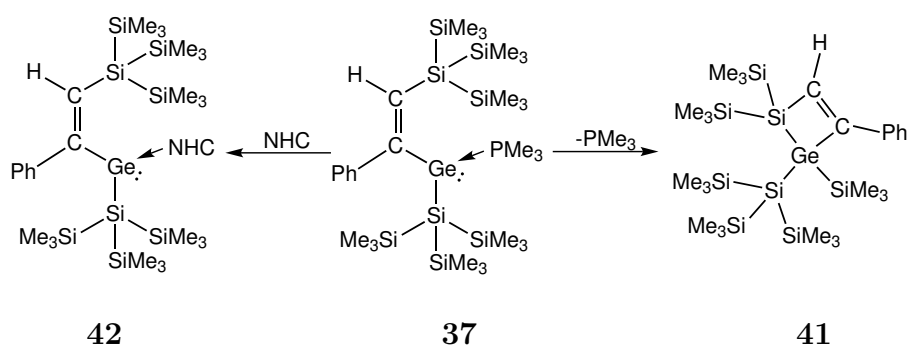
The PMe_3 adduct of divinylated germylene **38** was formed in the reaction of germylene **18** with two equivalents of phenylacetylene (Scheme 40). Again, the insertion reactions of the alkyne were regio- and stereoselective. The obtained product **38** seems to be far less stable than its single-inserted analog **37**. Attempts to crystallize **38** in pentane at -35 °C led to the intramolecular insertion of the germylene into the Si-SiMe₃ bond, causing the formation of silagermete **39**. It can be also obtained by abstraction of the phosphine in the chemical reaction of **38** with one equivalent of $\text{B}(\text{C}_6\text{F}_5)_3$. Due to the fast rearrangement, crystallization of **38** was very difficult, nevertheless a few crystals suitable for X-ray study were obtained. The fast rearrangement of **38** suggests that the interaction between the germylene and trimethylphosphine is very weak, however the fact that it was possible to isolate **38** demonstrates that it is stronger than in the starting material **18**. The stabilization of germylene **38** was possible by using a different Lewis base. Exchange trimethylphosphine for N-heterocyclic carbene proceeded immediately after mixing **38** with NHC, which resulted in the stabilization of the germylene and the formation of **40**.

Further reactivity study of germylene PMe_3 adduct **37** was carried out. Reaction of **37** with one equivalent of $\text{B}(\text{C}_6\text{F}_5)_3$ proceeded to silagermete **41** (right side in Scheme 41).



Scheme 40: Further reaction of **18**.

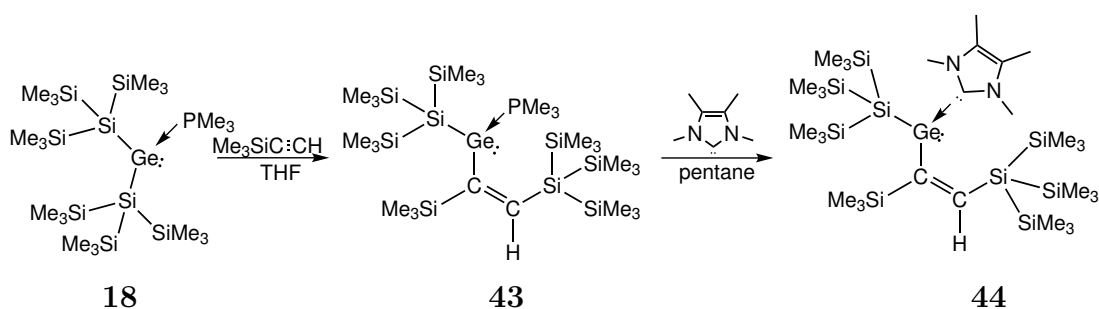
The Lewis acid, $\text{B}(\text{C}_6\text{F}_5)_3$, together with the Lewis base, PMe_3 , formed the stable adduct $\text{B}(\text{C}_6\text{F}_5)_3 \cdot \text{PMe}_3$, which led to the rearrangement of the germylene into **41**. Abstraction of the phosphine was also realized by heating **37** up to 120°C . The NHC-adduct of the single inserted germylene (**42**) was synthesized in the reaction of **37** with 1,3,4,5-tetramethylimidazole in the ratio of 1:1, similarly to the formation of **40**.



Scheme 41: Further reaction of **37**, NHC = 1,3,4,5-tetramethylimidazole-2-ylidene.

The successful reactions of germylene **18** with $\text{PhC}\equiv\text{CH}$ encouraged us to react **18** with trimethylsilylacetylene (Scheme 42). After mixing the starting materials at -35°C their color immediately changed from yellow to green, but after approximately 5 minutes it

turned back to yellow. The appearance of the green color for a short time suggests the formation of an intermediate, however attempts to confirm this presumption by NMR measurements were unsuccessful – the product of the insertion of acetylene into the silicon-germanium bond (**43**) was always detected. Addition of the second equivalent of the trimethylsilyl acetylene did not lead to the formation of the trimethylphosphine adduct of divinylated germylene, as it was the case for phenylacetylene. **43** is very stable and forms flashing yellow crystals, which are extremely soluble even in such an apolar solvent as pentane. Attempts to use a different solvent (e. g. toluene, benzene, THF-pentane 1:1, methylcyclohexane) as well as to crystallize at a different temperature (i. e. $-30\text{ }^{\circ}\text{C}$ and $23\text{ }^{\circ}\text{C}$) did not lead to the formation of crystals, which would give a satisfactory X-ray diffraction pattern. In order to confirm the formation of **43** it was necessary to replace the Lewis base, thus 1,3,4,5-tetramethylimidazole was added to the stirring pentane solution of **43** at room temperature, which led to the formation of the N-heterocyclic adduct of germylene **44**. Orange needles of **44**, suitable for X-ray study, precipitated from a benzene solution at room temperature within 18 hours.



Scheme 42: Synthesis of Lewis base adducts of vinylated germylene **43** and **44**.

Despite the successful synthesis of a germylene with two inserted phenylacetylenes, attempts to obtain a germylene with two inserted trimethylsilylacetylenes did not proceed as expected, which was already mentioned above. It was interesting to check the possibility of inserting one PHCCH and one TMSCH into the germanium-silicon bonds of **18**. The adduct of phenylacetylene inserted germylene **37** and trimethylsilylacetylene were submitted to the reaction carried out at room temperature. The synthesis proceeded relatively slowly – even after 7 days the full conversion was not observed. ^{29}Si NMR recorded in the course of this reaction did not show even traces of the expected product **45** (Scheme 43). Seven peaks were observed in the ^{29}Si NMR spectrum, instead of two signals corresponding to the quaternary silicon atoms and three resonances resulting from the trimethylsilyl groups (Figure 19). The signals observed in the spectrum could be assigned to the compound **46**, which is a product of intermolecular insertion of free asymmetric germylene into the Si–SiMe₃ bond in **45** (Scheme 43). The resonance located at -26.2 ppm is expected to originate from the silicon atom within the four membered ring, however its actual location in the spectra of similar compounds such as **41** and **39** is significantly farther upfield shifted than it is the case here. Regardless of such a large deviation from the typical value of this particular signal, the remaining peaks support the conclusion that silagermete **46**

was formed in this reaction. Although there are two possible isomers of **46** (see Scheme 43) only one of them was detected in the ^{29}Si NMR spectrum, which proves that the insertion of double-inserted germylene **45** into the Si–SiMe₃ bond is regioselective. Unfortunately, crystals of **46** could not be obtained, and it was not possible to discriminate between the two isomers using exclusively NMR technique.

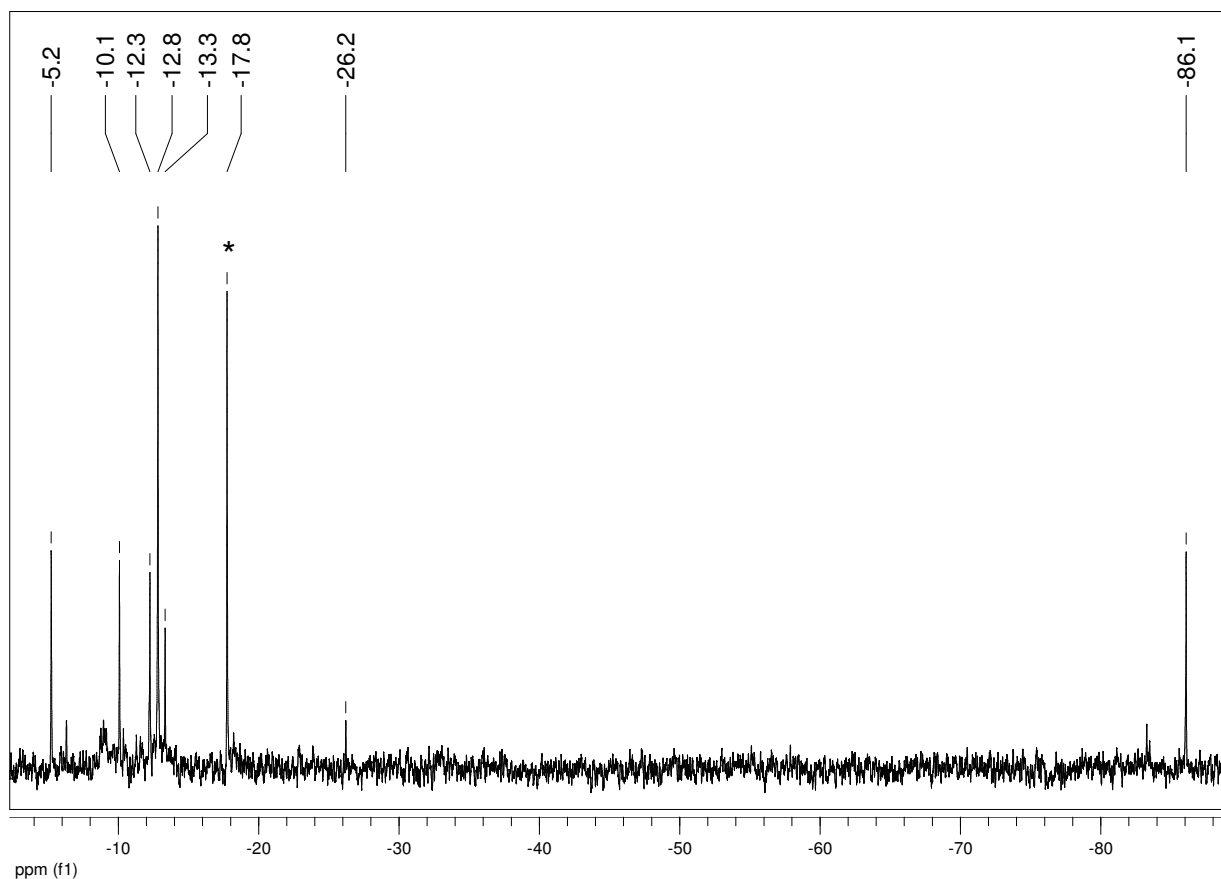
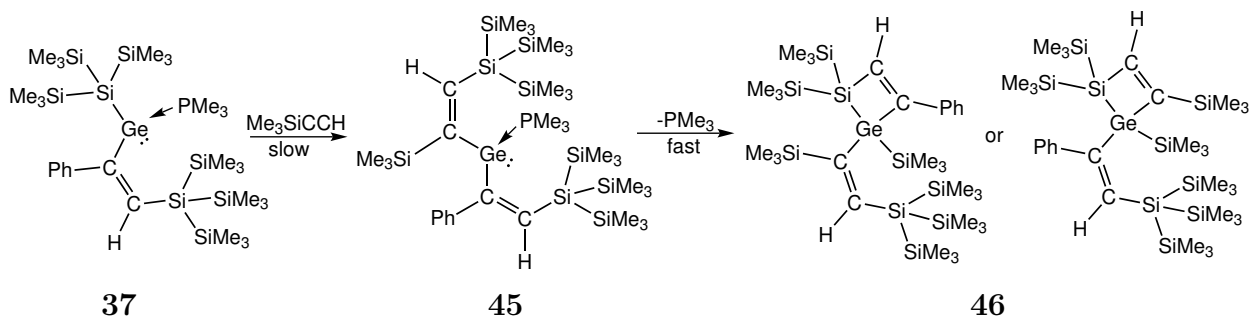


Figure 19: ^{29}Si NMR spectrum of the reaction mixture resulting from the reaction of **37** with TMSCH. The signal marked with * represents unreacted trimethylsilylacetylene.

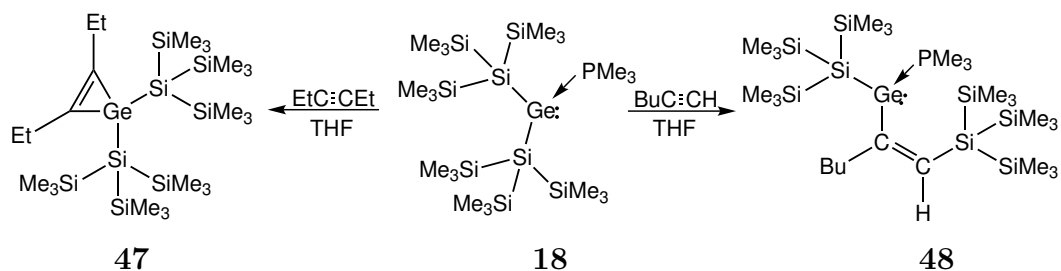


Scheme 43: Reaction of **37** with trimethylsilylacetylene.

Reactions of trimethylphosphine adduct of bis[tris(trimethylsilyl)silyl]germylene (**18**)

with bis(trimethylsilyl)acetylene carried out in THF at $-35\text{ }^{\circ}\text{C}$, room temperature and $50\text{ }^{\circ}\text{C}$ and also reaction of **18** with tris(trimethylsilyl)silylphenylacetylene did not lead to the formation of germacyclopropenes, probably due to the presence of too bulky substituents in acetylene species. It was interesting to check the influence of a less bulky group in the acetylene species on the reaction path. The hexyne isomers (1-hexyne and 3-hexyne) were chosen, due to their availability as liquids. Besides it was expected that the alkyl substituent would be of negligible lability, enhancing the chances of successful crystallization of the products.

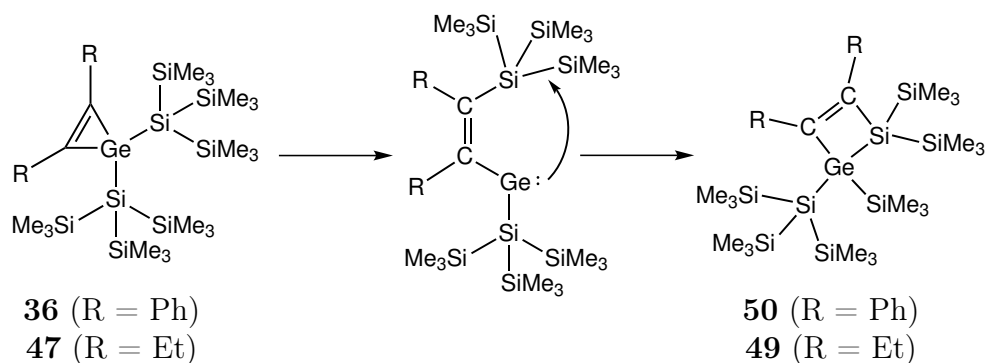
The PMe_3 adduct of bis[tris(trimethylsilyl)silyl]germylene (**18**) reacting with 3-hexyne formed germacyclopropene **47** (Scheme 44) similar to the reaction of **18** with diphenylacetylene. Addition of 1-hexyne into the solution of **18** in THF led to the regio- and stereoselective insertion of the alkyne into the germanium-silicon bond and the formation of **48**. Addition of the next equivalent of 1-hexyne did not lead to a doubly inserted germylene, similarly as in the case of trimethylsilylacetylene.



Scheme 44: Reaction of **18** with 1-hexyne and 3-hexyne.

Surprisingly, compound **47** is not stable, and after storage even at low temperature rearranged to the silagermete **49** (Scheme 45). Heating up of bis[tris(trimethylsilyl)silyl]diphenylgermacyclopropene (**36**) to $150\text{ }^{\circ}\text{C}$ gave similar result, i. e. it led to the formation of silagermete **50**. The mechanism of these reactions was proposed based on the analogous follow-up chemistry of vinylated germynes. The insertion of acetylene into germanium-silicon bond leading to the formation of free germylene is the first step of this reaction. The formation of silagermete **49** and **50** resulted from the insertion of free germylene into the Si-SiMe₃ bond. Compounds **49** and **50**, which are analogous to **41**, have not been crystallized yet.

The results obtained with PMe_3 adduct of bis[(tristrimethylsilyl)silyl]germylene (**18**) encouraged the attempts to extend the field of this research to N-heterocyclic carbene stabilized germylene and stannylene. Reactions of bis[tris(trimethylsilyl)silyl]germylene $\cdot \text{IME}_4$ (**1**) and bis[tris(trimethylsilyl)silyl]stannylene $\cdot \text{IME}_4$ (**34**) with PhCCH were carried out, but in both cases starting material was detected in the reaction mixture even after heating up to $50\text{ }^{\circ}\text{C}$ for 72 hours. Similar developments were observed, when PhCCPh was reacted with **1**. It demonstrated, that the coordination of NHC carbene to tetrylenes is very strong, thus this adduct should be considered as a germulenoid species rather than a germylene. In contrast, PMe_3 adduct of germylene reacts as a free tetrylene, due to the



Scheme 45: Proposed mechanism of the formation of silagermetes **49** and **50**.

very weak interaction between the phosphine and the germylene. Most probably, the first step of the reaction of the PMe_3 adduct of germylene (**18**) with acetylenes is the formation of germacyclopropene. This assumption is strongly supported by the observation that germacyclopropenes **36** and **47** rearranged to silagermetes **50** and **49**, respectively. It is assumed, that the above rearrangement involves transition of a Ge^{IV} into Ge^{II} system. If the proposed mechanism would get confirmed, it will provide one of the rare exceptions from the widely accepted viewpoint that the fourth oxidation state is preferred over the second for germanium. In the case of reaction of **18** with terminal acetylenes, the germylene adduct has lower energy than germacyclopropene. Attempt to confirm the formation of phenylgermyrene by lowering the temperature to -80°C during the addition of PhCCH to prepare *in situ* **18** in THF solution was unsuccessful, due to the impossibility of recording NMR spectrum at low temperature because of the usage of a D_2O capillary. Nevertheless, the fact, that diethylgermyrene and diphenylgermyrene rearranged to silagermetes suggests that the proposed mechanism is correct.

2.2.2 NMR Spectroscopy

The ^{29}Si NMR resonances of the tris(trimethylsilyl)silyl group of the vinylated germylenes as well as germacyclopropene **36** and **47** are compiled in Table 15. The ^{29}Si NMR shifts of germacyclopropene **36** (-92.6 and -9.2 ppm) resemble those of germacyclopropene **47** (-95.3 and -9.3 ppm). Similarity is also observed in the ^{13}C NMR spectra. The chemical shift of the carbon atoms within the three-membered ring of **36** (145.4 ppm) are almost the same as those of **47** (142.9 ppm) and differ by about 10 ppm with respect to the double bonded carbon in *cis*-stilbene (130.22 ppm) and *cis*-3-hexene (131.08 ppm).

The ^{29}Si NMR shifts of vinyl compounds are reminiscent of vinylsilanes [93, 94]. The ^{29}Si NMR spectrum of PMe_3 adduct of monoinserted PhCCH germylene (**37**) shows three doublets at -8.9 , -12.9 and -126.9 ppm (resulting from $\text{Ge}-\text{SiMe}_3$, $\text{C}-\text{SiMe}_3$ and $\text{Ge}-\text{Si}(\text{SiMe}_3)_3$, respectively) and one singlet at -83.4 ppm, which is assigned to quaternary silicon of tris(trimethylsilyl) group attached to the carbon atom. A coupling of silicon nuclei to phosphorous is not observed in ^{29}Si NMR of the divinylated germylene **38**. The chemical shifts of **38** (-86.2 and -12.9 ppm) are almost identical to chemical shifts

Table 15: ^{29}Si NMR data for tris(trimethylsilyl)silyl group of compounds resulting from reactions of germylene **18** with acetylenes, $\text{R} = (\text{Me}_3\text{Si})_3\text{Si}$.

| Compound | Group | | | |
|--------------------------------------------------------------|---------------------------------|--------------------------------|---------------------------------|--------------------------------|
| | Ge <i>Si</i> Si Me ₃ | C <i>Si</i> Si Me ₃ | Ge Si <i>Si</i> Me ₃ | C Si <i>Si</i> Me ₃ |
| germacyclopropene (36) | -92.6 (s) | n/a | -9.2 (s) | n/a |
| R HCCPh Ge R · PMe ₃ (37) | -126.9 (d) | -83.4 (s) | -8.9 (d) | -12.9 (d) |
| [R HCCPh] ₂ Ge · PMe ₃ (38) | n/a | -86.2 (s) | n/a | -12.9 (s) |
| [R HCCPh] ₂ Ge · IMe ₄ (40) | n/a | -87.6 (s) | n/a | -13.1 (s) |
| R HCCPh Ge R · IMe ₄ (42) | -128.0 (s) | -85.9 (s) | -8.7 (s) | -12.6 (s) |
| R HCCSiMe ₃ Ge R · PMe ₃ (43) | -128.2 (d) | -85.8 (d) | -8.9 (d) | -13.1 (d) |
| R HCCSiMe ₃ Ge R · IMe ₄ (44) | -126.7 (s) | -86.5 (s) | -8.7 (s) | -13.1 (s) |
| germacyclopropene (47) | -95.3 (s) | n/a | -9.3 (s) | n/a |
| R HCCBu Ge R · PMe ₃ (48) | -130.5 (d) | -85.5 (d) | -8.9 (d) | -13.2 (d) |

of its N-heterocyclic analog **40** (-87.6 and -13.1 ppm). The ^{29}Si NMR spectrum of **42** shows the following resonances at -12.6 and -85.9 ppm for tris(trimethylsilyl)silyl group attached to the carbon atom at -8.7 and -128.0 ppm for tris(trimethylsilyl)silyl group bonded to the germanium atom. The germylene PMe₃ with inserted trimethylsilylacetylene **43** contains three different trimethylsilyl groups (-7.9 ppm for C=C*Si*Me₃, -8.9 ppm for GeSi*Si*Me₃, and -13.1 ppm for C*Si**Si*Me₃). The resonances of the central silicon atoms are located at -128.2 and -85.8 ppm. The chemical shifts of **48** are almost identical to those of **43** and yield -8.9, -13.2, -85.5 and -130.5 ppm. Similarly to the adduct of germylene with inserted 1-hexyne (**48**), couplings to phosphorus are visible for all silicon atoms of **43**. Due to the very low intensity of the signal corresponding to silicon within trimethylsilyl group of acetylene part of **44**, its assignment was impossible based on ^{29}Si NMR. It was necessary to record 2D NMR spectrum with Si-H correlation, which shows that the resonance of the silicon atom within trimethylsilyl group of acetylene moiety is located at -8.2 ppm, other signals are located at -126.7 and -8.7 ppm for tris(trimethylsilyl)silyl group bonded to germanium -86.5 and -13.1 for tris(trimethylsilyl)silyl attached to carbon.

The ^{29}Si NMR spectrum of silagermete **39** exhibits unusual resonance at -45.0 ppm that represents the silicon atom in the four-membered ring (see Scheme 40). The three signals at -4.6, -10.0 and -12.5 ppm are associated with the trimethylsilyl groups attached to silicon and germanium atoms in the four-membered ring. The most intensive signal at -13.1 ppm corresponds to the three trimethylsilyl groups attached to the silicon bonded to the carbon atom in the non-cyclic part of the molecule. The central silicon atom of tris(trimethylsilyl)silyl group generates a resonance at -86.5 ppm, almost at the same chemical shift as the corresponding atomic site in **38** (-86.2 ppm). Spectra of the remaining compounds containing identical ring i. e. **41**, **50** and **49** look very similar.

The ^{31}P NMR chemical shifts of the trimethylphosphine adducts of vinylated germy-

Table 16: ^1H NMR data for vinylated compounds.

| Compound | Group | |
|-----------------------------------------------------------------------------------------------------------|-------|-------------|
| | TMS | C–H |
| $(\text{Me}_3\text{Si})_3\text{SiHCCPhGeSi}(\text{SiMe}_3)_3 \cdot \text{PMe}_3$ (37) | 0.39 | 6.86 |
| | 0.40 | |
| $[(\text{Me}_3\text{Si})_3\text{SiHCCPh}]_2\text{Ge} \cdot \text{PMe}_3$ (38) | 0.40 | 6.66 |
| | 0.42 | |
| silagermane (39) | 0.41 | 7.44 |
| | 0.41 | |
| $[(\text{Me}_3\text{Si})_3\text{SiHCCPh}]_2\text{Ge} \cdot \text{IME}_4$ (40) | 0.37 | 6.48 |
| | 0.35 | |
| silagermane (41) | 0.38 | 7.46 n/r |
| | 0.41 | |
| | 0.42 | |
| | 0.42 | |
| $(\text{Me}_3\text{Si})_3\text{SiHCCPhGeSi}(\text{SiMe}_3)_3 \cdot \text{IME}_4$ (42) | 0.37 | 6.48 |
| | 0.37 | |
| $(\text{Me}_3\text{Si})_3\text{SiHCCSiMe}_3\text{GeSi}(\text{SiMe}_3)_3 \cdot \text{PMe}_3$ (43) | 0.27 | 7.65 |
| | 0.32 | |
| | 0.00 | |
| $(\text{Me}_3\text{Si})_3\text{SiHCCSiMe}_3\text{GeSi}(\text{SiMe}_3)_3 \cdot \text{IME}_4$ (44) | 0.23 | 7.84 |
| | 0.41 | |
| | 0.46 | |
| $(\text{Me}_3\text{Si})_3\text{SiHCCBuGeSi}(\text{SiMe}_3)_3 \cdot \text{PMe}_3$ (48) | 0.42 | 6.45 |
| | 0.43 | |

n/r – resonance not resolved

lenes are up-field shifted compared to the starting material (-20.1 ppm) and are located at -24.6 ppm for PhCCH inserted germylene (**37** and **38**), -26.6 ppm for BuCCH inserted germylene **48** and -28.1 ppm for Me_3SiCCH inserted germylene **43**.

The vinyl protons of germylene as well as silagermete **39** and **41** described in this section are down-field shifted (Table 16) compared to the standard chemical shifts of the vinyl group ($4.6 - 5.9$ ppm).

The ^{13}C NMR spectrum of both vinylgermylenes and divinylgermylenes shows down-field shifted resonances of carbon bonded to germanium (173.0 ppm for **37**, 177.6 ppm for **38**, 172.9 ppm for **40**, 177.7 ppm for **43** and 172.3 ppm for **48**) compared to the spectrum of the related compounds [95]. The analogous signal of the product of the intramolecular insertion after loss of PMe_3 , **41**, is located at 140.8 ppm, however, the carbon atom attached to germanium belongs to the four-membered ring in this silagermete.

2.2.3 Crystallography

The structure of **36** was resolved by X-ray crystal structure analysis (Figure 20, Table 17). The endocyclic C=C double bond is relatively short (1.322(3) Å), which results in a small C–Ge–C angle (39.24(8)°). The distances between the germanium atom and each of the two carbon atoms within the ring in **36** are equal in length and yield approximately 1.969 Å.

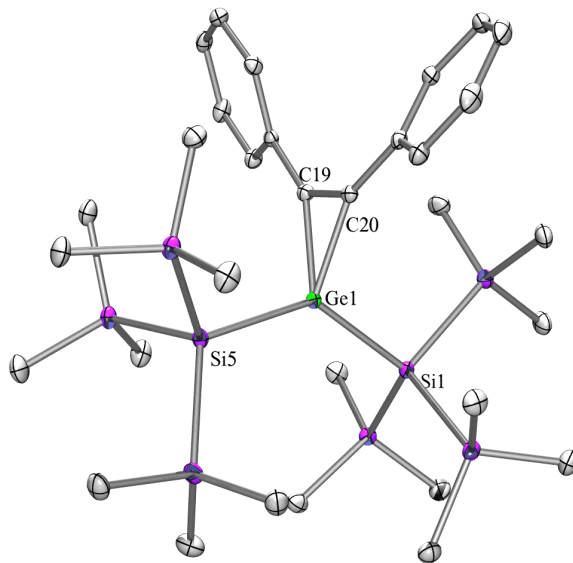


Figure 20: Crystal structure of **36**.

Table 17: Selected bond lengths and angles of **36**.

| Bond | Length [Å] | Bonds | Angle [°] |
|-------------|--------------|-------------------|-------------|
| Ge(1)–Si(1) | 2.4049(7) | Si(1)–Ge(1)–Si(5) | 133.88(2) |
| Ge(1)–Si(5) | 2.4102(7) | Si(1)–Ge(1)–C(20) | 109.73(6) |
| Ge(1)–C(19) | 1.9684(19) | Si(5)–Ge(1)–C(19) | 109.34(6) |
| Ge(1)–C(20) | 1.9695(18) | C(19)–C(20)–Ge(1) | 70.34(11) |
| C(19)–C(20) | 1.322(3) | C(20)–C(19)–Ge(1) | 70.43(11) |
| | | C(19)–Ge(1)–C(20) | 39.24(8) |
| | | C(19)–Ge(1)–Si(1) | 113.88(6) |

Crystalline **37** has the symmetry of orthorhombic space group $Pbca$ (Figure 21, Table 18). Typically for germylenes, elongated germanium–silicon bond yields 2.4816(8) Å and is much longer than in **36**. The distance of germanium–carbon bond yields 2.031(2) Å. The length of the carbon–carbon double bond is 1.347(3) Å.

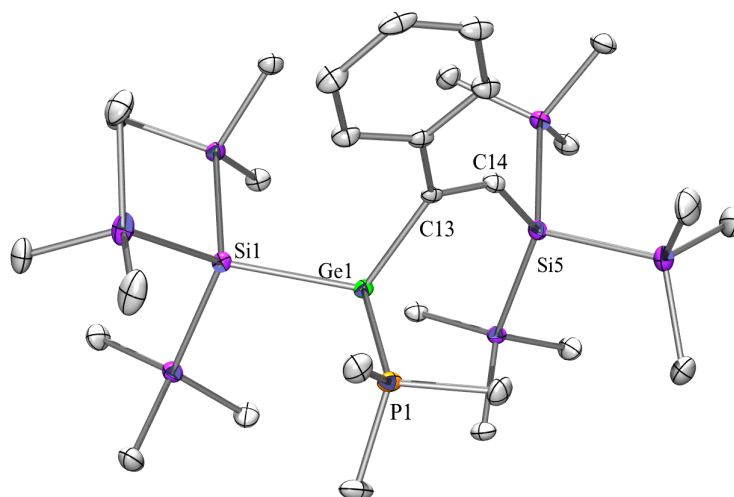


Figure 21: Crystal structure of **37**.

Table 18: Selected bond lengths and angles of **37**.

| Bond | Length [Å] | Bonds | Angle [°] |
|-------------|--------------|-------------------|-------------|
| Ge(1)–Si(1) | 2.4816(8) | Si(1)–Ge(1)–C(13) | 114.36(6) |
| Ge(1)–C(13) | 2.031(2) | Si(1)–Ge(1)–P(1) | 103.53(2) |
| Ge(1)–P(1) | 2.3900(7) | P(1)–Ge(1)–C(13) | 93.22(6) |
| C(13)–C(14) | 1.347(3) | Ge(1)–C(13)–C(14) | 112.85(15) |
| C(14)–Si(5) | 1.893(2) | C(13)–C(14)–Si(5) | 138.84(17) |

Crystalline **38** has the symmetry of triclinic space group $P\bar{1}$ (Figure 22, Table 19). The germanium – carbon bonds (2.043(2) and 2.035(2) Å) are slightly longer than in the monoinserted germylene **37** (2.031 Å). The bond between germanium and phosphorus atom has similar length as the corresponding bond in **37** which yields 2.4261(9) Å.

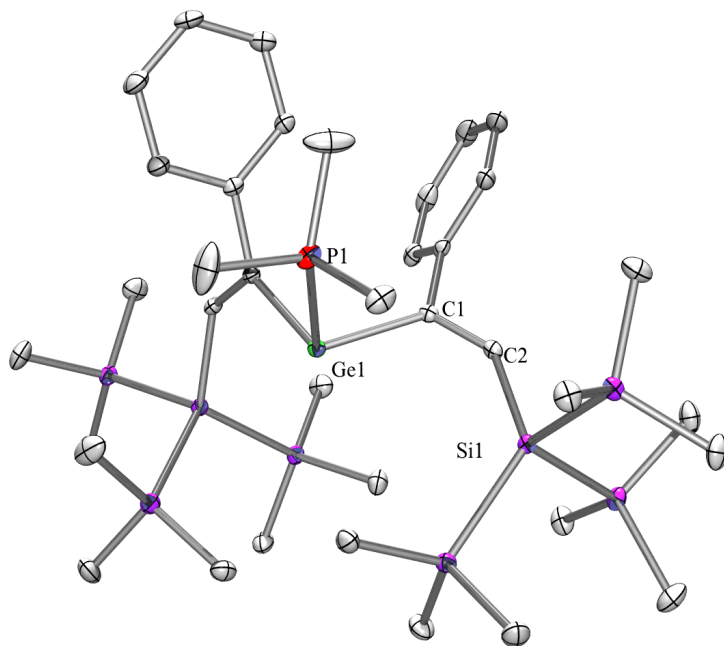


Figure 22: Crystal structure of **38**.

Table 19: Selected bond lengths and angles of **38**.

| Bond | Length [Å] | Bonds | Angle [°] |
|-------------|--------------|------------------|-------------|
| Ge(1)–C(1) | 2.043(2) | C(1)–Ge(1)–P(1) | 105.33(9) |
| Ge(1)–C(17) | 2.035(2) | Ge(1)–C(1)–C(2) | 123.72(16) |
| C(1)–C(2) | 1.347(3) | C(1)–C(2)–Si(1) | 141.72(17) |
| C(2)–Si(1) | 1.896(2) | C(17)–Ge(1)–C(1) | 105.33(9) |
| Ge(1)–P(1) | 2.4261(9) | | |

Compound **39** crystallized in monoclinic space group P2(1)/n (Figure 23, Table 20). It exhibits planar four-membered ring with sum of all angles yielding 359.89°. The lengths of Ge–Si bonds (2.4132(8) Å and 2.3959(8) Å) are typical. Also the distances between germanium–carbon atoms in **39** (2.008(2) Å and 1.997(2) Å) are slightly shorter compared to the corresponding bond in **38** (2.043(2) Å). Although the carbon=carbon double bond (C(7)–C(8)) is located within the ring, this fact does not have huge influence on its length (1.349(3)Å), which is similar to the length of C(18)–C(25) bond (1.347(3)Å).

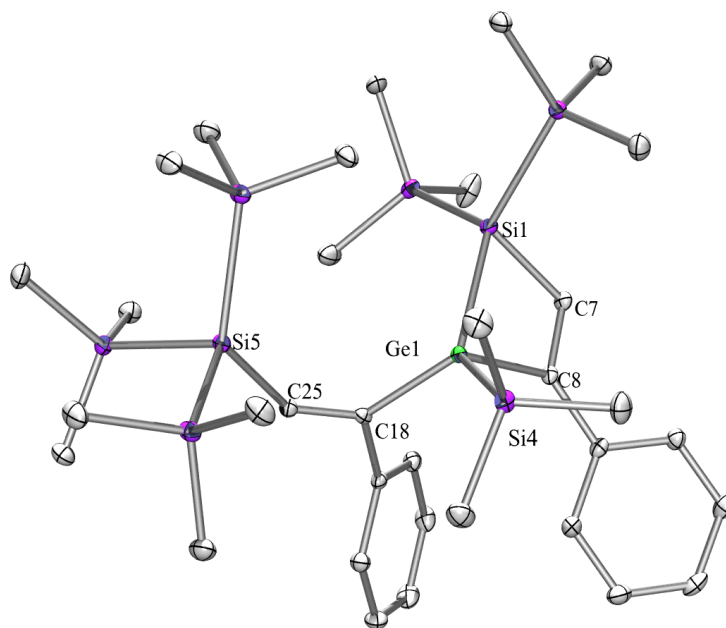


Figure 23: Crystal structure of **39**.

Table 20: Selected bond lengths and angles of **39**.

| Bond | Length [Å] | Bonds | Angle [°] |
|-------------|--------------|-------------------|-------------|
| Ge(1)–C(8) | 2.008(2) | Si(1)–Ge(1)–Si(4) | 126.80(3) |
| Ge(1)–Si(1) | 2.4132(8) | Si(1)–Ge(1)–C(8) | 72.78(7) |
| C(8)–C(7) | 1.349(3) | Ge(1)–C(8)–C(7) | 103.27(16) |
| Si(1)–C(7) | 1.887(2) | C(8)–C(7)–Si(1) | 108.40(17) |
| Ge(1)–Si(4) | 2.3959(8) | C(8)–Ge(1)–Si(4) | 104.08(7) |
| Ge(1)–C(18) | 1.997(2) | C(7)–Si(1)–Ge(1) | 75.44(8) |
| C(18)–C(25) | 1.347(3) | Si(1)–Ge(1)–C(18) | 118.99(7) |
| C(25)–Si(5) | 1.899(2) | C(8)–Ge(1)–C(18) | 113.89(9) |
| | | Si(4)–Ge(1)–C(18) | 110.71(7) |
| | | Ge(1)–C(18)–C(25) | 113.96(16) |
| | | C(18)–C(25)–Si(5) | 141.77(19) |

Compound **40** crystallizes in the monoclinic space group $P2(1)/c$ (Figure 24, Table 21). The replacement of the phosphine with NHC carbene does not have influence on the length of Ge–C(1) and Ge–C(3), which measures 2.042(4) Å in **40** and 2.043(2) Å in **38**. Not surprisingly, the distance between germanium and carbene carbon (2.070(4) Å) is greater than distance between germanium and vinylic carbon atoms (2.042(4) Å).

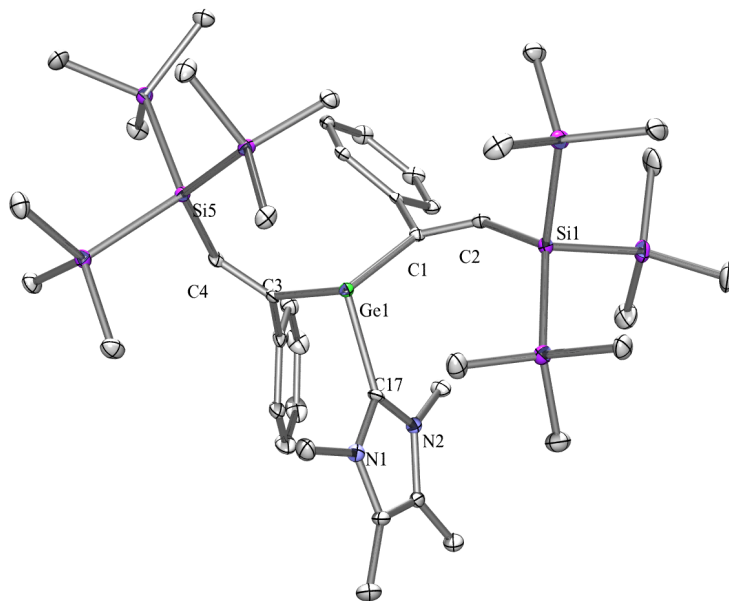


Figure 24: Crystal structure of **40**.

Table 21: Selected bond lengths and angles of **40**.

| Bond | Length [Å] | Bonds | Angle [°] |
|-------------|--------------|------------------|-------------|
| Ge(1)–C(1) | 2.042(4) | C(1)–Ge(1)–C(17) | 101.94(15) |
| C(1)–C(3) | 2.042(4) | C(1)–Ge(1)–C(3) | 101.83(15) |
| Ge(1)–C(17) | 2.070(4) | C(3)–Ge(1)–C(17) | 92.70(15) |
| C(1)–C(2) | 1.346(5) | C(2)–C1(1)–Ge(1) | 124.7(3) |
| C(4)–C(3) | 1.330(5) | C(1)–C(2)–Si(1) | 140.6(3) |
| C(2)–Si(2) | 1.882(4) | Ge(1)–C(3)–C(4) | 118.6(3) |
| C(4)–Si(5) | 1.899(4) | C(3)–C42)–Si(5) | 133.9(3) |

Colorless crystals of **41** suitable for X-ray study precipitated from toluene solution. Crystalline **41** has the monoclinic symmetry space group $P2(1)/n$ (Figure 25, Table 22). The length of germanium–carbon bond (1.9945(17) Å) is similar to the length of corresponding bond in vinylated germylenes. The distance between germanium and silicon atoms within the four-membered ring (2.4354(6) Å) is greater than that between germanium and the silicon of tris(trimethylsilyl)silyl group (2.4031(6) Å).

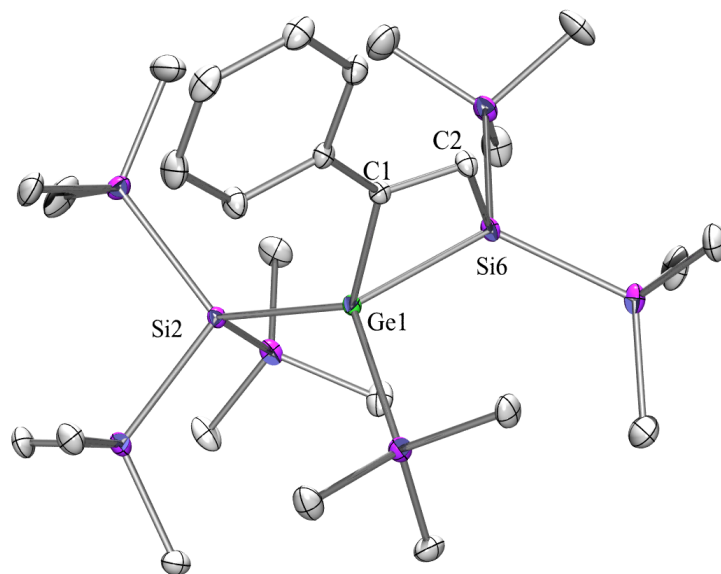


Figure 25: Crystal structure of **41**.

Table 22: Selected bond lengths and angles of **41**.

| Bond | Length [Å] | Bonds | Angle [°] |
|-------------|--------------|-------------------|-------------|
| Ge(1)–Si(2) | 2.4031(6) | Si(2)–Ge(1)–C(1) | 123.71(5) |
| Ge(1)–C(1) | 1.9945(17) | Si(6)–Ge(1)–C(1) | 72.12(5) |
| Ge(1)–Si(6) | 2.4354(6) | Si(6)–Ge(1)–Si(2) | 126.059(17) |
| C(1)–C(2) | 1.346(4) | Ge(1)–C(1)–C(2) | 103.95(11) |
| C(2)–Si(6) | 1.8879(17) | C(1)–C(2)–Si(6) | 107.75(12) |

Compound **42** crystallized in monoclinic space group P2(1)/c (Figure 26, Table 23). The length of Ge(1)–C(9) bond is about 0.04 Å greater than the length of Ge(1)–C(7) bond. The distance between germanium and silicon atom is slightly greater than in the phosphine adduct of germylene **37** and yields 2.5150(10) Å.

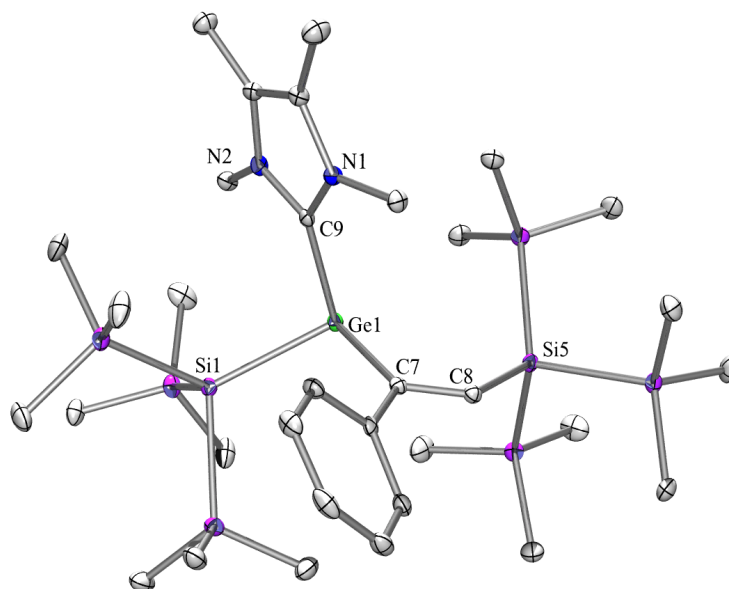


Figure 26: Crystal structure of **42**.

Table 23: Selected bond lengths and angles of **42**.

| Bond | Length [Å] | Bonds | Angle [°] |
|-------------|--------------|------------------|-------------|
| Ge(1)–Si(1) | 2.5150(10) | Si(1)–Ge(1)–C(7) | 105.12(8) |
| Ge(1)–C(7) | 2.033(3) | Si(1)–Ge(1)–C(9) | 98.29(8) |
| Ge(1)–C(9) | 2.070(3) | C(7)–Ge(1)–C(9) | 102.36(10) |
| C(7)–C(8) | 1.351(4) | Ge(1)–C(7)–C(8) | 115.8(2) |
| C(8)–Si(5) | 1.892(3) | C(7)–C(8)–Si(5) | 135.2(2) |

Compound **44** crystallized in orthorhombic space group $P2(1)2(1)2(1)$ (Figure 27, Table 24). In addition to one molecule of **44**, one molecule of benzene was found in the asymmetric unit. Compound **44** releases the longest Ge–Si(SiMe₃)₃ bond of 2.5363(10) Å within results presented in this work. The distances between the germanium and carbon atoms yield 2.078(3) Å for Ge(1)–C(1) and 2.036(3) Å for Ge(1)–C(8).

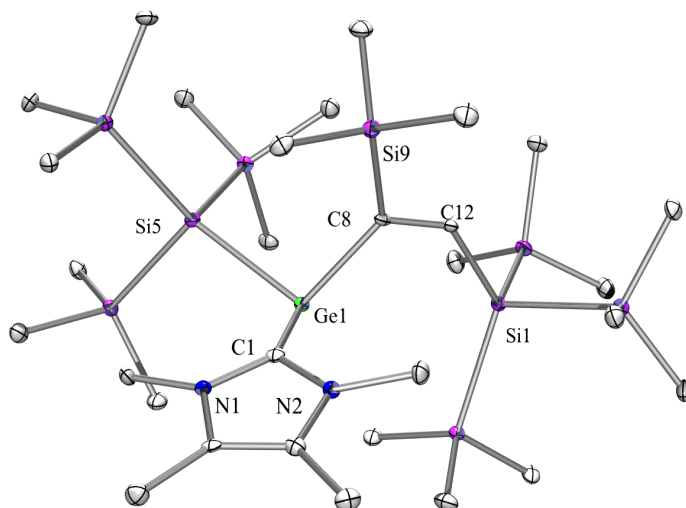


Figure 27: Crystal structure of **44**.

Table 24: Selected bond lengths and angles of **44**.

| Bond | Length [Å] | Bonds | Angle [°] |
|-------------|--------------|------------------|-------------|
| Ge(1)–Si(5) | 2.5363(10) | Si(5)–C(8)–C(7) | 103.67(9) |
| Ge(1)–C(8) | 2.036(3) | Si(5)–Ge(1)–C(1) | 109.46(9) |
| Ge(1)–C(1) | 2.078(3) | C(1)–Ge(1)–C(8) | 98.85(13) |
| C(12)–C(8) | 1.342(4) | Ge(1)–C(8)–C(12) | 116.8(2) |
| C(8)–Si(9) | 1.876(3) | Ge(1)–C(8)–Si(9) | 126.35(16) |
| C(12)–Si(1) | 1.911(3) | C(8)–C(12)–Si(1) | 136.6(2) |

48 crystallized in orthorhombic space group $P2(1)2(1)2(1)$ (Figure 28, Table 25). All bond lengths fall within ranges typical for this group of compounds.

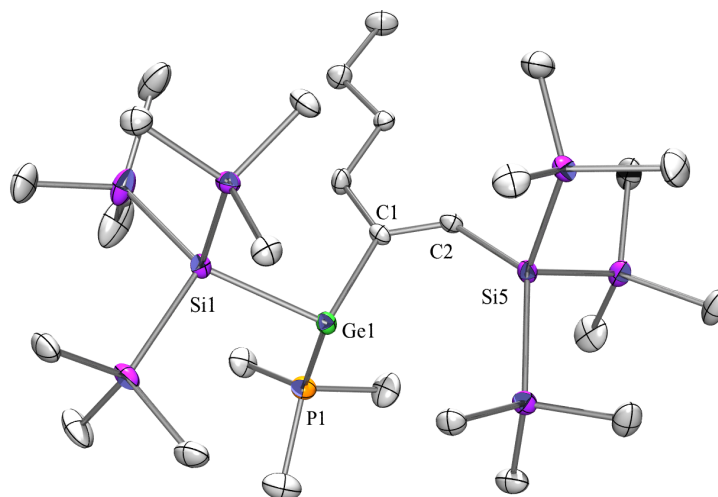


Figure 28: Crystal structure of **48**.

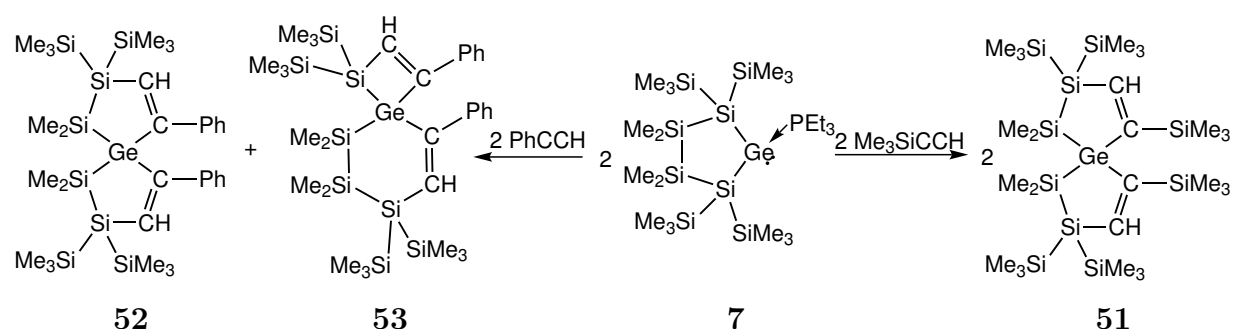
Table 25: Selected bond lengths and angles of **48**.

| Bond | Length [Å] | Bonds | Angle [°] |
|-------------|--------------|------------------|-------------|
| Ge(1)–Si(1) | 2.4640(12) | Si(1)–Ge(1)–C(1) | 104.18(10) |
| Ge(1)–C(1) | 1.998(3) | Si(1)–Ge(1)–P(1) | 102.76(4) |
| Ge(1)–P(1) | 2.3946(12) | C(1)–Ge(1)–P(1) | 95.16(10) |
| C(1)–C(2) | 1.340(5) | Ge(1)–C(1)–C(2) | 118.0(3) |
| C(2)–Si(5) | 1.887(4) | C(1)–C(2)–Si(5) | 137.0(3) |

2.3 Reactions of cyclic germylene adducts with acetylenes

2.3.1 Synthesis

The obtained results with acyclic germylenes **18** encourage the attempts to extend the field of research to phosphine adducts of cyclic germylene. As a starting material was chosen the five-membered ring disilylated germylene **7** due to its stability and quite easy synthetic approach [38]. The reaction of **7** with trimethylsilylacetylene led to the selective synthesis of a symmetric germane containing two five-membered rings (**51**) (Scheme 46). Each ring contains a PhCCH unit.

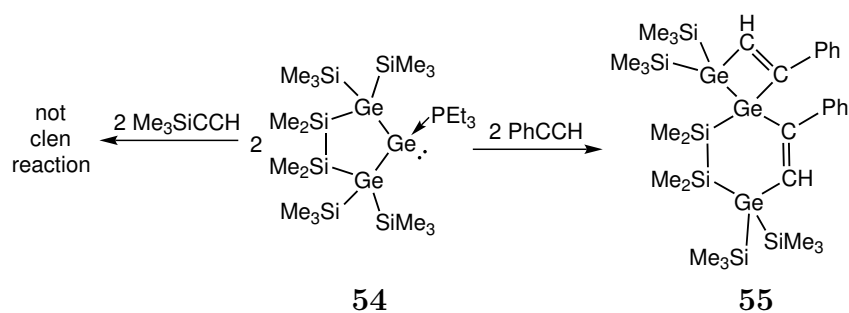


Scheme 46: Reaction of PEt₃ adduct of cyclic silylated germylene **7** with two equivalents of acetylene molecule.

Surprisingly, by changing trimethylsilylacetylene to phenylacetylene and using the same reaction conditions, two compounds were formed: the symmetric germane with two five-membered rings **52**, analogous to those obtained before, and the asymmetric germane with one six-membered and one four-membered ring **53** (Scheme 46). Attempt to separate the products **52** and **53** was unsuccessful. Nevertheless, the crystal structure of **53** was determined by X-ray measurement. The analysis confirmed, that the spirogermanium atom connects the four-membered ring with the six-membered ring. The PhCCH unit is present in both rings.

It was also interesting to check if this reaction occurs for digermylated germylene adduct. The reactivity of the PMe₃ adduct of the digermylated acyclic germylene could not be checked due to the lack of convenient starting material. Cyclic five-membered digermylated germylene adduct exists and is stable when stored under inert gas atmosphere [38]. The reaction of PEt₃ adduct of digermyleted germylene **54** with phenylacetylene is selective and only asymmetric product **55** was formed. At the same time the reaction of **54** with Me₃SiCCH proceeded to the formation of multiple inseparable products, none of them was identified.

The described above spirogermanium compounds are formed presumably *via* sequenced formation of germacyclopropene followed by the insertion of acetylene molecules into both Ge–Si or Ge–Ge bonds of germylene (Scheme 48). Similar to the acyclic germylene all these insertions are regio- and stereoselective. The nine-membered ring germylene is unstable and the intramolecular insertion of the germylene into Si–Si or Si–Ge bond occurred



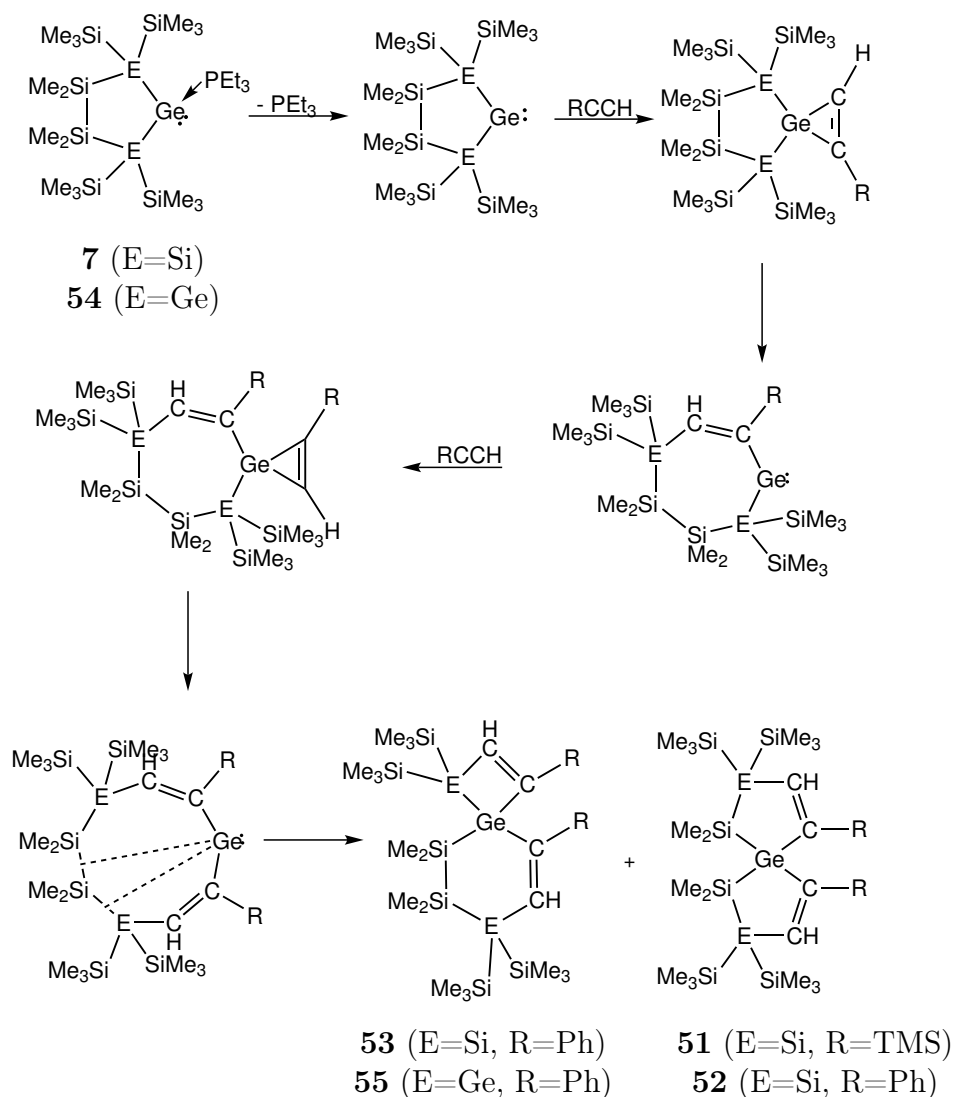
Scheme 47: Reaction of cyclic germylene PEt₃ adduct **54** with two equivalents of acetylene molecule.

(Scheme 48).

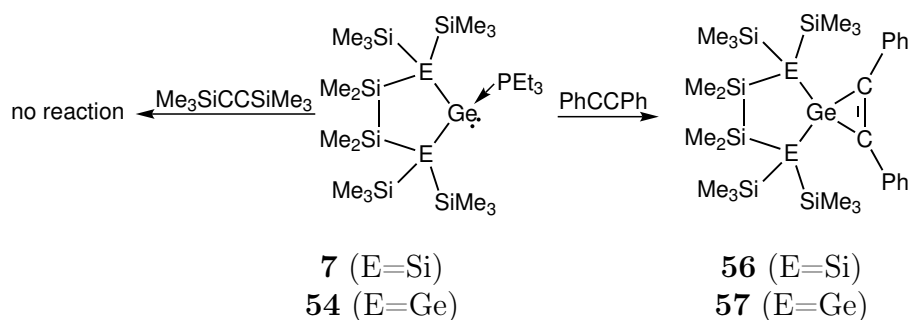
Cyclic germylene adduct **7** and **54** similar to the acyclic adduct **18** did not react with bis(trimethylsilyl)acetylene, but reactions of **7** and **54** with diphenylacetylene led to the formation of the expected products i. e. germacyclopropenes **56** and **57** (Scheme 49). Both compounds precipitated from pentane solution and formed pale yellow crystals, which were submitted to X-ray study. The structure of **56** was solved in contrast to **57**. Although the crystals of **57** looked nicely under the microscope and also diffracted very well, determination of the structure of **57** was impossible due to disorder in crystal structure. Nevertheless, all spectroscopic data confirm the formation of germacyclopropene **57**.

As discussed before, germacyclopropene-type compound rearranged to silagermane. It was interesting to check, if analogous follow-up chemistry occurs in the case of **56** and **57**. The results are positive, and in both cases an unexpected compounds were formed. Heating up of **56** to 150 °C led to the formation of a compound represented by the following resonances in ²⁹Si NMR spectrum: -127.5, -107.3, -27.3, -22.9, -11.4, -8.2, -8.0 and -3.9 ppm. Unfortunately, its crystallization was unsuccessful. Heating up of **56** to 60 °C for 18 hours followed by the increase of temperature to 150 °C led to the formation of multiple products according to ²⁹Si NMR spectrum (Figure 29). Heating up of **56** to 100 °C gave the same result. Crystallization from pentane gave colorless crystals analyzed using X-ray diffraction. One product of the reaction was identified as **58**, the other ones are still unknown (Scheme 50). A separation of the compounds was impossible.

Heating up of germacyclopropenes **57** led to the selective formation of **59** (Scheme 51). Compound **59** contains three germanium atoms within a four-membered ring. Surprisingly, the spirogermanium atom is not the middle germanium atom. It may suggest, that before the insertion of acetylene, double migration of trimethylsilyl group occurred, which resulted in transformation of the tetravalent germanium atom into a divalent one. However, this mechanism was excluded based on the observation that in the reaction of disilylated germacyclopropene described before, analogous product was formed. The proposed mechanism can explain the formation of **59**, but not the formation of **58** formation is impossible, what suggests that this mechanism is not correct at all. Although the mechanism of this rearrangement remains unknown, the reaction flow seems pretty stable, as demonstrated by the repeated procedure, which led to the exact same result.



Scheme 48: Proposed mechanism of reaction of cyclic germylenes **7** and **54** with 2 equivalent of acetylene molecules.



Scheme 49: Reactions of cyclic germylenes with acetylenes.

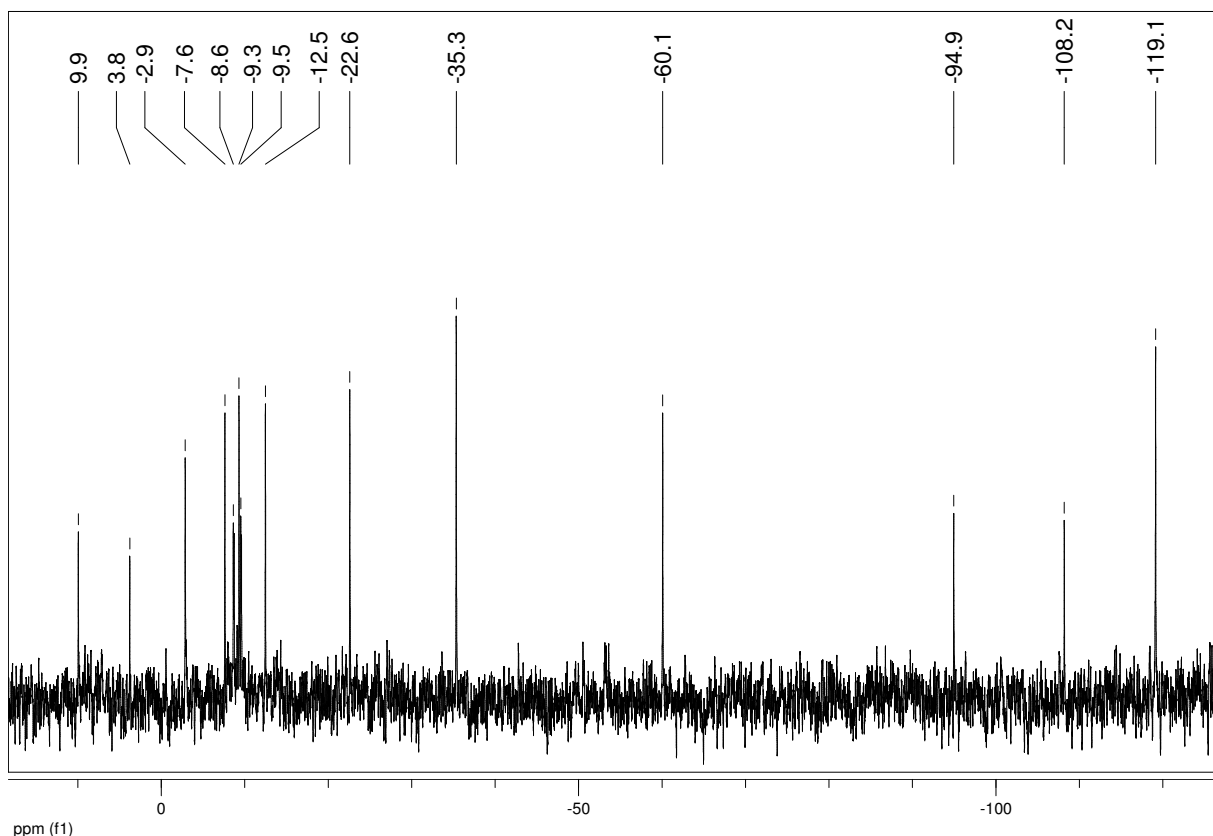
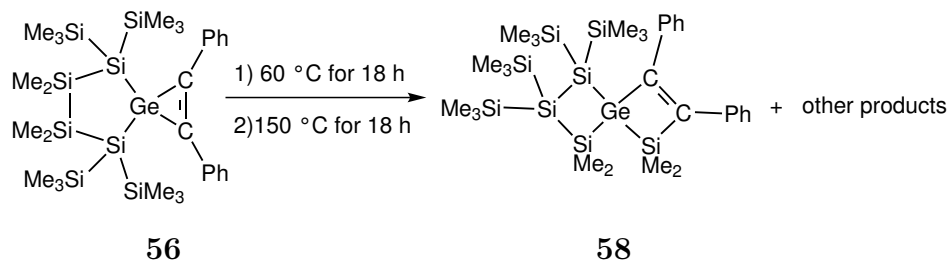
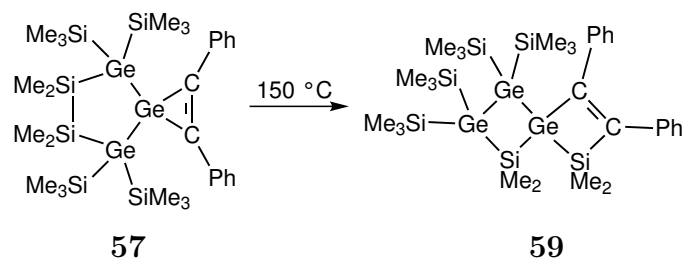


Figure 29: ^{29}Si NMR spectrum of the reaction mixture resulting from the heating up of **56**.

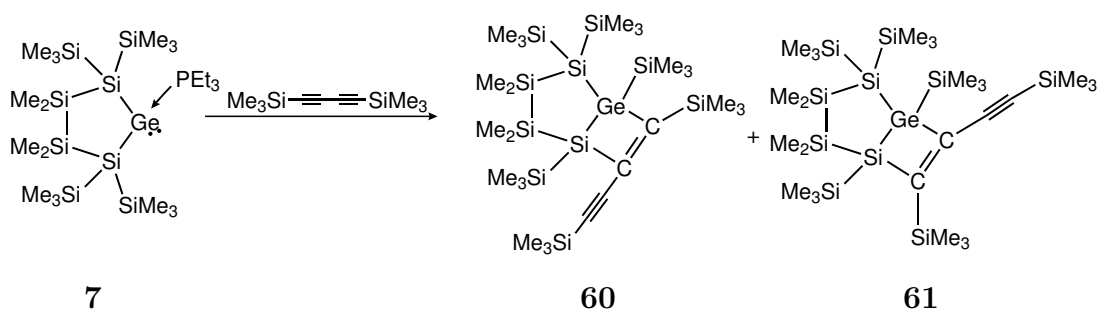


Scheme 50: Rearrangement of germacyclopropene **56**.



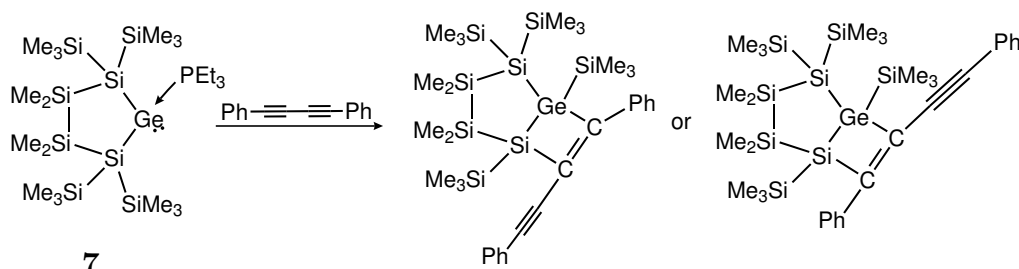
Scheme 51: Rearrangement of germacyclopropene **57**.

Cyclic germylene trimethylphosphine adduct **7** was treated with 1,4-bis(trimethylsilyl)-1,3-butadiyne, however, based on ^{29}Si NMR spectrum two difficult to separate compounds **60** and **61** were formed. The products indicate, that the synthesis occurred by the formation of base free germylene, which after 1,2-silyl shift formed products of [2+2] cycloaddition. The crystal of **60** was measured using X-ray technique.



Scheme 52: Reactions of cyclic germylene **7** with TMSCCCCTMS.

Analogous reaction of **7** with 1,4-diphenyl-1,3-butadiyne was carried out. According to the ^{29}Si NMR spectrum only one product was formed, however it was not possible to determine, which one, since its crystallization was unsuccessful (Scheme 53).



Scheme 53: Reactions of cyclic germylene **7** with PhCCCCPh.

2.3.2 NMR Spectroscopy

The ^{29}Si NMR spectrum of **51**, which is the product of the reaction between cyclic germylene adduct **7** and trimethylsilylacetylene, shows five resonances, as expected. Three of them located at: -6.9 , -12.1 and -12.7 ppm are assigned to trimethylsilyl groups, the signal at -28.2 ppm originates from silicon atom in the five-membered ring and the peak at -66.4 ppm is assigned to quaternary silicon. The latter resonance is about 20 ppm up-field shifted compared to the corresponding resonance within four-membered $-\text{C}=\text{C}-\text{Ge}-\text{Si}-$ ring. The signal of the vinyl protons are observed at 7.80 ppm in the ^1H NMR spectrum.

The ^{29}Si NMR spectrum of the mixture resulting from the reaction of **7** with phenylacetylene exhibits twelve resonances (Figure 30). The signals at -66.9 ppm, -27.3 ppm and the two peaks in the vicinity of -12 ppm are assigned to the symmetric compound **52**, the remaining resonances originate from asymmetric product **53**.

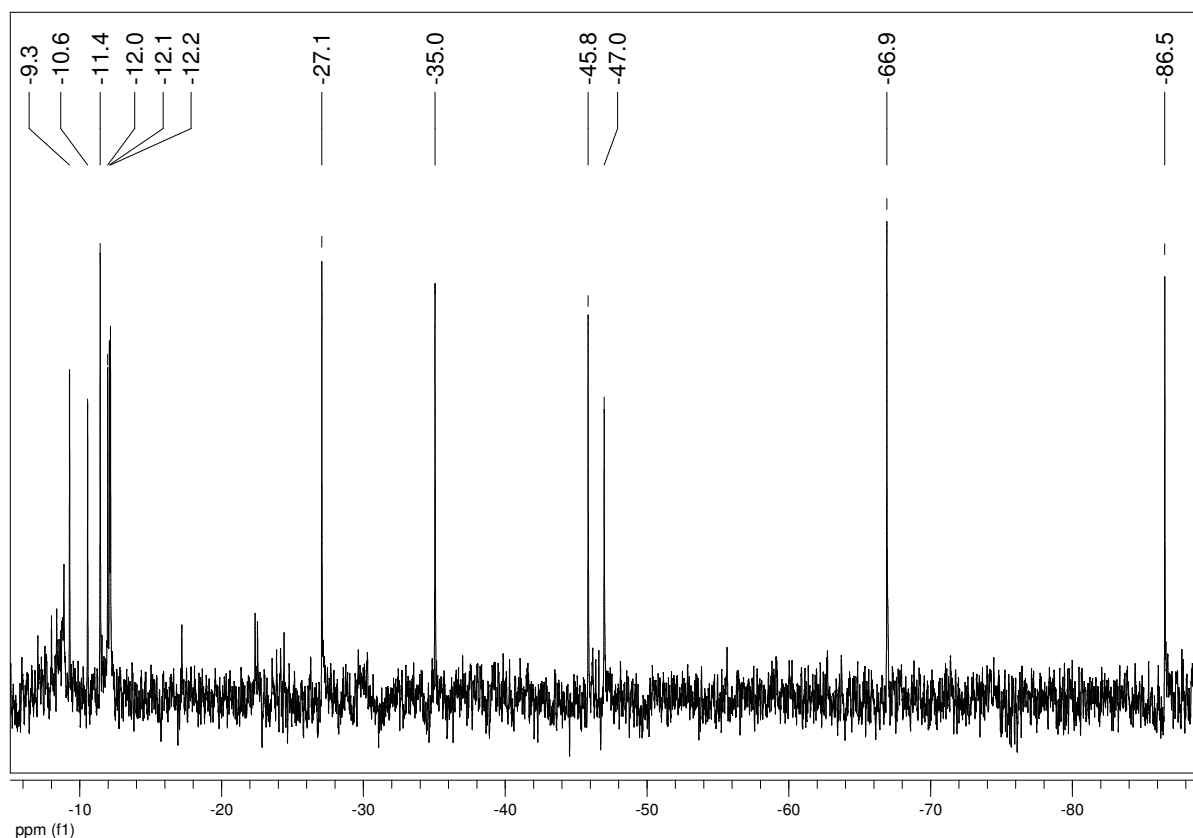


Figure 30: ^{29}Si NMR spectrum of the reaction mixture resulting from the reaction of **7** with PhCCH.

The selective formation of asymmetric product **55** in the reaction of digermylated germylene adduct **54** with phenylacetylene is confirmed by the presence of six resonances in the ^{29}Si NMR spectrum. The four of them located at: -3.3 , -3.7 , -4.7 and -5.5 are assigned to trimethylsilyl groups, the remaining signals at -35.5 and -37.3 ppm characterize silicon of SiMe_2 groups. In the ^1H NMR spectrum, the resonances of the vinyl protons

are observed at 7.41 and 7.78 ppm.

The resonance of quaternary silicon (-120.1 ppm) of the germacyclopropene **56** is 7 ppm down-field shifted compared to corresponding resonance in the starting germylene **7** (-127.1 ppm). This difference is much smaller than it is in the case of corresponding resonances of bis[tris(trimethylsilyl)silyl]germylene \cdot PMe_3 (**18**) (-119.9 ppm) and germacyclopropene **36** (-92.6 ppm). The remaining resonances of **56** are located at -30.3 and -7.3 ppm.

The peaks of digermylated germacyclopropene **57** located at -1.5 and -23.4 ppm are down-field shifted with respect to related resonances of disilylated germacyclopropene **56**, however the same trend was observed before for the triethylphosphine adduct of a five-membered disilylated germylene **7** and its digermylated analog **54** [38].

The ^{29}Si NMR spectrum of **59** exhibits low-field shifted resonances of the silicon atoms within the four-membered rings (18.3 and 3.5 ppm), four resonances at -2.5 , -2.8 , -3.2 and -4.5 ppm represent trimethylsilyl groups (Figure 31). The ^{29}Si NMR suggests the presence of four non-equivalent trimethylsilyl groups. The ^1H NMR spectrum confirmed the presence of different SiMe_3 group as well as showed four signals corresponding to SiMe_2 group located at: 0.60 , 0.64 , 0.91 and 0.94 ppm.

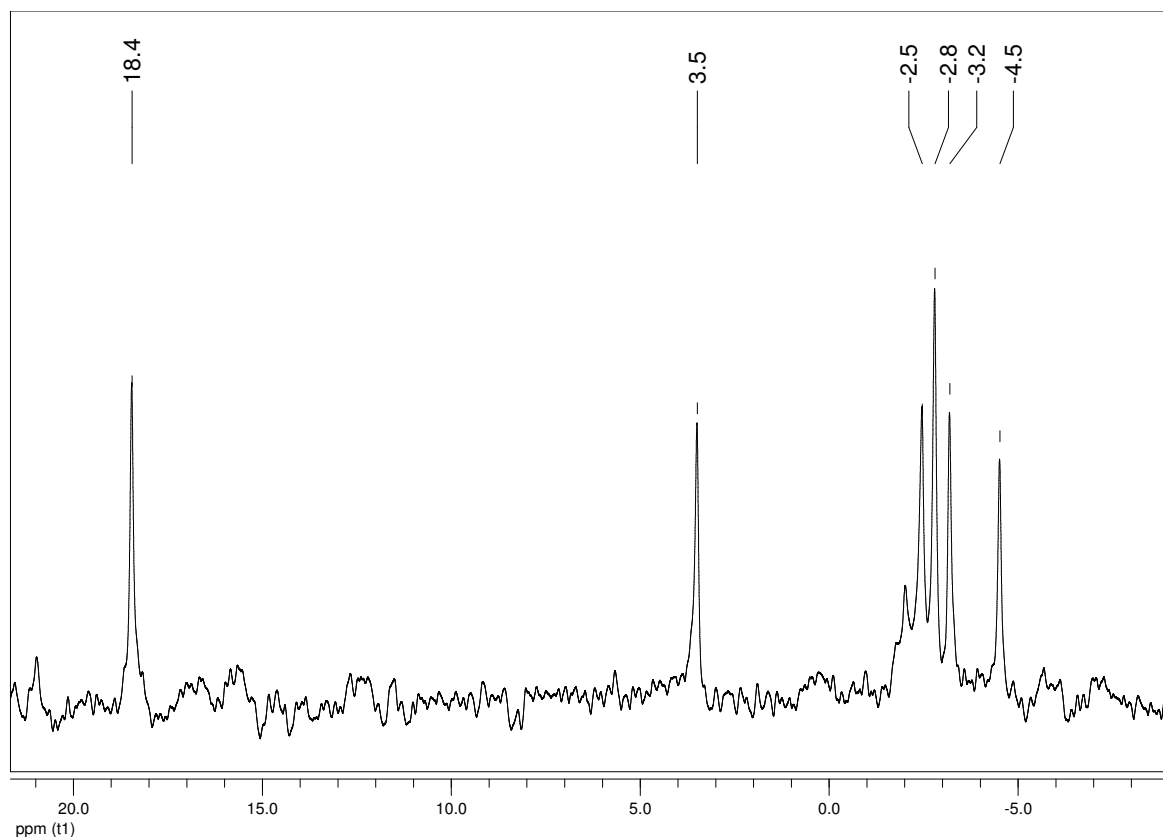


Figure 31: ^{29}Si NMR spectrum of **57**.

2.3.3 Crystallography

Colorless crystals suitable for X-ray study were obtained during storage in pentane at $-35\text{ }^{\circ}\text{C}$ (Figure 32, Table 26). Crystalline **51** has the orthorhombic symmetry with space group Fddd. A spirogermanium atom is a part of two electronically unsaturated identical heterocycles. One carbon atom of the endocyclic C=C double bond is bonded to the germanium atom and to the silyl group, the second one is attached to hydrogen and a quaternary silicon atom. The Ge(1)–C(1) bond yields $1.987(11)\text{ \AA}$ and is shorter compared to Ge–C bond in acyclic germylene adduct **44** ($2.036(3)\text{ \AA}$). The distance between Ge and Si is also smaller than in the starting germylene **7** and yields $2.4016(5)\text{ \AA}$.

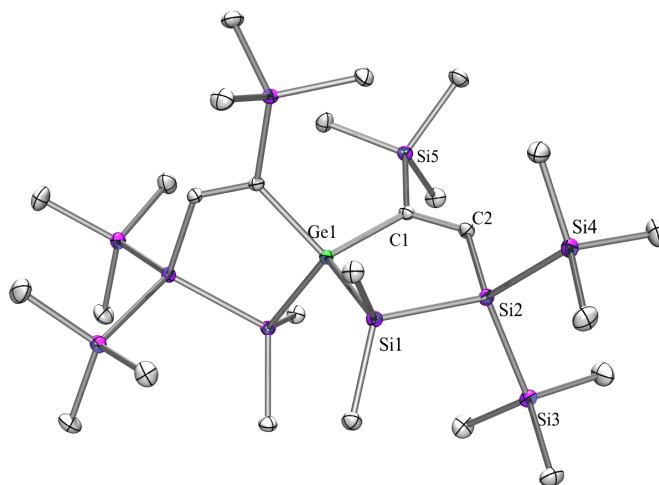


Figure 32: Crystal structure of **51**.

Table 26: Selected bond lengths and angles of **51**.

| Bond | Length [\AA] | Bonds | Angle [$^{\circ}$] |
|-------------|-------------------------|----------------------|----------------------|
| Ge(1)–Si(1) | 2.4016(5) | Si(1)–Ge(1)–C(1) | 99.81(4) |
| Ge(1)–C(1) | 1.987(11) | Ge(1)–C(1)–C(2) | 118.33(9) |
| C(1)–Si(5) | 1.8839(12) | Ge(1)–C(1)–Si(5) | 124.30(6) |
| C(1)–C(2) | 1.3518(17) | Si(5)–C(1)–C(2) | 117.33(9) |
| Si(1)–Si(2) | 2.3387(6) | C(2)–Si(2)–Si(1) | 100.53(4) |
| Si(2)–C(2) | 1.8953(12) | C(2)–Si(2)–Si(4) | 111.14(4) |
| Si(2)–Si(3) | 2.3473(5) | C(2)–Si(2)–Si(3) | 106.13(4) |
| Si(2)–Si(4) | 2.3470(6) | Si(4)–Si(2)–Si(3) | 111.92(2) |
| | | Ge(1)–Si(1)–Si(2) | 92.817(16) |
| | | C(1)#1–Ge(1)–C(1) | 110.65(7) |
| | | C(1)#1–Ge(1)–Si(1)#1 | 99.81(4) |
| | | C(1)–Ge(1)–Si(1)#1 | 115.63(3) |
| | | Si(1)#1–Ge(1)–Si(1) | 116.01(2) |

Compound **53** crystallized in monoclinic space group P2(1)/n (Figure 33, Table 27). A spirogermanium atom connects the four-membered unsaturated with the six-membered unsaturated ring. The acute endocyclic Si(6)–Ge(1)–C(19) angle of 72.70(14)° reveals that the germanium atom has a strongly distorted tetrahedral environment. The Ge(1)–Si(6) bond (2.4276(15) Å) is longer than Ge(1)–Si(1) bond (2.3899(15) Å), what combined with slightly elongated C(19)–C(20) bond (1.346(7) Å) with respect to C(11)–C(12) bond length of 1.342(7) ppm suggested steric stress within four-membered ring part of the molecule.

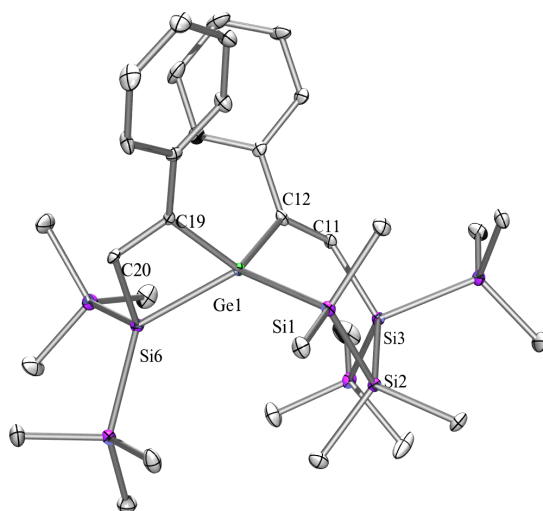


Figure 33: Crystal structure of **53**.

Table 27: Selected bond lengths and angles of **53**.

| Bond | Length [Å] | Bonds | Angle [°] |
|-------------|--------------|-------------------|-------------|
| Ge(1)–C(19) | 2.001(5) | Si(1)–Ge(1)–C(12) | 103.51(14) |
| Ge(1)–C(12) | 1.987(5) | C(12)–Ge(1)–C(19) | 116.7(2) |
| Ge(1)–Si(1) | 2.3899(15) | C(19)–Ge(1)–Si(1) | 111.31(14) |
| Ge(1)–Si(6) | 2.4276(15) | C(12)–Ge(1)–Si(6) | 120.68(14) |
| Si(1)–Si(2) | 2.3271(19) | Si(6)–Ge(1)–C(19) | 72.70(14) |
| Si(2)–Si(3) | 2.3568(19) | Si(1)–Ge(1)–Si(6) | 128.48(5) |
| Si(3)–C(11) | 1.889(5) | Ge(1)–C(12)–C(11) | 123.5(4) |
| C(11)–C(12) | 1.342(7) | Ge(1)–Si(1)–Si(2) | 98.98(6) |
| Si(6)–C(20) | 1.891(5) | Si(1)–Si(2)–Si(3) | 103.35(7) |
| C(19)–C(20) | 1.346(7) | Si(2)–Si(3)–C(11) | 114.50(16) |
| | | Si(3)–C(11)–C(12) | 134.7(4) |
| | | Ge(1)–C(19)–C(20) | 103.6(3) |
| | | C(19)–C(20)–Si(6) | 108.6(4) |
| | | C(20)–Si(6)–Ge(1) | 74.92(16) |

Colorless crystals of **55** suitable for X-ray study were obtained during storage in pentane at $-35\text{ }^{\circ}\text{C}$ (Figure 34, Table 28). Crystalline **55** has the symmetry of monoclinic space group $P2(1)/n$. Similar to the compound **53**, the germanium atom in **55** has a strongly distorted tetrahedral environment with acute endocyclic $\text{Ge}(2)\text{--Ge}(1)\text{--C}(9)$ angle of $74.07(8)^{\circ}$.

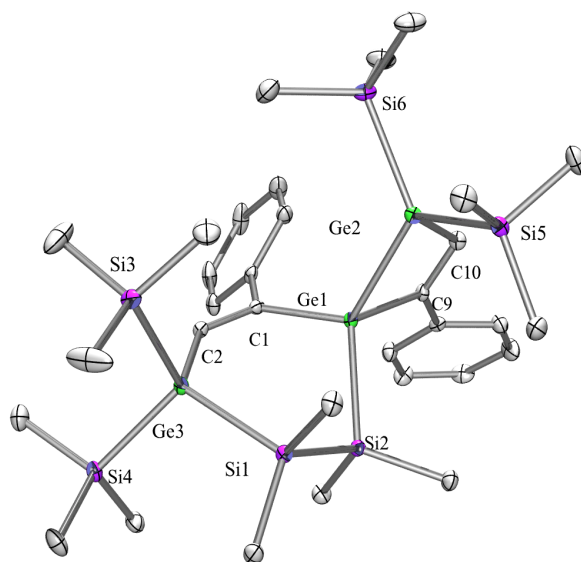


Figure 34: Crystal structure of **55**.

Table 28: Selected bond lengths and angles of **55**.

| Bond | Length [Å] | Bonds | Angle [°] |
|--------------|--------------|-------------------|-------------|
| Ge(1)–Ge(2) | 2.4741(6) | Ge(1)–Ge(2)–C(10) | 72.63(8) |
| Ge(1)–C(9) | 1.995(3) | Ge(2)–Ge(1)–C(9) | 74.07(8) |
| Ge(2)–C(10) | 1.976(3) | Ge(2)–C(10)–C(9) | 108.6(2) |
| Ge(2)–Si(6) | 2.4025(9) | Ge(1)–C(9)–C(10) | 104.4(2) |
| Ge(2)–Si(5) | 2.3895(10) | Ge(2)–Ge(1)–C(1) | 119.71(7) |
| Ge(1)–C(1) | 1.989(3) | Ge(2)–Ge(1)–Si(2) | 127.29(3) |
| Ge(1)–Si(2) | 2.3937(9) | Ge(1)–C(1)–C(2) | 123.6(2) |
| C(1)–C(2) | 1.334(4) | C(1)–C(2)–Ge(3) | 133.6(2) |
| C(2)–Ge(3) | 1.973(3) | C(2)–Ge(3)–Si(1) | 113.99(8) |
| Ge(3)–Si(1) | 2.3925(9) | Si(1)–Si(2)–Ge(1) | 99.49(4) |
| Si(11)–Si(2) | 2.3275(12) | C(1)–Ge(1)–C(9) | 116.33(11) |
| C(9)–C(10) | 1.340(4) | C(1)–Ge(1)–Si(2) | 104.54(8) |
| | | C(9)–Ge(1)–Si(2) | 11.73(8) |

56 crystallized in monoclinic space group $C2/c$ (Figure 35, Table 29). The Ge(1)–C(1) distance is slightly shorter than in the case of bis[tris(trimethylsilyl)silyl]germacyclopropene (**36**) and yields 1.958(2) Å. The C–Ge–C angle is almost the same as the related angle in **36** and measures 39.21(13)°.

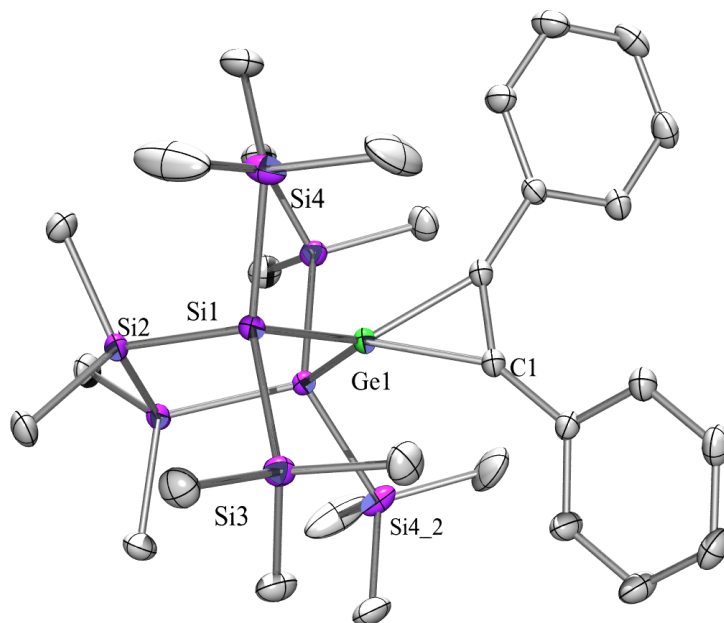


Figure 35: Crystal structure of **56**.

Table 29: Selected bond lengths and angles of **56**.

| Bond | Length [Å] | Bonds | Angle [°] |
|-------------|--------------|--------------------|-------------|
| Ge(1)–Si(1) | 2.3861(8) | C(1)–Ge(1)–C(1)#1 | 39.21(13) |
| Ge(1)–C(1) | 1.958(2) | C(1)–Ge(1)–Si(1) | 119.27(8) |
| Si(1)–Si(3) | 2.3461(11) | C(1)–Ge(1)–Si(1)#1 | 122.61(8) |
| Si(1)–Si(4) | 2.3381(12) | Ge(1)–Si(1)–Si(2) | 101.54(4) |
| | | Ge(1)–C(2)–C(1)#1 | 70.39(7) |
| | | C(1)#1–Ge(1)–Si(1) | 122.60(8) |

Both compounds, resulted from heating up of germacyclopropenes, **58** (Figure 36, Table 30) and **59** (Figure 37, Table 31) crystallized in monoclinic space group P2(1)/n. This spirogermanium compounds contain two different four-membered rings. The endocyclic C=C bond in **58** with length 1.361(5) Å is shorter than the related bond in **59** measuring 1.380(10) Å. The length of Ge(1)-Ge(2) bond in **59** measuring 2.4644(11) Å is slightly smaller than Ge(2)-Ge(3) bond length (2.4757(11) Å).

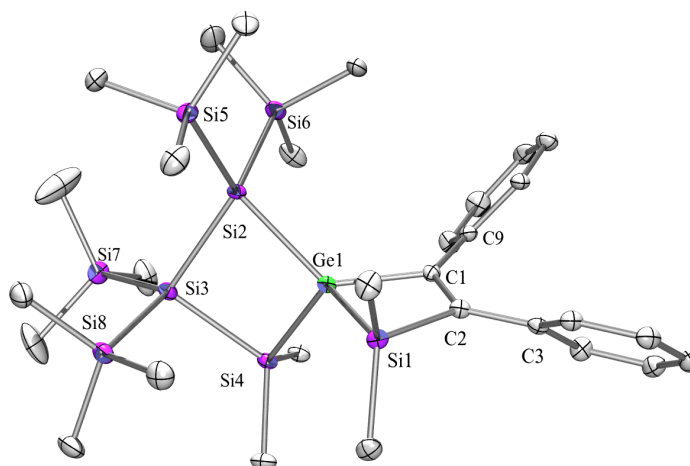


Figure 36: Crystal structure of **58**.

Table 30: Selected bond lengths and angles of **58**.

| Bond | Length [Å] | Bonds | Angle [°] |
|-------------|--------------|-------------------|-------------|
| Ge(1)–Si(1) | 2.3758(12) | Si(1)–Ge(1)–C(1) | 72.15(11) |
| Ge(1)–Si(2) | 2.4217(12) | Si(1)–Ge(1)–Si(2) | 131.33(4) |
| Ge(1)–Si(4) | 2.3984(12) | Si(1)–Ge(1)–Si(4) | 119.68(4) |
| Ge(1)–C(1) | 2.002(4) | Si(4)–Ge(1)–Si(2) | 88.17(4) |
| Si(1)–C(2) | 1.892(4) | C(1)–Ge(1)–Si(2) | 129.02(11) |
| C(2)–C(1) | 1.361(5) | C(1)–Ge(1)–Si(4) | 121.30(10) |
| C(1)–C(9) | 1.476(5) | Ge(1)–Si(1)–C(2) | 77.59(11) |
| C(2)–C(3) | 1.476(5) | Si(1)–C(2)–C(1) | 104.7(3) |
| Si(3)–Si(2) | 2.3818(15) | Ge(1)–C(1)–C(2) | 105.2(3) |
| Si(3)–Si(4) | 2.3557(16) | C(1)–C(2)–C(3) | 127.1(3) |
| Si(2)–Si(5) | 2.3605(16) | C(9)–C(1)–C(2) | 127.9(3) |
| Si(2)–Si(6) | 2.3608(16) | Ge(1)–Si(2)–Si(3) | 86.42(4) |
| Si(3)–Si(7) | 2.3586(16) | Si(2)–Si(3)–Si(4) | 90.12(5) |
| Si(3)–Si(8) | 2.3512(16) | Ge(1)–Si(4)–Si(3) | 87.54(5) |
| | | Ge(1)–C(1)–C(9) | 126.9(3) |

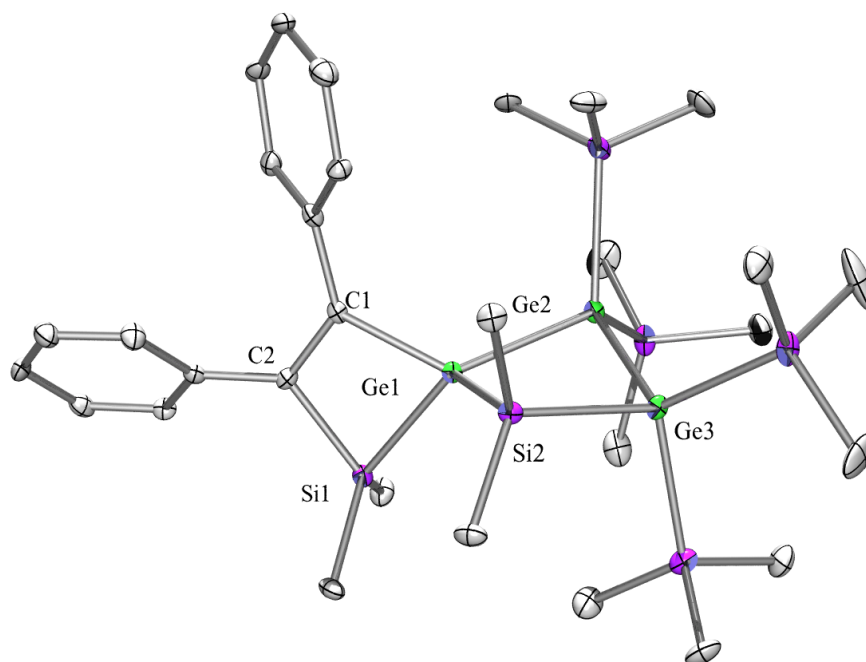


Figure 37: Crystal structure of **59**.

Table 31: Selected bond lengths and angles of **59**.

| Bond | Length [Å] | Bonds | Angle [°] |
|-------------|--------------|-------------------|-------------|
| Ge(1)–Ge(2) | 2.4644(11) | Ge(1)–Ge(2)–Ge(3) | 85.47(4) |
| Ge(1)–Si(1) | 2.376(2) | Ge(2)–Ge(3)–Si(2) | 88.95(6) |
| Ge(2)–Ge(3) | 2.4757(11) | Si(1)–Ge(1)–Ge(2) | 130.56(6) |
| Ge(1)–Si(2) | 2.392(2) | Si(1)–Ge(1)–C(1) | 72.7(2) |
| Ge(1)–C(1) | 1.988(7) | Si(1)–Ge(1)–Si(2) | 119.67(7) |
| C(2)–C(1) | 1.380(10) | Ge(1)–Si(2)–Ge(3) | 89.00(7) |
| Ge(3)–Si(2) | 2.391(2) | C(1)–Ge(1)–Si(2) | 121.08(19) |
| Si(1)–C(2) | 1.895(7) | C(1)–Ge(1)–Ge(2) | 128.1(2) |

Compound **60** crystallizes in triclinic space group $P\bar{1}$ (Figure 38, Table 32). Compound **60** contains a five-membered ring, annulated with a four membered cycle along a Ge–Si bond. The length of C(17)=C(18) double bond is greater than the length of double bond in germacyclopropenes **36**, **47**, **56** and **57** and yields 1.364(4) Å. The distance between Ge(1) and Si(1) measures 2.3885(8) Å, and is smaller than corresponding distance in **53**.

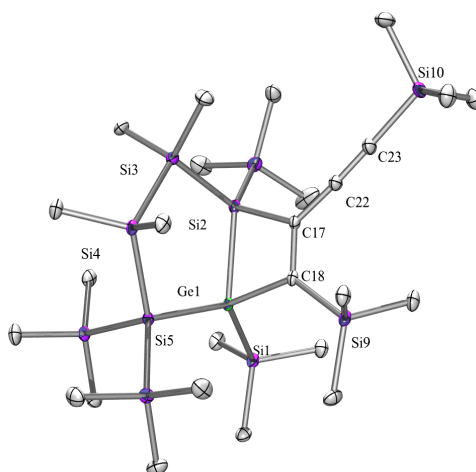


Figure 38: Crystal structure of **60**.

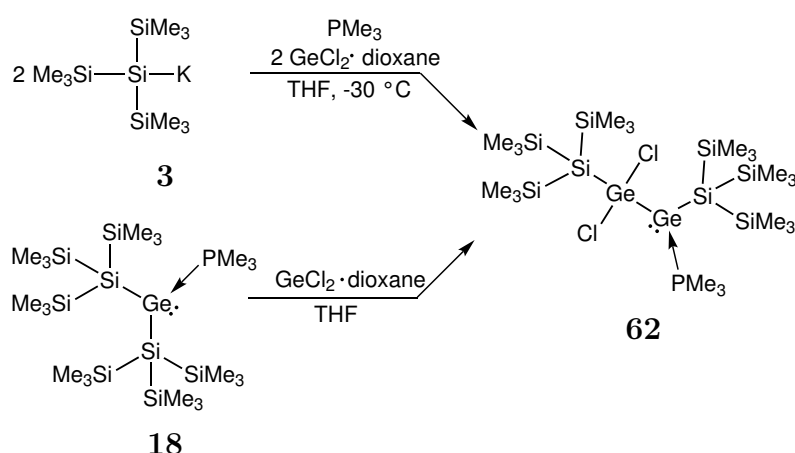
Table 32: Selected bond lengths and angles of **60**.

| Bond | Length [Å] | Bonds | Angle [°] |
|--------------|--------------|--------------------|-------------|
| Ge(1)–Si(1) | 2.3885(8) | Si(2)–Ge(1)–Si(5) | 106.25(3) |
| Ge(1)–Si(5) | 2.4022(8) | Si(2)–Ge(1)–Si(1) | 116.86(3) |
| Ge(1)–Si(2) | 2.4100(9) | Si(2)–Ge(1)–C(18) | 73.63(8) |
| Ge(1)–C(18) | 2.011(3) | Ge(1)–Si(5)–Si(4) | 103.47(3) |
| Si(2)–Si(3) | 2.3368(10) | Si(5)–Si(4)–Si(3) | 109.25(4) |
| Si(3)–Si(4) | 2.3553(11) | Si(3)–Si(2)–Ge(1) | 108.59(4) |
| C(18)–Si(9) | 1.871(3) | Si(3)–Si(2)–C(17) | 108.09(8) |
| C(18)–C(17) | 1.364(4) | Ge(1)–Si(2)–C(17) | 75.31(8) |
| C(17)–Si(2) | 1.907(3) | Si(2)–C(17)–C(18) | 108.16(18) |
| C(17)–C(22) | 1.428(4) | Ge(1)–C(18)–C(17) | 102.74(17) |
| C(22)–C(23) | 1.210(4) | C(17)–C(22)–C(23) | 175.6(3) |
| C(23)–Si(10) | 1.829(3) | C(22)–C(23)–Si(10) | 175.6(3) |
| | | Si(9)–C(18)–C(17) | 125.65(19) |
| | | C(18)–Ge(1)–Si(1) | 109.96(7) |
| | | C(18)–Ge(1)–Si(5) | 115.90(7) |
| | | Si(1)–Ge(1)–Si(5) | 123.68(3) |
| | | Si(2)–Si(3)–Si(4) | 105.58(4) |

2.4 Reactions of tetrylene adducts with group 14 halides

2.4.1 Synthesis

Reaction of two equivalents of tris(trimethylsilyl)silyl potassium (**3**) with two equivalents of germanium dichloride · dioxane and one equivalent of trimethylphosphine led to the formation of dichloro[tris(trimethylsilyl)silyl]germyl[tris(trimethylsilyl)silyl]germylene · PMe₃ adduct (**62**) (upper reaction in Scheme 54). The same product was obtained in the reaction of trimethylphosphine adduct of bis[tris(trimethylsilyl)silyl]germylene (**18**) with one equivalent of GeCl₂ · dioxane in THF at room temperature (lower reaction in Scheme 54). Although the ²⁹Si NMR spectra of both reaction mixtures are remarkably clean, compound **62** was isolated in low yield (close to 40 %).



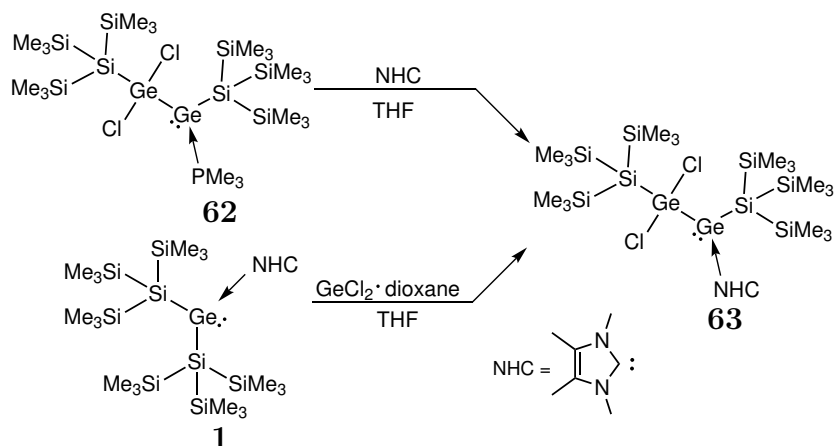
Scheme 54: Synthesis of dichlorogermyl substituted germylene PMe₃ adduct **62**.

Compound **62** contains two non-equivalent germanium atoms. The tetracoordinated germanium atom in the oxidation state IV is bonded to two chloride atoms, the second germanium atom and a tris(trimethylsilyl)silyl group. The tricoordinated germanium in oxidation state II is bonded to the tetracoordinated germanium atom, one trimethylphosphine ligand and a tris(trimethylsilyl)silyl group. **62** is not stable and even after storage at low temperature decomposes to tris(trimethylsilyl)silyl chloride. Nevertheless, a few crystals suitable to X-ray study were obtained and the crystal structure of **62** was determined.

The reaction between **18** and GeCl₂ · dioxane should be considered as an insertion of a germanium dichloride into a Ge–Si bond. It is the first known example of this type of insertion. However similar insertion of GeCl₂ into Ge–NHC bond with simultaneous preservation of the lone pair at germanium atom was observed before [85].

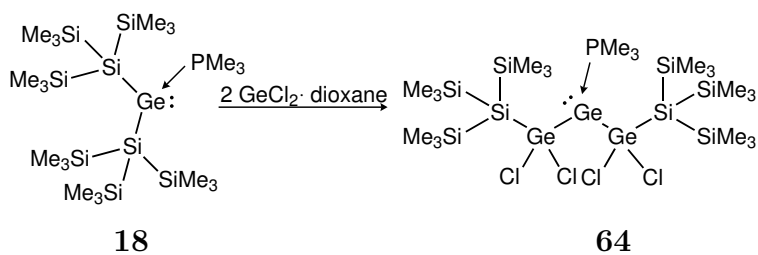
The addition of N-heterocyclic carbene into the stirring solution of α -dichlorogermyl substituted germylene PMe₃ adduct **62** led to the exchange of the Lewis base, that results in the formation of an NHC adduct of germylene **63** (upper reaction in Scheme 55). Compound **63** was also obtained in the reaction of NHC adduct of bis[tris(trimethylsilyl)silyl]germylene (**1**) with dioxane complex of germanium dichloride (lower reaction in Scheme 55). In that reaction GeCl₂ was inserted into Ge–Si bond of the NHC adduct of a germylene **1**,

in contrast to the analogous reaction of **1** with acetylenes, in which **1** was unreactive. Surprisingly, substitution of PMe_3 with NHC did not result in stabilization of the germylene, as it was the case for other germylenes. All attempts to crystallize **63** were unsuccessful and after few days in the reaction mixture tris(trimethylsilyl)silyl chloride was observed based on the ^{29}Si NMR spectrum.



Scheme 55: Synthesis of α -dichlorogermylene substituted germylene NHC adduct (**63**)

Reactions of trimethylphosphine adduct of germylene **18** with two equivalents of germanium dichloride \cdot dioxane led to the formation of bis{dichloro[tris(trimethylsilyl)silyl]germyl}germylene \cdot PMe_3 (**64**) (Scheme 56). Compound **64** is even less stable than the monoinserted germylene **62** and it was isolated in 15 % yield, nevertheless a few crystals suitable to X-ray study were obtained and the structure of **64** was determined.



Scheme 56: Synthesis of diinserted germylene **64**.

All above described compounds are potential precursors for preparation of digermenes. The reduction of **62** and **64** with: KC_8 and Mg resulted in the formation of tetrakis(trimethylsilyl)silane, what showed that they are too strong reducing agents. As a weaker reductant Rosenthal's reagent, $\text{Cp}_2\text{Ti}(\text{btmsa})$ was chosen, because of the hope that titanium II might be oxidized to $\text{Cp}_2\text{Ti}^{\text{IV}}\text{Cl}_2$, however in the reaction mixture even traces of non-coordinating bistrimethylsilylacetylene were not detected, what indicates that the titanocene derivative were not oxidized. This lack of success in the reduction of the α -dichlorogermyl substituted germylene PMe_3 adduct extorted the exchange of starting ma-

terial. Submitting a cyclic analog of **62** to the reduction reaction seemed to be a good idea. If GeCl_2 is inserted into Ge-Si bond of the five-membered ring germylene PEt_3 adduct **7**, the six-membered ring germylene adduct, formed in such reaction, should be more stable than the acyclic analog. Thus, reaction of cyclic germylene PEt_3 adduct **7** with dioxane complexes of germanium dichloride was investigated. The reaction proceeded in the optimal way at $-35\text{ }^\circ\text{C}$ using THF as a solvent, other temperatures and solvents resulted in the formation of a side product. The ^{29}Si NMR spectrum of the reaction mixture, with six resonances, fits well to the expected product (Figure 39). Moreover, doublets in the spectrum give an evidence, that coordinated phosphine is present in the solution, what was also confirmed by ^{31}P NMR spectrum. Surprisingly, after crystallization from pentane two different types of pale yellow crystals were formed. The X-ray structure analysis revealed, that instead of the expected six-membered ring, compounds **65** and **66** were present in the reaction mixture (Scheme 58). In spite of many attempts, separation of them was unsuccessful.

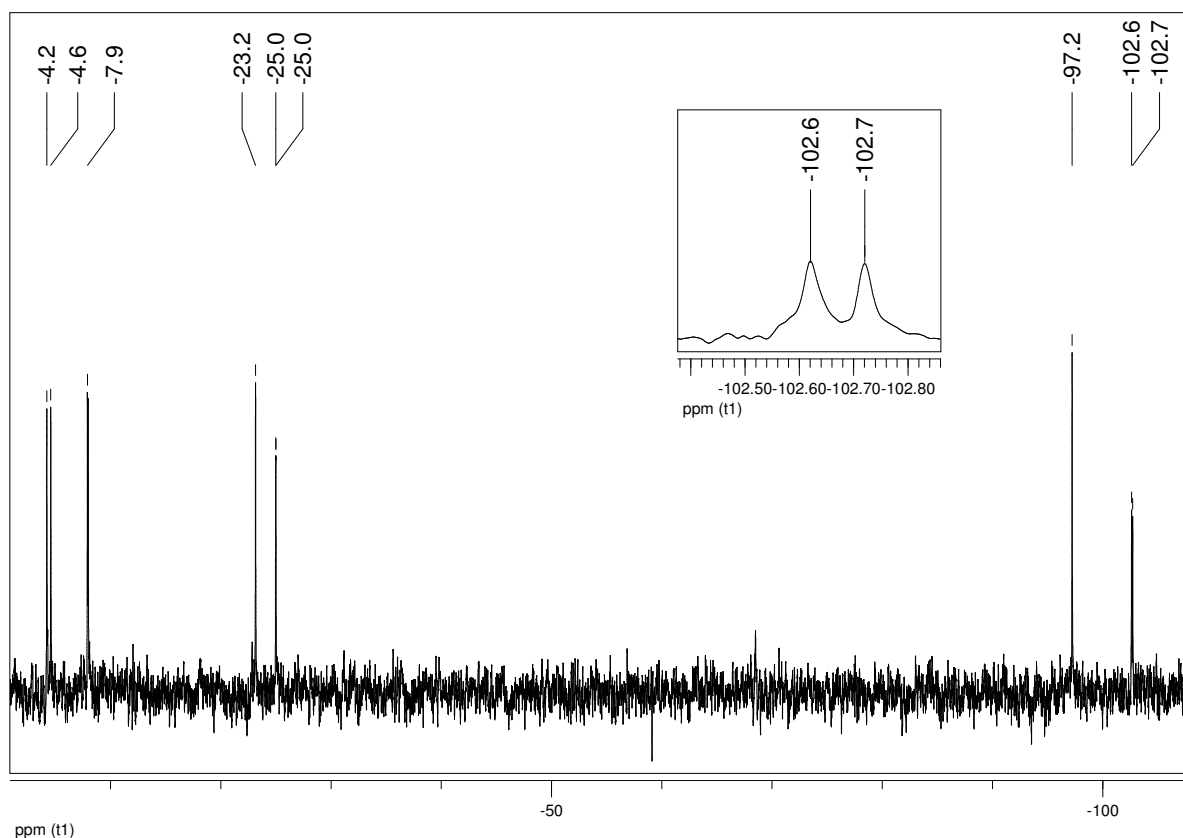
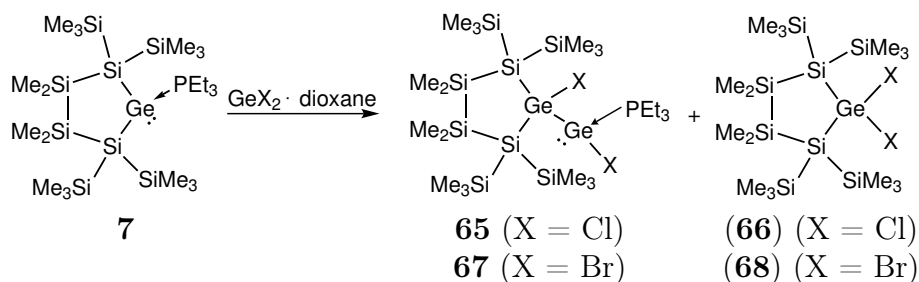


Figure 39: ^{29}Si NMR spectrum of the mixture resulting from the reaction of cyclic germylene **7** with $\text{GeCl}_2 \cdot \text{dioxane}$.

In spite of the fact, that the mechanism of this reaction remains unknown, compound **65** could be considered as a product of the insertion reaction of the five-membered germylene into a Ge-Cl bond of germanium dichloride. Although, such an insertion is already known in the literature [96], we were surprised that the silylated germylene PEt_3 adduct **7** showed



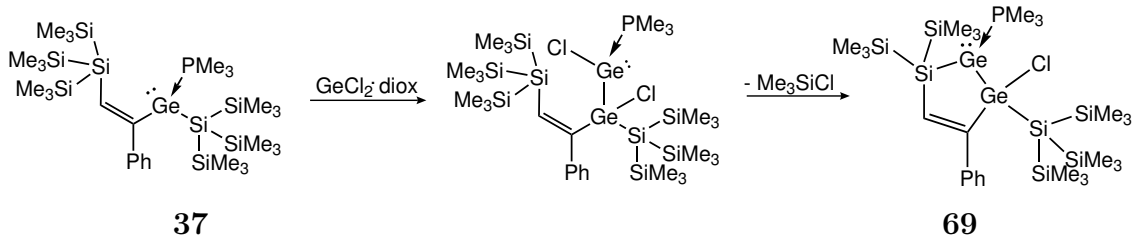
Scheme 58: Reaction of **7** with germanium halides.

different reactivity towards germanium dichloride from that of the acyclic germylene PEt_3 adduct **18**, i. e. **7** is inserted into the polar bond, typically for tetrylenes. Interesting is also the fact, that besides **65**, compound **66** was formed. At the same time, any sign of decomposition such as precipitation and formation of a metallic film was not observed during reaction. On the other hand, the formation of **66** suggests that an additional source of chloride should be present in the reaction mixture. Although both starting materials seem to be clean, when used in another reactions, the first guess was the contamination of $\text{GeCl}_2 \cdot \text{dioxane}$ with HCl or GeCl_4 resulting from its preparation. Thus, reaction of **7** with $\text{GeBr}_2 \cdot \text{dioxane}$ was carried out. The outcome is analogous to that observed for the reaction with dioxane complex of germanium dichloride, i. e. compound **67** and **68** were formed (Scheme 58). Moreover, both reactions are reproducible using different sources of starting materials. In contrast to these results, in the reaction of trimethylphosphine adduct of the five-membered ring stannylene **11** with germanium dichloride dioxane complex in the reaction mixture only one product was detected. The presence of the three resonances in the ^{29}Si NMR spectrum observed at -3.5 , -28.6 and -110.3 ppm, suggests that the GeCl_2 unit has been inserted into the tin–phosphorus bond. This conjecture was confirmed by ^{31}P NMR spectrum, in which only one signal at -0.7 ppm was found. Due to the fast decomposition of this compound, confirmation of the suggested structure by its crystallization and X-ray study was impossible.

The three reaction paths described above between base adduct of tetrylenes and group 14 halides i. e. insertion of GeCl_2 into Ge–Si bond, insertion of germylene into Ge–Cl or Ge–Br bond and proposed insertion of GeCl_2 into Sn–P bond of stannylene suggest that the reaction is sensitive with respect to base adduct of tetrylene. As an extension of this research the attempts to synthesize a compound containing one inserted GeCl_2 unit and one inserted phenylacetylene were carried out.

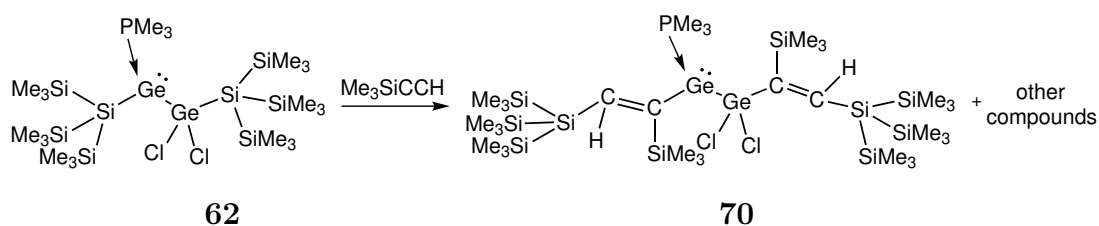
Reaction of the product of a single α -insertion of phenylacetylene into the Si–Ge bond of the bis[tris(trimethylsilyl)silyl]germylene (**37**) with dioxane complex of germanium dichloride, led to the insertion of germylene into a Ge–Cl bond. The formed product is unstable and rearranges to the cyclic germylene **69** *via* elimination of Me_3SiCl (Scheme 59). **69** is stable, probably due to its cyclic structure. Its colorless crystals, suitable for X-ray study, precipitated from a toluene solution at -35 °C.

Attempts to obtain **69** in the reaction of α -dichlorogermylene substituted germylene **62**



Scheme 59: Synthesis of **69**.

with PhCCH was unsuccessful. Not surprisingly, the product of the reaction depends on the order of the insertion. If, the starting material is **62** the insertion of phenylacetylene into the weakest bond, Ge–Ge, will probably occur. The second possible option is an insertion of acetylene into a Ge–Si bond. Although, the ^{29}Si NMR spectrum is remarkably clean, it is impossible to predict which scenario took place. Moreover, it is probable, that the formed product is not stable and its rearrangement occurred. What is clear, based on ^{31}P NMR spectrum, the coordinated phosphine is found in the solution, what suggests that the formed product is a PMe_3 adduct of a germylene. Because of its not successful crystallization, **62** was reacted with tris(trimethylsilyl)acetylene to check the outcome of another reaction of this type. Surprisingly, in this process multiple products were formed (Scheme 60), probably due to non-stoichiometric amount of the acetylene used in this process. Compound **70** was found among the products, but its isolation was impossible. Product **70** formed colorless crystal subjected to X-ray study. Compound **70** contains two inserted trimethylsilylacetylene molecules. Although insertion of the acetylene in the :Ge–Si bond was observed before, the insertion of second moiety in the Ge–Si bond remains enigmatic. There is no evidence in the literature of an insertion of an acetylene into a tetravalent germanium-silicon bond. It suggests that the mechanism of this reaction is different, however impossible to predict at this stage of study.



Scheme 60: Reaction of **62** with trimethylsilylacetylene.

69 did not react with phenylacetylene at room temperature within 5 days. In contrast, **69** treated with germanium dichloride, formed a new compound. The ^{29}Si NMR spectrum (Figure 40) suggests that the actual product contains ring-like structure, while the ^{31}P NMR resonances at -6.7 ppm indicates the presence of a PMe_3 adduct of germylene. There are three plausible pathways for this reaction: either the product of insertion of GeCl_2 into Ge–Ge or Ge–Si bond can be formed or germylene can be inserted into Ge–Cl bond of

GeCl₂ (Scheme 61). The obtained analytical data, however, did not provide the ultimate answer, regarding the final product.

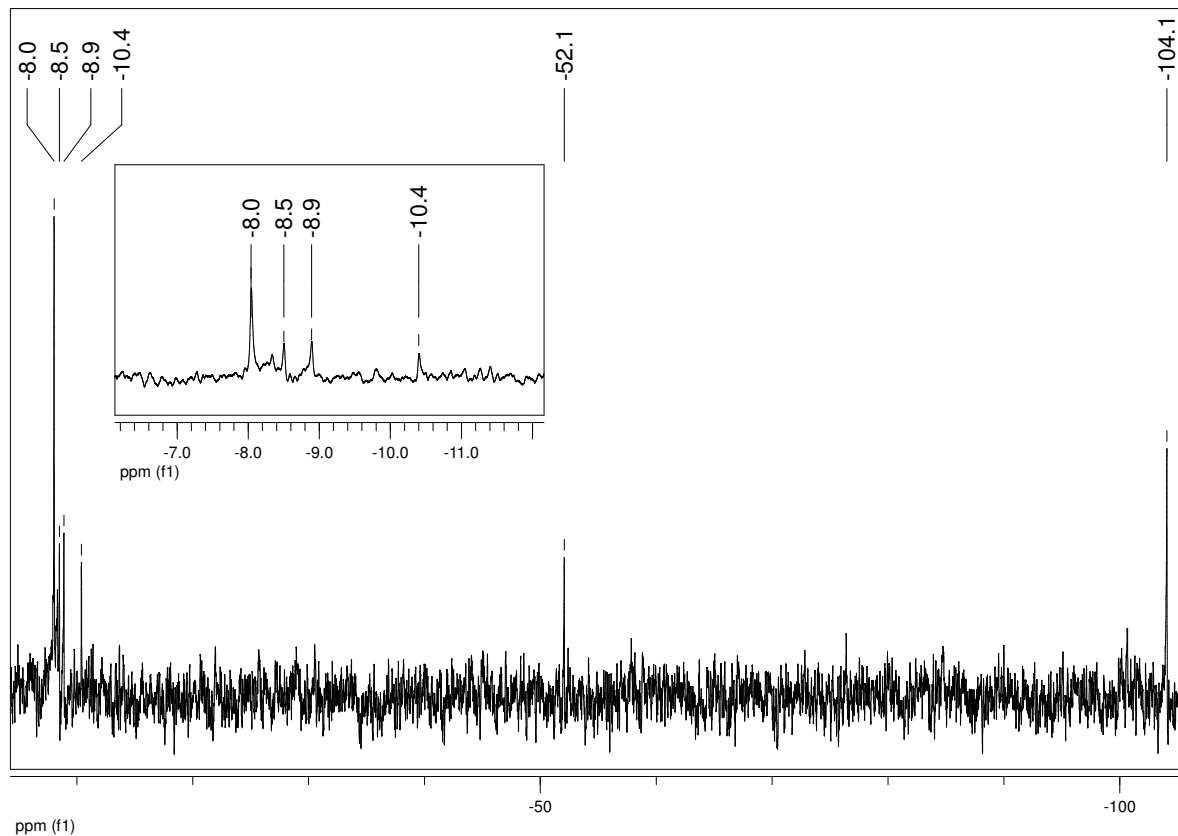
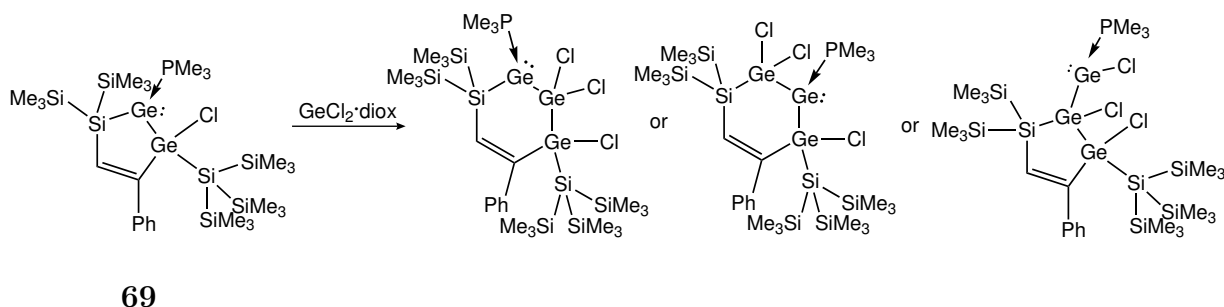


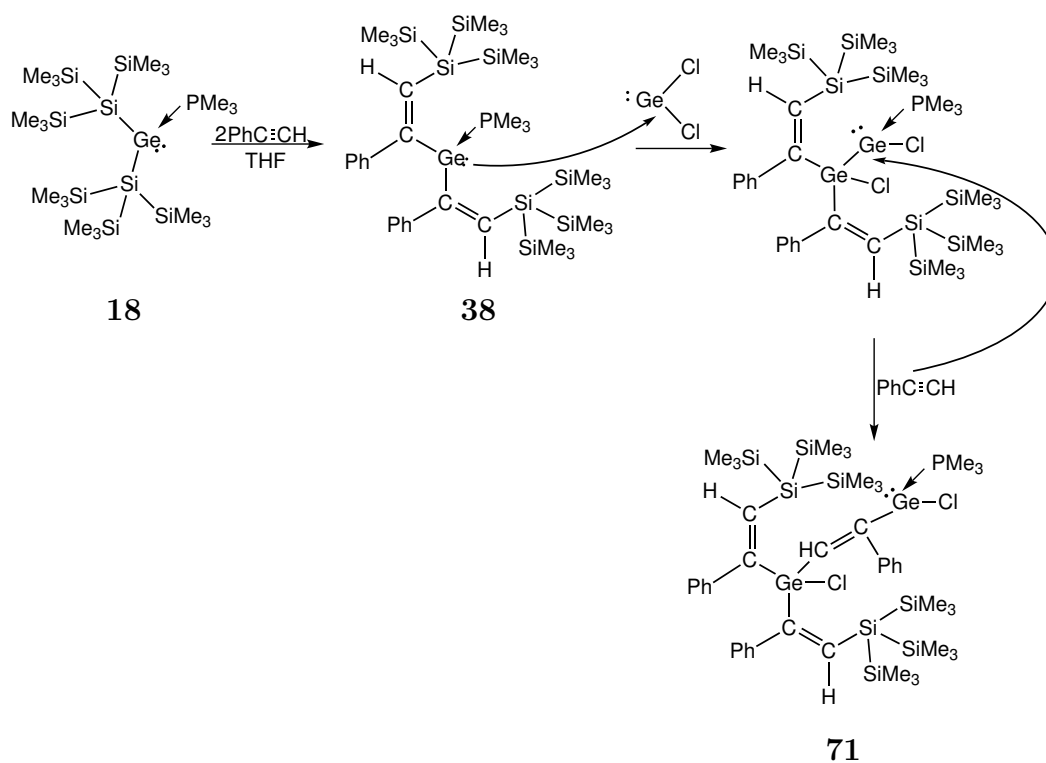
Figure 40: ²⁹Si NMR spectrum of the reaction mixture resulting from the reaction of cyclic germylene **69** with GeCl₂ · dioxane.



Scheme 61: Proposed products resulting from the reaction of **69** with GeCl₂·dioxane.

As mentioned above the trimethylphosphine adduct of bis[tris(trimethylsilyl)silyl]germylene (**18**) was reacted with two equivalents of phenylacetylene and formed the product of α -insertion of phenylacetylene into the Si–Ge bond of germylene adduct **38**. A third

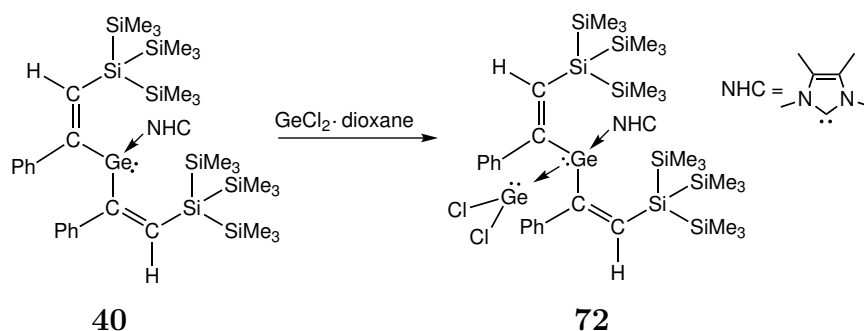
phenylacetylene molecule could not be inserted. However, addition of dioxane complex of germanium dichloride led to the insertion of the doubly inserted germylene adduct **38** into Ge–Cl bond of GeCl₂ and migration of trimethylphosphine to the second germanium atom (Scheme 62). This opened the possibility to insert another phenylacetylene molecule into Ge–Ge bond of the new intermediate germylene and to form **71**. However, the reaction of **38** with dioxane complex of germanium dichloride was not clean and at least few compounds were formed. Surprisingly, clean crystals of **38** treated with GeCl₂·dioxane also formed compound **71**, as confirmed by X-ray study of the crystal, which precipitated after work-up from pentane solution. It suggests an equilibrium probably between PMe₃ adduct of diinserted germylene and more stable PMe₃ adduct of monoinserted germylene. At the same time diinserted germylene could react with GeCl₂·dioxane and subsequently with phenylacetylene, which could be present in the solution due to formation of base adduct of monoinserted germylene. Compound **71** was isolated in very low yield, which did not enable its analytical characterization.



Scheme 62: Sequence formation of **71**

Reaction between the N-heterocyclic carbene adduct of germylene with two inserted phenylacetylene molecules **40** and dioxane complex of germanium dichloride did not lead to the insertion of GeCl₂, which was the case for the PMe₃ adduct of germylene. Instead, germanium dichloride was stabilized by germylene **40** and compound **72** was formed (Scheme 63).

Surprisingly repetition of this reaction with N-heterocyclic carbene adduct of monoin-



Scheme 63: Formation of germylene adduct **72**.

served germylene **42** did not lead to the formation of expected analog of **72**, but trimethylsilyl chloride and tris(trimethylsilyl)silyl chloride were obtained.

2.4.2 NMR Spectroscopy

The ^{29}Si NMR spectrum of α -dichlorogermyl substituted germylene PMe_3 adduct **62** (Figure 41) exhibits significantly down-field shifted resonance of the central silicon atom of the $\text{Si}(\text{SiMe}_3)_3$ ligand bonded to the tetracoordinated germanium atom (-76.7 ppm) as compared to the analogous resonance in tris(trimethylsilyl)silyl[tris(trimethylsilyl)silyl]germane (-122.3 ppm) [97]. The most intensive signal at -8.2 ppm corresponds to the three trimethylsilyl groups attached to the silicon atom bonded to the tetracoordinated germanium atom. The two peaks at -8.7 and -112.6 ppm are doublets that result from the coupling between silicon and phosphorus nuclei. The ^{31}P NMR resonance of **62** is observed at -15.2 ppm.

The ^{29}Si NMR spectrum of N-heterocyclic carbene adduct of doubly inserted germylene **63** shows four resonances, the signals located at -8.3 and -8.9 ppm are assigned to trimethylsilyl group, the peaks at -82.1 and -119.9 ppm are due to central silicons of tris(trimethylsilyl)silyl groups. The resonance of quaternary silicons of N-heterocyclic adduct of monoinserted germylene **63** located at -119.9 and -82.2 ppm are up field shifted by about 7 ppm compared to the related resonance (-112.6 and -76.7 ppm) of PMe_3 adduct analog **62**. Such a huge difference between corresponding resonances of PMe_3 and NHC adducts was not observed before, typically it yields about 2 ppm.

The ^{29}Si NMR spectrum of **64** shows two resonances: at -8.0 and -73.0 ppm, as expected. The signal, which originates from the central silicon atom (-73.0 ppm) is down-field shifted by about 5.7 ppm compared to the silicon bonded to the tetracoordinated germanium in **62**. The ^{31}P NMR spectrum reveals the up-field shifted resonance of -8.7 ppm compared to related signal of **62** (-15.2 ppm). The ^1H NMR and ^{13}C NMR chemical shifts are in their expected ranges.

Moving on to the product of the insertion of cyclic germylene into Ge–Cl bond of germanium dichloride, **65**, the resonance of quaternary silicon located at -102.6 ppm is by about 25 ppm up-field shifted compared to the corresponding resonance in the start-

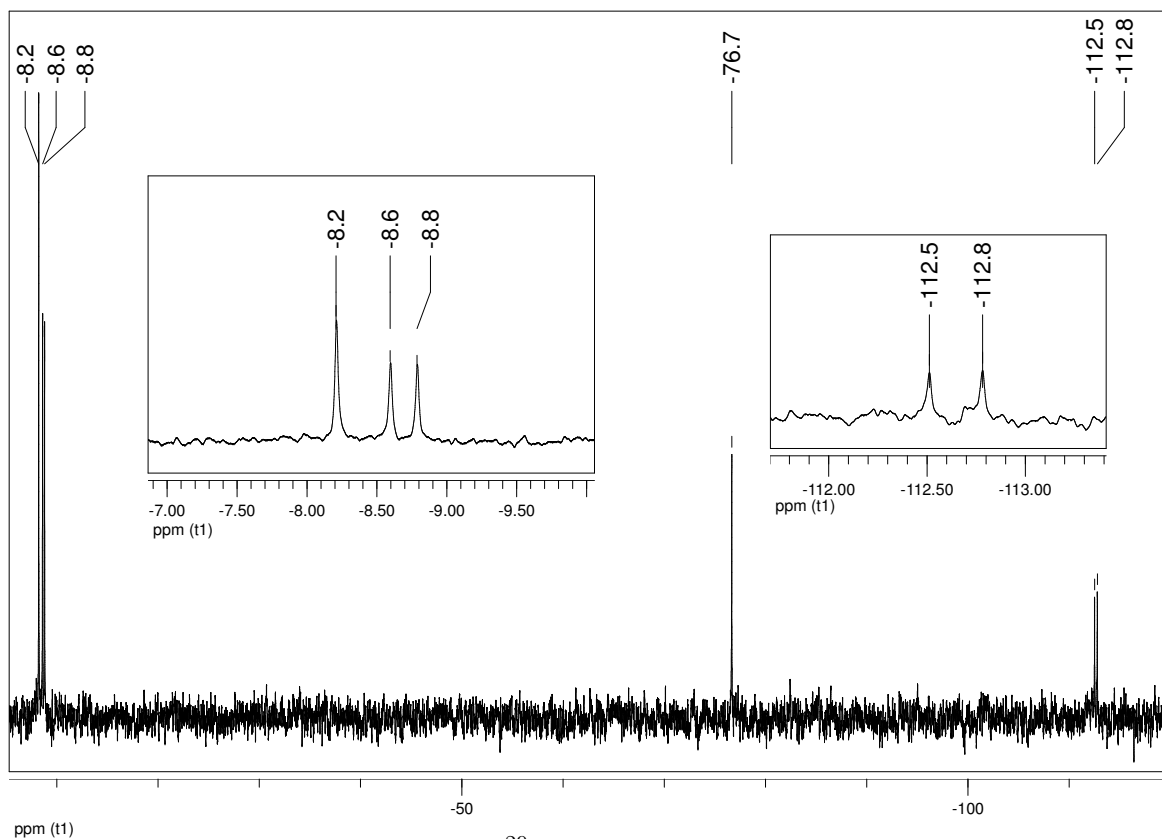


Figure 41: ^{29}Si NMR spectrum of **62**.

ing material **7** (-127.1 ppm). The remaining resonances are located at -25.0 and -4.6 and -4.4 ppm. Due to the presence in the compound coordinating phosphine, all above described resonances have multiplicity of two. In ^{31}P NMR the phosphorus atom resonates at 9.7 ppm. The signals originated from dichlorogermanium compound **66**, are observed at -97.2 , -23.2 and -7.9 ppm in ^{29}Si NMR spectrum.

Similarity of the ^{29}Si NMR spectrum of the mixture resulting from the reaction of **7** with $\text{GeBr}_2 \cdot \text{dioxane}$ to the ^{29}Si NMR spectrum described above (and shown in Figure 39) suggests that similar compounds were created in both reactions, as expected. The three doublets at -7.6 , -25.6 and -102.0 ppm result from the product of the insertion germylene into $\text{Ge}-\text{Br}$ bond (**67**), the three singlets at -3.5 , -22.6 and -95.1 ppm represent dibromogermanium compound **68**.

The ^{29}Si NMR spectrum of cyclic germylene PMe_3 adduct **69** shows five resonances. The doublet at -50.2 ppm originates from the silicon atom within the five-membered ring, two doublets at -11.1 and -11.6 ppm represent trimethylsilyl group attached to the silicon in the ring. The doublet at -100.6 ppm and singlet at -8.7 ppm are due to the tris(trimethylsilyl)silyl group. The resonance of a quaternary silicon -100.6 is by about 20 ppm down field shifted compared to the analogous resonance in tri(trimethylsilyl)[tris(trimethylsilyl)silyl]germane [97] and 1,1,1-tris(trimethylsilyl)-2,2-dichloro-2-methyldisilane [98]. The resonance of the vinylic hydrogen is observed at 7.07 ppm in ^1H NMR. ^{31}P NMR

spectrum of **69** reveals a resonance of -8.7 ppm.

The ^{29}Si NMR resonances of PMe_3 adduct of germylene **71** (-84.9 and -11.5 ppm) are almost the same as those of N-heterocyclic carbene adduct **72** (-84.3 and -12.4 ppm) and PMe_3 adduct of doubly inserted germylene **38** (-86.2 and -12.9 ppm), as expected.

2.4.3 Crystallography

Yellow crystals of α -dichlorogermyl substituted germylene PMe_3 adduct **62** precipitated from pentane solution over a period of 12 hours. Crystal was subjected to X-ray structure analysis (Figure 42, Table 33). Two independent molecules were found in the asymmetric unit cell, crystalline **62** belongs to the triclinic space group $P\bar{1}$. The length of the germanium–germanium bond yields 2.521 \AA . The distance between the tetracoordinated germanium (labeled Ge(2) in Figure 42) and the silicon atom Si(6) yields 2.428 \AA and is similar to the distance between the tricoordinated germanium Ge(1) and the silicon atoms Si(1), which yields 2.489 \AA .

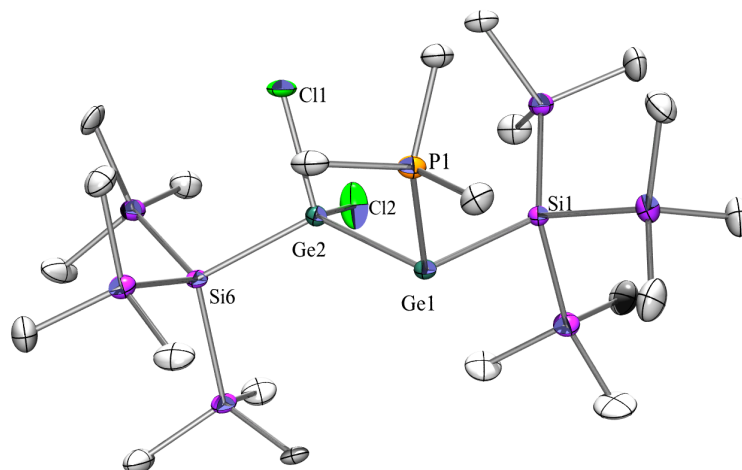


Figure 42: Crystal structure of **62**.

Table 33: Selected bond lengths and angles of **62**.

| Bond | Length [\AA] | Bonds | Angle [$^\circ$] |
|-------------|-------------------------|-------------------|--------------------|
| Ge(1)–Ge(2) | 2.5210(18) | Ge(2)–Ge(1)–Si(1) | 105.64(9) |
| Ge(1)–Si(1) | 2.489(3) | Ge(1)–Ge(2)–Si(6) | 125.38(10) |
| Ge(2)–Si(6) | 2.428(3) | Si(1)–Ge(1)–P(1) | 99.69(11) |
| Ge(1)–P(1) | 2.480(3) | Ge(1)–Ge(2)–Cl(1) | 116.19(10) |
| Ge(2)–Cl(1) | 2.253(3) | Ge(1)–Ge(2)–Cl(2) | 108.28(12) |
| Ge(2)–Cl(2) | 2.208(4) | Cl(1)–Ge(2)–Cl(2) | 99.49(17) |

Pale yellow crystals of **64** suitable for X-ray measurement were obtained during storage in pentane at $-35\text{ }^{\circ}\text{C}$ (Figure 43, Table 34). The compound crystallizes in the orthorhombic space group $P2(1)2(1)2(1)$. The germanium–silicon bonds (2.3966 \AA and 2.4101 \AA) are slightly shorter than the analogous bonds in compound **62**. The distances between two germanium atoms ($2.4980(9)\text{ \AA}$ and $2.5114(9)\text{ \AA}$) are shorter than related distances in linear tetrachlorodigermene adduct $\text{IPr}\cdot\text{GeCl}_2\text{GeCl}_2$, which yields $2.6304(9)\text{ \AA}$ [85]. The germanium–phosphorus bond is shorter by about 0.1 \AA than that in compound **62**.

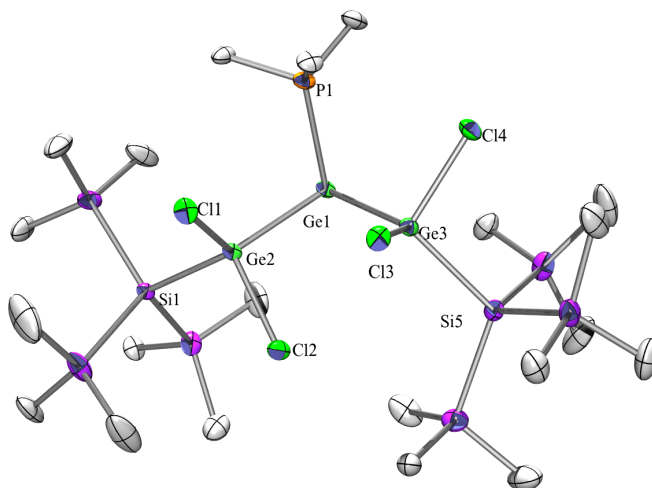


Figure 43: Crystal structure of **64**.

Table 34: Selected bond lengths and angles of **64**.

| Bond | Length [\AA] | Bonds | Angle [$^{\circ}$] |
|-------------|-------------------------|-------------------|----------------------|
| Ge(1)–P(1) | 2.3900(16) | P(1)–Ge(1)–Ge(2) | 96.91(5) |
| Ge(1)–Ge(2) | 2.4980(9) | P(1)–Ge(1)–Ge(3) | 95.39(4) |
| Ge(1)–Ge(3) | 2.5114(9) | Ge(2)–Ge(1)–Ge(3) | 97.31(3) |
| Ge(2)–Si(1) | 2.3966(15) | Cl(1)–Ge(2)–Cl(2) | 102.95(6) |
| Ge(2)–Cl(1) | 2.2177(15) | Cl(1)–Ge(2)–Si(1) | 104.52(6) |
| Ge(2)–Cl(2) | 2.2228(15) | Cl(2)–Ge(2)–Si(1) | 102.09(5) |
| Ge(3)–Si(5) | 2.4101(18) | Cl(1)–Ge(2)–Ge(1) | 116.31(5) |
| Ge(3)–Cl(3) | 2.2149(15) | Cl(2)–Ge(2)–Ge(1) | 100.48(5) |
| Ge(3)–Cl(4) | 2.2397(16) | Si(1)–Ge(2)–Ge(1) | 126.78(4) |
| | | Cl(3)–Ge(3)–Cl(4) | 100.37(7) |
| | | Cl(3)–Ge(3)–Si(5) | 105.94(6) |
| | | Cl(4)–Ge(3)–Si(5) | 99.11(6) |
| | | Cl(3)–Ge(3)–Ge(1) | 117.30(5) |
| | | Cl(4)–Ge(3)–Ge(1) | 99.98(5) |
| | | Si(5)–Ge(3)–Ge(1) | 128.04(5) |

Crystal structure of **65** was determined using X-ray measurement (Figure 44, Table 35). The Ge–Ge bond measures 2.5296(10) Å and is longer than Ge–Ge bond in **62** and **64**. The Ge–P bond of 2.4424(18) Å is longer than relevant bond of 2.390(4) Å in the starting germylene **7**. The slightly elongated Ge(2)–Cl(1) bond of 2.3170(19) Å compared to the Ge(1)–Cl(2) bond of 2.2830(17) Å reveals the germylene character of Ge(2) atom. The tetravalent germanium atom has a distorted tetrahedral environment with Ge(2)–Ge(1)–Si(4) angle of 120.60(5)°.

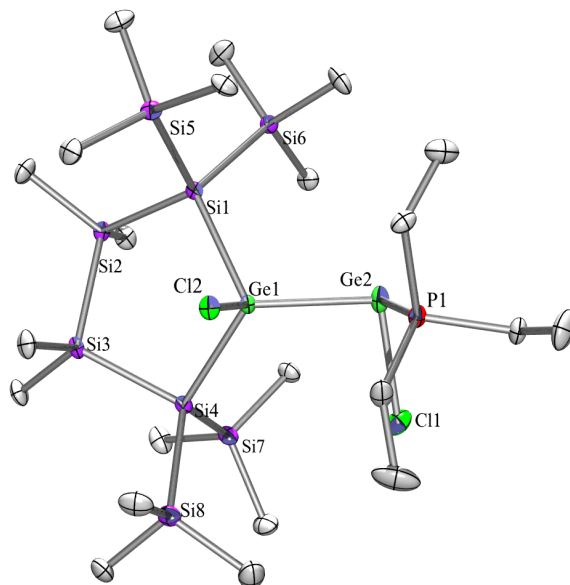


Figure 44: Crystal structure of **65**.

Table 35: Selected bond lengths and angles of **65**.

| Bond | Length [Å] | Bonds | Angle [°] |
|-------------|--------------|-------------------|-------------|
| Ge(2)–P(1) | 2.4424(18) | P(1)–Ge(2)–Ge(1) | 98.34(5) |
| Ge(1)–Ge(2) | 2.5296(10) | P(1)–Ge(2)–Cl(1) | 93.20(6) |
| Ge(1)–Cl(2) | 2.2830(17) | Cl(2)–Ge(1)–Ge(2) | 111.73(5) |
| Ge(2)–Cl(1) | 2.3170(19) | Si(1)–Ge(1)–Ge(2) | 111.90(5) |
| Ge(1)–Si(1) | 2.4302(17) | Si(4)–Ge(1)–Ge(2) | 120.60(5) |
| Si(4)–Ge(1) | 2.4236(18) | Ge(1)–Ge(2)–Cl(1) | 98.48(6) |
| Si(1)–Si(2) | 2.353(2) | Si(1)–Ge(1)–Cl(2) | 100.75(6) |
| Si(1)–Si(5) | 2.353(2) | Si(4)–Ge(1)–Cl(2) | 102.10(6) |
| Si(1)–Si(6) | 2.352(2) | Si(2)–Si(1)–Ge(1) | 104.21(7) |
| Si(2)–Si(3) | 2.340(2) | Si(3)–Si(2)–Si(1) | 104.52(8) |
| Si(3)–Si(4) | 2.355(2) | Si(2)–Si(3)–Si(4) | 105.73(8) |
| Si(4)–Si(7) | 2.371(2) | Si(5)–Si(1)–Si(6) | 108.32(9) |
| Si(4)–Si(8) | 2.357(2) | Si(8)–Si(4)–Si(7) | 108.34(9) |
| | | Si(4)–Ge(1)–Si(1) | 107.58(6) |
| | | Si(6)–Si(1)–Si(2) | 111.52(9) |
| | | Si(6)–Si(1)–Si(5) | 108.32(9) |
| | | Si(2)–Si(1)–Si(5) | 108.52(9) |
| | | Si(6)–Si(1)–Ge(1) | 112.23(8) |

69 crystallizes in orthorhombic space group *Pbca* (Figure 45, Table 36). An interesting feature of the compound **69** is the five-membered ring formed by two germanium, two carbon and one silicon atom, which is an unusual molecular pattern. The Ge–Ge bond length of 2.5052(5) Å falls in the lower range of usually observed values. The germanium–silicon bond is shorter than in **7** and yields 2.4410(8) Å. The Si(5)–Ge(2)–Ge(1) angle of 84.97(3)° is smaller by about 15° compared to the five membered ring found in triethylphosphine adducts of disilylated and digermylated germynes **7** and **54** [38].

Table 36: Selected bond lengths and angles of **69**.

| Bond | Length [Å] | Bonds | Angle [°] |
|-------------|--------------|-------------------|-------------|
| Ge(2)–P(1) | 2.3610(9) | Si(5)–Ge(2)–Ge(1) | 84.97(3) |
| Ge(1)–Ge(2) | 2.5052(5) | Ge(2)–Si(5)–C(16) | 106.15(9) |
| Ge(2)–Si(5) | 2.4410(8) | Si(5)–C(16)–C(17) | 121.4(2) |
| Si(5)–C(16) | 1.891(3) | C(16)–C(17)–Ge(1) | 114.66(18) |
| Ge(1)–Si(1) | 2.4285(8) | C(17)–Ge(1)–Ge(2) | 106.58(7) |
| C(17)–Ge(1) | 1.996(2) | Ge(1)–Ge(2)–P(1) | 95.24(2) |
| C(16)–C(17) | 1.343(4) | Si(1)–Ge(1)–C(17) | 118.46(8) |
| Ge(1)–Cl(1) | 2.2724(8) | Ge(2)–Ge(1)–Cl(1) | 113.27(2) |
| | | C(17)–Ge(1)–Cl(1) | 103.08(8) |

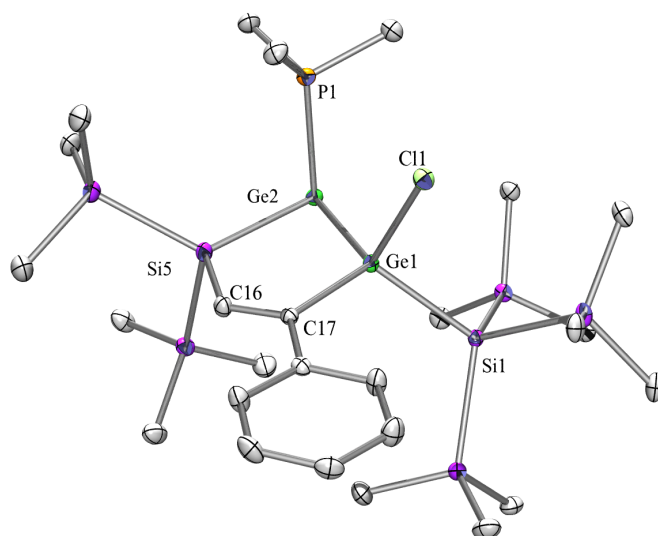


Figure 45: Crystal structure of **69**.

Compound **70** crystallizes in the monoclinic space group $P2(1)/c$ (Figure 46, Table 37). The germanium–germanium bond is quite long and yields 2.5477 Å. The C(21)–C(22) bond (1.3969(10) Å) is longer than C(1)–C(2) bond (1.338(11) Å). The Ge–Cl bond lengths yield 2.224(3) and 2.114(3) Å.

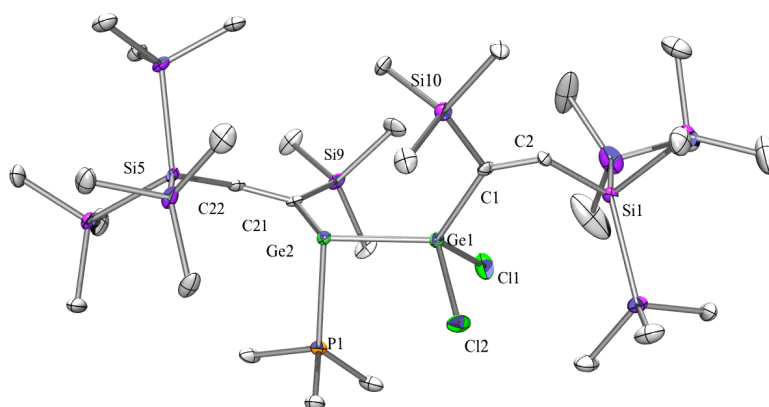


Figure 46: Crystal structure of **70**.

Table 37: Selected bond lengths and angles of **70**.

| Bond | Length [Å] | Bonds | Angle [°] |
|-------------|--------------|-------------------|-------------|
| Ge(1)–Ge(2) | 2.5477(14) | C(1)–Ge(1)–Cl(1) | 104.6(3) |
| Ge(2)–P(1) | 2.430(3) | C(1)–Ge(1)–Cl(2) | 102.4(3) |
| Ge(2)–C(21) | 2.016(8) | Cl(1)–Ge(1)–Cl(2) | 101.81(12) |
| C(21)–C(22) | 1.369(10) | C(1)–Ge(1)–Ge(2) | 120.6(3) |
| C(21)–Si(9) | 1.884(9) | Cl(1)–Ge(1)–Ge(2) | 122.43(9) |
| C(22)–Si(5) | 1.873(9) | Cl(2)–Ge(1)–Ge(2) | 101.26(9) |
| Ge(1)–Cl(2) | 2.224(3) | C(21)–Ge(2)–Ge(1) | 110.0(3) |
| Ge(1)–Cl(1) | 2.114(3) | C(21)–Ge(2)–P(1) | 96.7(2) |
| Ge(1)–C(1) | 1.980(9) | P(1)–Ge(2)–Ge(1) | 91.77(7) |
| C(1)–Si(10) | 1.893(9) | C(2)–C(1)–Ge(1) | 125.4(7) |
| C(1)–C(2) | 1.338(11) | C(2)–C(1)–Si(10) | 119.8(7) |
| C(2)–Si(1) | 1.3927(9) | C(2)–C(1)–Ge(1) | 125.4(7) |
| | | C(22)–C(21)–Ge(2) | 112.6(6) |
| | | C(22)–C(21)–Si(9) | 118.4(6) |
| | | Si(9)–C(21)–Ge(2) | 128.7(5) |
| | | Si(10)–C(1)–Ge(1) | 114.8(5) |
| | | C(1)–C(2)–Si(1) | 141.7(7) |
| | | C(21)–C(22)–Si(5) | 140.6(7) |

Compound **71** crystallizes in the orthorhombic space group Pccn (Figure 47, Table 38). It features three phenylacetylene molecules that are inserted into two germanium-silicon and one germanium-germanium bond. The Ge(2)–Cl(1) bond (2.2962(11) Å) is much longer than Ge(1)–Cl(3) (2.1662 Å). The length of Ge(1)–C(7) bond (1.963(3) Å) is almost equal to the length of Ge(1)–C(9) bond (1.961(3) Å). It is slightly larger than the length of Ge(1)–C(17) bond (1.942(3) Å). The small deviation of the latter Ge–C distance can be explained by different chemical surroundings of the C(17) atom, compared to those of C(7) and C(9).

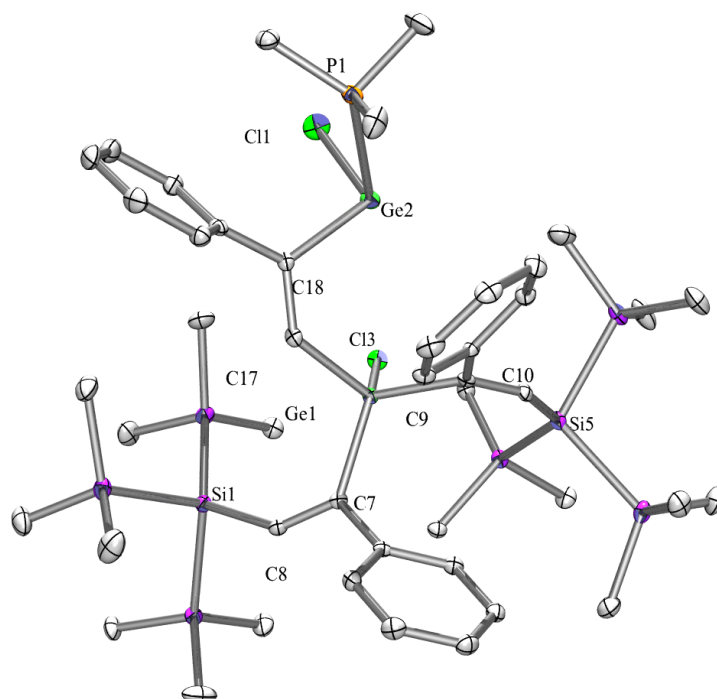


Figure 47: Crystal structure of **71**.

Table 38: Selected bond lengths and angles of **71**.

| Bond | Length [Å] | Bonds | Angle [°] |
|-------------|--------------|-------------------|-------------|
| Ge(2)–P(1) | 2.4306(10) | P(1)–Ge(2)–Cl(1) | 87.29(4) |
| Ge(2)–Cl(1) | 2.2962(11) | P(1)–Ge(2)–C(18) | 94.43(9) |
| Ge(2)–C(18) | 2.031(3) | Cl(1)–Ge(2)–C(18) | 100.27(10) |
| C(17)–C(18) | 1.327(4) | Ge(2)–C(18)–C(17) | 117.1(2) |
| Ge(1)–C(17) | 1.942(3) | C(18)–C(17)–Ge(1) | 129.1(2) |
| Ge(1)–Cl(3) | 2.1662(9) | C(17)–Ge(1)–Cl(3) | 105.58(10) |
| Ge(1)–C(7) | 1.963(3) | C(17)–Ge(1)–C(7) | 104.41(13) |
| Ge(1)–C(9) | 1.961(3) | C(17)–Ge(1)–C(9) | 116.70(13) |
| C(9)–C(10) | 1.329(4) | Cl(3)–Ge(1)–C(9) | 104.15(9) |
| C(10)–Si(5) | 1.897(3) | Cl(3)–Ge(1)–C(7) | 112.67(9) |
| C(7)–C(8) | 1.340(4) | C(9)–Ge(1)–C(7) | 113.29(13) |
| C(8)–Si(1) | 1.905(3) | Ge(1)–C(9)–C(10) | 125.4(2) |
| | | C(9)–C(10)–Si(5) | 144.3(3) |
| | | Ge(1)–C(7)–C(8) | 126.7(2) |
| | | C(7)–C(8)–Si(1) | 142.8(3) |

Germylene **72** crystallized in monoclinic space group $P2(1)/c$ (Figure 48, Table 39). The length of Ge–Ge bond yields 2.5628(7) Å and is larger than the Ge–Ge bond in **70**, which can be understood based on their chemical inequivalence. The Ge–Ge bond in **72** has a dative, whereas in **70** a much more covalent character. The Ge(1)–C(1) bond (2.007(4) Å) is slightly longer than Ge(1)–C(8) (1.999(4) Å) and Ge(1)–C(26) (1.995(4) Å). However, all these bonds are much shorter than the corresponding bonds in **40** and **42**. The distances between germanium and chloride atoms are typical and yield 2.3075(17) and 2.2994(14) Å.

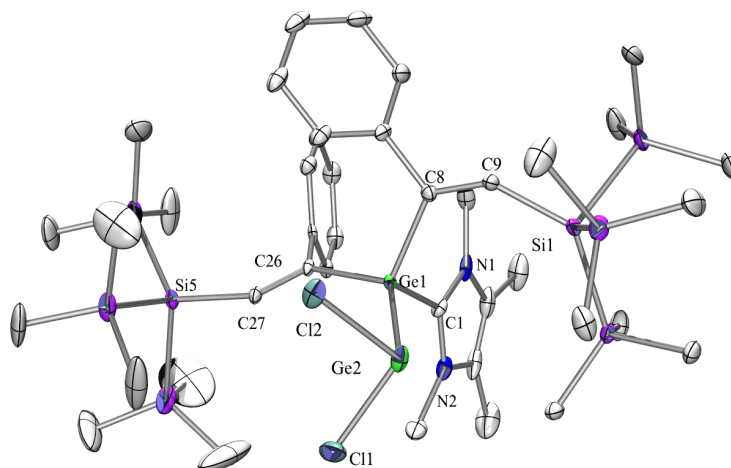


Figure 48: Crystal structure of **72**.

Table 39: Selected bond lengths and angles of **72**.

| Bond | Length [Å] | Bonds | Angle [°] |
|-------------|--------------|-------------------|-------------|
| Ge(1)–Ge(2) | 2.5628(7) | Ge(2)–Ge(1)–C(1) | 119.01(13) |
| Ge(1)–C(1) | 2.007(4) | Ge(2)–Ge(1)–C(8) | 101.25(12) |
| Ge(1)–C(8) | 1.999(4) | Ge(2)–Ge(1)–C(26) | 122.36(12) |
| C(8)–C(9) | 1.343(6) | C(1)–Ge(1)–C(8) | 105.09(18) |
| C(9)–Si(1) | 1.890(5) | C(1)–Ge(1)–C(26) | 96.85(17) |
| Ge(1)–C(26) | 1.995(4) | C(8)–Ge(1)–C(26) | 111.56(17) |
| C(26)–C(27) | 1.336(6) | Cl(1)–Ge(2)–Cl(2) | 95.78(6) |
| C(27)–Si(5) | 1.897(4) | Cl(1)–Ge(2)–Ge(1) | 99.61(5) |
| Ge(2)–Cl(1) | 2.3075(17) | Cl(2)–Ge(2)–Ge(1) | 90.62(4) |
| Ge(2)–Cl(2) | 2.2994(14) | Ge(1)–C(26)–C(27) | 117.4(3) |
| | | C(26)–C(27)–Si(5) | 132.7(3) |
| | | Ge(1)–C(8)–C(9) | 126.3(3) |
| | | C(8)–C(9)–Si(1) | 143.7(4) |

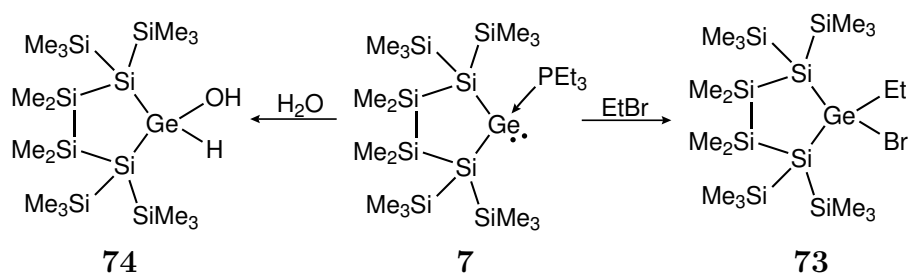
2.5 Reactions of tetrylene adducts with small molecules and carbonyl compounds

2.5.1 Synthesis

Although PMe_3 adduct of acyclic germyle **18** showed unexpected and interesting reactivity as a starting material for the reaction with small molecules and carbonyl compounds the PEt_3 adduct of cyclic germylene **7** was chosen due to its stability.

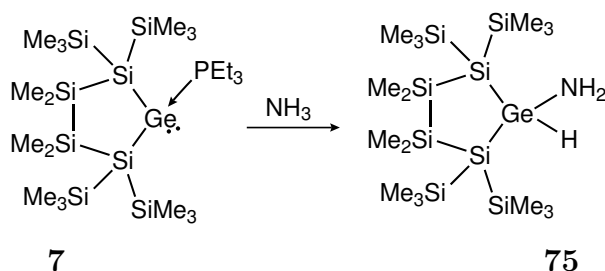
Treatment of triethylphosphine adduct of cyclic germylene **7** with EtBr afforded the tetravalent product **73** in a very high yield (right side in Scheme 64). Insertion of germylene into $\text{C}-\text{Br}$ bond was observed before [99, 100]. The product is stable and formed pale yellow crystals after storing it at -35°C for 18 hours.

Similar reactivity showed **7** towards water (left side in Scheme 64). Product of the insertion of germylene into $\text{O}-\text{H}$ bond of water **74** was formed only when stoichiometric amount of degassed H_2O was present in the solution. If excess of water was used, multiple products were formed, but none of them was identified. **74** form colorless needle suitable to X ray study.



Scheme 64: Reaction of germylene **7** with water and EtBr .

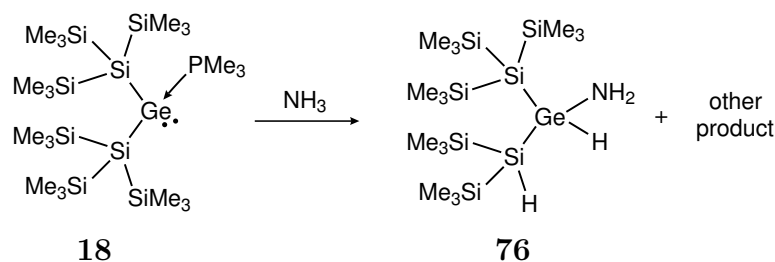
Triethylphosphine adduct of cyclic germylene **7** reacting with an excess of ammonia formed a product of the insertion of the germylene into the $\text{N}-\text{H}$ bond (**75**) (Scheme 65). The reaction proceeded rapidly and the reaction mixture lost its orange color and became colorless.



Scheme 65: Reaction of germylene **7** with ammonia.

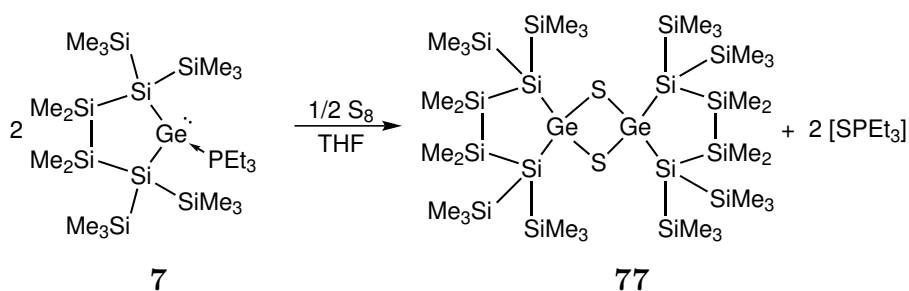
Because crystal structure of **75** was not determined, the reaction of acyclic germylene adduct **18** with ammonia was carried out with hope, that in this case the determination of the structure will be possible. Surprisingly, two compounds were formed in this

reaction. One of them is the product of the insertion of the germylene into the N-H bond with one trimethylsilyl group substituted with a hydrogen (**76**) (Scheme 66). The second compound remains unknown, however, the formation of trimethylsilylamine and 1,1,1,3,3,3-hexamethyl-2-(trimethylsilyl)trisilan-2-amine was ruled out based on ^{13}C NMR spectrum.



Scheme 66: Reaction of germylene **18** with ammonia.

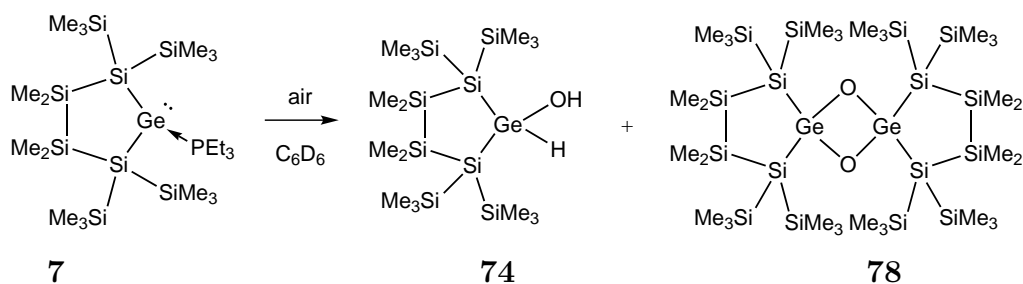
Reaction of cyclic germylene triethylphosphine adduct **7** with sulfur at room temperature led to the formation of a sulfido-bridged dimer **77** (Scheme 67). A similar dimerization was observed previously for the reaction of **7** with selenium and tellurium [37]. Although there are few examples of monomeric germanethione isolation at ambient temperature [101, 102], the majority of germylenes in the reaction with S_8 formed a dimer [103–107].



Scheme 67: Reaction of germylene **7** with sulfur.

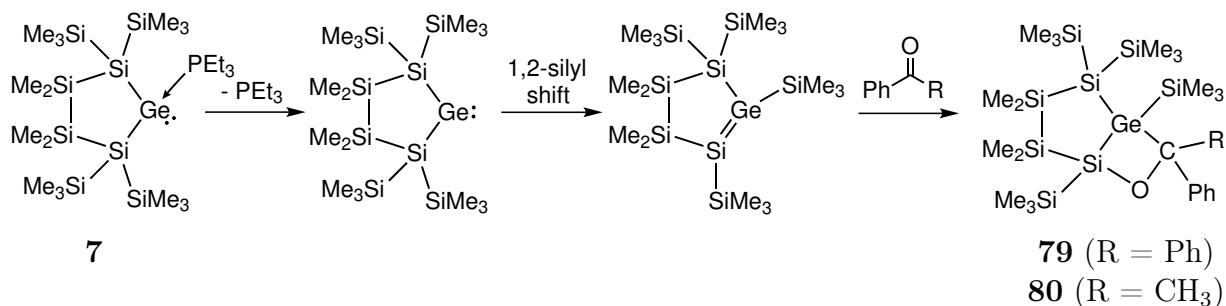
Reaction of cyclic germylene triethylphosphine adduct **7** with oxygen was carried out. After addition of excess of O_2 to the germylene **7** the initially orange solution turned immediately to colorless, however, ^{29}Si NMR spectrum recorded after this reaction did not show any signal. It could suggest a paramagnetic product, undetectable by NMR technique. Crystallization of the product of this reaction was unsuccessful.

The cyclic germylene triethylphosphine adduct **7** exposed to air immediately changes its color from yellow to colorless. Based on ^{29}Si NMR spectrum, which showed following resonances: -4.7 , -5.8 , -6.0 , -7.3 , -25.5 , -28.9 , -105.3 and -113.9 ppm, two compounds were formed. Resonances at -4.7 , -7.3 , -25.5 and -113.9 ppm was assigned to the product of the hydrolysis of five-membered ring germylene, **74**, which was synthesized earlier. The remaining peaks located at -5.8 , -6.0 , -28.9 and -105.3 ppm probably resulted from **78** (Scheme 68).



Scheme 68: Formation of **74** and **78** after exposition of **7** to air.

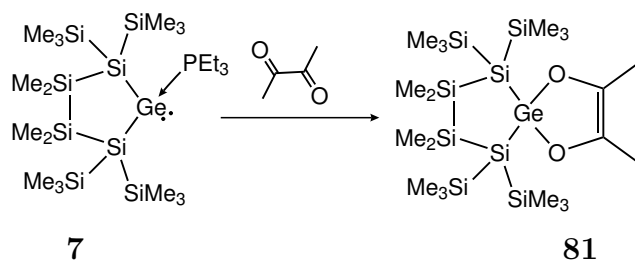
Triethylphosphine adduct of cyclic germylene **7** was reacted with benzophenone. The product of the reaction revealed significantly down-field shifted resonances at 40.3 ppm in the ²⁹Si NMR spectrum. The presence of eight signals suggested the formation of a highly asymmetric compound. Determination of the crystal structure showed that 2-sila-3-germaoxatene **79** was formed. Repetition of the reaction with acetophenone revealed the synthesis analogous 2-sila-3-germaoxatene **80**, although its crystal structure was not determined. Both cycloadditions proceeded regioselectively. The products indicate, that syntheses occurred by the formation of the free germylenes, which after 1,2-silyl shift give products of cycloaddition. This [2+2] addition was observed previously by Vittal and coworkers in the reaction of Mes₂Ge=GeMes₂ with a slightly different carbonyl compound [108].



Scheme 69: Reaction of germylene **7** with ketones.

The reaction of the acyclic germylene PMe₃ adduct **18** with benzophenone was also carried out in order to verify if the formation of related silagermaoxatene, but according to the ²⁹Si NMR spectrum mainly radicals were formed.

Reaction of the adduct of cyclic germylene **7** with diacetyl led to the formation 1,3-dioxa-2-germacyclopent-4-ene **81** (Scheme 70), related to 1,3-dioxa-2-stannacyclopent-4-ene obtained before [109]. The spirogermanium atom of **81** connects two the five-membered rings. One of them is composed of four silicon and one germanium atom, the second circle contains two carbon, two oxygen and germanium atoms.



Scheme 70: Reaction of germylene **7** with diacetyl.

2.5.2 NMR Spectroscopy

The ^{29}Si NMR spectrum of 1-bromo-1-ethylgermanium compound **73** shows four resonances located at -4.2 , -8.1 , -25.9 and -111.5 ppm. In ^{13}C NMR spectrum two signals for SiMe_2 group located at -2.6 and -2.1 ppm as well as two resonances for trimethylsilyl groups (3.3 and 3.2 ppm) are observed.

Four resonances located at -4.7 , -7.3 , -25.3 and -113.9 ppm are present in the ^{29}Si NMR spectrum of hydroxygermanium product **74**. Assignment of the signals in ^1H NMR spectrum was possible by comparing the spectra recorded before and after adding one drop of D_2O to the NMR tube. The proton bonded to germanium is represented by the signal at 6.38 ppm, the resonance at -0.44 ppm is due to the proton of the hydroxyl group. In ^{13}C NMR trimethylsilyl groups are represented by peaks at 1.8 and 2.6 ppm. One resonance located at -2.5 ppm originates from the two SiMe_2 groups.

In the ^{29}Si NMR spectrum of **75**, which is the product of an insertion of the cyclic germylene adduct **7** into N–H bond of ammonia, four resonances located at -7.1 , -8.1 , -24.9 , -122.0 ppm are observed. One signal corresponding to the SiMe_2 group is obtained in ^{13}C NMR spectrum, as for compound **74**. The signals resulting from the trimethylsilyl group are located at -2.0 and 3.1 ppm.

The ^{29}Si NMR spectrum of **77** shows three resonances located at -2.6 , -27.5 and -88.1 ppm, as expected.

The ^{29}Si NMR spectrum of bicyclic product of the reaction **7** with benzophenone, **79**, shows eight resonances. This compound features strongly low-field shifted ^{29}Si NMR signals for the silicon within the four-membered ring (40.3 ppm) compared to the related resonances (21.84 – 25.83 ppm) in similar systems [108]. The signal of the quaternary silicon bonded to the germanium atom is also down-field shifted (-104.7 ppm) compared to the starting germylene **7** (-127.1 ppm).

The ^{29}Si NMR spectrum of **80** shows eight resonances similar to those recorded in the spectrum of **79**, however, the signals corresponding to the quaternary silicon are in the expected region of the spectrum, in contrast to the spectrum of **79**. The signal at 17.3 ppm is assigned to silicon bonded to oxygen, the peak at -123.3 ppm represents the second quaternary silicon.

Three signals located at -6.1 , -30.4 and -117.0 ppm are present in ^{29}Si NMR spectrum of 1,3-dioxa-2-germacyclopent-4-ene **81**.

2.5.3 Crystallography

The crystal structure of **73** was determined using X-ray diffraction (Figure 49, Table 40). **73** crystallized in monoclinic space group C2/c. The length of Ge–Br and Ge–C bond are in good agreement with corresponding lengths in [$\{S(C_6H_3S)_2O\}Ge(Et)(Br)$] [110]. The Si(1)–Ge(1)–Si(4) angle of $110.86(4)^\circ$ is slightly greater than related angle of the starting germylene ($103.9(3)^\circ$).

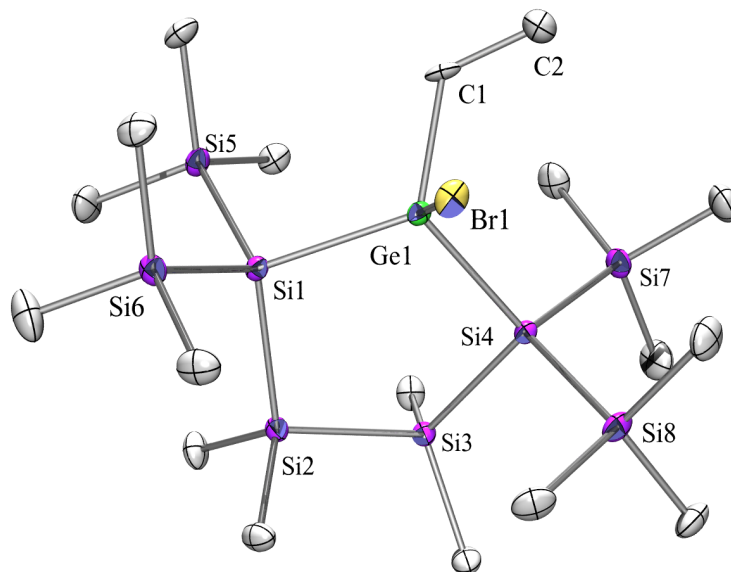


Figure 49: Crystal structure of **73**.

Table 40: Selected bond lengths and angles of **73**.

| Bond | Length [Å] | Bonds | Angle [°] |
|-------------|--------------|--------------------|-------------|
| Ge(1)–Si(1) | 2.4108(12) | Si(2)–Si(1)–Ge(1) | 103.26(5) |
| Ge(1)–Br(1) | 2.3672(9) | Si(1)–Ge(1)–Br(1) | 107.51(3) |
| Ge(1)–C(1) | 1.973(12) | Si(4)–Ge(1)–Br(1) | 108.95(3) |
| C(1)–C(2) | 1.500(15) | C(1)–Ge(1)–Br(1) | 99.1(4) |
| Si(1)–Si(5) | 2.3572(15) | Si(1)–Si(2)–Si(3) | 106.93(6) |
| Si(1)–Si(6) | 2.3510(15) | Si(2)–Si(3)–Si(4) | 108.93(6) |
| Si(1)–Si(2) | 2.3579(15) | Si(3)–Si(4)–Ge(1) | 102.20(5) |
| Si(2)–Si(3) | 2.3462(16) | Ge(1)–Si(1)–Si(5) | 106.58(5) |
| Si(3)–Si(4) | 2.3533(15) | Ge(1)–Si(1)–Si(26) | 113.35(5) |
| Si(4)–Si(7) | 2.3540(15) | Ge(1)–C(1)–C(2) | 117.3(8) |
| Si(4)–Si(8) | 2.3471(15) | Si(4)–Ge(1)–Si(1) | 110.86(4) |
| Ge(1)–Si(4) | 2.4083(13) | Si(6)–Si(1)–Si(5) | 110.51(6) |

Crystallization of **74** from pentane at $-30\text{ }^{\circ}\text{C}$ gave colorless crystals suitable to X-ray study. **74** has monoclinic symmetry space group $P2/c$ (Figure 50, Table 41). The Ge–OH bond of $1.778(4)\text{ \AA}$ is slightly longer than corresponding bond in $[\text{L}(\text{H})_2\text{GeGe}(\text{H})(\text{OH})\text{L}]$ $\text{L} = \text{N}(\text{SiMe}_3)(\text{Ar}^*)$; $\text{Ar}^* = \text{C}_6\text{H}_2\text{Me}\{\text{C}(\text{H})\text{Ph}_2\}_{2-4,2,6}$ and $(\text{Eind})_2\text{Ge}(\text{H})(\text{OH})$ ($\text{Eind} = 1,1,3,3,5,5,7,7$ -octaethyl-*s*-hydrindacen-4-yl) ($1.742(6)$ and $1.757(2)\text{ \AA}$, respectively) [28, 111]. The hydrogen atoms H(90) and H(91) are found not calculated. The Ge(1)–Si(1) bond distance of $2.3929(7)\text{ \AA}$ demonstrates that the germanium atom lost its germylene character.

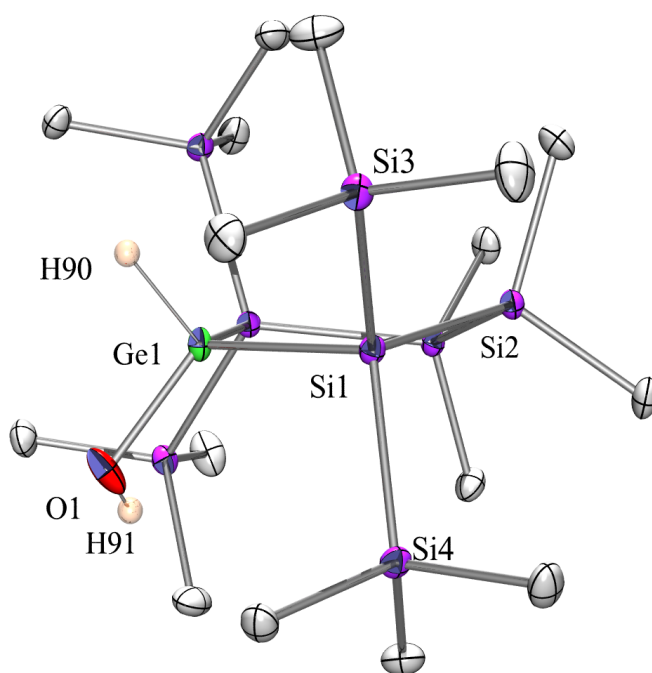


Figure 50: Crystal structure of **74**.

Table 41: Selected bond lengths and angles of **74**.

| Bond | Length [\AA] | Bonds | Angle [$^{\circ}$] |
|-------------|-------------------------|-------------------|----------------------|
| Ge(1)–Si(1) | $2.3929(7)$ | Si(2)–Si(1)–Ge(1) | $103.89(2)$ |
| Ge(1)–O(1) | $1.778(4)$ | Si(1)–Ge(1)–O(1) | $113.46(12)$ |

The crystal structure of **76** was determined by X-ray measurement (Scheme 51, Table 42). The product crystallized in triclinic space group $P\bar{1}$. The Ge–N bond length yields 1.795(8) Å. The Si(1)–Ge(1)–Si(5) bond angle (117.60(6) °) is almost the same to those found in the NHC adducts of bis[(tristrimethylsilyl)silyl]germylene (116.61(4)° in **1**, NHC = IMe₄; 117.39(2)° in **14**, NHC = ^{Me}LiPr) and they are larger than ideal tetrahedral angles.

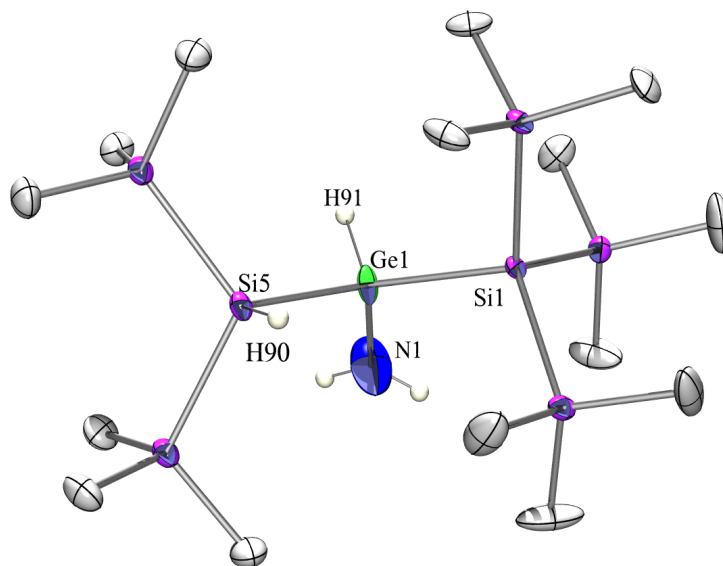


Figure 51: Crystal structure of **76**.

Table 42: Selected bond lengths and angles of **76**.

| Bond | Length [Å] | Bonds | Angle [°] |
|-------------|--------------|-------------------|-------------|
| Ge(1)–Si(1) | 2.3891(14) | Si(1)–Ge(1)–N(1) | 109.5(3) |
| Ge(1)–Si(5) | 2.396(2) | Si(5)–Ge(1)–N(1) | 114.5(3) |
| Ge(1)–N(1) | 1.795(8) | Si(1)–Ge(1)–Si(5) | 117.60(6) |

77 belongs to the monoclinic space group C2/c (Figure 52, Table 43). The germanium-sulfur bond in **77**, which measures 2.324(2) Å, is the longest Ge–S bond between tetracoordinated germanium and dicoordinated sulfur within four membered –Ge–S–Ge–S– ring, which normally is in the range of 2.21–2.25 Å [103–107, 112–116].

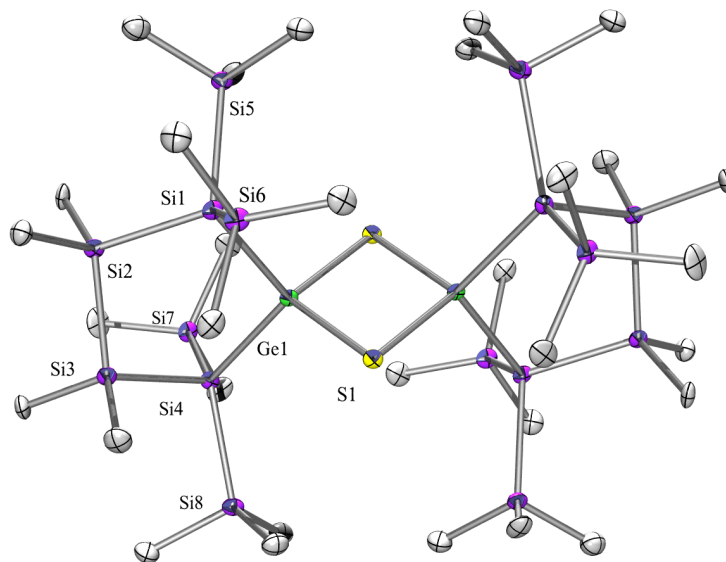


Figure 52: Crystal structure of **77**.

Table 43: Selected bond lengths and angles of **77**.

| Bond | Length [Å] | Bonds | Angle [°] |
|-------------|--------------|--------------------|-------------|
| Ge(1)–S(1) | 2.324(2) | Ge(1)–S(1)–Ge(1)#1 | 87.70(7) |
| Ge(1)–Si(4) | 2.510(3) | S(1)–Ge(1)–S(1)#1 | 92.30(7) |
| Ge(1)–Si(1) | 2.520(2) | | |

Crystallization of **79** from pentane gave colorless crystals suitable to X-ray study. **79** crystallized in orthorhombic space group *Pbca* (Figure 53, Table 44). The five-membered ring is joint with four-membered ring along Ge–Si bond. The length of Si–O bond of 1.6998(17) Å is significantly longer than in related 2-sila-3-germaoxetane compounds [108], however discussed bond is almost the same like in the 2,3-disilaoxetane (1.681(3) Å) [117] and silaoxetane (1.696 Å) [118].

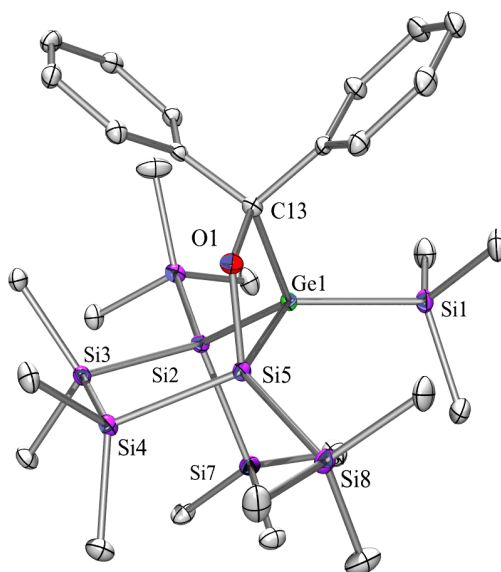


Figure 53: Crystal structure of **79**.

Table 44: Selected bond lengths and angles of **79**.

| Bond | Length [Å] | Bonds | Angle [°] |
|-------------|--------------|-------------------|-------------|
| Ge(1)–Si(5) | 2.3824(7) | Si(5)–Ge(1)–C(13) | 69.34(6) |
| Ge(1)–C(13) | 2.118(2) | Ge(1)–C(13)–O(1) | 98.7(13) |
| O(1)–C(13) | 1.446(3) | C(13)–O(1)–Si(5) | 109.26(13) |
| O(1)–Si(5) | 1.6998(17) | O(1)–Si(5)–Ge(1) | 82.45(6) |
| Si(5)–Si(8) | 2.3431(9) | C(13)–Ge(1)–Si(1) | 116.32(6) |
| Ge(1)–Si(1) | 2.4050(8) | O(1)–Si(5)–Si(8) | 111.12(6) |
| Ge(1)–Si(2) | 2.4307(8) | Si(5)–Ge(1)–Si(1) | 121.39(3) |
| | | C(13)–Ge(1)–Si(2) | 119.77(6) |

The compound **81** crystallized in triclinic space group $P\bar{1}$ (Figure 54, Table 45). The Ge–O bond distances (1.833(4) and 1.839(4) Å) are greater than related bond in $(\text{Me}_3\text{SiN}=\text{PPh}_2)_2\text{C}=\text{Ge}[\text{O}(\text{Ph})\text{C}=\text{C}(\text{Ph})\text{O}]$ (1.781(3) and 1.794(3) Å) [119], however they are comparable to those of compounds containing Ge–O single bonds (1.75–1.85 Å) [120].

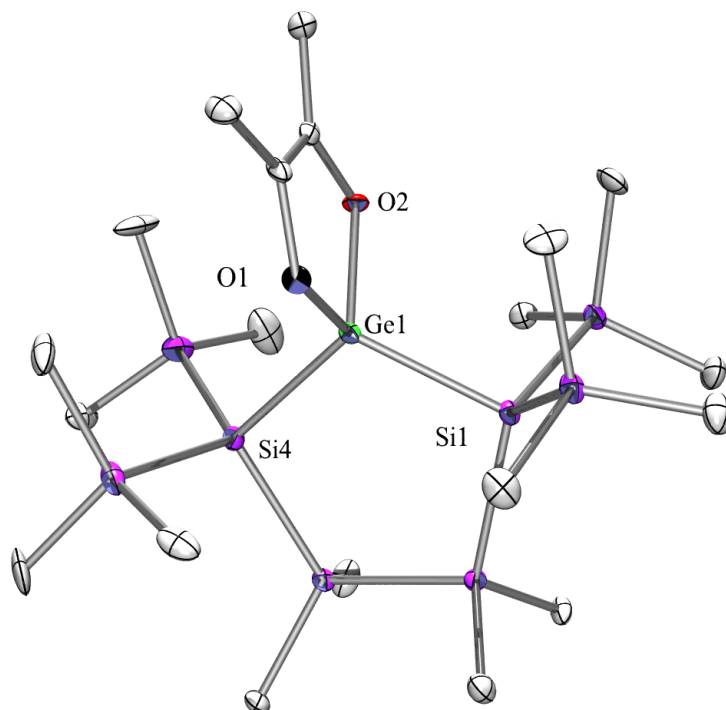


Figure 54: Crystal structure of **81**.

Table 45: Selected bond lengths and angles of **81**.

| Bond | Length [Å] | Bonds | Angle [°] |
|-------------|--------------|-------------------|-------------|
| Ge(1)–O(1) | 1.833(4) | O(1)–Ge(1)–O(2) | 91.1(2) |
| Ge(1)–O(2) | 1.839(4) | Si(4)–Ge(1)–Si(1) | 114.44(7) |
| Ge(1)–Si(1) | 2.396(2) | Si(4)–Ge(1)–O(1) | 109.70(15) |
| Ge(1)–Si(4) | 2.400(2) | Si(4)–Ge(1)–O(2) | 112.48(16) |
| | | Si(1)–Ge(1)–O(2) | 112.98(15) |
| | | Si(1)–Ge(1)–O(1) | 113.91(16) |

Although compound **82** was synthesized earlier in the reaction of cyclic five-membered ring germylene **7** with selenium [37], its structure was not determined. Current study aims at its comparison to other known compounds. As expected **82** is isostructural to sulfur analog **77**. It crystallized in triclinic space group P-1 (Figure 55, Table 46). The torsion angle of $-0.52(5)$ of four-membered ring Se(2)-Ge(2)-Se(1)-Ge(1) demonstrates that four-membered ring is planar, whereas the corresponding angle for 1,3,2,4-dithiadigermetanes are 37.8° and 43.8° [102]. The lengths of Ge–Se bonds fall in the upper range of value [102, 114, 116, 121–123].

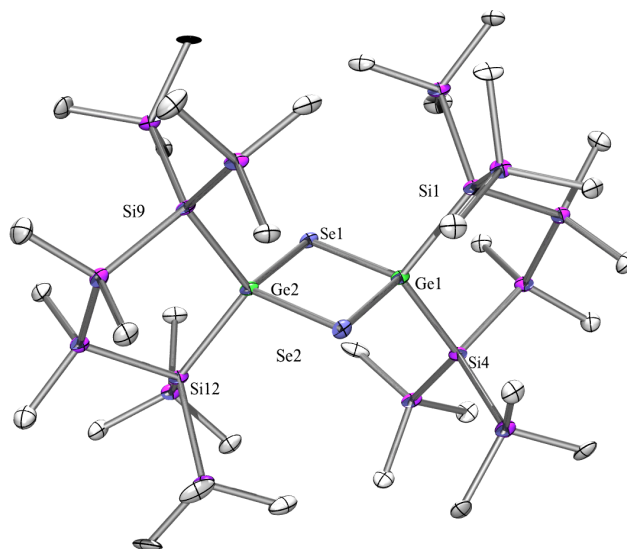


Figure 55: Crystal structure of **82**.

Table 46: Selected bond lengths and angles of **82**.

| Bond | Length [Å] | Bonds | Angle [°] |
|--------------|--------------|--------------------|-------------|
| Ge(1)–Se(2) | 2.4199(18) | Ge(1)–Se(1)–Ge(2) | 87.56(6) |
| Ge(1)–Se(1) | 2.4224(18) | Ge(1)–Se(2)–Ge(2) | 87.74(6) |
| Ge(1)–Si(4) | 2.448(3) | Se(1)–Ge(1)–Se(2) | 92.17(6) |
| Ge(1)–Si(1) | 2.483(4) | Se(1)–Ge(2)–Se(2) | 92.52(6) |
| Ge(2)–Se(2) | 2.4114(18) | Si(9)–Ge(2)–Si(12) | 106.44(12) |
| Ge(2)–Se(1) | 2.4168(18) | Si(1)–Ge(1)–Si(4) | 106.32(12) |
| Ge(2)–Si(9) | 2.447(3) | | |
| Ge(2)–Si(12) | 2.461(4) | | |

2.6 Conclusions

The phosphine adducts of disilylated and digermylated germylenes were found to be compounds with interesting reactivity towards acetylenes. The isolated products strongly depend on the type of both: germylene adduct and acetylene species. Proposed first step of these reactions is always the formation of the corresponding germacyclopropene. Then, for terminal acetylenes the regio- and stereoselective insertion into germanium–silicon or germanium–germanium bond occurred.

For the acyclic germylene adduct **18** such insertions led to the formation of the vinylated and divinylated germylenes PMe_3 adducts. In this process a crucial role played the phosphine. The coordination of a phosphine to a germylene is very weak, thus germylene adduct could react as a free germylene. On the other hand, this coordination is sufficient to stabilize such reactive molecules and able for its crystallization and characterization. The preferable reaction of the vinylated germylene adducts is intramolecular insertion of the germylene into a Si-SiMe_3 bond. A silagermetes formed in this process, contain tetravalent germanium atom and are stable, when stored under inert atmosphere. Interestingly, germacyclopropenes which were formed in the reactions of **18** with PhCCPh and EtCCEt also rearranged to such silagermetes. It suggests that this rearrangement involved transformation of Ge^{IV} to Ge^{II} species, although the products of such reactions, similar to the starting germacyclopropenes, formally are in oxidation state IV.

The nine-membered ring germylenes are formed as a result of the regio- and stereoselective insertion of terminal acetylenes into Ge-Si and Ge-Ge bond of cyclic germylenes adducts **7** and **54**. Such nine-membered ring systems rapidly rearrange to the much more stable spirogermanium compounds.

The reactions of germylene phosphine adducts with dioxane complex of germanium dichloride demonstrates, that the GeCl_2 could be inserted into a Ge-Si or Ge-P bond as well as a germylene could be inserted into Ge-Cl bond of germanium dichloride. Which scenario takes place strongly depends on the type of germylene, however at this point of study, is impossible to predict.

The reactivity of phosphine adduct of disilylated germylene with small molecules such as H_2O , EtBr , NH_3 , S_8 showed, that phosphine adduct was reacted as a typical tetraylene, i. e. the insertion of germylene into polar bond occurred or a dimer was formed in the case of reaction with sulfur. That process confirmed, that coordination between germylene and phosphene is very weak. In the reaction of **7** with diacetyl the typical dioxagermapentene was formed, in contrast to the reaction with benzophenone, where 2-sila-3-germaoxatene was obtained.

3 Reactions of tetrylenes with transition metal complexes

3.1 Introduction

The coordination chemistry of heavier tetrylenes is much more neglected than that of parent carbenes. Due to the fundamental differences in the electronic ground state structure of carbenes and heavier tetrylenes different chemical reactivities are observed. While carbenes react as diradicals, heavier tetrylenes exhibit dual Lewis acid-base character. Their ground state is characterized by both an electron lone-pair and a vacant p orbital, which enables them to react with transition metal complexes as a σ -donor- π -acceptor ligands (Figure 56).

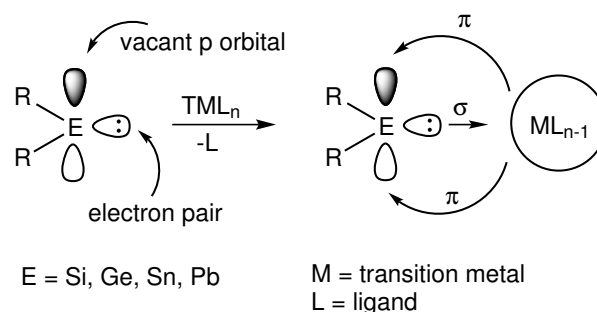
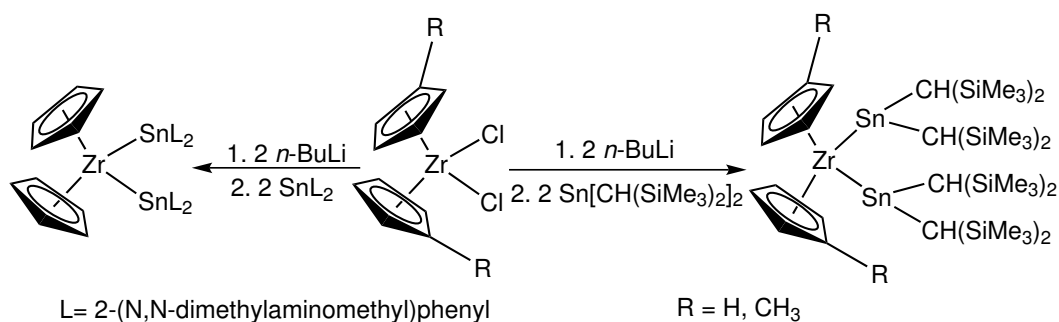


Figure 56: Formation of a heavier tetrylene-transition metal complex.

The first tetrylene-transition metal complexes $[\text{Cr}(\text{CO})_5\text{ER}_2(\text{THF})]$ ($\text{ER}_2 = \text{GeMe}_2, \text{SnMe}_2, \text{Sn}^t\text{Bu}_2$) were obtained in 1971 [124]. Since that time many transition metal complexes of silicon, germanium, tin and lead were synthesized using different synthetic approaches in which tetrylenes play a critical role. Among other possibilities, a tetrylene can act as a terminal or bridging ligand or insert into a $M-L$ bond of a transition metal complex. Tetrylenes can also behave as nucleophiles and form new $\text{E}(\text{ML}_n)_2$ tetrylenes as well as they can act as R group-transfer reagents or reducing agents. They can also participate in oxidative addition reactions with transition metal complexes in low oxidation state [125].

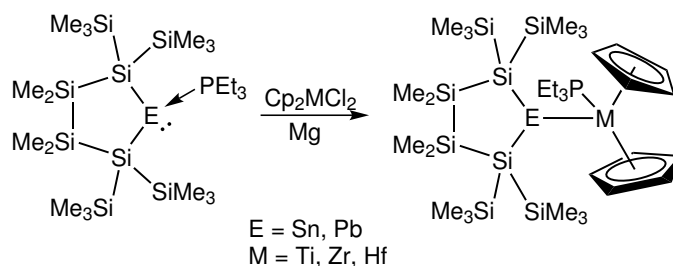
3.1.1 Early transition metal complexes

Group 4 transition metal complexes were synthesized in the reaction of tetrylenes with metallocene derivatives. In the earliest study, Lappert's monomeric stannylene $\text{Sn}[\text{CH}(\text{SiMe}_3)_2]_2$ was reacted with a 'zirconocene' derivative [126], obtained by reducing Cp_2ZnCl_2 using *n*-butyllithium [127, 128] (right side in Scheme 71). A similar approach was used almost 20 years later [129] to obtain $\text{Cp}_2\text{Zr}(\text{SnL}_2)_2$, $L = 2\text{-(N,N-dimethylaminomethyl)phenyl}$ (left side in Scheme 71).



Scheme 71: Formation of zirconocene stannylene complexes.

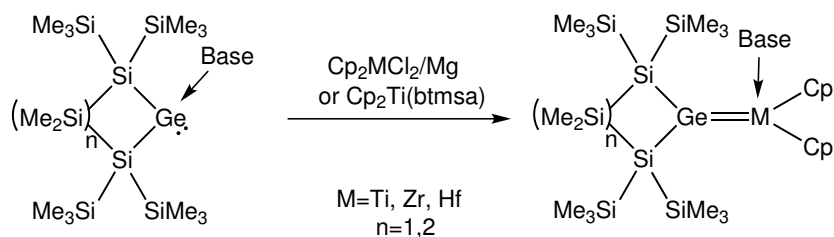
The reduction of group 4 metallocene dichlorides with magnesium instead of *n*-butyllithium opened new possibilities in the synthesis of tetrylene–metal complexes. Reactions of trimethylphosphine adducts of the five-membered ring stannylene **11** and plumbylene with group 4 metallocene dichlorides were carried out in the presence of magnesium [130] (Scheme 72). The coordination of silylated tetrylenes to metallocenes was accompanied by the transfer of PEt_3 from a tetrylene adduct to the empty metal orbital. All complexes were obtained in 80 % yield.



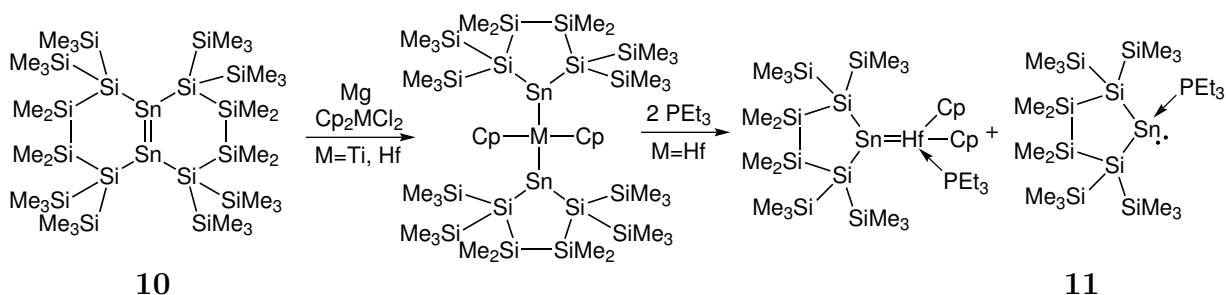
Scheme 72: Formation of group 4 metallocene stannylene and plumbylene complexes.

The same reaction path as for the five-membered ring stannylene **11** and plumbylene was observed for the five-membered ring germylene **7** [61], but the reaction yields (about 50 %) were much lower than for the corresponding stannylene and plumbylene complexes (Scheme 73). In contrast to the five-membered ring tetrylenes, the four-membered ring germylene stabilized by NHC-carbene did not react with Cp_2TiCl_2 under the same conditions. Using Rosenthal's complex $\text{Cp}_2\text{Ti}(\text{btmsa})$ instead of Cp_2TiCl_2 led to the formation of a titanocene germylene NHC adduct (Scheme 73) [61]. Replacing the Ti-coordinating PEt_3 with an N-heterocyclic carbene was demonstrated for a five-membered germylene-titanocene complex [61].

Reaction of the distannene **10** [43], which is the direct dimerization product of monocyclic stannylene, with metallocene dichloride in the presence of magnesium led to the formation of distannylene complexes (Scheme 74). Addition of 2 equivalents of PEt_3 to the hafnocene-distannylene complex led to the formation of a triethylphosphine adduct of cyclic stannylene **11** and a hafnocene-stannylene complex, which was also formed in the

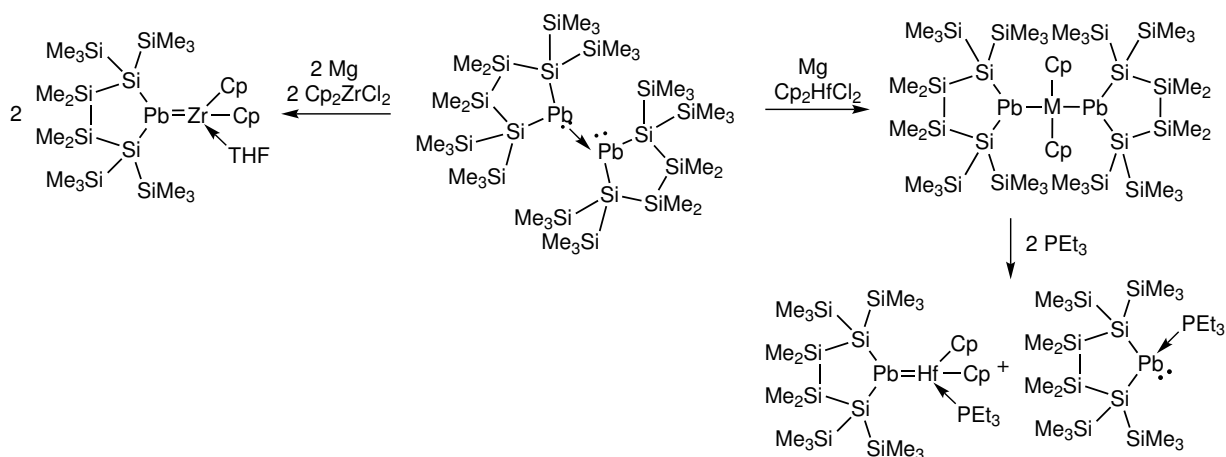


Scheme 73: Formation of group 4 metallocene germylene complex base adducts.



Scheme 74: Formation of titanocene and hafnocene-di(stannylene) complexes, and – in the case of the hafnocene complex – its transformation to hafnocene-mono(stannylene).

reduction of hafnocene dichloride in the presence of **11**. Under very similar conditions, the reduction of hafnocene dichloride with magnesium in the presence of a plumbylene dimer led to the formation of hafnocene-di(plumbylene) complex (right side in Scheme 75). After addition of trimethylphosphine, a plumbylene phosphine adduct and a hafnocene-plumbylene complex were formed selectively. Under the same conditions, the reaction of the plumbylene dimer with zirconocene dichloride in the presence of magnesium gave the THF adduct of the monoplumbylene-zirconocene complex (left side in Scheme 75).

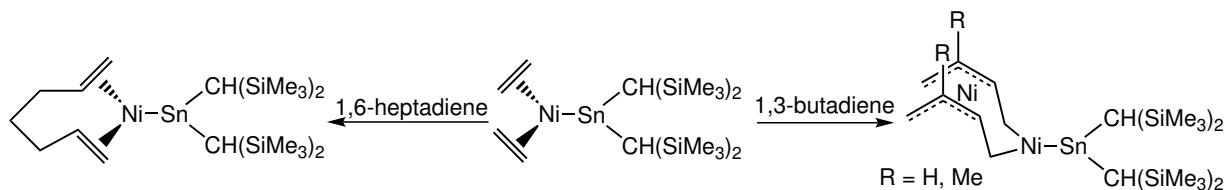


Scheme 75: Formation of group 4 metallocene plumbylene complexes.

3.1.2 Late transition metal complexes

The coordination chemistry of tetrylenes with late transition metal complexes is better explored than that of the early transition metals. The major motivation for pursuing research in this area is the fact, that such compounds can be used in catalytic reactions. Most of the efforts were devoted to N-heterocyclic silylenes, whose palladium complexes were found to be catalytically active in Heck coupling [131] and in Suzuki reactions [132]. A cobalt complex of an N-heterocyclic silylene was successfully investigated in a [2+2+2] cyclootrimerization reaction of triphenylbenzene [133]. An iridium complex served as pre-catalyst in C–H borylation [134]. Nickel complexes of N-heterocyclic silylenes and germylenes were active in Sonogashira cross-coupling reactions [135]. Other applications of N-heterocyclic silylene complexes are known [136]. However, not only N-heterocyclic tetrylene complexes play an important role in catalytic reactions. Cationic ruthenium silylene complexes were found to perform as catalysts for olefin hydrosilylation [137–139]. The catalytic properties of $[\text{MeN}(\text{CH}_2\text{CH}_2\text{NC}_6\text{F}_5)_2\text{Sn}]_4\text{Pd}$ and $[\text{MeN}(\text{CH}_2\text{CPh}_2\text{O})(\text{CH}_2\text{CH}_2\text{O})\text{Ge}]_4\text{Pd}$ were tested in the Suzuki–Miyaura cross-coupling and Heck arylation of olefins [140].

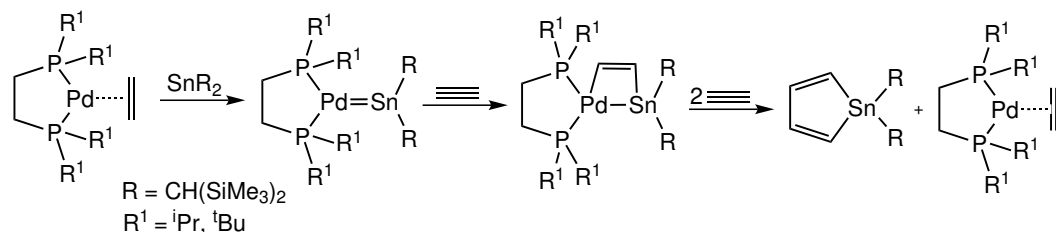
Lappert's stannylene $\text{Sn}[\text{CH}(\text{SiMe}_3)_2]_2$, reacted with $(\text{Et}_3\text{P})\text{PtCl}_2$, gave $[\text{PtCl}(\text{Et}_3\text{P})-(\text{SnR}_2)(\text{SnR}_2\text{Cl})]$, $\text{R} = \text{CH}(\text{SiMe}_3)_2$ [141]. Its formation can be explained as an insertion of $\text{Sn}[\text{CH}(\text{SiMe}_3)_2]_2$ into the platinum-chloride bond and a simultaneous exchange of the phosphine ligand with the stannylene. Lappert's stannylene reacted with $(\text{C}_2\text{H}_4)_3\text{Ni}$ giving $(\text{C}_2\text{H}_4)_2\text{Ni}-\text{Sn}[\text{CH}(\text{SiMe}_3)_2]_2$ [142]. Addition of a donor (NH_3 , pyridine and HMPA) to $(\text{C}_2\text{H}_4)_2\text{Ni}-\text{Sn}[\text{CH}(\text{SiMe}_3)_2]_2$ led to the formation of adducts. Reaction of $(\text{C}_2\text{H}_4)_2\text{Ni}-\text{Sn}[\text{CH}(\text{SiMe}_3)_2]_2$ with CO resulted in the replacement of the ethylene moieties by CO ligands. The reaction of the resulting product with NH_3 , pyridine and HMPA donors led to the formation of adducts, $(\text{CO})_3\text{Ni}-\text{Sn}[\text{CH}(\text{SiMe}_3)_2]_2(\text{donor})$. A reactivity study of $(\text{C}_2\text{H}_4)_2\text{Ni}-\text{Sn}[\text{CH}(\text{SiMe}_3)_2]_2$ with dienes was carried out [143]. The reaction with 1,6-heptadiene led to the replacement of both ethylene species with a heptadiene, in contrast to 1,3-butadienes which led to the formation of dinuclear diallyl complex *via* double addition of butadienes across the Ni–Sn bond (Scheme 76) [143].



Scheme 76: Reaction of nickel-stannylene complex with dienes.

Lappert's stannylene $\text{Sn}[\text{CH}(\text{SiMe}_3)_2]_2$ was also reacted with palladium complexes $[(\text{R}_2\text{P}-\text{C}_2\text{H}_4\text{PR}_2)\text{Pd}(\text{C}_2\text{H}_4)]$ ($\text{R} = {}^i\text{Pr}$, ${}^t\text{Bu}$), which led to the formation of $\text{Pd}^0\text{-Sn}^{\text{II}}$ compounds (Scheme 77). The latter reacted with acetylene giving stannole *via* addition of ethyne to palladium-stannylene complexes [144].

An asymmetric alkylarylstannylene $\text{RR}'\text{Sn}$: [$\text{R} = 2,4,6\text{-}{}^t\text{Bu}_3\text{C}_6\text{H}$; $\text{R}' = \text{CH}_2\text{C}(\text{CH}_3)\text{-}$

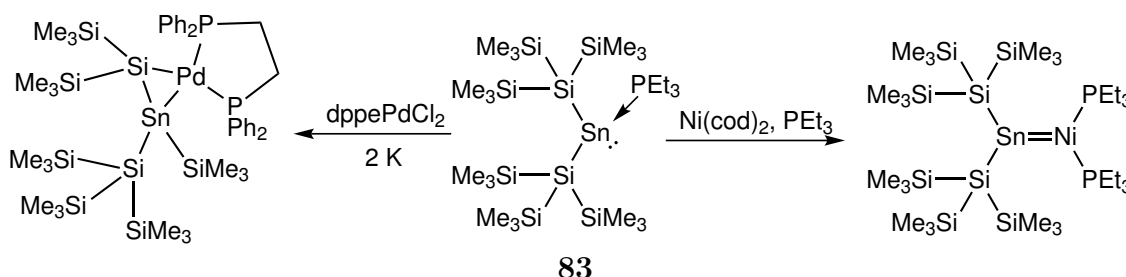


Scheme 77: Formation of palladium stannylene complexes and their reactions with acetylene.

3,5-*t*Bu₂] treated with tetracarbonylnickel formed light yellow crystals of (OC)₃Ni=SnRR', which slowly decomposed in a solution upon exposure to daylight [145].

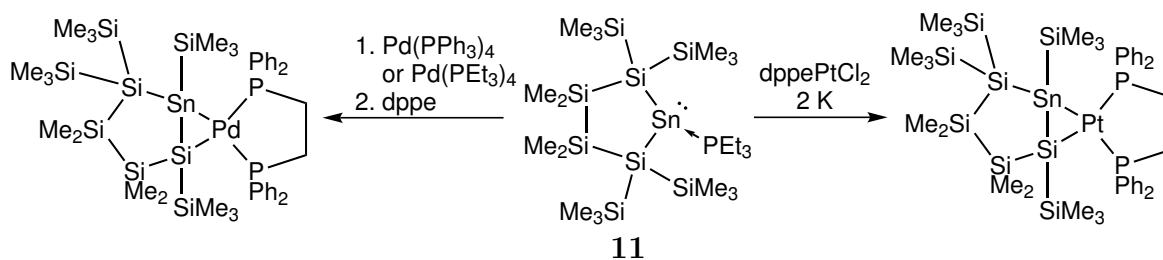
The same reactivity was observed by Kira and coworkers for a silylene. The authors synthesized a series of dialkylsilylene-group 10 metal complexes, R^H₂SiM(PMe₃)₂ (M = Ni, Pd, Pt; R^H = 1,1,4,4-tetrakis(trimethylsilyl)butane-1,4-diyl) in the reaction of the silylene with M⁽⁰⁾ complexes [146].

Reaction of the triethylphosphine adduct of bis[(trimethylsilyl)silyl]stannylene (**83**) with Ni(cod)₂ and an additional equivalent of PEt₃ led to the nickel-stannylene complex (right side in Scheme 78) [63]. A different reactivity pattern was observed for the coordination of the same stannylene adduct **83** to a palladium complex. Reaction of **83** with dppePdCl₂ in the presence of potassium resulted in the formation of a silastannene palladium complex by migration of a trimethylsilyl group to the tin atom (left side in Scheme 78).



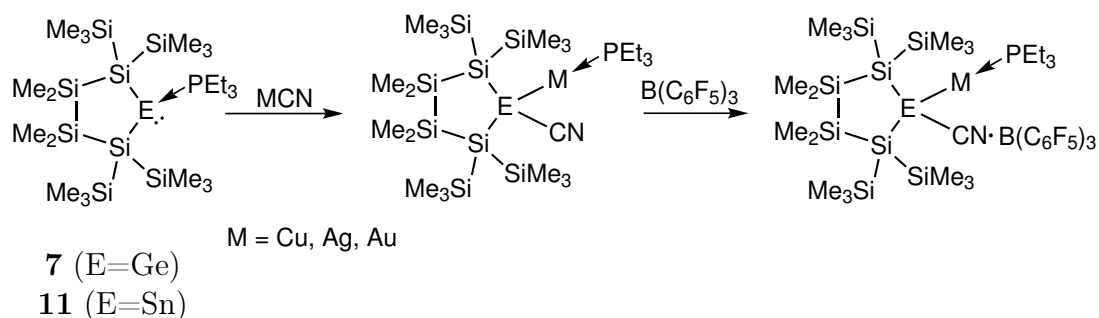
Scheme 78: Reaction of acyclic stannylene (**83**) with nickel and palladium complexes.

The five-membered ring stannylene **11** showed similar reactivity with the platinum complex: reaction of **11** with dppePtCl₂ in the presence of potassium led to the formation of a complex, containing a platinum-tin-silicon (Pt–Sn–Si) three-membered ring [63] (right side in Scheme 79). Reaction of **11** with the palladium complexes, i. e. Pd(PPh₃)₄ and Pd(PEt₃)₄, was carried out in order to verify that the similar structural pattern (Pt–Sn–Si ring) could be found among the products [63]. Due to the very high solubility of the two complexes, their isolation was unsuccessful, however, the exchange of PPh₃ and PEt₃ with dppe resulted in the crystallization of a palladium-stannene complex (left side in Scheme 79).



Scheme 79: Reaction of five-membered ring stannylyene **11** with palladium and platinum complexes.

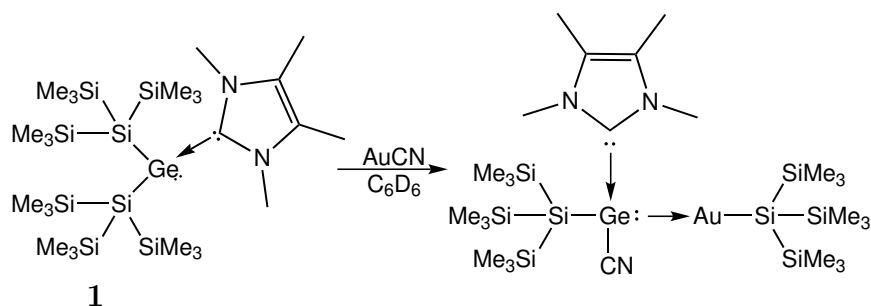
The reactivity of group 11 metal complexes is far less explored than that of group 10 metals. The reactions of the five-membered cyclic germylene **7** and stannylyene **11** with CuCN, AgCN and AuCN led to the formation of light-sensitive cyanogermyl and -stannyl complexes of the respective metals, with PEt₃ attached to the metal atoms [147] (Scheme 80). Contrary to expectations, the addition of B(C₆F₅)₃ did not lead to the abstraction of a phosphine, but instead resulted in the formation of a more stable adduct, featuring borane coordinated to the cyanide nitrogen atom.



Scheme 80: Reactions of five-membered ring germylene **7** and stannylyene **11** with group 11 cyanides.

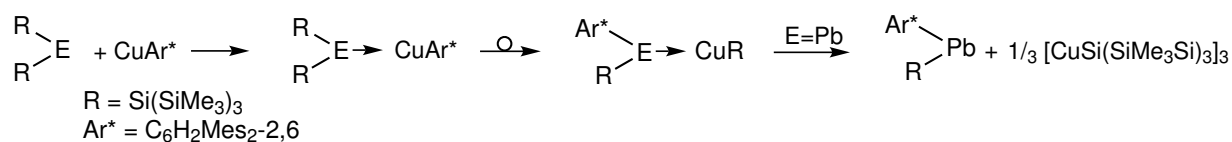
Interestingly, the reaction of bis[tris(trimethylsilyl)silyl]germylene (**1**) – an acyclic analog of germylene **7** – with gold cyanide, gave an unexpectedly different result. The obtained product should be formally treated as a cyanogermylene complex of gold, featuring a tris(trimethylsilyl)silyl group migrated to the gold atom (Scheme 81). The nature of this compound is fundamentally different from that of cyanogermyl complex, obtained in the reaction of the cyclic germylene with AuCN (Scheme 80). The emergence of cyanogermylene is enabled by the migration of the tris(trimethylsilyl)silyl group from the germanium to the gold atom, and the simultaneous transfer of the CN group to the Ge. As it will be discussed later (see Section 3.3) such a migration results – presumably – from the fact, that the reaction was driven by the N-heterocyclic carbene and not the phosphine, which improves the stabilization of the starting germylene.

A similar migration of the Si(SiMe₃)₃ group was observed before in the case of the bis[tris(trimethylsilyl)silyl]stannylyene and plumblyene [148]. Their reactions with an aryl-



Scheme 81: Reaction of acyclic germylene (**1**) with AuCN.

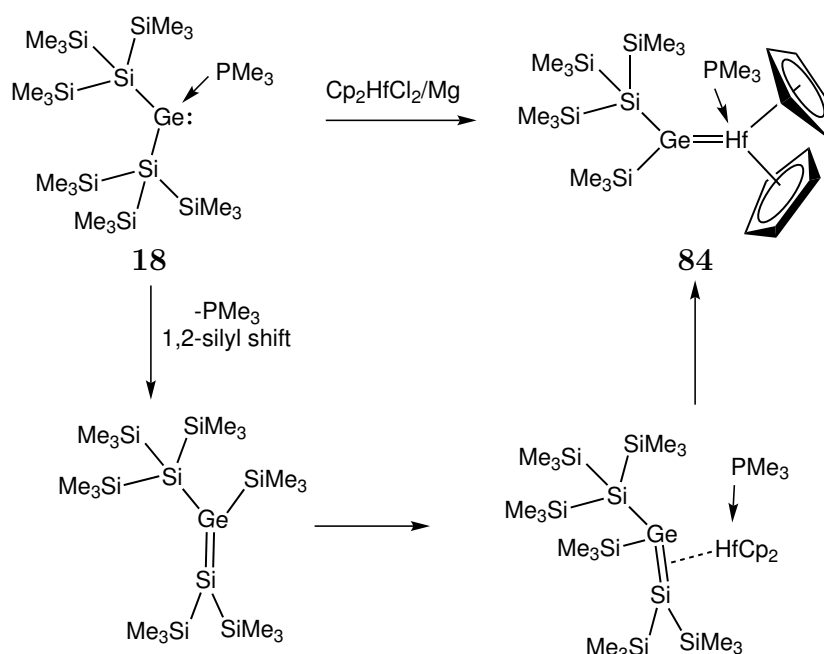
copper complex led to the formation of copper-stannylene and copper-plumbylene complexes, characterized by one of tris(trimethylsilyl)silyl groups exchanged for an aryl group (Scheme 82). Although the stannylene complex is stable and its crystal structure has been determined, the corresponding plumbylene complex decomposed to the asymmetric plumbylene $\text{Pb}[\text{Si}(\text{SiMe}_3)_3]\text{Ar}^*$ and the trimerized tris(trimethylsilyl)silylcopper $[\text{CuSi}(\text{SiMe}_3)_3]_3$.



Scheme 82: Reaction of bis[tris(trimethylsilyl)silyl]stannylene and plumbylene with aryl-copper complex.

3.2 Reaction of germylene with group 4 metal complexes

Reaction of the bis[tris(trimethylsilyl)silyl]germylene PMe_3 adduct (**18**) with Cp_2HfCl_2 in the presence of magnesium at room temperature led to the formation of the germylene-hafnocene complex **84** (Scheme 83). Dark red crystals of **84** precipitated from pentane solution at $-35\text{ }^\circ\text{C}$. Weak coordination of PMe_3 to the germanium atom of **18** enabled the 1,2-silyl shift. The resulting transformation of the germylene into the silagermane was followed by the coordination of hafnocene to the $\text{Ge}=\text{Si}$ double bond. The elimination of $\text{Si}(\text{SiMe}_3)_2$ was possible, probably because of the formation of a complex with hafnocene, which was present in the reaction mixture in excess. However, there is no evidence for the formation of this unstable compound in the ^{29}Si NMR spectrum. Attempt to stabilize it with PMe_3 was unsuccessful and instead of $(\text{Me}_3\text{Si})_2\text{SiHfCp}_2\cdot\text{PMe}_3$ formation, a $(\eta^1:\eta^5\text{-C}_5\text{H}_4)$ -bridged dimer of hafnocene and PMe_3 was formed [149].



Scheme 83: Reaction of bis[tris(trimethylsilyl)silyl]germylene PMe_3 adduct (**18**) with hafnocene dichloride in the presence of magnesium.

The ^{29}Si NMR spectrum of **84** shows three doublets at -97.5 , -8.3 and 1.8 ppm. The resonance of the central silicon atom of **84** (-97.5 ppm) is more than 20 ppm downfield shifted, compared to the analogous signal of the starting material **18** (-119.9 ppm). In the ^1H NMR spectrum two resonances originate from hydrogen atoms of the Cp rings, which suggests multiple-bond character of the Ge–Hf bond. Compound **84** crystallized in triclinic space group $\text{P}\bar{1}$ (Figure 57, Table 47). The Ge(1)–Si(5) bond is slightly shorter than the Ge(1)–Si(1) one, however, both bonds are much shorter than in bis[tris(trimethylsilyl)silyl]-

germylene adducts **1** and **14**. The Ge–Hf bond length of 2.5867(8) Å is almost equal to the corresponding bond in the five-membered ring germylene-hafnocene complex (2.599 Å) [61] and significantly shorter than the Ge–Hf bond in hafnocene 1,1,2,2-tetrakis(trimethylsilyl)digermene (2.8413(8) and 2.8670(4) Å) [150] and in a hafnocene-germyl complex Cp*Cl₂HfGe(SiMe₃)₃ (2.740(1) Å) [151]. Shortened distance between Hf and Ge compared to the latter hafnocene-germyl compound reveals the bond order higher than one between the metal and the germanium atom in **84**. The planar geometry of germanium atom (sum of angle yielding 359.95°) indicates its sp² hybridization.

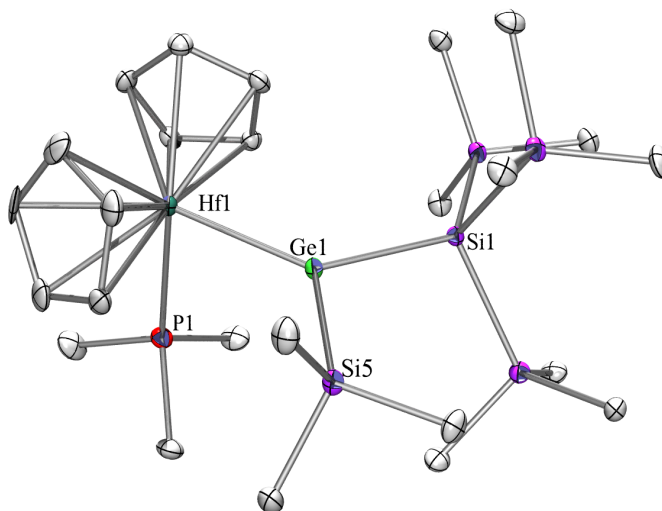


Figure 57: Crystal structure of **84**.

Table 47: Selected bond lengths and angles of **84**.

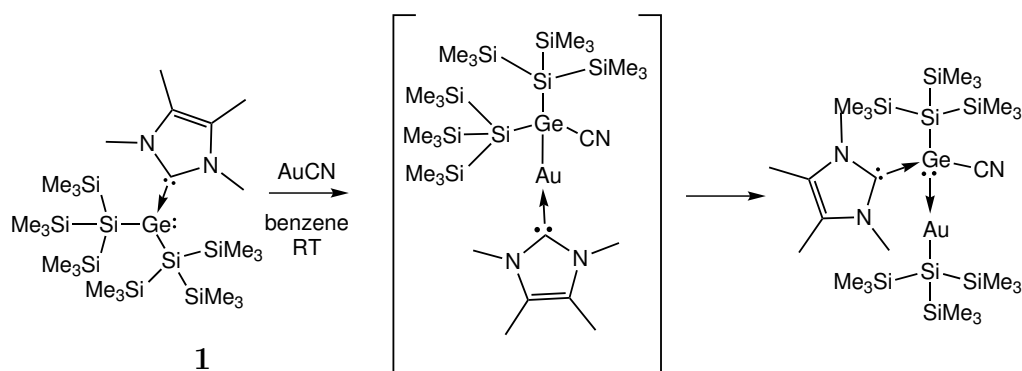
| Bond | Length [Å] | Bonds | Angle [°] |
|-------------|--------------|-------------------|-------------|
| Ge(1)–Hf(1) | 2.5867(8) | Hf(1)–Ge(1)–Si(1) | 130.97(5) |
| Ge(1)–Si(1) | 2.430(18) | P(1)–Hf(1)–Ge(1) | 89.14(4) |
| Hf(1)–P(1) | 2.6465(18) | Hf(1)–Ge(1)–Si(5) | 123.41(5) |
| Ge(1)–Si(5) | 2.4230(18) | Si(1)–Ge(1)–Si(5) | 105.57(6) |

Complex **84** reacted neither with acetylenes, such as phenylacetylene and trimethylsilylacetylene, nor with benzaldehyde. Substitution of trimethylphosphine with an N-heterocyclic carbene was not successful either.

3.3 Reactions of tetrylenes with group 11 metal complexes

3.3.1 Synthesis

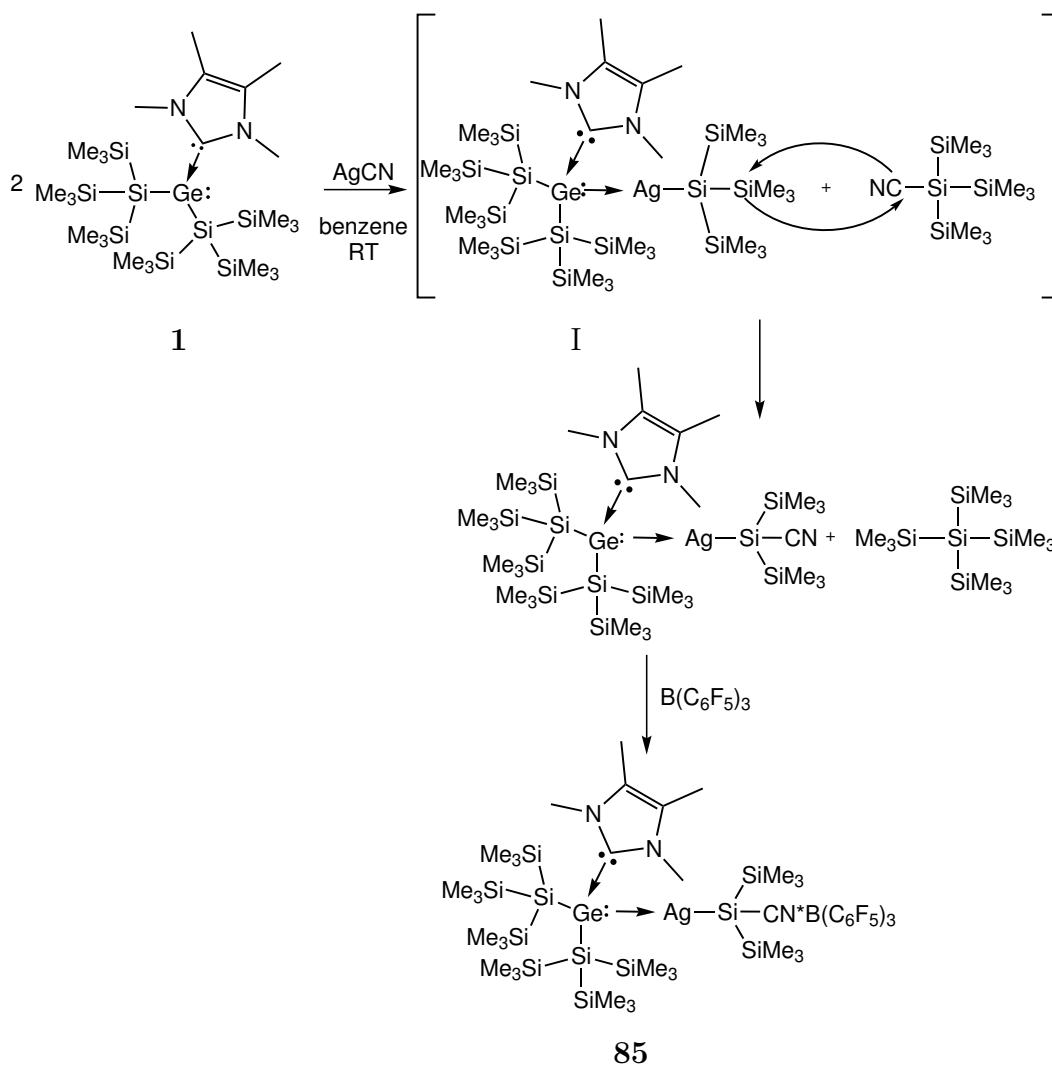
As mentioned in the introduction (see Section 3.1), the reaction of 1,3,4,5-tetramethylimidazol-2-ylidene adduct of [bis(trimethylsilyl)silyl]germylene (**1**) with AuCN led to the formation of tris(trimethylsilyl)silyl{cyano[tris(trimethylsilyl)silyl]germylene · IMe₄}gold(I). The product contains a tris(trimethylsilyl)silyl group bonded to the gold atom [37]. The reaction was repeated for verification. The ²⁹Si NMR spectrum recorded immediately after mixing **1** with AuCN differs by about two signals from the one recorded one hour later. This difference suggested that during the reaction an intermediate was formed. The observed locations of the additional resonances (−8.4 and −99.9 ppm) agree with the expected locations of the proposed product formed by the insertion of the germylene into the Au–CN bond and the migration of the carbene to the gold atom (Scheme 84). Subsequently, the migration of the NHC carbene to the germanium atom and of the tris(trimethylsilyl)silyl group to the gold atom occurred.



Scheme 84: Proposed reaction path of **1** with AuCN.

Analogous reactions with AgCN and CuCN were carried out in order to verify that the tris(trimethylsilyl)silyl group migration takes place in silver and copper germylene complexes. The 1,3,4,5-tetramethylimidazol-2-ylidene adduct of [bis(trimethylsilyl)silyl]germylene (**1**) was reacted with AgCN in benzene at room temperature. After two hours tris(pentafluorophenyl)borane was added to prevent decomposition of the formed product. Based on the ²⁹Si NMR spectrum all starting material was consumed after 6 hours. The crystal structure analysis of **85** showed a novel Ge–Ag–Si compound with the silicon center substituted with two trimethylsilyl and one cyanide group, with borane coordinated to it. Product **85** provides the first example of a compound containing a Ge–Ag–Si structural unit. A plausible first step of the reaction is the formation of a germanium-silver complex with two tris(trimethylsilyl)silyl groups attached to the germanium atom and one bonded to the silver atom (Scheme 85). Unfortunately, the NMR spectrum did not confirm the presence of the latter complex (see compound I in Scheme 85) in the reaction mixture due to recording time, which was too short. The two signals in the spectrum were assigned to

tris(trimethylsilyl)silylcyanide (-11.0 and -103.3 ppm). Compound **85** was obtained as a product of the addition of $B(C_6F_5)_3$ to the reaction mixture. It suggests that the exchange of a trimethylsilyl group with CN took place before the addition of borane. Additionally, the presence of tetrakis(trimethylsilyl)silane was confirmed by ^{29}Si NMR spectrum.



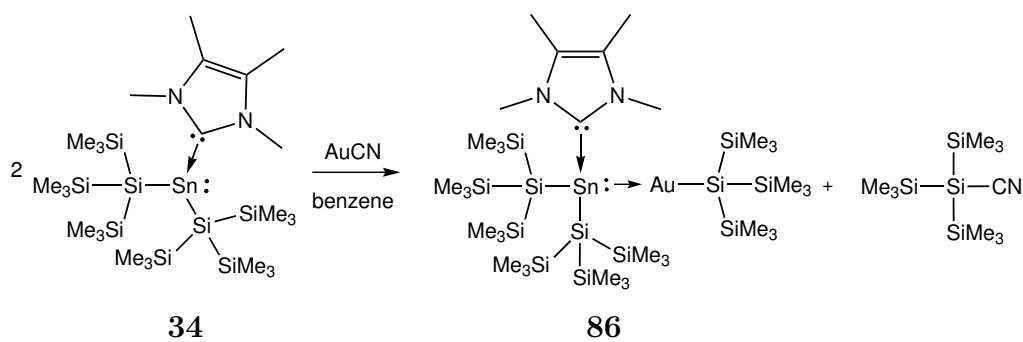
Scheme 85: Proposed mechanism of the formation of **85** complex.

The N-heterocyclic carbene adduct of acyclic germylene (**1**) did not react with CuCN regardless of whether the reaction was conducted in benzene or THF. Repetition of this reaction with CuCl instead CuCN led to the formation of a compound characterized by the two peaks at -109.0 and -8.8 ppm in the ^{29}Si NMR spectrum. The presence of only one signal originating from the trimethylsilyl group suggests that no migration similar to the one described above, did occur in this case. The structure of the obtained compound was not determined.

Surprisingly, reaction of the germylene **14**, stabilized by a more bulky N-heterocyclic

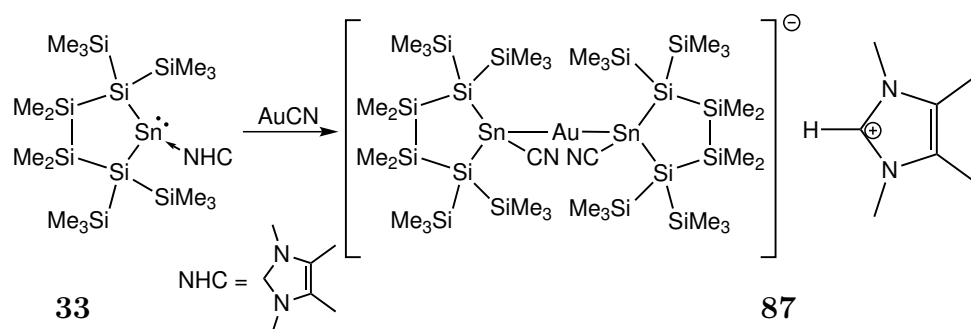
carbene ($^{\text{Me}}\text{IiPr}$), with AuCN in benzene did not proceed and after 2 days only the starting material was detected in the reaction mixture instead of the expected product. It suggests that in germylene **14** the germanium center is protected by $^{\text{Me}}\text{IiPr}$, which does not allow for contact between germylene and the gold atom.

The reaction of bis[tris(trimethylsilyl)silyl]stannylene N-heterocyclic carbene adduct **34** with AuCN was carried out in order to check whether the migration of the tris(trimethylsilyl)silyl group takes place also for stannylene, as observed previously in the case of germylene. The result was positive: during the reaction complex **86** was obtained. Surprisingly, it proceeded only with fourfold excess of gold cyanide. Additionally to **86** during the reaction a black precipitation was formed. Compound **34** formed colorless crystals, suitable for X-ray study. In contrast to AuCN, stannylene **34** did not react even with huge excess of AgCN or CuCN, and even when heated up to 70°C.



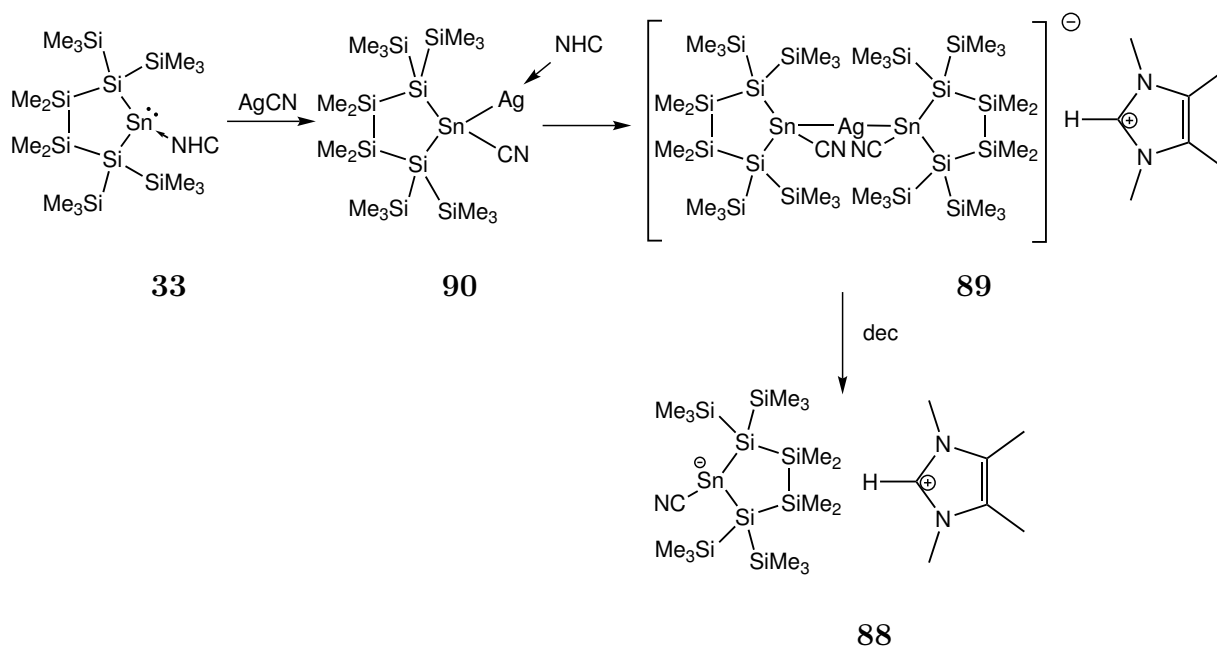
Scheme 86: Reaction of bis[tris(trimethylsilyl)silyl]stannylene NHC adduct (**34**) with AuCN.

The surprising products of the reaction of N-heterocyclic carbene adducts of stannylene and germylene with group 11 metal cyanide motivated an attempt to react a cyclic stannylene adduct with AuCN, AgCN and CuCN. The reaction of five-membered ring stannylene NHC adduct **33** with AuCN led to the formation of the ionic compound **87** (Scheme 87). Slow evaporation of benzene gave colorless crystals of **87**.



Scheme 87: Reaction of cyclic stannylene NHC adduct **33** with AuCN.

As an outcome of the reaction of the five-membered ring stannylene N-heterocyclic carbene adduct **33** with AgCN were colorless crystals of **88** obtained (Scheme 88). Compound **88** was probably formed as a product of the decomposition of the ionic silver complex **89**, which is similar to **87**, obtained in the reaction of **33** with gold cyanide (Scheme 87). Although the resonances present in the ^{29}Si NMR spectrum recorded 18 hours after mixing the starting materials could fit to the proposed compound **89**, lack of the ^1H NMR signal characteristic for the protonated N-heterocyclic carbene, suggests that **89** was not present in the measured solution. Thus, it is conceivable that another intermediate is formed on the early stage of this reaction. The stannyl-silver complex **90**, analogous to that reported by Hlina *et al.* [147], is a plausible candidate. The rearrangement of **90** into **89** can be rationalized by the fact that the N-heterocyclic carbene is not a suitable ligand for group 11 metals, as observed before in the case of AgCN and AuCN reacting with bis[tris(trimethylsilyl)silyl]germylene and stannylene NHC adducts **2** and **34**. The ionic compound **88** is also unstable and, according to the ^1H NMR spectrum, decomposed to several unknown products. An attempt to obtain **88** in the reaction of stannylene **33** and KCN in the presence of crown ether (18-crown-6), which helps to solubilize potassium, was unsuccessful. It suggests that reactions of **33** with cyanides are metal specific.



Scheme 88: Proposed reaction path resulting in the formation of **88**.

It is very surprising that the protonated N-heterocyclic carbene was formed at all in the above mentioned reactions, due to the hydrogen, necessary to protonate the carbene, whose source is completely unclear. The solvent, which is the usual suspect in such cases, can be safely ruled out as a donor, since the reactions were carried out in benzene solution. It will be necessary to investigate this issue in future studies.

3.3.2 NMR spectroscopy

The ^{29}Si NMR spectrum of silver complex **85** shows five resonances: two doublets at -8.9 and -107.3 ppm, which are assigned to the silicon atoms of the tris(trimethylsilyl)silyl groups bonded to the germanium atom, one doublet at -5.3 ppm and two doublets at -124.3 ppm originating from the group attached to the silver atom (Figure 58). The presence of the two latter doublets ($^1J_{\text{Si}-\text{Ag}}=214$ Hz, $^1J_{\text{Si}-\text{Ag}}=255$ Hz) provides evidence that the silicon atom is directly bonded to the silver center. Comparison of ^{29}Si NMR spectra of the starting material **1** and the silver complex **85** indicates a 17 ppm downfield shifted resonance of the silicon atom bonded to the germanium of the silver complex. This observation is in line with recently published results for cyanogermyl and cyanostannyl complexes [147]. The ^{11}B NMR resonances (-22.6 ppm) of **85** is about 10 ppm upfield shifted, compared to the resonance of $\text{B}(\text{C}_6\text{F}_6)_3$ group coordinated to the nitrile substituent attached to germanium and tin [147].

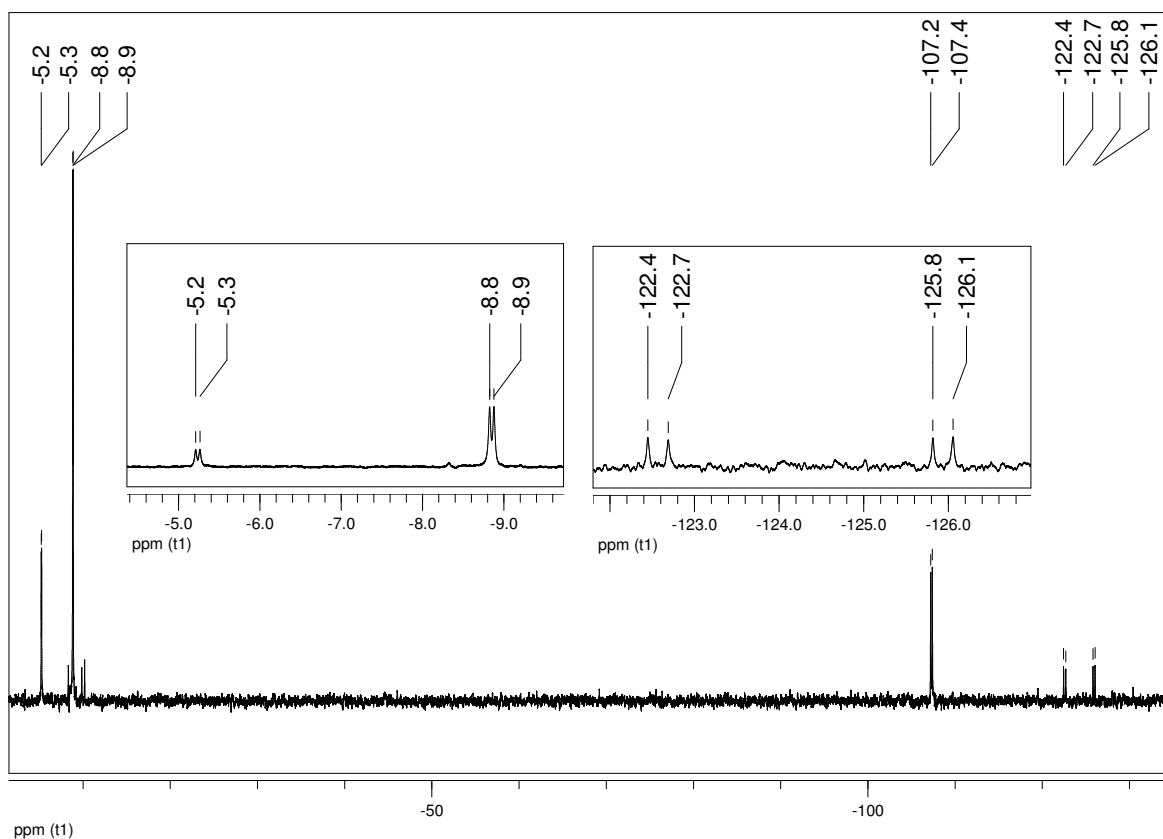


Figure 58: ^{29}Si NMR spectrum of **85**.

Moving on to the ^{29}Si NMR spectrum of the gold-stannylene complex **86**, two pairs of resonances corresponding to two chemically different tris(trimethylsilyl)silyl groups are observed, as expected. The resonance of -114.2 ppm originates from the quaternary

silicon of the $(\text{Me}_3\text{Si})_3\text{Si}$ group attached to germanium. It is shifted upfield by about 20 ppm, compared to the corresponding signal of the starting material **34**, which is in good agreement with the previously described chemical shift difference of silver-germylene complex **85** and bis[tris(trimethylsilyl)]germylene IMe_4 adduct (**1**). The signal of silicon atoms of trimethylsilyl groups within $(\text{Me}_3\text{Si})_3\text{Si}$ groups attached to germanium is located at -7.0 ppm. The resonances of -99.4 and -4.9 ppm originating from the tris(trimethylsilyl)silyl group attached to gold are very similar to those of gold germylene complex (-95.7 and -4.7 ppm) [37]. **86** exhibits the ^{119}Sn NMR shift of 136.8 ppm, which is down-field shifted by about 434 ppm, compared to the starting material (-297.2 ppm). It suggests that the contribution of the stannylene-like character to the overall properties of this complex (**86**) is bigger than it is the case for the N-heterocyclic adduct of bis[tris(trimethylsilyl)silyl]stannylene **34**.

The ^{29}Si NMR spectrum of the ionic compound **87** shows four resonances: at -4.4 , -7.6 , -19.2 and -121.8 ppm, while the ^{119}Sn NMR spectrum exhibits one resonance at -70.9 ppm. The signal originating from the protonated N-heterocyclic carbene is observed in the ^1H NMR spectrum at 8.89 ppm, that is in the spectral range reported before for a similar compound [152].

If the formation of **88** follows the proposed reaction pathway depicted in Scheme 88, the observed ^{29}Si NMR chemical shifts (-130.3 , -18.0 , -7.8 and -4.4 ppm) will originate from **90**. Assuming that the above is true, the signal of quaternary silicon (-130.3 ppm) is shifted upfield by about 8 ppm, compared to the corresponding resonance (-122.7 ppm) of phosphine stabilized gold-stannyl complex [147]. The resonances present in the ^{29}Si NMR spectrum of the decomposed compound **88** do not differ significantly from those of **90**. At the same time the chemical shift of the quaternary silicon in **88** is upfield shifted by as much as 12 ppm with respect to the corresponding silicon atom in the gold ionic compound **87**. In the ^1H NMR spectrum the signal of the protonated N-heterocyclic carbene is located at 8.51 ppm.

3.3.3 Crystallography

The crystalline silver-germylene complex **85** has a monoclinic symmetry with space group $\text{P}2(1)/c$ (Figure 59, Table 48). The Ag–Ge bond measures 2.502 \AA and is almost equally long as two such bonds in Roesky’s germylene-silver complex ($2.4732(10)$ and $2.4551(8) \text{ \AA}$) [153]. The silver–silicon distance of $2.4226(10) \text{ \AA}$ is slightly shorter than in the [tris(trimethylsilyl)silyl]silver·NHC adducts [154], and is almost equal to that found in the silver-silylene complex [155]. Compound **85** features nearly linear Ge–Ag–Si arrangement with an angle of $176.11(3)^\circ$ (see lower panel in Figure 59). The other three bonds, Si–C–N–B, form another close-to-linear pattern at approximately tetragonal angle (precisely $108.42(10)^\circ$) to the Ge–Ag–Si fragment.

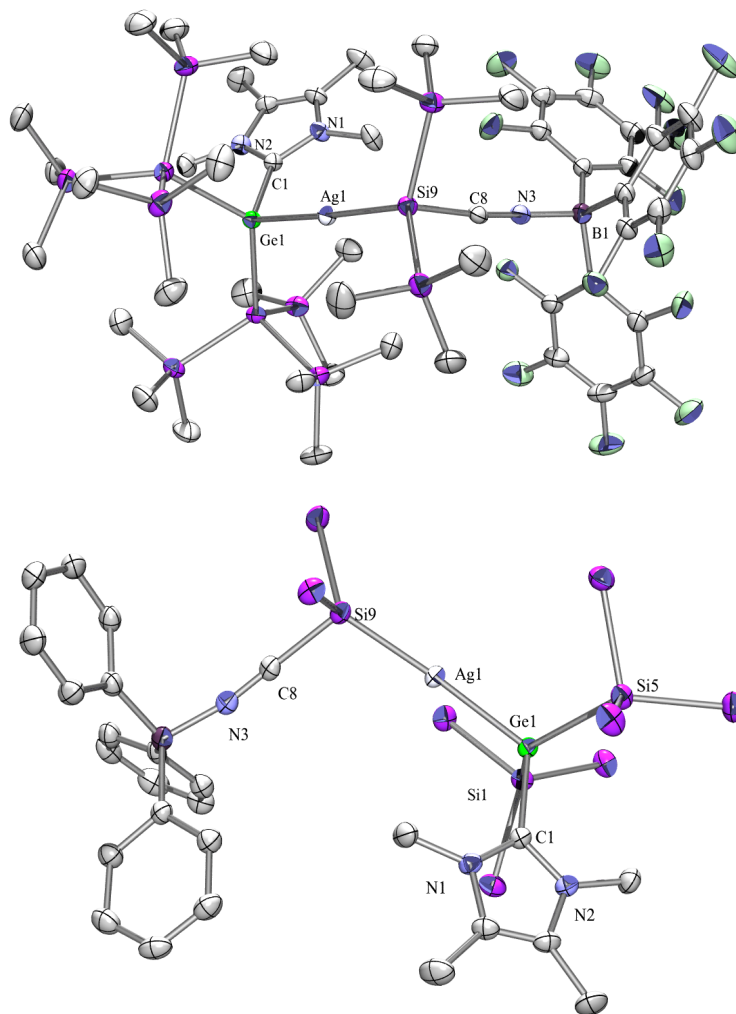


Figure 59: Crystal structure of **85**

Table 48: Selected bond lengths and angles of **85**.

| Bond | Length [Å] | Bonds | Angle [°] |
|-------------|--------------|-------------------|-------------|
| Ag(1)–Ge(1) | 2.5022(6) | Si(9)–Ag(1)–Ge(1) | 176.11(3) |
| Ge(1)–Si(5) | 2.4649(11) | Ag(1)–Ge(1)–Si(5) | 106.79(3) |
| Ge(1)–Si(1) | 2.4569(11) | Ag(1)–Ge(1)–C(1) | 108.82(9) |
| Ge(1)–C(1) | 2.037(3) | Ag(1)–Ge(1)–Si(1) | 110.35(3) |
| Ag(1)–Si(9) | 2.4226(10) | Si(1)–Ge(1)–Si(5) | 125.56(4) |
| Si(9)–C(8) | 1.888(4) | C(1)–Ge(1)–Si(5) | 101.66(9) |
| C(8)–N(3) | 1.150(4) | C(1)–Ge(1)–Si(1) | 102.35(9) |
| | | Ag(1)–Si(9)–C(8) | 108.42(10) |
| | | Si(9)–C(8)–N(3) | 174.6(3) |

The crystalline gold-stannylene complex **86** has a triclinic symmetry with space group $P\bar{1}$ (Figure 60, Table 49). The Sn–Au bond that yields 2.6389 Å is the longest among all known bonds involving tin and the two-coordinated gold atoms, which fall within the range of 2.565–2.614 Å [147, 156, 157]. At the same time the distance between Si and Au yields 2.345(3) Å, which is the shortest among all Si–Au bonds reported in the literature [158–163].

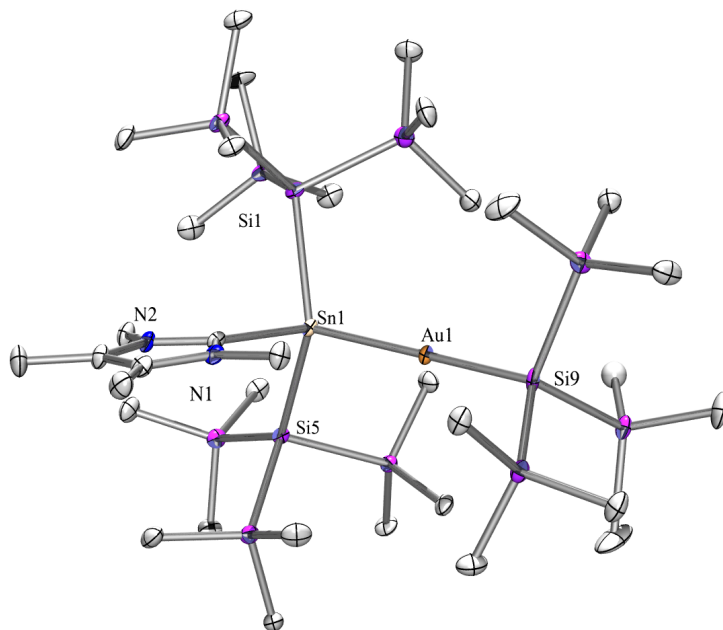


Figure 60: Crystal structure of **86**.

Table 49: Selected bond lengths and angles of **86**.

| Bond | Length [Å] | Bonds | Angle [°] |
|-------------|--------------|-------------------|-------------|
| Au(1)–Sn(1) | 2.6389(12) | Si(9)–Au(1)–Sn(1) | 177.75(7) |
| Sn(1)–C(1) | 2.258(8) | Au(1)–Sn(1)–Si(1) | 114.09(6) |
| Sn(1)–Si(1) | 2.632(2) | Au(1)–Sn(1)–C(1) | 106.6(2) |
| Sn(1)–Si(5) | 2.644(2) | Au(1)–Sn(1)–Si(5) | 111.23(6) |
| Au(1)–Si(9) | 2.345(3) | C(1)–Sn(1)–Si(1) | 100.3(2) |
| | | C(1)–Sn(1)–Si(5) | 97.8(2) |
| | | Si(1)–Sn(1)–Si(5) | 123.20(8) |

Crystals of compound **87** have triclinic symmetry with space group $P\bar{1}$ (Figure 61, Table 50). Two independent molecules of **87**, two protonated NHC, and two benzenes appear in the asymmetric unit. The length of the Au–Sn bond (2.5960(7) Å) falls into the typical range for this type of bonds. Compound **87** displays the well-known linear geometry with Sn–Au–Sn angle of 177.283(9)°, as observed previously for two-coordinated group 11 metal complexes. The Sn–Si bonds of 2.5961(17) and 2.6045(12) Å are much shorter compared to the corresponding bonds in the starting stannylene **33** (2.6639(9) and 2.6734(9) Å), which indirectly suggests that the tin atom lost its stannylene character.

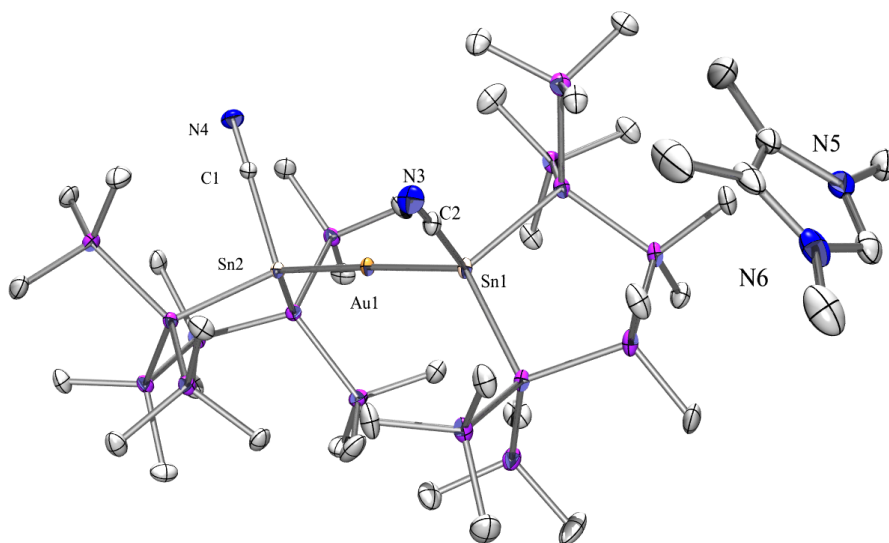


Figure 61: Crystal structure of **87**.

Table 50: Selected bond lengths and angles of **87**.

| Bond | Length [Å] | Bonds | Angle [°] |
|-------------|--------------|-------------------|-------------|
| Sn(1)–Au(1) | 2.5960(7) | Au(1)–Sn(1)–C(2) | 107.00(10) |
| Sn(2)–Au(1) | 2.5947(7) | Sn(1)–Au(1)–Sn(2) | 177.283(9) |
| Sn(1)–C(2) | 2.211(4) | Au(1)–Sn(2)–C(1) | 109.60(10) |
| C(2)–N(3) | 1.144(4) | Sn(2)–C(1)–N(4) | 177.2(3) |
| C(1)–N(4) | 1.142(5) | | |

The crystal structure of **89** was determined by X-ray measurement (Figure 62, Table 51). The five-membered ring exhibits an *envelope* conformation with one of the $\text{Si}(\text{SiMe}_3)_2$ units sticking out of plane. The Sn–Si bond lengths are very similar to those in the starting material **33**. The Sn–C bond of 2.248(3) Å is slightly longer than the one found in **87** (2.211(4) Å).

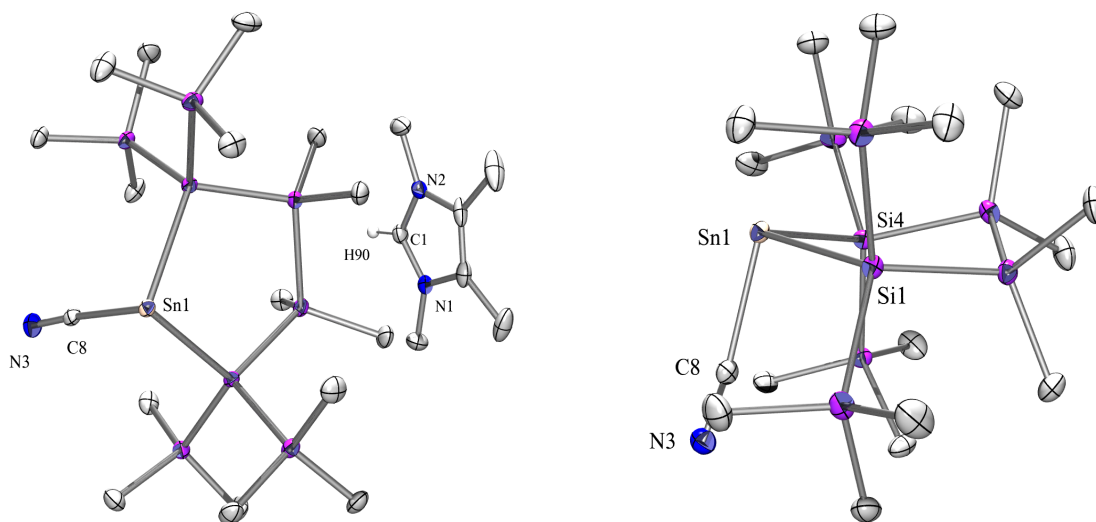


Figure 62: Crystal structure of **89**.

Table 51: Selected bond lengths and angles of **87**.

| Bond | Length [Å] | Bonds | Angle [°] |
|-------------|--------------|-------------------|-------------|
| Sn(1)–C(8) | 2.248(3) | C(8)–Sn(1)–Si(4) | 93.79(8) |
| Sn(1)–Si(4) | 2.6573(11) | C(8)–Sn(1)–Si(1) | 91.43(8) |
| Sn(1)–Si(1) | 2.6650(9) | Si(4)–Sn(1)–Si(1) | 94.39(3) |
| N(3)–C(8) | 1.146(4) | N(3)–C(8)–Sn(1) | 173.1(3) |

3.4 Conclusions

The present study of group 4 transition metal complexes demonstrates that the product of the reaction between the bis[tris(trimethylsilyl)silyl]germylene \cdot PMe_3 adduct (**18**) and hafnocene dichloride in the presence of magnesium, differs from the products obtained in similar reactions of cyclic germylene, although in both cases a germylene-metallocene complex was formed. The NMR spectroscopy as well as the X-ray structure analysis confirmed the Hf–Ge multiple bond character of **84**.

The N-heterocyclic carbene adducts of germylenes and stannylenes studied here showed interesting reactivity towards group 11 cyanides. The products of these reactions differ fundamentally from the compounds obtained previously, when phosphine adducts of tetrylenes were reacted with AuCN, AgCN and CuCN. Most importantly, the products formed in the reaction of NHC adduct of tetrylenes with group 11 cyanides were highly specific to both tetrylene and cyanide reagents. In the case of PEt_3 germylene and stannylene adducts reacted with AuCN, AgCN and CuCN, tetrylenes were inserted into M–CN bonds and the products featured the phosphine ligand coordinating to the metal atom. The analogous reaction using N-heterocyclic adducts of acyclic germylene led to the migration of a tris(trimethylsilyl)silyl group from Ge to Au atom and the subsequent transfer of the CN group to the Ge atom. Exchanging either the germylene for stannylene or AuCN for AgCN in the latter reaction activated a very different pathway, i. e. in both cases the third tris(trimethylsilyl)silyl group was added to the gold and silver atom resulting in the formation of an additional product, $(\text{Me}_3\text{Si})_3\text{SiCN}$. In the case of reactions involving the cyclic stannylene, the treatment with AuCN and AgCN resulted in the formation of ionic compounds. In all compounds mentioned above, an N-heterocyclic carbene is not coordinating to the group 11 metal, as it was the case for phosphine. Although examples of the NHC-gold, -silver and -copper compounds are known, their abundance in the literature is much more limited than it is the case for the phosphine complexes. The assumption, that a phosphine is a much more suitable ligand for soft acids such as Au^+ , Ag^+ and Cu^+ than N-heterocyclic carbenes, is strongly supported by the hard and soft acids and bases (HSAB) principle [164]. If germanium and tin complexes of NHC-carbene coordinated gold or silver are formed as suggested here, either they will rearrange to compounds, in which the carbene is located at germanium or tin atom or the protonation of the carbene will occur.

4 Experimental details

4.1 General experimental

4.1.1 General remarks

All reactions involving air-sensitive compounds were carried out in the atmosphere of dry nitrogen employing Schlenk techniques or using glovebox UNILAB 150, supplied by M.BROWN.

THF, DME, toluene, benzene and pentane were dried using a column solvent purification system by Innovative Technologies [165].

Deuterated benzene ordered from Deutero was distilled from sodium under nitrogen atmosphere. Deuterated THF and toluene was purchased from Deutero and used without further purification.

4.1.2 Chemical substances

Potassium *tert*-butoxide and sulfur was purchased exclusively from Merck. Magnesium turnings were obtained from Acros Organics. Trimethylphosphine was purchased from ABCR. Diphenylacetylene, phenylacetylene, trimethylsilylacetylene, 1-hexyne, 3-hexyne, 1,4-bis(trimethylsilyl)-1,3-butadiyne, triethylphosphine, 2,6-dimethylphenylisocyanide, *tert*-butylisocyanide, benzophenone, diacetyl, silver cyanide, gold cyanide, hafnocene dichloride, tin dichloride and bromoethane was purchased exclusively from Sigma Aldrich. All chemicals were used without further purification.

Tetrakis(trimethylsilyl)silane [166], tris(trimethylsilyl)silyl potassium (**3**) [167], tris(trimethylsilyl)germyl potassium (**4**) [97], bis[tris(trimethylsilyl)]silyl magnesium · 2 THF (**6**) [168], tris(trimethylsilyl)silatranysilane (**19**) [169], bis[tris(trimethylsilyl)germyl] magnesium · 2 THF (**24**) [170], 1,3-dipotassio-1,1,3,3,-tetrakis(trimethylsilyl)dimethyltrisilane (**12**) [171], 1,4-dipotassio-1,1,4,4-tetrakis(trimethylsilyl)tetramethyltetrasilane (**8**) [171, 172], 2-germa-1,1,3,3-tetrakis(trimethylsilyl)-2,2,3,3,-tetramethylcyclopentasilan-2-ylidene · PEt₃ (**7**) [38], germanium dichloride · dioxane [173], germanium dibromide · dioxane [173], 1,3,4,5-tetramethylimidazol-2-ylidene (IMe₄) [66], 1,3,-diisopropyl-4,5-dimethylimidazol-2-ylidene (^{Me}LiPr) [66], B(C₆F₅)₃ [174] were prepared by following known procedures. ^{Me}LiPr adduct of tris(trimethylsilyl)silyl(chloro)germylene (**5**) was prepared by slightly modified protocol presented by Katir *et al.* [33] i. e. changing the order in which starting material was added.

4.1.3 Analytical methods

NMR spectroscopy

^1H (300 MHz), ^{13}C (75.4 MHz), ^{11}B (96.0 MHz), ^{19}F (282.2 MHz) ^{29}Si (59.3 MHz), ^{31}P (121.4 MHz) and ^{119}Sn (111.8 MHz) NMR spectra were recorded on Varian INOVA 300 spectrometer. Temperature dependent NMR experiments were carried out with VARIAN VT setup, allowing the sample temperature to equilibrate for 15 minutes. Chemical shifts are reported in ppm. Samples for ^{29}Si NMR spectra were either dissolved in deuterated solvents or in the cases of reaction samples measured with D_2O capillary in order to provide a lock frequency signal. The completeness of reactions was usually controlled by NMR spectroscopy using solvent residual signals for referencing. To compensate for the low isotopic abundance of ^{29}Si , the INEPT pulse sequence was applied for amplification of the signal [175, 176].

X-ray structure analysis

The crystals were mounted onto the tip of glass fiber, the data collection was performed using Bruker-AXS SMART APEX CCD diffractometer (wavelength 0.710 73 Å). The data was reduced to F_0^2 and corrected for absorption effects with SAINT [177] and SADABS [178], respectively. The structures were solved using direct methods and refined by full-matrix least-squares method (SHELXL97) [179]. All non-hydrogen atoms were refined with anisotropic displacement parameters. Positions of the hydrogen atoms were determined using standard bond lengths and angles.

Elemental Analysis

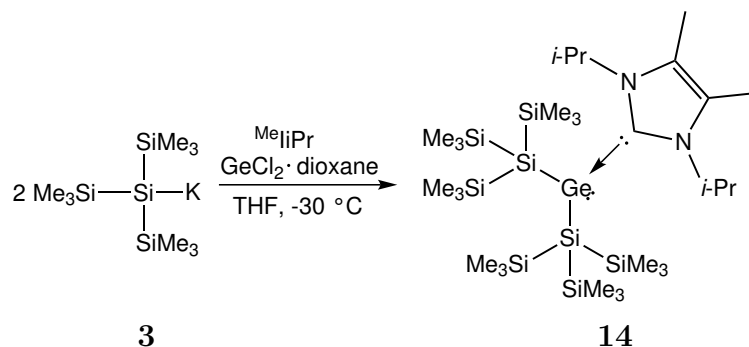
Elementary analysis were carried out using Heraeus Vario Elementar.

Melting points

Melting point determination was carried out on melting point apparatus with microscope from Mueller Optronic equipped with JM628 digital thermometer with Pt–100 thermocouple.

4.2 Experimental procedure

4.2.1 Bis[tris(trimethylsilyl)silyl]germylene · MeTiPr (**14**)



A solution of tris(trimethylsilyl)silyl potassium (**3**) (1.56 mmol) in THF (40 mL) was slowly added dropwise to a vigorously stirred solution of germanium dichloride · dioxane (180 mg, 1.78 mmol) and 1,3-diisopropyl-4,5-dimethylimidazol-2-ylidene (140 mg, 0.78 mmol) in THF (20 mL) at $-30\text{ }^{\circ}\text{C}$. The stirring of the reaction mixture was continued for 14 hours at room temperature. The solvent was removed under reduced pressure and the product was extracted with pentane (3 x 20 mL). The solvent was removed to yield **14** as an orange solid (469 mg, 77%). Crystallization from toluene at $-35\text{ }^{\circ}\text{C}$ gave orange crystals suitable for X-ray study.

Mp = 108–110 $^{\circ}\text{C}$.

$^1\text{H NMR}$ (300 MHz, C_6D_6): δ = 6.56 (br, 1H, CHMe_2), 5.73 (br, 1H, CHMe_2), 1.55 (s, 6H, $\text{NHC}-\text{Me}_3$), 1.30 (br, 12H, $\text{CH}(\text{Me})_2$) and 0.41 (s, 54H, SiMe_3) ppm.

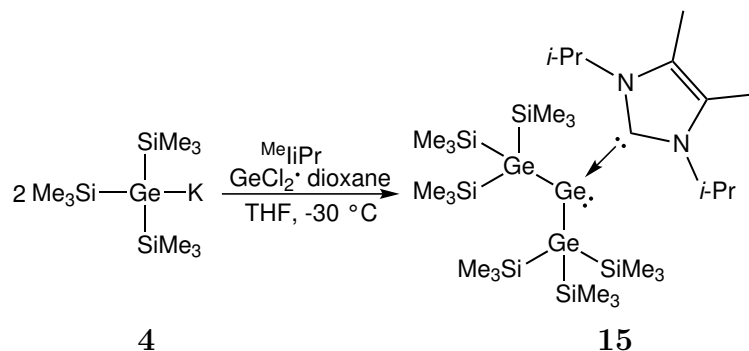
$^1\text{H NMR}$ (300 MHz, Toluene- d_8 , $-20\text{ }^{\circ}\text{C}$): δ = 6.55 (m, 1H, CHMe_2), 5.58 (m, 1H, CHMe_2), 1.55 (s, 3H, $\text{NHC}-\text{Me}$), 1.49 (s, 3H, $\text{NHC}-\text{Me}$), 1.24 (d, 6H, $\text{CH}(\text{Me})_2$, $^3J = 7.0\text{ Hz}$), 1.05 (d, 6H, $\text{CH}(\text{Me})_2$, $^3J = 7.0\text{ Hz}$) and 0.37 (s, 54H, SiMe_3) ppm.

$^{13}\text{C NMR}$ (75.4 MHz, C_6D_6): δ = 173.2 (N–C–N), 126.5 ($\text{MeC}=\text{CMe}$), 54.8 (CHMe_2), 52.3 (CHMe_2), 22.7 ($\text{CH}(\text{Me})_2$), 21.7 ($\text{CH}(\text{Me})_2$), 10.0 ($\text{NHC}-\text{Me}$) and 4.7 (SiMe_3) ppm.

$^{29}\text{Si NMR}$ (59.3 MHz, C_6D_6): δ = -8.8 (SiMe_3), -122.9 ($\text{Si}(\text{SiMe}_3)_3$) ppm.

Anal. calcd for $\text{C}_{29}\text{H}_{76}\text{GeN}_2\text{Si}_8$ (776.29): C 46.55, H 9.97, N 3.74. Found: C 46.84, H 9.65, N 3.89.

4.2.2 Bis[tris(trimethylsilyl)germyl]germylene · ^{Me}IiPr (15)



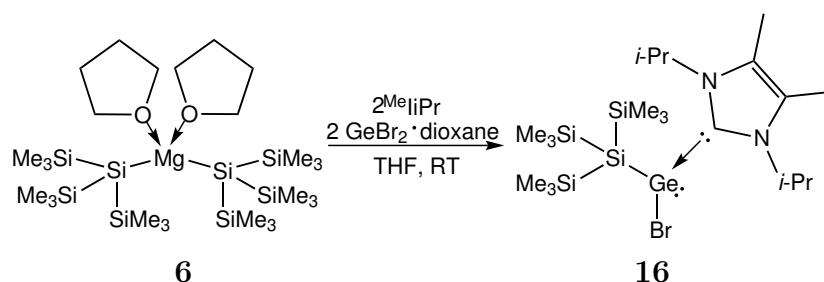
A solution of tris(trimethylsilyl)germyl potassium (**4**) (0.40 mmol) in THF (5 mL) was slowly added dropwise to a vigorously stirred solution of germanium dichloride · dioxane (51 mg, 0.22 mmol) and 1,3-diisopropyl-4,5-dimethylimidazol-2-ylidene (39 mg, 0.22 mmol) in THF (2 mL) at $-30\text{ }^{\circ}\text{C}$. The stirring of the reaction mixture was continued for 14 hours at room temperature. The solvent was removed under reduced pressure and the product was extracted with pentane (3 x 5 mL). The solvent was removed to yield **15** as an orange solid (148 mg, 88%).

¹H NMR (300 MHz, C_6D_6): $\delta = 6.45$ (m, 1H, N(1,3)-CH(CH₃)), 5.64 (m, 1H, N(1,3)-CH(CH₃)), 1.62 (s, 3H, C(4,5)-CH₃), 1.56 (s, 3H, C(4,5)-CH₃), 1.31 (d, 6H, N(1,3)-CH(CH₃)₂, ²*J* = 7.1 Hz), 1.10 (d, 6H, N(1,3)-CH(CH₃)₂, ²*J* = 7.1 Hz) and 0.42 (s, 54H, SiMe₃) ppm.

¹³C NMR (75.4 MHz, C_6D_6): $\delta = 174.8$ (N-C-N), 126.5 (MeC=CMe), 126.2 (MeC=CMe), 54.7 (N(1,3)-CH(CH₃)₂), 52.0 (N(1,3)-CH(CH₃)₂), 22.7 (N(1,3)-CH(CH₃)₂), 21.6 (N(1,3)-CH(CH₃)₂), 10.1 C(4,5)-CH₃, 9.7 C(4,5)-CH₃ and 5.1 (SiMe₃) ppm.

²⁹Si NMR (59.3 MHz, C_6D_6): $\delta = -4.1$ (SiMe₃) ppm.

4.2.3 Tris(trimethylsilyl)silyl(bromo)germylene · ^{Me}LiPr (16)



A solution of bis[tris(trimethylsilyl)]silyl magnesium · 2 THF (**6**) (0.15 mmol) in THF (2 mL) was slowly added dropwise to a vigorously stirred solution of germanium dibromide · dioxane (95 mg, 0.30 mmol) and 1,3-diisopropyl-4,5-dimethylimidazol-2-ylidene (54 mg, 0.30 mmol) in THF (2 mL) at room temperature. After 1 hour the solvent was removed under reduced pressure and the product was extracted with pentane (3 x 5 mL). The solvent was removed to yield **16** as an orange solid (53 mg, 62%).

Mp: 109–113 °C (dec).

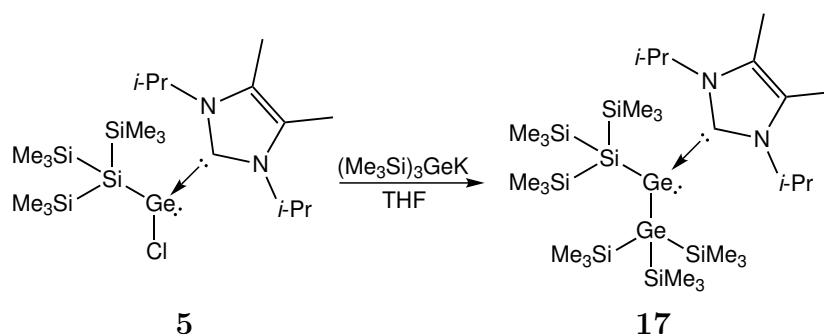
¹H NMR (300 MHz, C₆D₆): δ = 5.59 (sept, 2H, N(1,3)–CH(CH₃), ³J = 6.9 Hz), 1.45 (s, 6H, C(4,5)–CH₃), 1.26 (d, 6H, N(1,3)–CH(CH₃)₂, ³J = 7.0 Hz), 1.11 (d, 6H, N(1,3)–CH(CH₃)₂, ³J = 7.0 Hz) and 0.49 (s, 27H, SiMe₃) ppm.

¹³C NMR (75.4 MHz, C₆D₆): δ = 170.0 (N–C–N), 125.3 (MeC=CMe), 53.0 (CH(CH₃)₂), 21.7 (N(1,3)–CH(CH₃)₂), 9.6 (C(4,5)–CH₃) and 3.5 (SiMe₃) ppm.

²⁹Si NMR (59.3 MHz, C₆D₆): δ = –7.2 (SiMe₃), –121.2 (Si(SiMe₃)₃) ppm.

Anal. calcd for C₂₀H₂₇BrGeN₂Si₄ (580.49): C 41.38, H 8.16, N 4.83. Found: C 42.53, H 7.85, N 4.88.

4.2.4 Tris(trimethylsilyl)germyltris(trimethylsilyl)silylgermylene · ^{Me}IiPr (17)

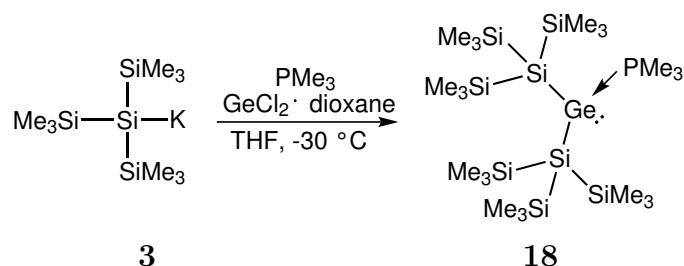


A solution of tris(trimethylsilyl)germyl potassium (**4**) (0.28 mmol) in THF (2 mL) was slowly added dropwise to a vigorously stirred solution of tris(trimethylsilyl)silyl(chloro)germylene · ^{Me}IiPr (**5**) (75 mg, 0.14 mmol) in THF (2 mL) at room temperature. After 3 hours the solvent was removed under reduced pressure and the product was extracted with pentane (3 x 5 mL). The solvent was removed to yield **17** as an orange solid (64 mg, 58%).

¹H NMR (300 MHz, C₆D₆): δ = 6.52 (m, 1H, N(1,3)-CH(CH₃)), 5.66 (m, 1H, N(1,3)-CH(CH₃)), 1.59 (s, 3H, C(4,5)-CH₃), 1.53 (s, 3H, C(4,5)-CH₃), 1.33 (br, 12H, N(1,3)-CH(CH₃)₂), 0.43 (s, 27H, SiSiMe₃) and 0.41 (s, 27H, GeSiMe₃) ppm.

²⁹Si NMR (59.3 MHz, C₆D₆): δ = -4.2 (GeSiMe₃), -8.7 (SiSiMe₃) and -123.3 (Si(SiMe₃)₃) ppm.

4.2.5 Bis[tris(trimethylsilyl)silyl]germylene · PMe₃ (**18**)



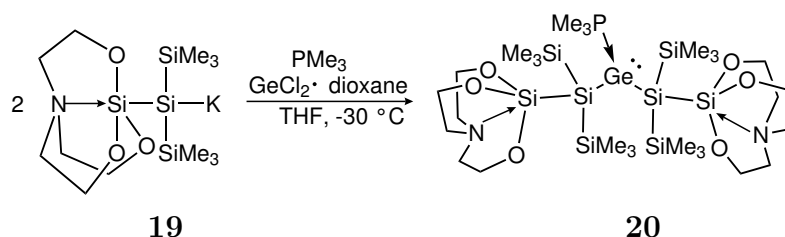
A solution of tris(trimethylsilyl)silyl potassium (**3**) (0.62 mmol) in THF (2 mL) was slowly added dropwise to a vigorously stirred solution of germanium dichloride · dioxane (72 mg, 0.31 mmol) and trimethylphosphine (23 mg, 0.31 mmol) in THF (2 mL) at $-30\text{ }^\circ\text{C}$. The full conversion was detected by ^{29}Si NMR spectrum after 15 minutes. Compound **18** was used without further purification. An approximate yield of 60% was estimated by comparison of the SiMe_3 ^1H NMR signal of **18** to that of $\text{Me}_3\text{Si O } t\text{-Bu}$, which is present in the solution resulting from the formation of tris(trimethylsilyl)silyl potassium.

^1H NMR (300 MHz, D_2O capillary): $\delta = 1.37$ (s, 9H, PMe_3) and 0.43 (s, 54H, SiMe_3) ppm.

^{29}Si NMR (59.3 MHz, D_2O capillary): $\delta = -8.9$ (d, SiMe_3 , $^3J_{\text{Si-P}} = 11$ Hz) and -119.9 ($\text{Si}(\text{SiMe}_3)_3$, $^2J_{\text{Si-P}} = 15$ Hz) ppm.

^{31}P NMR (121.4 MHz, D_2O capillary): $\delta = -20.1$ (PMe_3) ppm.

4.2.6 Bis[bis(trimethylsilyl)silatranlysilyl]germylene · PMe₃ (**20**)



A solution of **19** (0.12 mmol) in THF (1 mL) freshly prepared from tris(trimethylsilyl)silatranlysilane (50 mg, 0.12 mmol) and *t*-BuOK (15 mg, 0.12 mmol) was slowly added dropwise to a stirred solution of germanium dichloride · dioxane (14 mg, 0.06 mmol) and PMe₃ (5 mg, 0.06 mmol) in THF (1 mL) at $-30\text{ }^{\circ}\text{C}$. After 1 hour the solvent was evaporated and product was extracted with pentane (3 x 8 mL). The solvent was evaporated to give yellowish solid of **20** (45 mg, 88%).

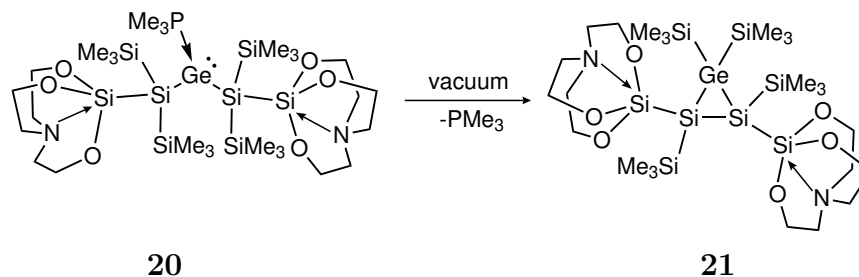
¹H NMR (300 MHz, C₆D₆): $\delta = 3.37$ (t, 12H, OCH₂, $^3J = 5.4\text{ Hz}$), 2.10 (t, 12H, NCH₂, $^3J = 5.2\text{ Hz}$), 1.59 (d, 9H, PMe₃, $^2J_{H-P} = 10.5\text{ Hz}$) and 0.64 (s, 36H, SiMe₃) ppm.

¹³C NMR (75.4 MHz, C₆D₆): $\delta = 59.5$ (OCH₂), 51.5 (NCH₂), 18.1 (d, PMe₃, $^1J_{C-P} = 22\text{ Hz}$), 3.8 (SiMe₃) and 3.8 (SiMe₃) ppm.

²⁹Si NMR (59.3 MHz, C₆D₆): $\delta = -8.1$ (d, SiMe₃, $^3J_{Si-P} = 9\text{ Hz}$), -8.4 (s, SiMe₃), -43.7 (d, Sa, $^3J_{Si-P} = 16\text{ Hz}$) and -125.7 (Si(SiMe₃)₃, $^2J_{Si-P} = 13\text{ Hz}$) ppm.

³¹P NMR (121.4 MHz, C₆D₆): $\delta = -18.2$ (PMe₃) ppm.

4.2.7 *trans*-1,1,2,3-Tetrakis(trimethylsilyl)-2,3-silatranylcyclopropa-1-germadi-silane (**21**)

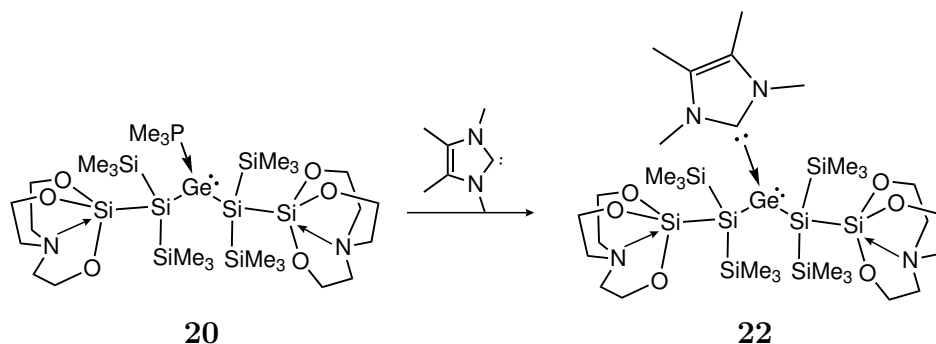


Applying vacuum to **20** (45 mg, 0.05 mmol) for 90 minutes gave **21** (41 mg, 100%).

^1H NMR (300 MHz, C_6D_6): $\delta = 3.38$ (t, 12H, OCH_2 $^3J = 5.6\text{Hz}$), 1.93 (t, 12H, NCH_2 , $^3J = 5.6\text{Hz}$), 0.73 (s, 18H, SiMe_3) and 0.66 (s, 18H, SiMe_3) ppm.

^{29}Si NMR (59.3 MHz, C_6D_6): $\delta = -0.6$ (GeSiMe_3), -6.5 (s, SiSiMe_3), -53.1 (Sa) and -168.6 ($\text{Si}(\text{SiMe}_3)_3$) ppm.

4.2.8 Bis[bis(trimethylsilyl)silatranlysilyl]germylene · IMe₄ (**22**)



I₄Me₄ (7 mg, 0.06 mmol) was added to the stirred solution of **20** (0.06 mmol) in THF (10 mL) at room temperature. After 1 hour the solvent was removed under reduced pressure and the product was extracted with pentane/toluene 1:1 (3 x 5 mL). The solvent was removed to yield **22** as an orange solid. (47 mg, 88%).

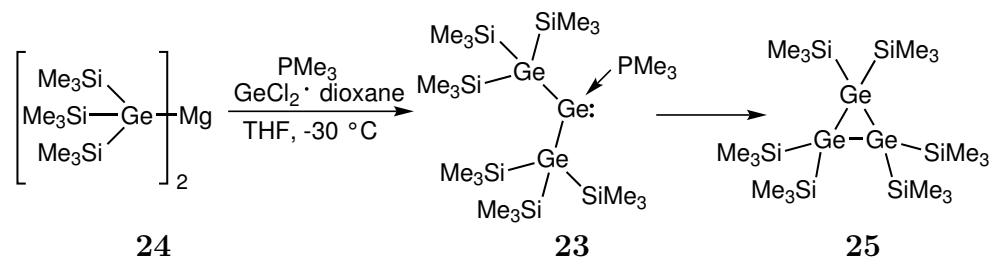
Mp = 128–129 °C

¹H NMR (300 MHz, THF-d₈): δ = 3.97 (s, 3H, N–CH₃), 3.94 (s, 3H, N–CH₃), 3.49 (t, 12H, OCH₂, ³J = 5.4 Hz), 2.66 (t, 12H, NCH₂, ³J = 5.4 Hz), 2.17 (s, 3H, C–CH₃), 2.16 (s, 3H, C–CH₃), 0.23 (s, 18H, SiMe₃) and 0.02 (s, 18H, SiMe₃) ppm

¹³C NMR (75.4 MHz, THF-d₈): δ = 174.8 (N–C–N), 125.8 (C–Me), 125.7 (C–Me), 60.5 (OCH₂), 53.1 (NCH₂), 38.9 (N–CH₃), 35.4 (N–CH₃), 9.4 (C–CH₃), 8.9 (C–CH₃), 3.3 (SiMe₃) and 2.8 (SiMe₃) ppm.

²⁹Si NMR (59.3 MHz, THF-d₈): δ = –8.3 (SiMe₃), –8.5 (SiMe₃), –41.9 (Sa) and –130.6 (Si(SiMe₃)₃) ppm.

4.2.9 Bis[tris(trimethylsilyl)germyl]germylene · PMe₃ (**23**)



A solution of bis[tris(trimethylsilyl)germyl] magnesium (**24**) (0.068 mmol) in THF (2 mL) was slowly added dropwise to a vigorously stirred solution of germanium dichloride · dioxane (17 mg, 0.075 mmol) and trimethylphosphine (6 mg, 0.075 mmol) in THF (2 mL) at -30 °C. The two products were detected by ²⁹Si NMR spectrum after 15 minutes.

23:

¹H NMR (300 MHz, D₂O capillary): δ = 1.08 (br, 9H, PMe₃) and 0.39 (s, 54H, SiMe₃) ppm.

²⁹Si NMR (59.3 MHz, D₂O capillary): δ = -5.3 (d, SiMe₃, ³J_{Si-P} = 2 Hz) ppm.

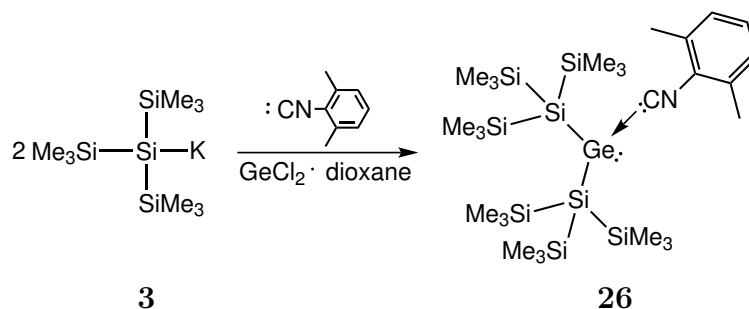
³¹P NMR (121.4 MHz, D₂O capillary): δ = -17.3 (PMe₃) ppm.

25:

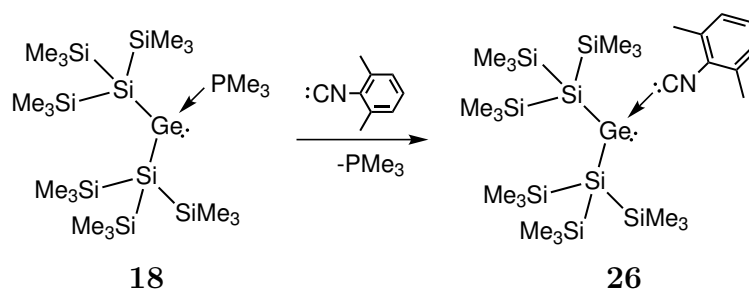
²⁹Si NMR (59.3 MHz, D₂O capillary): δ = -0.5 (s, SiMe₃) ppm.

The remaining analytical data for **25** are shown by Mallela *et al.* [36]

4.2.10 Bis[tris(trimethylsilyl)silyl]germylene · 2,6-dimethylphenylisocyanide (**26**)



Method A: **3** (1.56 mmol) in THF (5 mL) was dropped to the stirring solution of $\text{GeCl}_2 \cdot \text{dioxane}$ and 2,6-dimethylphenylisocyanide in THF (5 mL) at -30°C . After 30 minutes the solvent was removed under reduced pressure and the product was extracted with pentane (3 x 10 mL). The extract was concentrated to 3 mL and stored at -35°C . Dark red crystals of **26** (200 mg, 37%) were obtained.



Method B: 2,6-dimethylphenylisocyanide (37 mg, 0.28 mmol) was added to the stirring solution of **18** (0.28 mmol) in THF (3 mL) at -30°C . The color immediately turned to deep red. The reaction mixture was slowly warmed up to room temperature and stirred for two hours. The solvent was evaporated under reduced pressure, dark red residue was extracted with pentane (3 x 5 mL). After concentration to 1.5 mL and storage at -35°C the dark red crystals of **26** (171 mg, 87%) were obtained.

Mp = $94-116^\circ\text{C}$

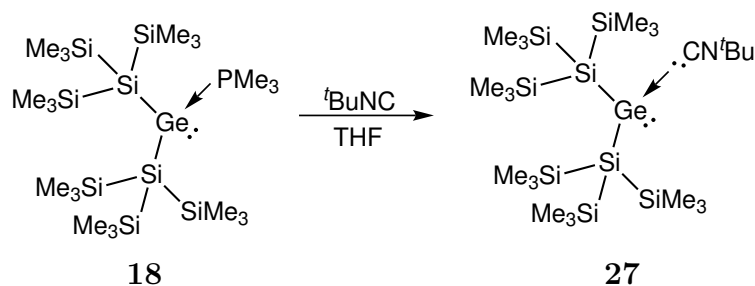
$^1\text{H NMR}$ (300 MHz, C_6D_6): δ = 6.66 (t, 1H, *p-H*), 6.55 (d, 2H, *m-H*), 2.31 (s, 6H, *CMe*) and 0.39 (s, 54H, *SiMe}_3*) ppm.

$^{13}\text{C NMR}$ (75.4 MHz, C_6D_6): δ = 165.0 *CN*, 137.2, 129.6, 128.3, one signal missing (*Ph*), 18.7 (*CMe*) and 3.0 (*SiMe}_3*) ppm.

$^{29}\text{Si NMR}$ (59.3 MHz, C_6D_6): δ = -8.3 (*SiMe}_3*) and -115.7 (*Si(SiMe}_3)_3*) ppm.

Anal. calcd for $\text{C}_{27}\text{H}_{63}\text{GeNSi}_8$ (699.23): C 46.39, H 9.08, N 2.00. Found: C 44.53, H 8.74, N 1.90

4.2.11 Bis[tris(trimethylsilyl)silyl]germylene · *tert*-butylisocyanide (**27**)



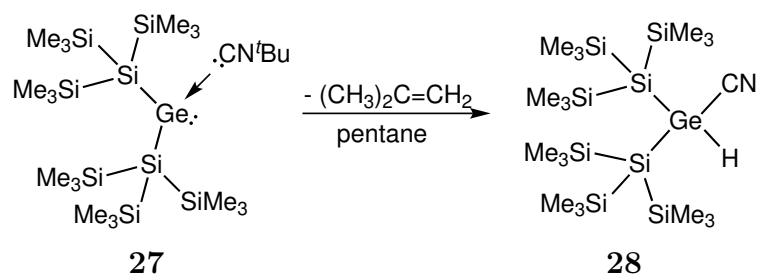
Tert-butylisocyanide (24 mg, 0.28 mmol) was added to the stirring solution of **18** (0.28 mmol) in THF (3 mL) at -30 °C. The reaction mixture was warmed up to room temperature and stirred for 1 hour. The solvent was evaporated under reduced pressure, the orange residue was extracted with pentane (3 x 5 mL). Slow evaporation of pentane gave yellow crystals of **27** (111 mg, 61%) were obtained.

^1H NMR (300 MHz, C_6D_6): δ = 0.99 (s, 9H, *t*-Bu) and 0.45 (s, 54H, SiMe₃) ppm.

^{13}C NMR (75.4 MHz, C_6D_6): δ = 155.4 (CN), 23.7 (CMe₃), 2.7(CMe₃) and 2.2 (SiMe₃) ppm.

^{29}Si NMR (59.3 MHz, C_6D_6): δ = -8.0 (SiMe₃) and -118.8 (Si(SiMe₃)₃) ppm.

4.2.12 Cyanobis[tris(trimethylsilyl)silyl]germane (**28**)



Storage of the **27** in the pentane solution for 2 weeks gave colorless crystals of **28**.

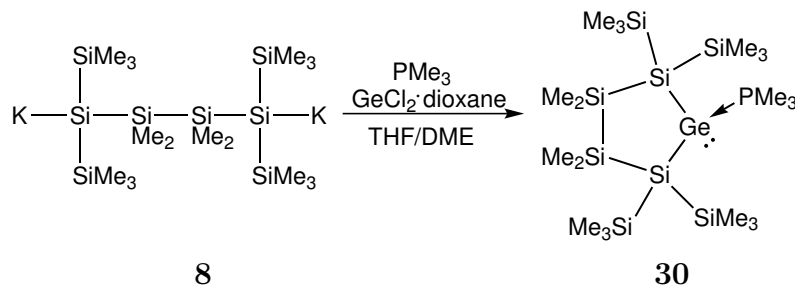
¹H NMR (300 MHz, C₆D₆): δ = 4.10 (s, 1H, Ge–H) and 0.31 (s, 54H, SiMe₃) ppm.

¹³C NMR (75.4 MHz, C₆D₆): δ = 128.9 (CN) and 2.2 (SiMe₃) ppm.

²⁹Si NMR (59.3 MHz, C₆D₆): δ = –8.5 (SiMe₃) and –107.2 (Si(SiMe₃)₃) ppm.

Anal. calcd for C₁₉H₅₅GeNSi₈ (594.97): C 38.36, H 9.32, N 2.35 Found: C 38.47, H 8.47, N 1.70.

4.2.13 1-Germa-2,2,5,5-tetrakis(trimethylsilyl)-3,3,4,4-tetramethylcyclopentasilan-1-ylidene · PMe₃ (**30**)



A solution of 1,4-dipotassio-1,1,4,4-tetrakis(trimethylsilyl)tetramethyltetrasilane (**8**) (0.33 mmol) in DME (2 mL) was slowly added dropwise to a stirred solution of germanium dichloride · dioxane (91 mg, 0.39 mmol) and PMe₃ (30 mg, 0.39 mmol) in THF (4 mL) at $-30\text{ }^\circ\text{C}$. After 4 hours the solvent was evaporated and product was extracted with pentane (3 x 5 mL). The solvent was removed to yield **30** as an orange solid (160 mg, 80%). Crystallization from pentane at $-35\text{ }^\circ\text{C}$ gave orange crystals suitable to X-ray study.

Mp = 161–162 $^\circ\text{C}$.

¹H NMR (300 MHz, C₆D₆): δ = 1.11 (d, 9H, PMe₃, ²J_{H-P} = 9.9 Hz), 0.44 (s, 12H, SiMe₂), 0.41 (s, 18H, SiMe₃) and 0.32 (s, 18H, SiMe₃) ppm

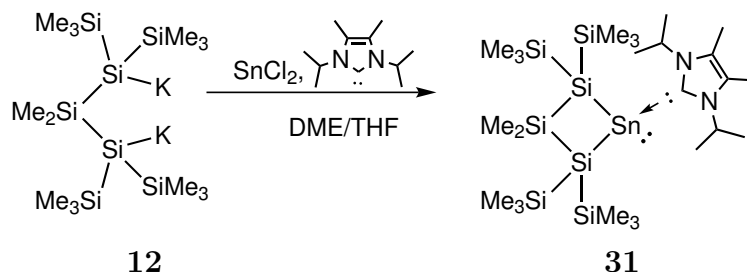
¹³C NMR (75.4 MHz, C₆D₆): δ = 18.3 (d, PMe₃, ¹J_{C-P} = 23.2 Hz), 4.3 (SiMe₃), 2.8 (SiMe₃), -1.1 (SiMe₂) and -1.6 (SiMe₂) ppm.

²⁹Si NMR (59.3 MHz, C₆D₆): δ = 4.3 (br, SiMe₃), 8.5 (br, SiMe₃), 22.3 (d, SiMe₂, ³J_{Si-P} = 10.1 Hz) and 126.0 (d, Si(SiMe₃)₃, ³J_{Si-P} = 15.7 Hz) ppm.

³¹P NMR (121.4 MHz, C₆D₆): δ = -20.0 (PMe₃) ppm.

Anal. calcd for C₁₉H₅₇GeSi₈ (613.95): C 37.17, H 9.36 Found: C 36.38, H 9.12.

4.2.14 1-Stanna-2,2,4,4-tetrakis(trimethylsilyl)-3,3-dimethylcyclobutasilan-1-ylidene · ^{Me}IiPr (31)



1,3-dipotassio-1,3,3-tetrakis(trimethylsilyl)dimethyltrisilane (**12**) (0.32 mmol) in DME (2 mL) was slowly added dropwise to the stirring solution of tin dichloride (49 mg, 0.26 mmol) and 1,3-diisopropyl-4,5-dimethylimidazol-2-ylidene (45 mg, 0.26 mmol) in THF at $-30\text{ }^\circ\text{C}$. The stirring was continued for 18 hours at room temperature. The solvent was evaporated under reduced pressure and the residue was extracted with pentane (3 x 5 mL). The extract was concentrated to 2 mL and stored at $-35\text{ }^\circ\text{C}$. Orange crystals of **31** (135 mg, 83%) were obtained.

Mp = $140\text{--}142\text{ }^\circ\text{C}$.

¹H NMR (300 MHz, C₆D₆): δ = 5.12 (sept, 2H, N(1,3)-CH(CH₃), 1.47 (s, 6H, C(4,5)-CH₃), 1.21 (d, 12H, N(1,3)-CH(CH₃)₂, ²J = 7.0 Hz), 0.78 (s, 3H, SiMe₂), 0.69 (s, 3H, SiMe₂), 0.52 (s, 18H, SiMe₃) and 0.44 (s, 18H, SiMe₃) ppm.

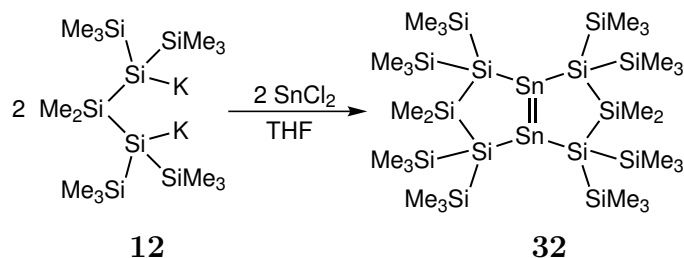
¹³C NMR (75.4 MHz, C₆D₆): δ = 171.4 (N-C-N), 126.8 (MeC=CMe), 53.9 (CH(CH₃)₂), 21.7 (CH(CH₃)₂), 10.1 C(4,5)-CH₃, 6.9 (SiMe₂), 5.2 (SiMe₂), 3.3 (SiMe₃) and 3.2 (SiMe₃) ppm.

²⁹Si NMR (59.3 MHz, C₆D₆): δ = -6.5 (SiMe₃), -10.3 (SiMe₃), -15.0 (SiMe₂) and -121.3 (Si(SiMe₃)₃) ppm.

¹¹⁹Sn NMR (111.8 MHz, C₆D₆): -272.9 ppm.

Anal. calcd for C₂₅H₆₂N₂Si₇Sn (706.08): C 42.53, H 8.85, N 3.97. Found: C 39.84, H 8.18, N 3.67

4.2.15 1,5-Distanna-2,2,4,4,6,6,8,8-octakis(trimethylsilyl)bicyclo[3.3.0]hexasilaoct-1,5-ene (**32**)



1,3-dipotassio-1,1,3,3-tetrakis(trimethylsilyl)dimethyltrisilane (**12**) (0.60 mmol) in DME (5 mL) was slowly added dropwise to the stirring solution of tin dichloride (0.60 mmol, 114 mg) in THF (5 mL) at room temperature. The stirring was continued for 18 h. The solvent was evaporated under reduced pressure and the residue was extracted with pentane (3 x 7 mL). The extract was concentrated to 2 mL and stored at $-35\text{ }^\circ\text{C}$. Dark violet crystals of **32** (60 mg, 58%) were obtained.

Mp = 178–181 $^\circ\text{C}$.

$^1\text{H NMR}$ (300 MHz, C_6D_6): $\delta = 0.75$ (s, 12H, SiMe_2) and 0.37 (s, 72H, $(\text{SiMe}_3)_3$) ppm.

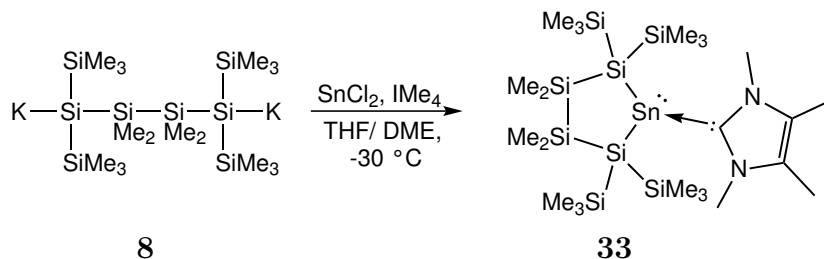
$^{13}\text{C NMR}$ (75.4 MHz, C_6D_6): $\delta = 4.1$ (SiMe_2) and 3.3 (SiMe_3) ppm.

$^{29}\text{Si NMR}$ (59.3 MHz, C_6D_6): $\delta = -2.0$ (SiMe_3), -8.4 (SiMe_2) and -83.6 (Si^q) ppm.

$^{119}\text{Sn NMR}$ (111.8 MHz, C_6D_6): 730.7 ppm.

Anal. calcd for $\text{C}_{30}\text{H}_{84}\text{Si}_{12}\text{Sn}$ (1019.43): C 35.35, H 8.31. Found: C 32.13, H 7.59.

4.2.16 1-Stanna-2,2,5,5-tetrakis(trimethylsilyl)-3,3,4,4-tetramethylcyclopentasilan-1-ylidene · IMe₄ (**33**)



A solution of 1,4-dipotassio-1,1,4,4-tetrakis(trimethylsilyl)tetramethyltetrasilane (**8**) (0.82 mmol) in DME (10 mL) was slowly added dropwise to a stirred solution of tin dichloride (169 mg, 0.85 mmol) and IIme₄ (105 mg, 0.85 mmol) in THF (10 mL) at -30 °C. After 2 hours the solvent was evaporated and the residue was extracted with pentane (4 x 20 mL). The brown extract was concentrated to 3 mL and stored at -35 °C. Yellow crystals (260 mg, 44%) of **33** were obtained.

Mp = 164–166 °C.

¹H NMR (300 MHz, C₆D₆): δ = 3.39 (s, 6H, N-Me), 1.21 (s, 6H, C-Me), 0.55 (overlapping, SiMe₂), 0.54 (s, 18H, SiMe₃), 0.53 (s, 6H, SiMe₂) and 0.20 (s, 18H, (SiMe₃) ppm.

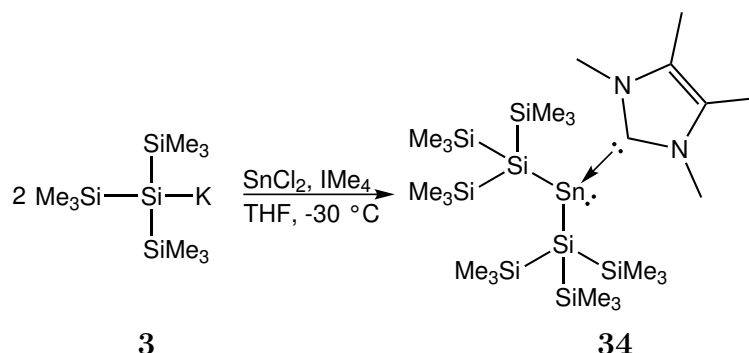
¹³C NMR (75.4 MHz, C₆D₆): δ = 125.4 (C-Me), 37.6 (N-Me), 8.0 (C-Me), 4.4 (SiMe₃), 3.9 (SiMe₃), 0.6 (SiMe₂) and -0.3 (SiMe₂) ppm; N-C-N not found.

²⁹Si NMR (59.3 MHz, C₆D₆): δ = -5.1 (SiMe₃), -7.1 (SiMe₃), -15.9 (SiMe₂) and -133.7 (Si^q) ppm.

¹¹⁹Sn NMR (111.8 MHz, C₆D₆): -318.8 ppm.

Anal. calcd for C₂₄H₆₀N₂Si₈Sn (708.13): C 39.01, H 8.54, N 3.96 Found: C 37.10, H 8.08, N 3.96.

4.2.17 Bis[tris(trimethylsilyl)silyl]stannylene · IMe₄ (**34**)



A solution of tris(trimethylsilyl)silyl potassium (**3**) (1.56 mmol) was slowly added dropwise to a vigorously stirred solution of tin dichloride (162 mg, 0.86 mmol) and IMe₄ (108 mg, 0.86 mmol) in THF (5 mL) at -30°C . The stirring of the dark brown reaction mixture was continued for 30 minutes at room temperature. The solvent was removed under reduced pressure and the residue was extracted with pentane (5 x 8 mL). The red extract was concentrated to 3 mL and stored at -35°C . Yellow crystals of **34** (396 mg, 69%) were obtained.

Mp = $152\text{--}155^\circ\text{C}$.

¹H NMR (300 MHz, C₆D₆): δ = 3.66 (s, 3H, C-CH₃), 3.38 (s, 3H, C-CH₃), 1.38 (s, 3H, N-CH₃), 1.24 (s, 3H, N-CH₃) and 0.36 (s, 54H, SiMe₃).

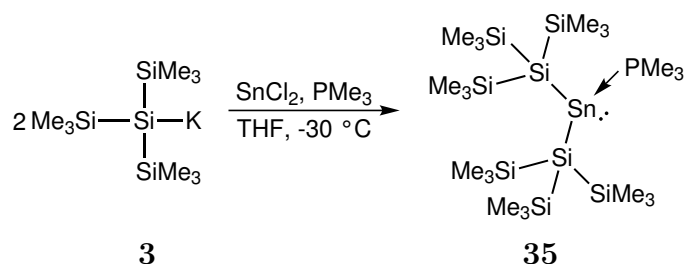
¹³C NMR (75.4 MHz, C₆D₆): δ = 169.9 (N-C-N), 126.2 (CMe), 125.3 (CMe), 41.1 (N-CH₃), 35.9 (N-CH₃), 8.2 (C-CH₃), 7.9 (C-CH₃) and 3.9 (SiMe₃) ppm.

²⁹Si NMR (59.3 MHz, C₆D₆): δ = -7.2 (SiMe₃), -136.5 (Si(SiMe₃)₃) ppm.

¹¹⁹Sn NMR (111.8 MHz, C₆D₆): -297.2 ppm.

Anal. calcd for C₂₅H₆₆N₂Si₈Sn (738.20): C 40.68, H 9.01, N 3.79 Found: C 42.78, H 9.24, N 3.64.

4.2.18 Bis[tris(trimethylsilyl)silyl]stannylene · PMe₃ (**35**)



A solution of tris(trimethylsilyl)silyl potassium (**3**) (1.56 mmol) was slowly added dropwise to a vigorously stirred solution of tin dichloride (177 mg, 0.94 mmol) and trimethylphosphine (71 mg, 0.94 mmol) in THF (5 mL) at $-30\text{ }^\circ\text{C}$. The stirring of the dark red reaction mixture was continued for 1 hour at room temperature. The solvent was removed under reduced pressure and the residue was extracted with pentane (5 x 8 mL). The red extract was concentrated to 3 mL and stored at $-35\text{ }^\circ\text{C}$. Yellow crystals (159 mg, 29%) of **35** were obtained.

Mp = 101–103 $^\circ\text{C}$.

¹H NMR (300 MHz, C₆D₆): δ = 1.09 (d, 9H, PMe₃, ²J_{H-P} = 7.9 Hz) and 0.40 (s, 54H, SiMe₃) ppm.

¹³C NMR (75.4 MHz, C₆D₆): δ = 18.9 (d, PMe₃, ¹J_{P-C} = 12 Hz) and 4.9 (SiMe₃) ppm.

²⁹Si NMR (59.3 MHz, C₆D₆): δ = -7.4 (SiMe₃), -126.8 (Si(SiMe₃)₃) ppm.

³¹P NMR (121.4 MHz, C₆D₆): δ = -61.7 (br, PMe₃) ppm.

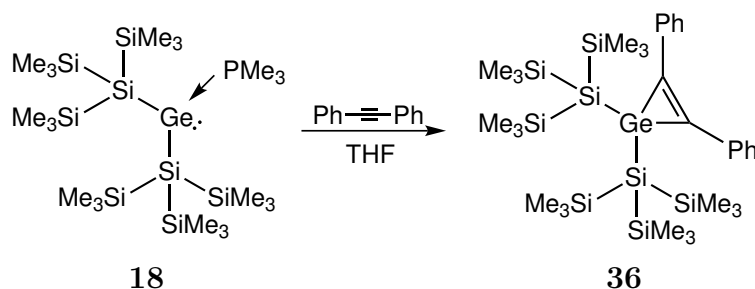
³¹P NMR (121.4 MHz, Toluene-d₈, $-30\text{ }^\circ\text{C}$): δ = -61.1 (br, PMe₃, ¹J_{P-¹¹⁷Sn/¹¹⁹Sn} = 1980/1896 Hz, satellite signals for ¹¹⁷Sn and ¹¹⁹Sn broad) ppm.

¹¹⁹Sn NMR (111.8 MHz, C₆D₆): -43.5 (bd, ¹J_{Sn-P} = 2060 Hz) ppm.

¹¹⁹Sn NMR (111.8 MHz, Toluene-d₈, $-30\text{ }^\circ\text{C}$): -89.9 (d, ¹J_{Sn-P} = 1980 Hz) ppm.

Anal. calcd for C₂₁H₆₃PSi₈Sn (690.09): C 36.55, H 9.20 Found: C 35.84, H 8.82.

4.2.19 1,1-Bis[tris(trimethylsilyl)silyl]-2,3-diphenyl-1-germacyclopropene (**36**)



Diphenylacetylene (138 mg, 0.76 mmol) was added to the solution of bis[tris(trimethylsilyl)silyl]germylene·PMe₃ (**18**) (0.78 mmol) in THF (10 mL) at room temperature and stirred for 12 hours. The solvent was removed under reduced pressure and the product was extracted with pentane (3 x 5 mL). The solvent was removed to yield **36** as an orange solid (248 mg, 43%). Crystallization from pentane gave orange crystals suitable for X-ray measurement.

Mp = 104-106 °C.

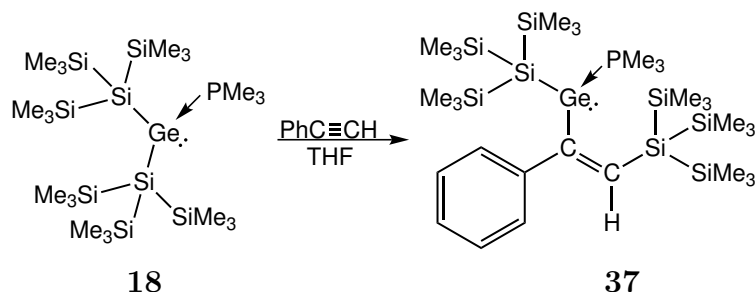
¹H NMR (300 MHz, C₆D₆): δ = 7.92 (d, 4H, *o*-H), 7.23 (t, 4H, *m*-H), 7.02 (t, 2H, *p*-H) and 0.26 (s, 54H, SiMe₃) ppm.

¹³C NMR (75.4 MHz, C₆D₆): δ = 145.4, 134.4, 131.6, 130.0, 128.2 and 2.9 (SiMe₃) ppm.

²⁹Si NMR (59.3 MHz, C₆D₆): δ = -9.2 (SiMe₃) and -92.6 (Si(SiMe₃)₃) ppm.

Anal. calcd for C₃₂H₆₄GeSi₈ (746.17): C 51.51, H 8.65. Found: C 50.54, H 8.38.

4.2.20 [*Z*-1-Phenyl-2-(tris(trimethylsilyl)silyl)vinyl]tris(trimethylsilyl)silyl]germylene · PMe₃ (**37**)



Phenylacetylene (79 mg, 0.78 mmol) was added to a stirred solution bis[tris(trimethylsilyl)silyl]germylene · PMe₃ (**18**) (0.78 mmol) in THF (10 mL) at room temperature. After 1 hour the solvent was evaporated under reduced pressure, orange residue was extracted with pentane (3 x 5 mL). After concentration to 1.5 mL and storage at -35 °C orange crystals of **37** (108 mg, 19%) were obtained.

Mp = 119–130 °C.

¹H NMR (300 MHz, C₆D₆): δ = 7.52 (d, 2H, *o*-H), 7.15 (t, 2H, *m*-H), 6.94 (t, 1H, *p*-H), 6.86 (s, 1H, CH), 0.87 (d, 9H, PMe₃, ²J_{H-P} = 9.6 Hz), 0.40 (s, 27H, CSi(SiMe₃)₃) and 0.39 (s, 27H, GeSi(SiMe₃)₃) ppm.

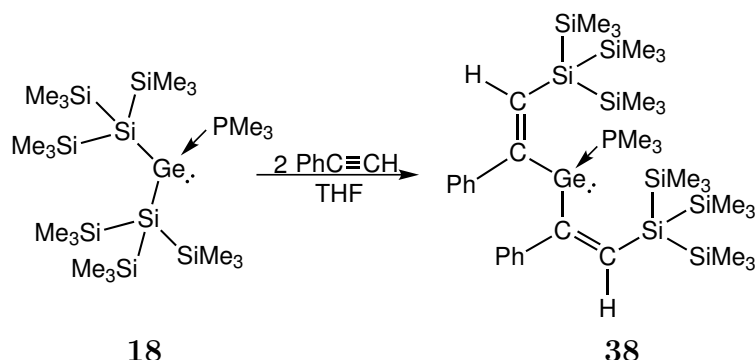
¹³C NMR (75.4 MHz, C₆D₆): δ = 173.0 (d, C=CH, ²J_{P-C} = 7 Hz), 153.2 (d, C_qPh, ³J = 3 Hz), 142.0 (d, C=CH, ³J_{P-C} = 16 Hz), 127.7, 127.7, 125.5, 15.1 (d, PMe₃, ¹J_{P-C} = 20 Hz), 3.9(SiMe₃) and 2.2 (SiMe₃) ppm.

²⁹Si NMR (59.3 MHz, C₆D₆): δ = -8.9 (d, GeSi(SiMe₃)₃, ³J_{P-Si} = 12 Hz), -12.9 (d, CSi(SiMe₃)₃, ⁵J_{P-Si} = 2 Hz), -83.4 (Si(SiMe₃)₃) and -126.9 (d, GeSi(SiMe₃)₃, ⁴J_{P-Si} = 15 Hz) ppm.

³¹P NMR (121.4 MHz, C₆D₆): δ = -24.6 (PMe₃) ppm.

Anal. calcd for C₂₉H₆₉GePSi₈ (746.16): C 46.68, H 9.32. Found: C 46.25, H 9.14.

4.2.21 Bis[*Z*-1-phenyl-2-(tris(trimethylsilyl)silyl)vinyl]germylene · PMe₃ (**38**)



Phenylacetylene (60 mg, 0.587 mmol) was added to the stirred solution of **18** (0.466 mmol) in THF (10 mL) at room temperature. After 1 hour the solvent was removed under reduced pressure and the residue was extracted with pentane (3 x 5 mL). The solvent was removed to yield **38** as an orange solid (232 mg, 93%). Crystallization from pentane at $-30\text{ }^{\circ}\text{C}$ gave orange crystals suitable for X-ray study.

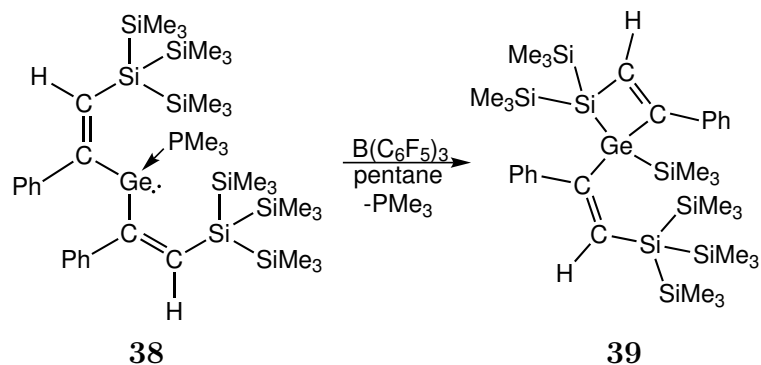
¹H NMR (300 MHz, C₆D₆): $\delta = 7.02$ (m, 4H, *m-H*), 6.83 (m, 6H, *o-H*, *p-H*), 6.66 (s, 2H, *CH*), 0.87 (d, 9H, P*Me*₃, ²*J*_{H-P}=8.7 Hz) and 0.40 (s, 54H, Si*Me*₃) ppm.

¹³C NMR (75.4 MHz, C₆D₆): $\delta = 177.6$ (C=C*Ph*), 156.1 (C^{*q*}*Ph*), 138.7 (C-H), 126.2, 124.7, (Ph, one signal overlapping with C₆D₆), 15.4 (d, P*Me*₃, ¹*J* = 21 Hz) and 2.1 (Si*Me*₃) ppm.

²⁹Si NMR (59.3 MHz, C₆D₆): $\delta = -12.9$ (Si*Me*₃) and -86.2 (Si(Si*Me*₃)₃) ppm.

³¹P NMR (121.4 MHz, C₆D₆): $\delta = -24.6$ (P*Me*₃) ppm.

4.2.22 (Z)-1-(2-(tris(trimethylsilyl)silyl)-1-phenylvinyl)-4-phenyl-1,2,2-tris(trimethylsilyl)-1,2-dihydro-1,2-silagermete (**39**)



Method A: $B(C_6F_5)_3$ (45 mg, 0.088 mmol) in pentane (3 mL) was added dropwise to the stirring solution of **38** (75 mg, 0.088 mmol) in pentane (2 mL). During the reaction a white precipitate was formed. The suspension was filtrated through glass wool and celite. The solvent was evaporate to give **39** (42 mg, 62%) as a yellowish solid.

Method B: Storage of **38** in pentane for 1 week at $-35\text{ }^\circ\text{C}$ led to the formation of **39**.
Mp = 131–132 $^\circ\text{C}$.

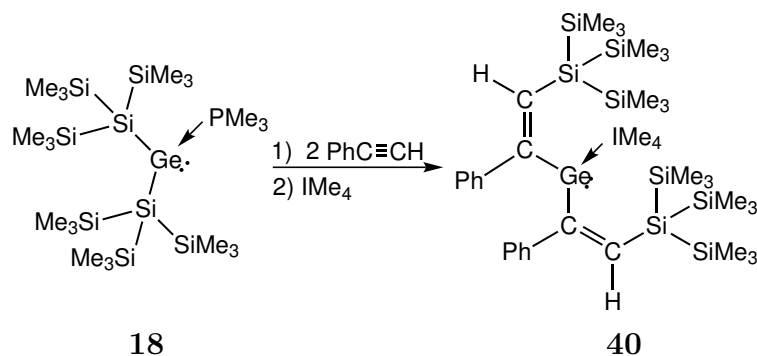
$^1\text{H NMR}$ (300 MHz, C_6D_6): 7.46 (s, 1H, *CH*), 7.41 (m, 1H, *p-H*), 7.27 (d, 2H, *o-H*), 6.85 (m, 4H), 6.79 (m, 2H), 6.67 (m, 2H), 0.49 (s, 9H, $SiMe_3$), 0.40 (s, 9H, $SiMe_3$), 0.33 (s, 9H, $SiMe_3$) and 0.30 (s, 27H, $SiMe_3$) ppm.

$^{13}\text{C NMR}$ (75.4 MHz, C_6D_6): 173.1, 163.4, 153.2, 141.1, 140.8, 138.9, 138.2, 128.5, 127.5, 126.9, 126.2, 126.1, 3.9 ($SiMe_3$), 2.1 ($SiMe_3$), 1.7 ($SiMe_3$) and 1.1 ($SiMe_3$) ppm.

$^{29}\text{Si NMR}$ (59.3 MHz, C_6D_6): -4.6 ($SiMe_3$), -10.0 ($SiMe_3$), -12.5 ($SiMe_3$), -13.1 ($CSi(SiMe_3)_3$), -45.0 (Si-Ge) and -86.5 ($CSi(SiMe_3)_3$) ppm.

Anal. calcd for $C_{34}H_{66}GeSi_8$ (772.21): C 52.88, H 8.61. Found: C 52.99, H 8.31.

4.2.23 Bis[*Z*-1-Phenyl-2-tris(trimethylsilyl)silylvinyl]germylene · IMe₄ (**40**)



Phenylacetylene (100 mg, 0.920 mmol) was added to a stirred solution of **18** (0.466 mmol) in THF (10 mL) at room temperature. After 1 hour to the stirring solution ImMe₄NHC (59 mg, 0.466 mmol) was added. After 15 minutes the solvent was removed under reduced pressure and the residue was extracted with pentane (3 x 5 mL). The solvent was removed to yield **40** as an orange solid (337 mg, 80%). Crystallization from pentane at -30 °C gave orange crystals suitable for X-ray study.

Mp = 63–65 °C.

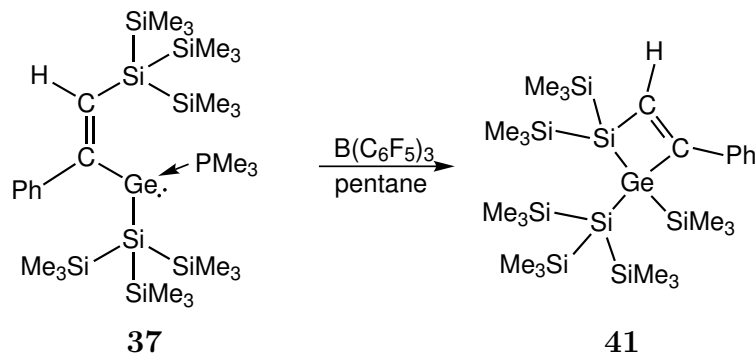
¹H NMR (300 MHz, C₆D₆): δ = 7.11 (2H), 6.97 (4H), 6.87 (4H), 6.48 (s, 2H, CH), 3.11 (s, 6H, N-Me), 1.29 (s, 6H, C-Me) and 0.37 (s, 54H, SiMe₃) ppm.

¹³C NMR (75.4 MHz, C₆D₆): δ = 179.9 (N-C-N), 172.9 (C-Ge), 155.8 (Cipso), 131.8 (C-H), 128.3 (Ph), 128.1 (Ph), 126.7 (Ph), 124.6 (C-Me), 33.5 (N-Me), 7.8 (C-Me) and 1.8 (SiMe₃) ppm.

²⁹Si NMR (59.3 MHz, C₆D₆): δ = -13.1 (SiMe₃) and -87.6 (Si(SiMe₃)₃) ppm.

Anal. calcd for C₄₁H₇₈GeN₂Si₈ (896.40): C 54.94, H 8.77, N 3.13 Found: C 55.83, H 8.36, N 3.34.

4.2.24 1-[Tris(trimethylsilyl)silyl]-4-phenyl-1,2,2-tris(trimethylsilyl)-1,2-dihydro-1,2-silagermete (**41**)



$B(C_6F_5)_3$ (66 mg, 0.13 mmol) in pentane (3 mL) was added dropwise to stirring solution of **37** (100 mg, 0.13 mmol) in pentane (2 mL). During the reaction a white precipitate was formed. The suspension was filtrated through glass wool and celite. The solvent was evaporate to give **41** (72 mg, 82%) as a white solid.

Mp = 108–110 °C.

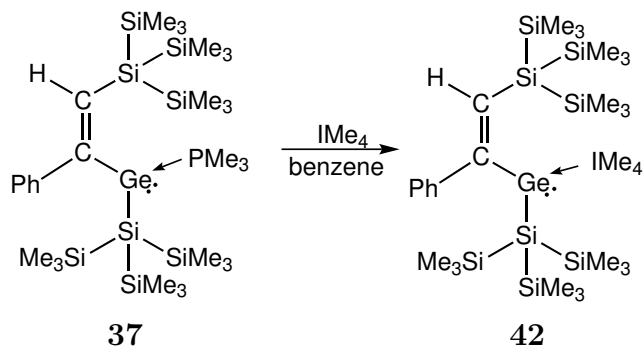
1H NMR (300 MHz, C_6D_6): δ = 7.44 (s, 1H, *CH*), 7.44 (2H, *o-H*), 7.17 (t, 2H, *m-H*), 7.03 (t, 1H, *p-H*), 0.42 (s, 9H, $SiMe_3$), 0.41 (s, 9H, $SiMe_3$), 0.38 (s, 9H, $SiMe_3$) and 0.35 (s, 27H, $SiMe_3$) ppm.

^{13}C NMR (75.4 MHz, C_6D_6): 169.0 (C_{ipso}), 140.8 ($C-Ph$), 140.0 ($C-H$), 127.8, 126.5, one signal missing, 3.5 ($SiMe_3$), 2.5 ($SiMe_3$) and 2.1 ($SiMe_3$) ppm

^{29}Si NMR (59.3 MHz, C_6D_6): -3.7 ($SiMe_3$), -8.4 ($SiMe_3$), -9.0 ($SiMe_3$), -14.6 ($CSi(SiMe_3)_3$), -50.9 (Si-Ge) and -116.6 ($GeSi(SiMe_3)_3$) ppm.

Anal. calcd for $C_{26}H_{60}GeSi_8$ (670.08): C 46.60, H 9.03. Found: C 44.38, H 5.39.

4.2.25 [Z-1-phenyl-2-tris(trimethylsilyl)silylvinyl]tris(trimethylsilyl)silylgermylene · IMe₄ (**42**)



37 (75 mg, 0.1 mmol) and IMe₄ (13 mg, 0.1 mmol) was stirred in benzene (2 mL) for 2 hours at room temperature. Slow evaporation of the solvent gave orange crystals of **42** (78 mg, 98%) suitable for X-ray study.

Mp = 158–160 °C.

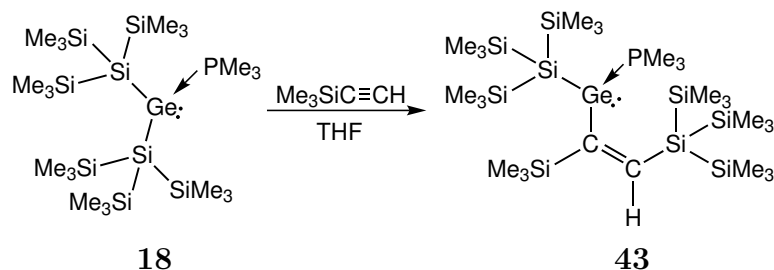
¹H NMR (300 MHz, C₆D₆): δ = 7.28 (2H), 7.12 (2H), 6.93 (2H), 6.48 (s, 1H, CH), 3.26 (s, 6H, N–Me), 1.30 (s, 6H, C–Me), 0.37 (s, 27H, SiMe₃) and 0.37 (s, 27H, SiMe₃) ppm.

¹³C NMR (75.4 MHz, C₆D₆): δ = 177.4, 176.6, 151.5, 141.4, 128.7 (*Ph*), 126.0 (*Ph*), 125.1 (*C*–Me), one signal overlapping with C₆D₆, 34.3 (N–Me), 7.9 (*C*–Me), 4.0 (SiMe₃) and 2.1 (SiMe₃) ppm.

²⁹Si NMR (59.3 MHz, C₆D₆): δ = –8.7 (GeSiMe₃) –12.6 (CSiMe₃), –85.9 (CSi(SiMe₃)₃) and –128.0 (GeSi(SiMe₃)₃) ppm.

Anal. calcd for C₃₃H₇₂GeN₂Si₈ (794.26): C 49.90, H 9.14, N 3.53 Found: C 47.06, H 8.63, N 3.30.

4.2.26 [Z-1-Trimethylsilyl-2-(tris(trimethylsilyl)silyl)vinyl]tris(trimethylsilyl)-silyl]germylene · PMe₃ (**43**)



Trimethylsilylacetylene (46 mg, 0.46 mmol) was added to a solution of bis[tris(trimethylsilyl)silyl]germylene · PMe₃ (**18**) (0.46 mmol) in THF (5 mL) at room temperature. The color immediately turned green and after next 15 minutes turned yellow. The stirring was continued for 12 hours. The solvent was removed under reduced pressure and the product was extracted with pentane (3 x 5 mL). The extract was concentrated to 3 mL and storage at -35 °C gave **36** as yellow crystals (205 mg, 60%).

Mp = 106-108°C.

¹H NMR (300 MHz, C₆D₆): δ = 7.65 (d, 1H, C-H, ⁴J_{H-P} = 1.7 Hz), 1.03 (d, 9H, PMe₃, ²J_{H-P} = 9.4 Hz), 0.36 (s, 27H, SiMe₃), 0.32 (s, 27H, SiMe₃) and 0.27 (s, 9H, SiMe₃) ppm.

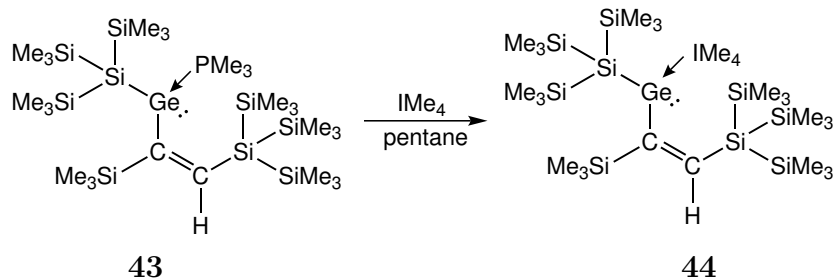
¹³C NMR (75.4 MHz, C₆D₆): δ = 177.7 (d, C=C*Si*Me₃, ³J_{C-P} = 7 Hz), 158.8 (d, C-H, ³J_{C-P} = 20 Hz), 16.1 (d, PMe₃, ¹J_{C-P} = 19 Hz), 4.3 (SiMe₃), 2.5 (SiMe₃) and 2.0 (SiMe₃) ppm.

²⁹Si NMR (59.3 MHz, C₆D₆): δ = -7.9 (d, C=C*Si*Me₃, ³J_{Si-P} = 3 Hz), -8.9 (d, GeSi*Si*Me₃, ³J_{Si-P} = 12 Hz), -13.1 (d, C*SiSi*Me₃, ⁵J_{Si-P} = 2 Hz), -85.8 (d, C*Si*(SiMe₃)₃, ⁴J_{Si-P} = 2 Hz) and -128.2 (d, Ge*Si*(SiMe₃)₃, ²J_{Si-P} = 15 Hz) ppm.

³¹P NMR (121.4 MHz, C₆D₆): δ = -28.1 (PMe₃) ppm.

Anal. calcd for C₂₆H₇₃GePSi₉ (742.24): C 42.07, H 9.91 Found: C 42.05, H 9.08.

4.2.27 [Z-1-Trimethylsilyl-2-(tris(trimethylsilyl)silyl)vinyl]tris(trimethylsilyl)-silyl]germylene · IMe₄ (44)



43 (50 mg, 0.067 mmol) and ImMe₄NHC (8 mg, 0.067 mmol) was stirred in pentane (1 mL) for 1 hour at room temperature. The solvent was removed under reduced pressure and the product was extracted with pentane (3 x 5 mL). The extract was concentrated to 1 mL and storage at $-35\text{ }^\circ\text{C}$ gave **44** as yellow crystals (29 mg, 55%).

Mp = 112–114 $^\circ\text{C}$.

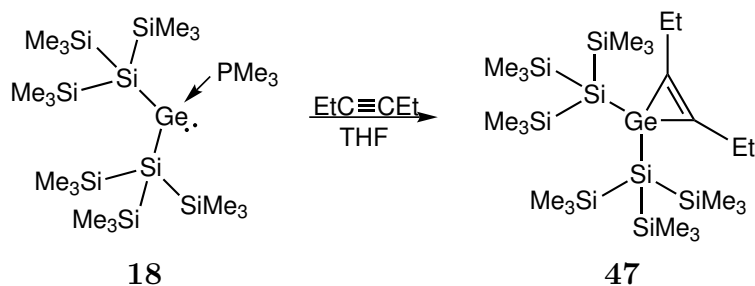
¹H NMR (300 MHz, C₆D₆): δ = 7.84 (s, 1H, CH), 3.45 (s, 6H, N–Me), 1.21 (s, 6H, C–Me), 0.46 (s, 27H, SiMe₃), 0.41 (s, 27H, SiMe₃) and 0.23 (s, 9H, SiMe₃) ppm.

¹³C NMR (75.4 MHz, C₆D₆): δ = 154.9, 124.8 (C–Me), 36.1 (N–Me), 7.8 (C–Me), 4.9 (SiMe₃), 2.6 (CSiMe₃) and 2.3 (SiMe₃) ppm; (signals of N–C–N and C=C not detected).

²⁹Si NMR (59.3 MHz, C₆D₆): δ = -8.2 (C=CSiMe₃)– 8.7 (GeSiMe₃)– 13.1 (CSiMe₃), -86.5 (CSi(SiMe₃)₃) and -126.7 (GeSi(SiMe₃)₃) ppm.

Anal. calcd for C₃₀H₇₈GeN₂Si₉ (792.36): C 45.47, H 9.92, N 3.53 Found: C 45.27, H 9.31, N 3.64.

4.2.28 2,3-Diethyl-1,1-bis[tris(trimethylsilyl)silyl]-1-germacyclopropene (47)



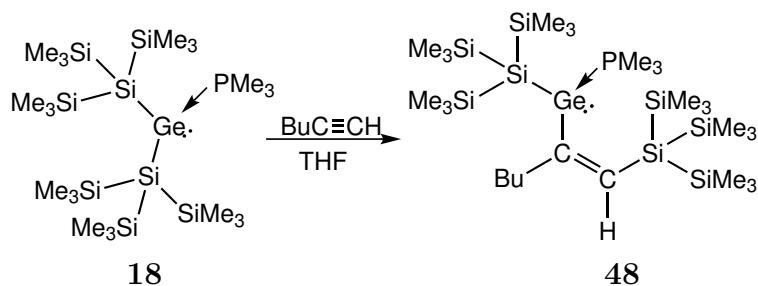
3-Hexyne (38 mg, 0.47 mmol) was added to a stirred solution bis[tris(trimethylsilyl)silyl]germylene·PMe₃ (**18**) (0.23 mmol) in THF (10 mL) at room temperature. After 1 hour the solvent was evaporated under reduced pressure and the brown residue was extracted with pentane (3 x 5 mL). Solvent was evaporated to give **47** as a brown solid (124 mg, 83%).

¹H NMR (300 MHz, C₆D₆): δ = 2.74 (q, 4H, CH₂–CH₃, ³J = 7.5 Hz), 1.28 (t, 6H, CH₂–CH₃, ³J = 7.4 Hz) and 0.31 (s, 54H, SiMe₃) ppm.

¹³C NMR (75.4 MHz, C₆D₆): δ = 142.9 (C=C), 24.5 (CH₂–CH₃), 14.2 (CH₂–CH₃) and 3.0 (SiMe₃) ppm.

²⁹Si NMR (59.3 MHz, C₆D₆): δ = –9.5 (SiMe₃) and –95.4 (Si(SiMe₃)₃) ppm.

4.2.29 [Z-1-Butyl-2-(tris(trimethylsilyl)silyl)vinyl]tris(trimethylsilyl)silylgermylene · PMe₃ (**48**)



1-Hexyne (25 mg, 0.31 mmol) was added to a stirred solution bis[tris(trimethylsilyl)silyl]germylene · PMe₃ (**18**) (0.23 mmol) in THF (10 mL) at room temperature. After 1 hour the solvent was evaporated under reduced pressure, the orange residue was extracted with pentane (3 x 5 mL). After concentration to 0.5 mL and storage at $-35\text{ }^{\circ}\text{C}$ orange crystals of **48** (128 mg, 77%) were obtained.

Mp = 120–121 $^{\circ}\text{C}$.

¹H NMR (300 MHz, C₆D₆): δ = 6.45 (s, 1H, CH), 2.87–2.98 and 2.39–2.49 (2 m, 1H each, CH₂), 1.55–1.72 (m, 2H, CH₂), 1.37–1.51 (m, 2H, CH₂), 1.06 (d, 9H, PMe₃, ²J_{H–P} = 9.3 Hz), 0.97 (t, 3H, CH₃, ³J = 7.2 Hz), 0.43 (s, 27H, SiMe₃) and 0.42 (s, 27H, SiMe₃) ppm.

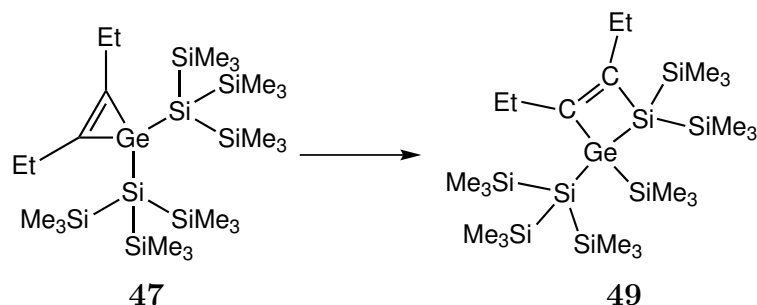
¹³C NMR (75.4 MHz, C₆D₆): δ = 172.3 (d, C=CH, ²J_{P–C} = 7 Hz), 131.0 (d, C=CH, ³J_{P–C} = 15 Hz), 51.2 (d, CH₂, ⁴J_{P–C} = 4 Hz), 31.4 (CH₂), 23.3 (CH₂), 16.2 (d, PMe₃, ¹J_{P–C} = 19 Hz), 14.7 (CH₃), 4.2 (SiMe₃) and 2.5 (SiMe₃) ppm.

²⁹Si NMR (59.3 MHz, C₆D₆): δ = –8.9 (d, GeSi(SiMe₃)₃, ³J_{P–Si} = 12 Hz), –13.2 (d, CSi(SiMe₃)₃, ⁵J_{P–Si} = 2 Hz), –85.5 (d, Si(SiMe₃)₃, ⁴J_{P–Si} = 1 Hz) and –130.5 (d, GeSi(SiMe₃)₃, ⁴J_{P–Si} = 16 Hz) ppm.

³¹P NMR (121.4 MHz, C₆D₆): δ = –26.6 (PMe₃) ppm.

Anal. calcd for C₂₇H₇₃GePSi₈ (726.17): C 44.66, H 10.13. Found: C 43.77, H 9.93.

4.2.30 3,4-Diethyl-1-[tris(trimethylsilyl)silyl]-1,2,2-tris(trimethylsilyl)-1,2-dehydro-2-silagermete (**49**)



Storing of **47** (124 mg, 0.19 mmol) in pentane for 1 week at $-35\text{ }^{\circ}\text{C}$ followed by evaporation of the solvent under reduced pressure gave **49** (124 mg, 100%) as a brownish solid.

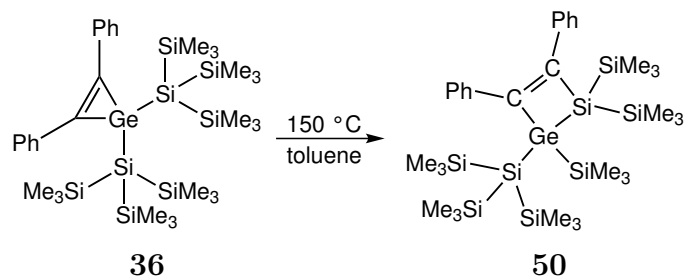
Mp = $124\text{--}126\text{ }^{\circ}\text{C}$

$^1\text{H NMR}$ (300 MHz, C_6D_6): δ = 2.41–1.92 (m, 4H, CH_2CH_3), 1.02 and 1.00 (2t, overlapping, 6H, CH_2CH_3), 0.39 (s, 9H, SiMe_3), 0.37 (s, 9H, SiMe_3) and 0.33 (s, 27H, SiMe_3) ppm.

$^{13}\text{C NMR}$ (75.4 MHz, C_6D_6): δ = 165.4 ($\text{C}=\text{C}$), 157.8 ($\text{C}=\text{C}$), 28.1 (CH_2CH_3), 26.8 (CH_2CH_3), 14.7 (CH_2CH_3), 14.5 (CH_2CH_3), 3.5 (SiMe_3), 2.9 (SiMe_3) and 2.7 (SiMe_3) ppm.

$^{29}\text{Si NMR}$ (59.3 MHz, C_6D_6): δ = -3.9 (GeSiMe_3), -9.3 (SiMe_3), -11.5 ($\text{CSi}(\text{SiMe}_3)_3$), -15.0 ($\text{CSi}(\text{SiMe}_3)_3$), -46.7 (Si-Ge) and -116.5 ($\text{GeSi}(\text{SiMe}_3)_3$) ppm.

4.2.31 1-[Tris(trimethylsilyl)silyl]-3,4-diphenyl-1,2,2-tris(trimethylsilyl)-1,2-dehydro-2-silagermete (**50**)



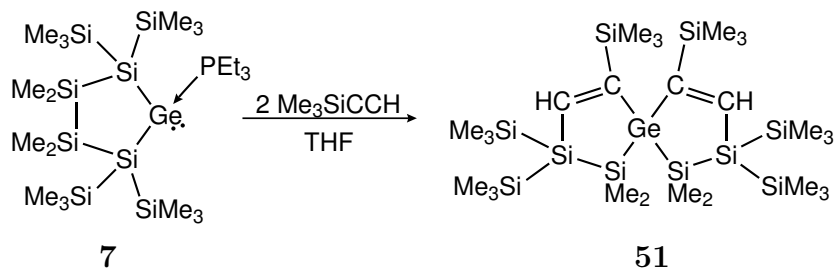
36 (30 mg, 0.04 mmol) in toluene was heated up to 150 °C for 18 hours. The solvent was removed under reduced pressure and the residue was extracted with pentane (3 x 5 mL). The solvent was evaporated to give **50** as a pale yellow solid (28 mg, 93%).

¹H NMR (300 MHz, C₆D₆): δ = 7.48 (1H), 7.27–7.23 (m, 4H), 7.04 (m, 3H), 6.95 (d, 2H), 0.39 (s, 9H, GeSiMe₃), 0.36 (s, 36H, Ge(SiMe₃)₃ and CSiSiMe₃) and 0.34 (s, 9H, CSiSiMe₃)

¹³C NMR (75.4 MHz, C₆D₆): 162.9, 156.9, 143.6, 142.0, 126.4, 125.9, four signals overlapping with C₆D₆, 3.7 (SiMe₃), 3.0 (SiMe₃) and 2.9 (2 x SiMe₃).

²⁹Si NMR (59.3 MHz, C₆D₆): δ = -0.6 (SiMe₃), -8.9 (SiMe₃), -9.7 (SiMe₃), -13.9 (GeSi(SiMe₃)₃), -42.7 (Si–Ge) and -115.5 (GeSi(SiMe₃)₃) ppm.

4.2.32 5-Germa-1,3,3,6,8,8-hexakis(trimethylsilyl)-4,4,9,9-tetramethylspiro[4.4]-3,4,7,8-tetrasilanon-1,6-diene (51)



7 (65 mg, 0.1 mmol) and trimethylsilylacetylene (20 mg, 0.2 mmol) were stirred in THF (2 mL) for 18 hours at room temperature. The solvent was removed under reduced pressure and the residue was extracted with pentane (3 x 5 mL). The solvent was evaporated to give **56** as a white solid (63 mg, 86%). Crystallization from pentane at $-35\text{ }^{\circ}\text{C}$ gave colorless crystals suitable to X-ray study.

Mp = 113-116 $^{\circ}\text{C}$

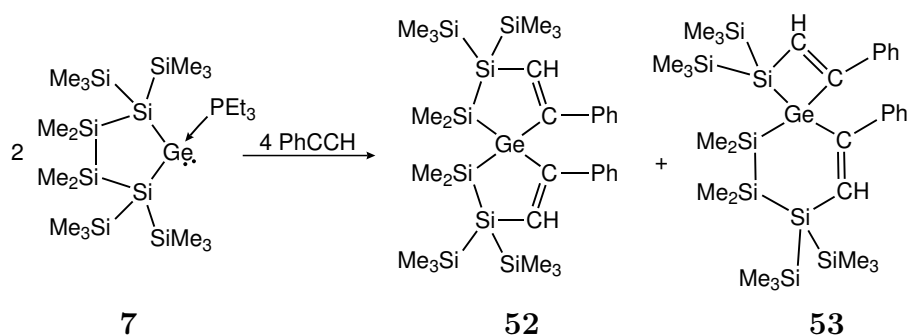
$^1\text{H NMR}$ (300 MHz, C_6D_6): δ = 7.80 (s, 2H, CH), 0.55 (s, 12H, SiMe₂), 0.28 (s, 18H, SiMe₃), 0.21 (s, 18H, SiMe₃) and 0.20 (s, 18H, SiMe₃) ppm.

$^{13}\text{C NMR}$ (75.4 MHz, C_6D_6): δ = 176.6, 158.2, 1.2 (SiMe₃), 1.1 (SiMe₃), 0.3 (SiMe₃), -0.3 (SiMe₂) and -1.4 (SiMe₂) ppm.

$^{29}\text{Si NMR}$ (59.3 MHz, C_6D_6): δ = -6.9 (SiMe₃), -12.1 (SiMe₃), -12.7 (SiMe₃), -28.2 (SiMe₂) and -66.4 (Si(SiMe₃)₃) ppm.

Anal. calcd for $\text{C}_{26}\text{H}_{68}\text{GeSi}_{10}$ (734.31): C 42.53, H 9.33 Found: C 44.24, H 9.03.

4.2.33 52 and 53



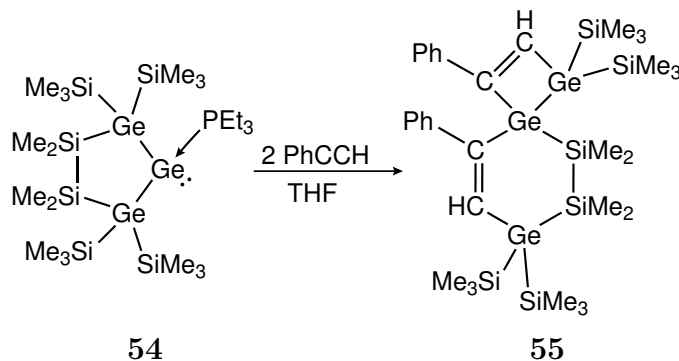
7 (130 mg, 0.2 mmol) and phenylacetylene (41 mg, 0.4 mmol) were stirred in THF (2 mL) for 18 hours at room temperature. The solvent was removed under reduced pressure and the residue were extracted with pentane (3 x 5 mL). The solvent was evaporated to give **52** and **53** as white solids. Separation of the products was unsuccessful.

¹H NMR (300 MHz, C₆D₆): δ = 7.66 (1H), 7.63 (1H), 7.51 (2H), 7.48 (3H), 7.24 (1H), 7.16 (2H), 7.12–7.07 (3H), 7.04–6.98 (m, 5H), 6.95–6.92 (m, 5H), 6.85–6.80 (1H), 0.48 (s, 6H, SiMe₂), 0.45 (s, 6H, SiMe₂), 0.40 (s, 6H, SiMe₂), 0.36 (s, 9H, SiMe₃), 0.36 (s, 9H, SiMe₃), 0.30 (s, 9H, SiMe₃), 0.30 (s, 9H, SiMe₃), 0.26 (s, 32H, SiMe₃), 0.25 (s, 9H, SiMe₃), 0.25 (s, 9H, SiMe₃) and 0.22 (s, 6H, SiMe₂) ppm.

¹³C NMR (75.4 MHz, C₆D₆): δ = 172.2, 167.9, 165.3, 149.8.6, 147.7, 143.5, 142.1, 140.1, 137.5, 128.3, 126.9, 126.6, 126.3, 126.2, seven signals overlapping with C₆D₆, 1.9 (SiMe₃), 1.5 (SiMe₃), 1.0 (SiMe₃), 0.9 (overlapping, 2 x SiMe₃), 0.4 (SiMe₃), -2.0 (SiMe₂), -2.4 (SiMe₂), -2.9 (SiMe₂), -3.4 (SiMe₂), -3.9 (SiMe₂) and -4.7 (SiMe₂) ppm.

²⁹Si NMR (59.3 MHz, C₆D₆): δ = -9.6, -10.9, -11.8, -12.1, -11.4, -12.5, -27.3, -35.1, -46.1, -46.8, -66.9, -86.6 ppm.

4.2.34 3,4,7-Trigerma-3,3,6,6-tetrakis(trimethylsilyl)-8,9-dimethyl-1,5-diphenylspiro[3.5]-8,9-disilanon-1,5-diene (55)



54 (37 mg, 0.05 mmol) and phenylacetylene (10 mg, 0.1 mmol) were stirred in THF (2 mL) for 2 hours at room temperature. The solvent was removed under reduced pressure and the product was extracted with pentane (3 x 5 mL). The solvent was evaporated to give **55** as pale yellow solid (38 mg, 90%). Crystallization from pentane at $-35\text{ }^{\circ}\text{C}$ gave colorless crystals suitable for X-ray study.

Mp = 101-102 $^{\circ}\text{C}$

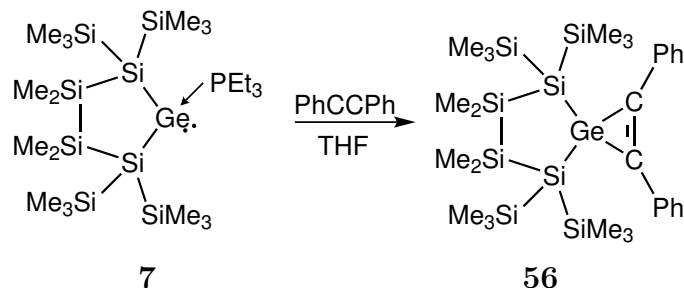
$^1\text{H NMR}$ (300 MHz, C_6D_6): δ = 7.78 (s, 1H, CH), 7.58 (d, 2H, *o*-H), 7.41 (s, 1H, CH), 7.00–7.07 (m, 4H, Ph), 6.85–6.95 (m, 2H, Ph), 0.54 (s, 3H, SiMe₂), 0.52 (s, 3H, SiMe₂), 0.43 (s, 9H, SiMe₃), 0.41 (s, 3H, SiMe₂), 0.40 (s, 9H, SiMe₃), 0.38 (s, 3H, SiMe₂), 0.32 (s, 9H, SiMe₃) and 0.31 (s, 9H, SiMe₃) ppm.

$^{13}\text{C NMR}$ (75.4 MHz, C_6D_6): δ = 169.7, 162.5, 149.4, 146.5, 142.6, 140.1, 126.5, 126.1, two signals overlapping with C_6D_6 , 125.9 (2 signals, overlapping), 2.6 (SiMe₃), 2.2 (SiMe₃), 1.8 (SiMe₃), 1.5 (SiMe₃), -2.0 (SiMe₂), -3.1 (SiMe₂), -3.8 (SiMe₂) and -5.1 (SiMe₂) ppm.

$^{29}\text{Si NMR}$ (59.3 MHz, C_6D_6): δ = -3.3 (SiMe₃), -3.7 (SiMe₃), -4.7 (SiMe₃), -5.0 (SiMe₃), -35.5 (SiMe₂) and -37.3 (SiMe₂) ppm.

Anal. calcd for $\text{C}_{32}\text{H}_{60}\text{Ge}_3\text{Si}_6$ (831.25): C 46.24, H 7.28. Found: C 44.22, H 6.15.

4.2.35 3-Germa-4,4,7,7-tetrakis(trimethylsilyl)-5,5,6,6-tetramethyl-1,2-diphenylspiro[2.4]-4,5,6,7-tetrasilhept-1-ene (**56**)



7 (65 mg, 0.1 mmol) and diphenylacetylene (18 mg, 0.1 mmol) were stirred in THF (2 mL) for 24 hours at room temperature. The solvent was removed under reduced pressure and the product was extracted with pentane (3 x 5 mL). The solvent was evaporated to give **56** as a yellowish solid (62 mg, 86%). Crystallization from toluene at $-35\text{ }^\circ\text{C}$ gave colorless crystals suitable for X-ray study.

Mp = 167–169 $^\circ\text{C}$

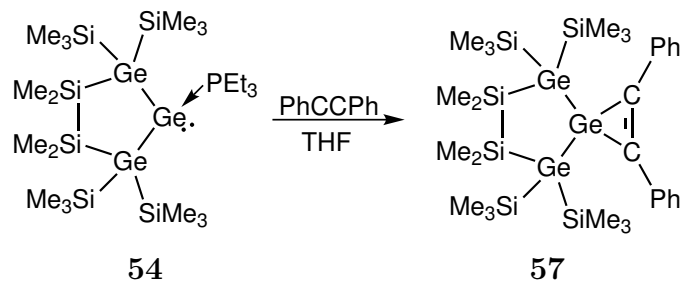
$^1\text{H NMR}$ (300 MHz, C_6D_6): δ = 7.3 (d, 4H, *o*-H), 7.19 (t, 4H, *m*-H) 7.00 (t, 2H, *p*-H), 0.43 (s, 12H, SiMe₂) and 0.25 (s, 36H, SiMe₃) ppm.

$^{13}\text{C NMR}$ (75.4 MHz, C_6D_6): δ = 144.4, 134.7, 131.6, 129.0, 128.2, 2.4 (SiMe₃) and -2.7 (SiMe₂) ppm.

$^{29}\text{Si NMR}$ (59.3 MHz, C_6D_6): δ = -7.3 (SiMe₃) -30.3 (SiMe₂) and -120.1 (Si(SiMe₃)₃) ppm.

Anal. calcd for C₃₀H₅₈GeSi₈ (716.11): C 50.32, H 8.16 Found: C 66.60, H 5.48.

4.2.36 3,4,7-Trigerma-4,4,7,7-tetrakis(trimethylsilyl)-5,5,6,6-tetramethyl-1,2-diphenylspiro[2.4]-5,6-disilahept-1-ene (57)



54 (74 mg, 0.10 mmol) and phenylacetylene (18 mg, 0.1 mmol) were stirred in THF (2 mL) for 12 hours at room temperature. The solvent was removed under reduced pressure and the product was extracted with pentane (3 x 5 mL). The solution was concentrated to 1 mL and stored at $-35\text{ }^{\circ}\text{C}$ to give **57** as yellow crystals (52 mg, 64%).

Mp = 168–169 $^{\circ}\text{C}$

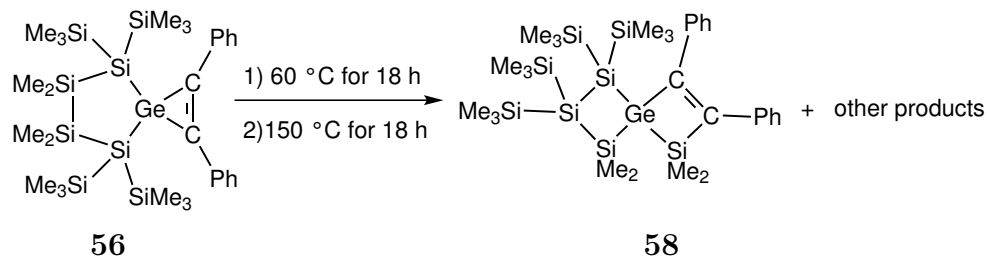
$^1\text{H NMR}$ (300 MHz, C_6D_6): δ = 7.82 (d, 4H, *o*-H), 7.19 (t, 4H, *m*-H), 7.00 (t, 2H, *p*-H), 0.46 (s, 12H, *SiMe*₂), 0.28 (s, 36H, *SiMe*₃) ppm.

$^{13}\text{C NMR}$ (75.4 MHz, C_6D_6): δ = 147.7, 135.4, 131.6, 128.8, 128.2, 3.0 (*SiMe*₃) and -2.2 (*SiMe*₂) ppm.

$^{29}\text{Si NMR}$ (59.3 MHz, C_6D_6): δ = -1.5 (*SiMe*₃) and -23.4 (*SiMe*₂) ppm.

Anal. calcd for $\text{C}_{30}\text{H}_{58}\text{Ge}_3\text{Si}_6$ (805.21): C 44.75, H 7.20 Found: C 44.98, H 6.59.

4.2.37 4-Germa-5,5,6,6-tetrakis(trimethylsilyl)-3,3,5,5-tetramethyl-1,2-diphenyl-spiro[3.3]-3,5,6,7-tetrasilhept-1-ene (**58**)

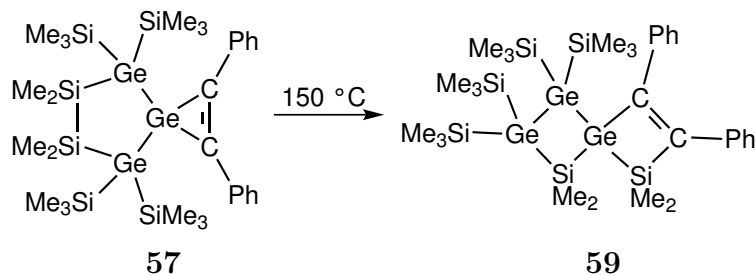


56 (50 mg, 0.07 mmol) in toluene (1 mL) was heated up to 60 °C for 18 hours and then to 150°C for the next 18 hours. After the NMR confirmed formation of the new products the solvent was concentrate to 0.5 mL and the products was stored at -35 °C. Inseparable mixture of **58** and other unknown products was obtained.

²⁹Si NMR (59.3 MHz, C₆D₆): 10.2, 3.9, -2.7, -7.5, -8.5, -8.6, -9.4, -9.5, -12.4, -22.5, -35.2, -59.9, -94.6, -108.1, -119.0 ppm.

The ¹H NMR and ¹³C NMR spectra could not be interpreted due to inability to separation of the products.

4.2.38 4,5,6-Trigerma-5,5,6,6-tetrakis(trimethylsilyl)-3,3,5,5-tetramethyl-1,2-diphenylspiro[3.3]-3,7-disilahept-1-ene (59)



54 (35 mg, 0.043 mmol) in C_6D_6 was heated up to $150\text{ }^\circ\text{C}$ for 18 hours. The solvent was removed under reduced pressure and the product was extracted with pentane (3 x 5 mL). The extract was concentrate to 0.5 mL and stored at $-35\text{ }^\circ\text{C}$. Colorless crystals (20 mg, 58%) of **59** were obtained.

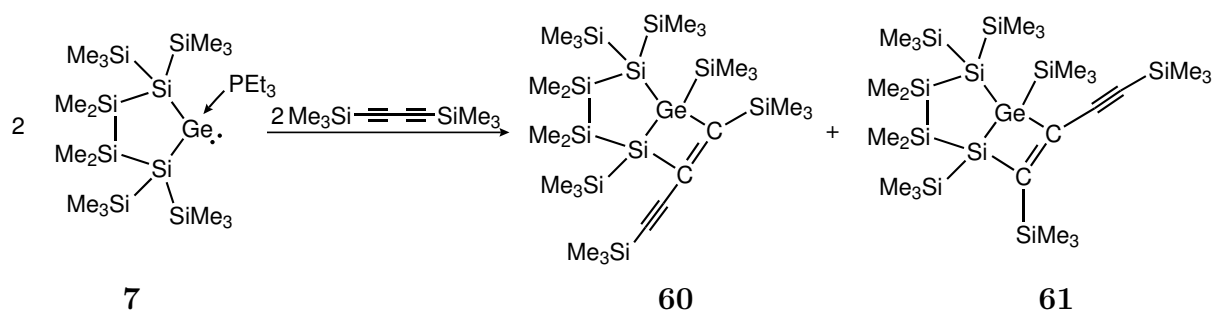
Mp = $168\text{--}170\text{ }^\circ\text{C}$.

^1H NMR (300 MHz, C_6D_6): δ = 7.28 (2H, *o*-H), 7.09–7.21 (4H), 6.91–7.04 (m, 4H), 0.94 (s, 3H, *SiMe*₂), 0.91 (s, 3H, *SiMe*₂), 0.64 (s, 3H, *SiMe*₂), 0.60 (s, 3H, *SiMe*₂), 0.44 (s, 18H, 2x*SiMe*₃), 0.34 (s, 9H, *SiMe*₃) and 0.21 (s, 9H, *SiMe*₃) ppm.

^{13}C NMR (75.4 MHz, C_6D_6): δ = 170.6, 156.9, 144.0, 141.0, 126.6, 126.1, 126.0, three signals overlapping with C_6D_6 , 5.4 (*SiMe*₂), 3.7 (*SiMe*₃), 3.7 (*SiMe*₃), 3.6 (*SiMe*₃), 3.5 (*SiMe*₃), 1.9 (*SiMe*₂), 1.6 (*SiMe*₂) and 0.2 (*SiMe*₂) ppm.

^{29}Si NMR (59.3 MHz, C_6D_6): 18.4 (*SiMe*₂), 3.5 (*SiMe*₂), -2.5 (*SiMe*₃), -2.8 (*SiMe*₃), -3.2 (*SiMe*₃) and -4.5 (*SiMe*₃).

4.2.39 60 and 61

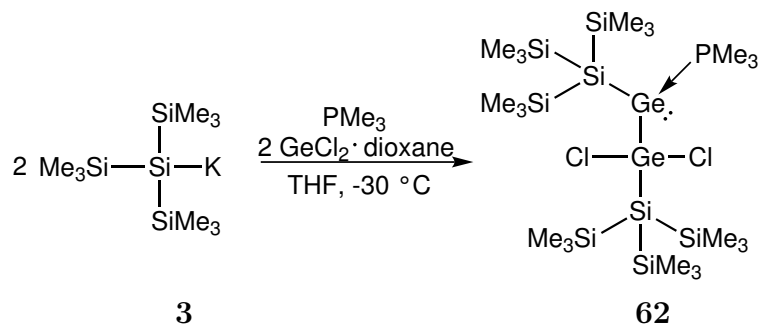


7 (33 mg, 0.05 mmol) and 1,4-bis(trimethylsilyl)-1,3-butadiyne (8 mg, 0.05 mmol) was stirred in THF (1 mL) for 3 days at 70 °C. The solvent was removed under reduced pressure and the product was extracted with pentane (3 x 5 mL). The solvent was evaporated to give a mixture of **60** and **61** (31 mg, 85%).

²⁹Si NMR (59.3 MHz, C₆D₆): δ = -3.8, -4.1, -7.7, -8.1, -8.3, -8.8, -11.1, -11.5, -12.7, -13.1, -16.2, -16.7, -19.2, -24.7, -26.8, -28.4, -35.8, -38.0, -112.7 and -113.1 ppm

The ¹H NMR and ¹³C NMR spectra could not be interpreted due to inability to separate products.

4.2.40 {Dichloro[tris(trimethylsilyl)silyl]germyl}[tris(trimethylsilyl)silyl]germylene · PMe₃ (**62**)



Method A: A solution of tris(trimethylsilyl)silyl potassium (**3**) (0.31 mmol) in THF (2 mL) was slowly added dropwise to a vigorously stirred solution of germanium dichloride · dioxane (72 mg, 0.31 mmol) and trimethylphosphine (11 mg, 0.16 mmol) in THF (4 mL) at -30°C . The stirring of the reaction mixture was continued for 1 hour at room temperature. The solvent was removed under reduced pressure and the product was extracted with pentane (3 x 5 mL). The orange extract was concentrated to 3 mL and stored at -35°C . Yellow crystals (25 mg, 20%) of **62** were obtained.

Method B: GeCl₂ · dioxane (194 mg, 0.84 mmol) in THF (2 mL) was added to a stirred solution of **18** (1.40 mmol) in THF (15 mL) at -30°C . After 1 hour the solvent was removed under reduced pressure and the product was extracted with pentane (3 x 5 mL). The extract was concentrated to 5 mL and stored at -35°C . Yellow crystals (262 mg, 39%) of **62** were obtained.

Mp = 116-119 °C.

¹H NMR (300 MHz, C₆D₆): δ = 1.20 (d, PMe₃, ²J_{H-P} = 10.7 Hz), 0.46 (s, 27H, SiMe₃) and 0.43 (s, 27H, SiMe₃) ppm.

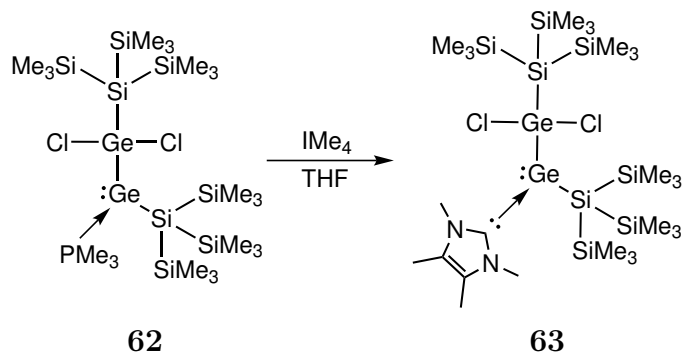
¹³C NMR (75.4 MHz, C₆D₆): δ = 17.1 (d, PMe₃, ¹J_{C-P} = 25 Hz), 4.2 (SiMe₃) and 3.1 (SiMe₃) ppm.

²⁹Si NMR (59.3 MHz, C₆D₆): δ = -8.2 (GeCl₂Si(SiMe₃)₃), -8.7 (d, :GeSi(SiMe₃)₃, ³J_{Si-P} = 11 Hz), -76.7 (GeSi(SiMe₃)₃) and -112.6 (d, SiSi(SiMe₃)₃, ²J_{Si-P} = 16 Hz) ppm.

³¹P NMR (121.4 MHz, C₆D₆): δ = -15.2 (PMe₃) ppm.

Anal. calcd for C₂₁H₆₃Cl₂Ge₂PSi₈ (787.57): C 32.03, H 8.06. Found: C 30.63, H 7.35.

4.2.41 {Dichloro[tris(trimethylsilyl)silyl]germyl}[tris(trimethylsilyl)silyl]germylene · IMe₄ (**63**)

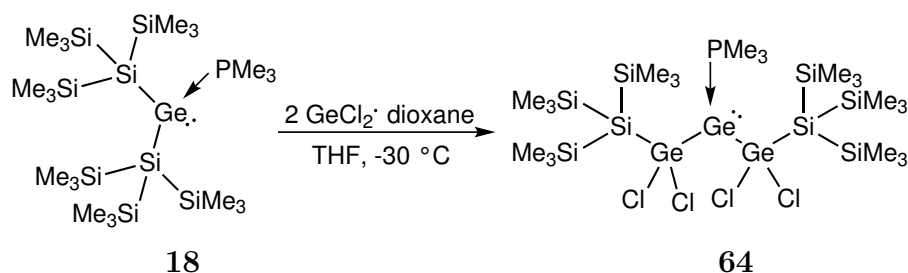


62 (79 mg, 0.1 mmol) and IMe₄ (13 mg, 0.1 mmol) were stirred in THF (1 mL) for 1 hours at room temperature. The solvent was removed under reduced pressure and the product was extracted with toluene (3 x 5 mL). The solvent was evaporated to give **63** as an orange oil (78 mg, 93 %).

¹H NMR (300 MHz, D₂O capillary): δ = 2.34 (s, 6H, C–Me), 0.35 (s, 27H, SiMe₃) and 0.31 (s, 27H, SiMe₃) ppm; signal of N–Me overlapping with THF (removal of THF leads to decomposition of **63** due to its instability).

²⁹Si NMR (59.3 MHz, D₂O capillary): δ = –8.3 (SiMe₃) –8.9 (CSiMe₃), –82.2 (Si(SiMe₃)₃) and –119.9 (Si(SiMe₃)₃) ppm.

4.2.42 Bis{dichloro[tris(trimethylsilyl)silyl]germyl}germylene · PMe₃ (**64**)



Germanium dichloride · dioxane (173 mg, 0.75 mmol) in THF (2 mL) was added to the stirred solution of bis[tris(trimethylsilyl)silyl]germylene · PMe₃ (**18**) (0.45 mmol) in THF (10 mL) at $-30\text{ }^{\circ}\text{C}$. After 10 min the solvent was removed under reduced pressure and the product was extracted with pentane (3 x 5 mL). The solution was concentrated to 5 mL and stored at $-35\text{ }^{\circ}\text{C}$. Pale yellow crystals of **64** (52 mg, 15%) were obtained.

Mp = 90–92 °C.

¹H NMR (300 MHz, C₆D₆): δ = 1.27 (d, 9H, PMe₃, $^2J_{H-P}$ = 11.7 Hz) and 0.45 (s, 54H, SiMe₃) ppm.

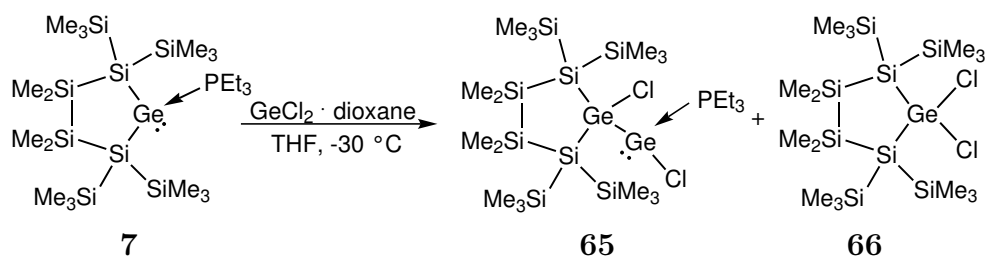
¹³C NMR (75.4 MHz, C₆D₆): δ = 29.9 (PMe₃) and 2.9 (SiMe₃) ppm.

²⁹Si NMR (59.3 MHz, C₆D₆): δ = -8.0 (SiMe₃), -73.0 (Si(SiMe₃)₃) ppm.

³¹P NMR (121.4 MHz, C₆D₆): δ = -8.7 (PMe₃) ppm.

Anal. calcd for C₂₁H₆₃Cl₄Ge₃PSi₈ (931.11): C 27.09, H 6.82. Found: C 26.80, H 6.69.

4.2.43 65 and 66



7 (65 mg, 0.10 mmol) and $\text{GeCl}_2 \cdot \text{dioxane}$ (22 mg, 0.1 mmol) were stirred in THF (1 mL) for 10 minutes at $-30\text{ }^\circ\text{C}$. The solvent was removed under reduced pressure and the products were extracted with toluene (3 x 5 mL). The solvent was evaporated to give **65** and **66** as brown solids. Separation of the products was unsuccessful.

65

^{29}Si NMR (59.3 MHz, C_6D_6): $\delta = -4.2$ (SiMe_3), -4.6 (SiMe_3), -25.0 (d, SiMe_2 , $^3J_{\text{Si}-\text{P}} = 1$ Hz) and -102.6 ($\text{Si}(\text{SiMe}_3)_3$, $^2J_{\text{Si}-\text{P}} = 6$ Hz) ppm.

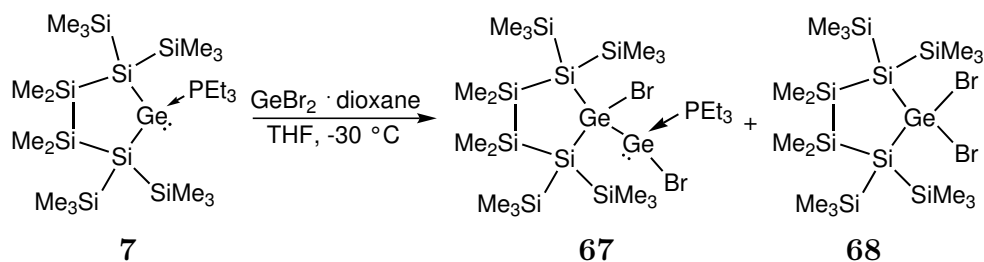
^{31}P NMR (121.4 MHz, C_6D_6): $\delta = +9.7$ (PMe_3) ppm.

66

^{29}Si NMR (59.3 MHz, C_6D_6): $\delta = -4.7$ (SiMe_3), -23.1 (SiMe_2) and -96.7 ($\text{Si}(\text{SiMe}_3)_3$) ppm.

The ^1H NMR spectrum could not be interpreted due to the inability to separate product.

4.2.44 67 and 68



7 (55 mg, 0.08 mmol) and $\text{GeBr}_2 \cdot \text{dioxane}$ (27 mg, 0.08 mmol) were stirred in benzene (1 mL) for 2 hours at room temperature. The solvent was removed under reduced pressure and the products were extracted with toluene (3 x 5 mL). The solvent was evaporated to give **67** and **68** as brown solids. Separation of the products was unsuccessful.

67

^{29}Si NMR (59.3 MHz, C_6D_6): $\delta = -7.5$ (SiMe_3), -7.6 (d, SiMe_3), -25.6 (d, SiMe_2 , $^3J_{\text{Si-P}} = 2$ Hz) and -102.1 ($\text{Si}(\text{SiMe}_3)_3$, $^2J_{\text{Si-P}} = 8$ Hz) ppm.

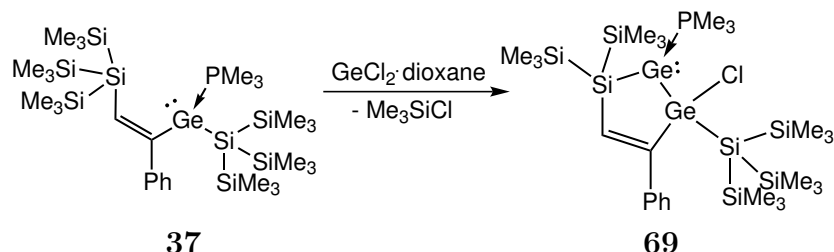
^{31}P NMR (121.4 MHz, C_6D_6): $\delta = +4.6$ (PMe_3) ppm.

68

^{29}Si NMR (59.3 MHz, C_6D_6): $\delta = -3.5$ (SiMe_3), -22.6 (SiMe_2) and -95.1 ($\text{Si}(\text{SiMe}_3)_3$) ppm.

The ^1H NMR spectrum could not be interpreted due to the inability to separate product.

4.2.45 2-Chloro-2-tris(trimethylsilyl)silyl-5,5-bis(trimethylsilyl)-3-phenyl-1,2-digerma-5-silacyclopent-3-en-1-ylidene · PMe₃ (**69**)



Dioxane complex of germanium dichloride (23 mg, 0.1 mmol) was added to the stirring solution of **37** (75 mg, 0.1 mmol) in THF (2 mL). After 2 hours the solvent was removed under reduced pressure, the residues was extracted with pentane (3 x 5 mL). The solution was concentrated to 0.5 mL and stored at $-35\text{ }^{\circ}\text{C}$. Pale yellow crystals of **69** (57 mg, 74%) suitable to X-ray study were obtained.

Mp = 122-124 $^{\circ}\text{C}$.

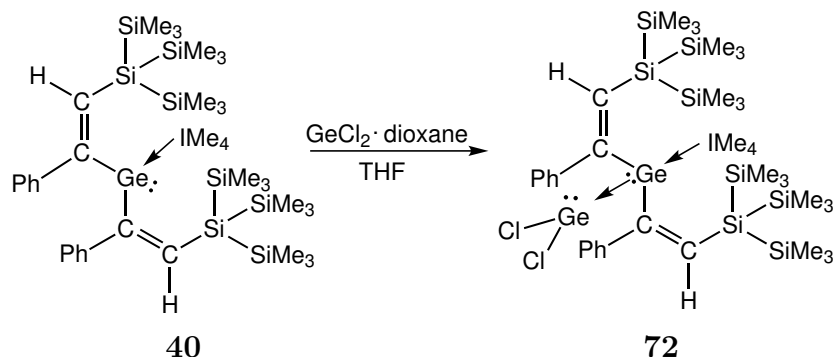
¹H NMR (300 MHz, C₆D₆): δ = 7.90 (d, 2H, *o*-H), 7.13 (m, 2H, *m*-H), 7.07 (s, 1H, CH), 6.98 (t, 1H, *p*-H), 1.12 (d, PMe₃, ²J_{H-P} = 10.7 Hz), 0.33 (s, 9H, SiMe₃), 0.30 (s, 27H, SiMe₃) and 0.14 (s, 9H, SiMe₃) ppm.

¹³C NMR (75.4 MHz, C₆D₆): δ = 171.3, 147.4, 146.6, 128.2, 126.7, one signal overlapping with C₆D₆, 17.0 (d, PMe₃, ¹J_{C-P} = 26 Hz), 3.0 (SiMe₃), 1.9 (SiMe₃) and 1.2 (SiMe₃) ppm.

²⁹Si NMR (59.3 MHz, C₆D₆): δ = -8.7 (SiMe₃), -11.1 (d, SiMe₃, ³J_{Si-P} = 13 Hz), -11.7 (d, SiMe₃, ³J_{Si-P} = 17 Hz), -50.1 (d, Si-Ge, ²J_{Si-P} = 15 Hz) and -100.7 (d, SiMe₃, ³J_{Si-P} = 2 Hz) ppm.

³¹P NMR (121.4 MHz, C₆D₆): δ = -13.9 (PMe₃) ppm.

4.2.46 Germanium dichloride · bis[*Z*-1-phenyl-2-tris(trimethylsilyl)silylvinyl]-germylene · IMe₄ (**72**)



40 (40 mg, 0.045 mmol) and GeCl₂ · dioxane (10 mg, 0.045 mmol) were stirred in THF (1 mL) at room temperature for 48 hours. To the solution 1 mL of pentane was added and after storing at -35 °C yellow crystals of **40** (22 mg, 47%) were obtained.

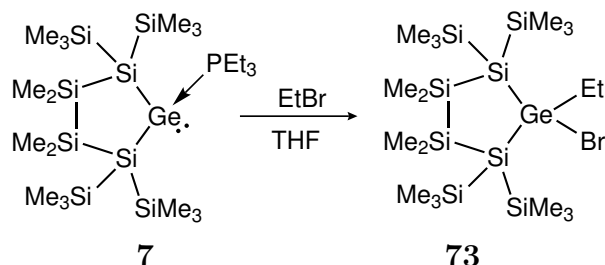
Mp = 121–122 °C.

¹H NMR (300 MHz, C₆D₆): δ = 7.12 (2H), 6.99 (4H), 6.61 (br, 4H), 6.28 (s, 1 H), 3.33 (s, 6H, N-Me), 2.10 (s, 6H, C-Me) and 0.20 (s, 54H, SiMe₃) ppm.

¹³C NMR (75.4 MHz, C₆D₆): δ = 150.6, 150.4, 147.0, 145.2, 130.8, 128.7, 127.5, 126.8, 34.0 (N-Me), 9.5 (C-Me) and 1.5 (SiMe₃) ppm.

²⁹Si NMR (59.3 MHz, C₆D₆): δ = -12.4 (SiMe₃) and -84.3 (Si(SiMe₃)₃) ppm.

4.2.47 1-Bromo-1-ethylgerma-2,2,5,5-tetrakis(trimethylsilyl)tetramethylcyclopentasilane (**73**)



EtBr (5 mg, 0.05 mmol) was added to a stirring solution of **7** (33 mg, 0.05 mmol) in THF (1 mL). After 2 hours the solvent was evaporated and the residues was extracted with pentane (3 x 5 mL). The solution was concentrated to 1 mL and stored at $-35\text{ }^\circ\text{C}$. Yellow crystals of **73** (29 mg, 91%) suitable to X-ray study were obtained.

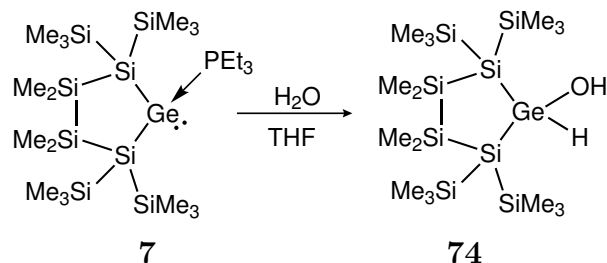
Mp = 136–138 $^\circ\text{C}$.

$^1\text{H NMR}$ (300 MHz, C_6D_6): δ = 1.56 (m, 2H, Ge- CH_2), 1.43 (m, 3H, CH_3), 0.43 (s, 18H, SiMe_3), 0.41 (s, 6H, SiMe_2), 0.32 (s, 6H, SiMe_2) and 0.22 (s, 18H, SiMe_3) ppm.

$^{13}\text{C NMR}$ (75.4 MHz, C_6D_6): δ = 19.0 (Ge- CH_2), 12.1 (CH_3), 3.3 (SiMe_3), 3.2 (SiMe_3), -2.1 (SiMe_2) and -2.6 (SiMe_2) ppm.

$^{29}\text{Si NMR}$ (59.3 MHz, C_6D_6): δ = -4.1 (SiMe_3), -8.1 (SiMe_3), -25.9 (SiMe_2) and -111.5 ($\text{Si}(\text{SiMe}_3)_3$) ppm.

4.2.48 1-Hydroxy-1-germa-2,2,5,5-tetrakis(trimethylsilyl)-3,3,4,4-tetramethylcyclopentasilane (**74**)



Degassed H₂O (1.8 μl, 0.1 mmol) was added to a stirring solution of **7** (65 mg, 0.1 mmol) in THF (1 mL). After 18 hours the solvent was evaporated and the residues was extracted with pentane (3 x 5 mL). The solvent was evaporated to give **74** as a yellowish solid (50 mg, 90%).

Mp = 123–125°C

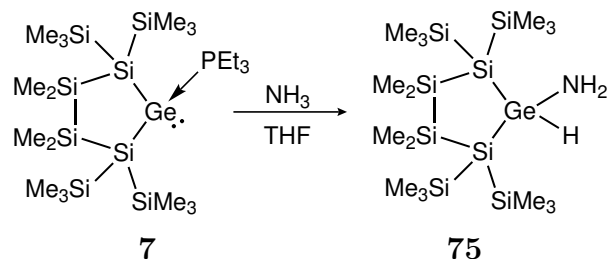
¹H NMR (300 MHz, C₆D₆): δ = 6.38 (d, 1H, Ge–H, ³J_{H–H} = 1.6 Hz), 0.34 (s, 18H, SiMe₃), 0.39 (s, 6H, SiMe₂), 0.28 (s, 6H, SiMe₂), 0.27 (s, 18H, SiMe₃) and –0.44 (d, 1H, O–H, ³J_{H–H} = 1.7 Hz) ppm.

¹³C NMR (75.4 MHz, C₆D₆): δ = 2.6 (SiMe₃), 1.8 (SiMe₃) and –2.5 (SiMe₂) ppm.

²⁹Si NMR (59.3 MHz, C₆D₆): δ = –4.7 (SiMe₃), –7.3 (SiMe₃), –25.3 (SiMe₂) and –113.9 (Si(SiMe₃)₃) ppm.

Anal. calcd for C₁₆H₅₀GeOSi₈ (555.89): C 34.57, H 9.07 Found: C 30.81, H 6.75.

4.2.49 1-Aminogerma-2,2,5,5-tetrakis(trimethylsilyl)-3,3,4,4-tetramethylcyclopentasilane (**75**)



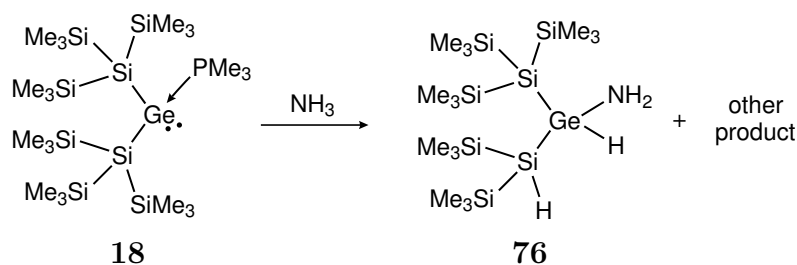
An orange solution of **7** (65 mg, 0.1 mmol) in toluene (2 mL) was exposed to ammonia gas for 3 min at $-40\text{ }^\circ\text{C}$. The solution turned colorless and was stirred for 1 hour at ambient temperature. The solvent was removed to give **75** as a yellowish solid (57 mg, 99%).

^1H NMR (300 MHz, C_6D_6): 5.35 (s, 1H, GeH), 1.33 (br, 2H, NH_2), 0.35 (br, 12H, SiMe_2) and 0.28 (br, 36H, SiMe_3) ppm.

^{13}C NMR (75.4 MHz, C_6D_6): $\delta = 3.1$ (SiMe_3), 2.0 (SiMe_3) and -2.3 (SiMe_2) ppm.

^{29}Si NMR (59.3 MHz, C_6D_6): $\delta = -7.1$ (SiMe_3), -8.1 (SiMe_3), -24.9 (SiMe_2) and -122.0 ($\text{Si}(\text{SiMe}_3)_3$) ppm.

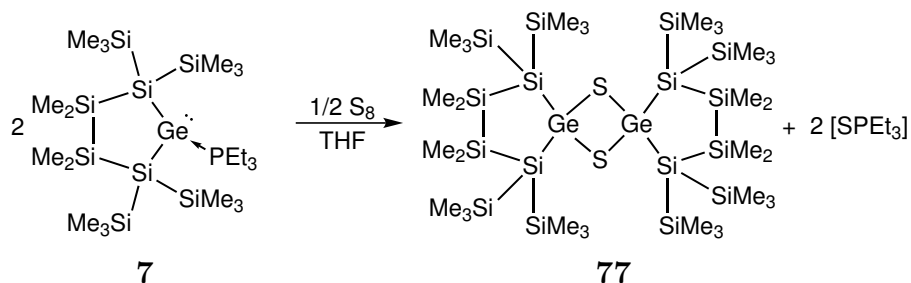
4.2.50 Amino[tris(trimethylsilyl)silyl][bis(trimethylsilyl)silyl]germane (**76**)



An orange solution of **18** (0.1 mmol) in THF (5 mL) was exposed to ammonia gas for 3 minutes at $-40\text{ }^\circ\text{C}$. The solution was stirred for 1 hour at ambient temperature. The solvent was removed and the residue was extracted with pentane (3 x 5 mL). The solution was concentrated to 1 mL and stored at $-35\text{ }^\circ\text{C}$. Yellow crystals of **76** suitable for X-ray study and a second compound were obtained. Separation of these two products was unsuccessful.

The NMR spectra could not be interpreted due to the inability to separate products.

4.2.51 5,7-Digerma-6,13-disulfo-1,1,4,4,8,8,11,11-octakis(trimethylsilyl)octamethyldispiro[4.1.4.1]dodecasilane (**77**)



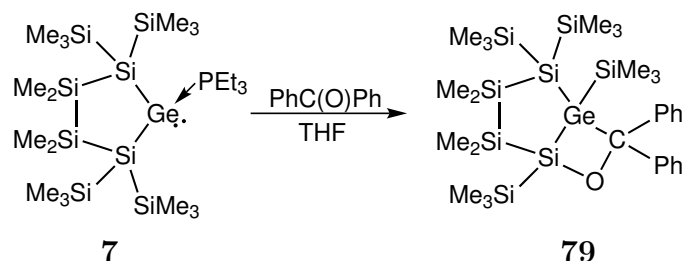
Germylene **7** (33 mg, 0.05 mmol) and S₈ (3 mg, 0.013 mmol) were stirred in THF (1 mL). After 18 hours the solvent was removed under reduced pressure and the residue was extracted with pentane (3 x 5 mL). The solution was concentrated to 1 mL and stored at -35 °C. Yellow crystals of **77** and white crystals of SPEt₃ were obtained. Separation of the compounds was unsuccessful.

¹H NMR (300 MHz, C₆D₆): δ = 0.50 (s, 72H, SiMe₃) and 0.37 (s, 24H, SiMe₂) ppm.

¹³C NMR (75.4 MHz, C₆D₆): δ = 4.6 (SiMe₃) and 1.6 (SiMe₂) ppm.

²⁹Si NMR (59.3 MHz, C₆D₆): δ = -5.4 (SiMe₃), -30.1 (SiMe₂) and -90.7 (Si(SiMe₃)₃) ppm.

4.2.52 1,2,2,5-Tetrakis(trimethylsilyl)-7,7-diphenyl-bicyclo[3.2.0]-7-carba-1-germa-6-oxa-heptasilane (**79**)



Germylene (**7**, 33 mg, 0.05 mmol) and benzophenone (10 mg, 0.05 mmol) were stirred in THF. After 18 hours the solvent was removed under reduced pressure and the residues were extracted with pentane (3 x 3 mL). The solution was concentrated to 1 mL and stored at $-35\text{ }^\circ\text{C}$. Colorless crystals of **79** (35 mg, 97%) were obtained.

Mp = 185–187 $^\circ\text{C}$

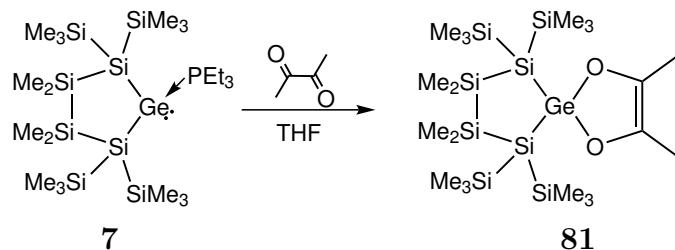
$^1\text{H NMR}$ (300 MHz, C_6D_6): δ = 7.08 (m, 6H *m-H*, *p-H*), 6.99 (d, 4H *o-H*), 0.51 (s, 3H, *SiMe*₂), 0.45 (s, 6H, *SiMe*₃), 0.44 (s, 6H, *SiMe*₃), 0.29 (s, 3H, *SiMe*₂), 0.28 (s, 3H, *SiMe*₂), 0.18 (s, 6H, *SiMe*₃), 0.11 (s, 6H, *SiMe*₃) and -0.50 (s, 3H, *SiMe*₂) ppm.

$^{13}\text{C NMR}$ (75.4 MHz, C_6D_6): δ = 152.1, 151.3, 137.9, 131.7, 129.8, 126.0, 125.1, 124.4, 97.7, 4.1, 4.1, 2.5, -0.5 , -2.9 , -4.6 and -5.6 ppm

$^{29}\text{Si NMR}$ (59.3 MHz, C_6D_6): δ = 40.3 (*Si-O*), -2.1 (*SiMe*₃), -7.9 (*SiMe*₃), -8.5 (*SiMe*₃), -14.0 (*SiMe*₃), -25.3 (*SiMe*₂), -37.2 (*SiMe*₂) and -104.7 (*Si^q*) ppm.

Anal. calcd for $\text{C}_{29}\text{H}_{58}\text{GeOSi}_8$ (720.09): C 48.37, H 8.12. Found: C 36.79, H 7.35.

4.2.53 2,3,7,7,8,8-Hexamethyl-6,6,9,9-tetrakis[tris(trimethylsilylsilyl)-spiro[4.4]-5-germa-1,4-dioxa-6,7,8,9-tetrasilanon-2-ene (81)



7 (33 mg, 0.05 mmol) and diacetyl (5 mg, 0.05 mmol) were stirred in THF. After 24 hours the solvent was removed under reduced pressure and the residue was extracted with pentane (3 x 3 mL). The solution was concentrated to 1 mL and stored at $-35\text{ }^{\circ}\text{C}$. Yellowish crystals of **81** (31 mg, 100%) were obtained.

Mp = 153–155 $^{\circ}\text{C}$.

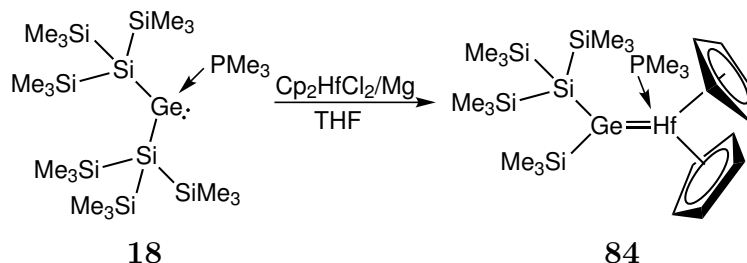
$^1\text{H NMR}$ (300 MHz, C_6D_6): δ = 1.93 (s, 6H, *CMe*), 0.36 (s, 12H, *SiMe*₂) and 0.35 (s, 36H, *SiMe*₃) ppm.

$^{13}\text{C NMR}$ (75.4 MHz, C_6D_6): δ = 131.3 (*CO*), 14.5 (*CMe*), 2.6 (*SiMe*₃) and -2.7 (*SiMe*₂) ppm.

$^{29}\text{Si NMR}$ (59.3 MHz, C_6D_6): δ = -6.1 (*SiMe*₃), -30.4 (*SiMe*₂) and -117.0 (*Si*(*SiMe*₃)₃) ppm.

Anal. calcd for $\text{C}_{20}\text{H}_{54}\text{GeO}_2\text{Si}_8$ (623.97): C 38.50, H 8.72. Found: C 40.43, H 7.85.

4.2.54 Trimethylsilyl[tris(trimethylsilyl)silyl]germylene–hafnocene · PMe₃ complex (**84**)



Hafnocene dichloride (177 mg, 0.47 mmol) was added to a solution of bis[tris(trimethylsilyl)silyl]germylene · PMe₃ (**18**) (0.28 mmol) in THF (5 mL) at room temperature. The color turned red-violet after 2 hours. The stirring was continued for 18 hours. The solvent was removed under reduced pressure and the product was extracted with pentane (3 x 5 mL). The extract was concentrated to 3 mL and storage at -35 °C gave **84** as dark red crystals (68 mg, 35%).

Mp = 148-151 °C.

¹H NMR (300 MHz, C₆D₆): δ = 5.35 (d, 5H, Cp, ⁴J_{H-P} = 1.1 Hz), 5.23 (d, 5H, Cp, ⁴J_{H-P} = 1.1 Hz), 0.85 (d, 9H, PMe₃, ²J_{H-P} = 6.7 Hz), 0.73 (s, 9H, GeSiMe₃) and 0.53 (s, 27H, SiSiMe₃) ppm.

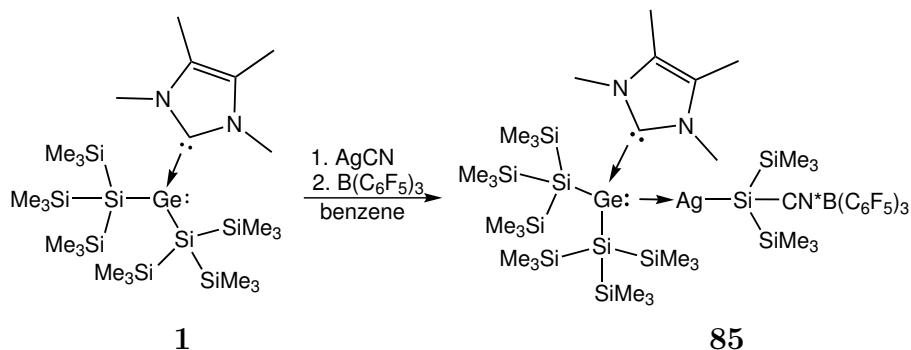
¹³C NMR (75.4 MHz, C₆D₆): δ = 96.8 (d, Cp, ³J_{C-P} = 19 Hz), 22.9 (d, PMe₃, ¹J_{C-P} = 25 Hz), 8.7 (SiMe₃) and 5.6 (SiMe₃) ppm.

²⁹Si NMR (59.3 MHz, C₆D₆): δ = 1.8 (d, GeSiMe₃, ³J_{Si-P} = 2 Hz), -8.3 (d, SiSiMe₃, ⁴J_{Si-P} = 2 Hz) and -97.5 (d, Si(SiMe₃)₃, ³J_{Si-P} = 3 Hz) ppm.

³¹P NMR (121.4 MHz, C₆D₆): δ = -2.7 (PMe₃) ppm.

Anal. calcd for C₂₂H₄₆GeHfSi₅ (702.16): C 37.63, H 6.60. Found: C 38.09, H 6.55.

4.2.55 Cyano[bis(trimethylsilyl)]silyl{bis[tris(trimethylsilyl)silyl]germylene · IMe₄}-silver(I) · B(C₆F₅)₃ (**85**)



1 (289 mg, 0.3 mmol) and AgCN (40 mg, 0.3 mmol) were stirred in benzene in a vial wrapped with tin foil for light protection. After 2 hours B(C₆F₅)₃ (154 mg, 0.3 mmol) was added. Slow evaporation of benzene gave **85** as colorless crystals (183 mg, 40%).

Mp = 121-122 °C.

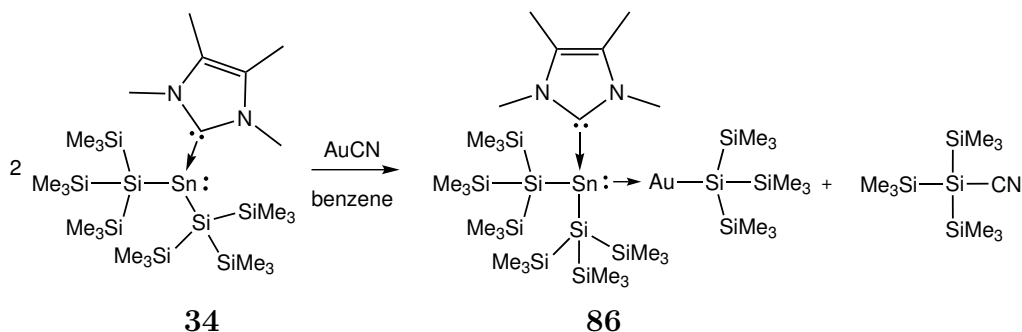
¹H NMR (300 MHz, C₆D₆): δ = 4.08 (s, 3H, NMe), 3.43 (s, 3H, NMe), 1.42 (s, 3H, CMe), 1.24 (s, 3H, CMe), 0.38 (s, 18H, SiMe₃) and 0.18 (s, 54H, SiMe₃) ppm.

¹¹B NMR (96.2 MHz, C₆D₆): -22.6 ppm.

¹⁹F NMR (282.2 MHz, C₆D₆): -132.9 (dd, ³J_{F-F} = 23 Hz, ⁴J_{F-F} = 9 Hz, *o*-ArF), -157.3 (t, ³J_{F-F} = 21 Hz, *p*-ArF) and -164.3 (dt, ³J_{F-F} = 23 Hz, ⁴J_{F-F} = 8 Hz, *m*-ArF) ppm.

²⁹Si NMR (59.3 MHz, C₆D₆): δ = -5.3 (d, AgSiSiMe₃²J_{Si-Ag} = 3 Hz), -8.8 (d, GeSiSiMe₃, ³J_{Si-Ag} = 3 Hz), -107.3 (d, GeSi(SiMe₃)₃, ³J_{Si-Ag} = 11 Hz), -124.3 (2d, AgSi, ¹J_{Si-Ag} = 214 Hz, ¹J_{Si-Ag} = 255 Hz) ppm.

4.2.56 Tris(trimethylsilyl)silyl{bis[tris(trimethylsilyl)silyl]stannylene · IMe₄} gold(I)
(86)



34 (42 mg, 0.057 mmol) and AuCN (12 mg, 0.228 mmol) were stirred in benzene in a vial wrapped with tin foil for light protection. The solvent was evaporated and the residue was redissolved in toluene (3 mL). The concentrated solution was stored at $-35\text{ }^{\circ}\text{C}$ yielding **86** as colorless crystals (12 mg, 17%).

¹H NMR (300 MHz, C₆D₆): $\delta = 4.28$ (s, 3H, NMe), 3.46 (s, 3H, NMe), 1.27 (s, 3H, CMe), 1.18 (s, 3H, CMe), 0.59 (s, 27H, SiMe₃) and 0.33 (s, 54H, SiMe₃) ppm.

¹³C NMR (75.4 MHz, C₆D₆): $\delta = 165.4$ (N-C-N), 126.1 (br, 2 x CMe), 40.0 (NMe), 37.2 (NMe), 8.2 (CMe), 7.7 (CMe), 4.7 (SiMe₃) and 4.0 (SiMe₃) ppm.

²⁹Si NMR (59.3 MHz, C₆D₆): $\delta = -4.9$ (AuSiSiMe₃), -7.0 (SnSiSiMe₃), -99.4 (AuSi(SiMe₃)₃) and -114.2 (SnSi(SiMe₃)₃) ppm.

¹¹⁹Sn NMR (111.8 MHz, C₆D₆): 136.8 ppm.

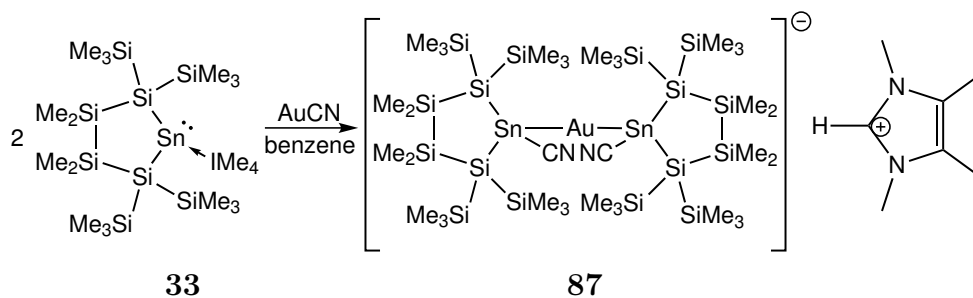
Tris(trimethylsilyl)silyl cyanide:

¹H NMR (300 MHz, D₂O capillary): $\delta = 0.44$ (s, 54H, SiMe₃) ppm.

²⁹Si NMR (59.3 MHz, D₂O capillary): $\delta = -10.4$ (SiMe₃) and -103.0 (Si(SiMe₃)₃) ppm.

Full analytical data for tris(trimethylsilyl)silyl cyanide is shown by Ballestri *et al.* [180].

4.2.57 87



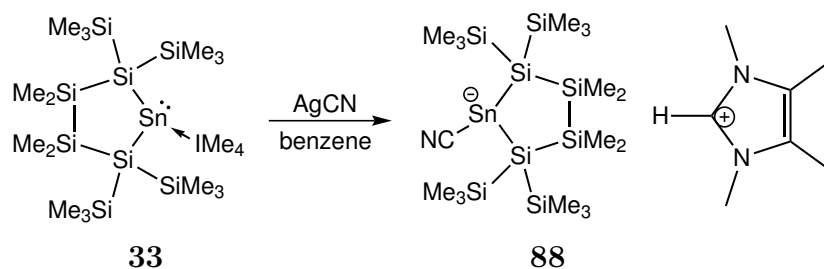
33 (60 mg, 0.083 mmol) and AuCN (18 mg, 0.083 mmol) were stirred in benzene in a vial wrapped with tin foil for light protection for 18 hours. Slow evaporation of benzene give **87** as colorless crystals (32 mg, 25%).

^1H NMR (300 MHz, C_6D_6): δ = 8.89 (s, 1H, NCHN), 3.27 (s, 6H, NMe), 1.21 (s, 6H, CMe), 0.56 (s, 36H, SiMe₃), 0.54 (s, 36H, SiMe₃), 0.29 (s, 12H, SiMe₂) and 0.25 (s, 12H, SiMe₂) ppm.

^{29}Si NMR (59.3 MHz, C_6D_6): δ = -4.4 (SiMe₃), -7.6 (SiMe₃), -19.2 (SiMe₂) and -121.8 (Si_g) ppm.

^{119}Sn NMR (111.8 MHz, C_6D_6): -70.9 ppm.

4.2.58 88



33 (60 mg, 0.083 mmol) and AgCN (11 mg, 0.083 mmol) were stirred in benzene for 18 hours.

$^1\text{H NMR}$ (300 MHz, C_6D_6): $\delta = 3.17$ (s, 6H, *NMe*), 1.38 (s, 6H, *CMe*), 0.62 (s, 18H, *SiMe_3*), 0.55 (s, 6H, *SiMe_2*), 0.46 (s, 6H, *SiMe_2*) and 0.38 (s, 18H, *SiMe_3*) ppm.

$^{29}\text{Si NMR}$ (59.3 MHz, C_6D_6): $\delta = -4.4$ (*SiMe_3*), -7.8 (*SiMe_3*), -18.0 (*SiMe_2*) and -130.3 (*Si_q*) ppm.

Slow evaporation of the solvent gave colorless crystal of **88** (32 mg, 52%).

$^1\text{H NMR}$ (300 MHz, C_6D_6): $\delta = 8.51$ (s, 1H, *NCHN*), 2.99 (s, 6H, *NMe*), 1.15 (s, 6H, *CMe*), 0.67 (s, 6H, *SiMe_2*), 0.64 (s, 18H, *SiMe_3*), 0.58 (s, 6H, *SiMe_2*) and 0.52 (s, 18H, *SiMe_3*) ppm.

$^{29}\text{Si NMR}$ (59.3 MHz, C_6D_6): $\delta = -4.3$ (*SiMe_3*), -7.7 (*SiMe_3*), -14.5 (*SiMe_2*) and -133.6 (*Si_q*) ppm.

Abbreviations

| | |
|--------------------|------------------------------------------------|
| btmsa | Bis(trimethylsilyl)acetylene |
| Bu | Butyl |
| Cp | cyclopentadienyl |
| Cp* | pentamethylcyclopentadienyl |
| Dipp | 2,6-diisopropylphenyl |
| DME | Dimethoxyethane |
| dppe | 1,2-Bis(diphenylphosphino)ethane |
| EPR | Electron paramagnetic resonance |
| Et | Ethyl |
| IMe ₄ | 1,3,4,5-tetramethylimidazol-2-ylidene |
| ^{Me} LiPr | 1,3-diisopropyl-4,5-dimethylimidazol-2-ylidene |
| <i>i</i> -Pr | Isopropyl |
| Me | Methyl |
| Mp | Melting point |
| NHC | N-heterocyclic carbene |
| NMR | Nuclear Magnetic Resonance |
| ppm | parts per milion |
| <i>t</i> -Bu | 1,1-Dimethylethyl |
| <i>t</i> -BuOK | Potassium <i>tert</i> -butoxide |
| TIPS | Triisopropylsilyl |
| THF | Tetrahydrofuran |
| TMS | Trimethylsilyl |

X-ray Crystallographic Tables

Table 52: Bis[tris(trimethylsilyl)silyl]germylene · IMe₄ (**1**)

| | | |
|-----------------------------------|----------------------------------------------------------------------------------|-------------|
| Empirical formula | C ₆₂ H ₁₄₄ Ge ₂ N ₄ Si ₁₆ | |
| Formula weight | 1540.43 | |
| Temperature | 100(2) K | |
| Wavelength | 0.71073 Å | |
| Crystal system, space group | Orthorhombic, Pca2(1) | |
| Unit cell dimensions | a = 31.634(6) Å, | α = 90 deg. |
| | b = 16.787(3) Å, | β = 90 deg. |
| | c = 17.540(4) Å, | γ = 90 deg. |
| Volume | 9314(3) Å ³ | |
| Z, Calculated density | 4, 1.099 Mg/m ³ | |
| Absorption coefficient | 0.885 mm ⁻¹ | |
| F(000) | 3328 | |
| Crystal size | 0.38 × 0.22 × 0.18 mm | |
| Theta range for data collection | 1.29 to 26.37 deg. | |
| Limiting indices | -39 ≤ h ≤ 39, -20 ≤ k ≤ 20, -21 ≤ l ≤ 21 | |
| Reflections collected / unique | 72640 / 18943 [R(int) = 0.0611] | |
| Completeness to θ = 26.37 | 99.9 % | |
| Absorption correction | SADABS | |
| Max. and min. transmission | 0.8570 and 0.7298 | |
| Refinement method | Full-matrix least-squares on F ² | |
| Data / restraints / parameters | 18943 / 1 / 802 | |
| Goodness-of-fit on F ² | 1.097 | |
| Final R indices [I > 2σ(I)] | R1 = 0.0475, wR2 = 0.0983 | |
| R indices (all data) | R1 = 0.0554, wR2 = 0.1012 | |
| Absolute structure parameter | 0.489(6) | |
| Largest diff. peak and hole | 1.024 and -0.296 e.Å ⁻³ | |

Table 53: Bis[tris(trimethylsilyl)silyl]germylene · MeLiPr (14)

| | | |
|-----------------------------------|-------------------------------------------------------------------|---------------------------------------------------|
| Empirical formula | C ₂₉ H ₇₄ Ge N ₂ Si ₈ | |
| Formula weight | 748.21 | |
| Temperature | 273(2) K | |
| Wavelength | 0.71073 Å | |
| Crystal system, space group | monoclinic, P2(1)/n | |
| Unit cell dimensions | a = 12.106(3) Å, b = 23.293(5) Å, c = 16.666(4) Å, | α = 90 deg. β = 103.081(4) deg. γ = 90 deg. |
| Volume | 4577.9(18) Å ³ | |
| Z, Calculated density | 4, 1.086 Mg/m ³ | |
| Absorption coefficient | 0.898 mm ⁻¹ | |
| F(000) | 1624 | |
| Crystal size | 0.33 × 0.22 × 0.15 mm | |
| Theta range for data collection | 1.53 to 26.37 deg. | |
| Limiting indices | -15 ≤ h ≤ 15, -29 ≤ k ≤ 28, -20 ≤ l ≤ 20 | |
| Reflections collected / unique | 36156 / 9341 [R(int) = 0.0533] | |
| Completeness to θ = 26.37 | 99.8 % | |
| Absorption correction | SADABS | |
| Max. and min. transmission | 0.8771 and 0.7559 | |
| Refinement method | Full-matrix least-squares on F ² | |
| Data / restraints / parameters | 9341 / 0 / 385 | |
| Goodness-of-fit on F ² | 1.056 | |
| Final R indices [I > 2σ(I)] | R1 = 0.0433, wR2 = 0.1045 | |
| R indices (all data) | R1 = 0.0564, wR2 = 0.1097 | |
| Largest diff. peak and hole | 0.845 and -0.298 e.Å ⁻³ | |

Table 54: Bis[tris(trimethylsilyl)silyl]germylene · 2,6-dimethylphenylisocyanide (**26**)

| | | |
|--------------------------------------|----------------------------------------------------------|----------------------------------------------------------------------------------|
| Empirical formula | C ₂₇ H ₆₃ Ge N Si ₈ | |
| Formula weight | 699.09 | |
| Temperature | 100(2) K | |
| Wavelength | 0.71073 Å | |
| Crystal system, space group | triclinic, P-1 | |
| Unit cell dimensions | a = 11.751(2) Å, b = 12.289(3) Å, c = 15.337(3) Å, | $\alpha = 97.97(3)$ deg. $\beta = 105.95(3)$ deg. $\gamma = 96.71(3)$ deg. |
| Volume | 2080.8(7) Å ³ | |
| Z, Calculated density | 2, 1.116 Mg/m ³ | |
| Absorption coefficient | 0.983 mm ⁻¹ | |
| F(000) | 752 | |
| Crystal size | 0.42 × 0.36 × 0.34 mm | |
| Theta range for data collection | 1.40 to 26.34 deg. | |
| Limiting indices | -14 ≤ h ≤ 14, -15 ≤ k ≤ 15, -19 ≤ l ≤ 19 | |
| Reflections collected / unique | 16696 / 8355 [R(int) = 0.0193] | |
| Completeness to $\theta = 26.34$ | 98.5 % | |
| Absorption correction | SADABS | |
| Max. and min. transmission | 0.7310 and 0.6829 | |
| Refinement method | Full-matrix least-squares on F ² | |
| Data / restraints / parameters | 8355 / 0 / 354 | |
| Goodness-of-fit on F ² | 1.047 | |
| Final R indices [$I > 2\sigma(I)$] | R1 = 0.0278, wR2 = 0.0717 | |
| R indices (all data) | R1 = 0.0301, wR2 = 0.0730 | |
| Largest diff. peak and hole | 0.826 and -0.323 e.Å ⁻³ | |

Table 55: Bis[tris(trimethylsilyl)silyl]germylene · *tert*-butylisocyanide (**27**)

| | | |
|--------------------------------------|----------------------------------------------------------|----------------------------------------------------------------------|
| Empirical formula | C ₂₃ H ₆₃ Ge N Si ₈ | |
| Formula weight | 651.05 | |
| Temperature | 100(2) K | |
| Wavelength | 0.71073 Å | |
| Crystal system, space group | monoclinic, P2(1)/n | |
| Unit cell dimensions | a = 14.362(5) Å, b = 12.627(5) Å, c = 21.716(8) Å, | $\alpha = 90$ deg. $\beta = 91.429(6)$ deg. $\gamma = 90$ deg. |
| Volume | 3937(3) Å ³ | |
| Z, Calculated density | 4, 1.098 Mg/m ³ | |
| Absorption coefficient | 1.035 mm ⁻¹ | |
| F(000) | 1408 | |
| Crystal size | 0.24 × 0.14 × 0.08 mm | |
| Theta range for data collection | 1.68 to 26.38 deg. | |
| Limiting indices | -17 ≤ h ≤ 17, -15 ≤ k ≤ 15, -27 ≤ l ≤ 27 | |
| Reflections collected / unique | 30327 / 8014 [R(int) = 0.0782] | |
| Completeness to $\theta = 26.38$ | 99.4 % | |
| Absorption correction | SADABS | |
| Max. and min. transmission | 0.9218 and 0.7893 | |
| Refinement method | Full-matrix least-squares on F ² | |
| Data / restraints / parameters | 8014 / 0 / 319 | |
| Goodness-of-fit on F ² | 1.028 | |
| Final R indices [$I > 2\sigma(I)$] | R1 = 0.0519, wR2 = 0.1212 | |
| R indices (all data) | R1 = 0.0654, wR2 = 0.1288 | |
| Largest diff. peak and hole | 1.730 and -0.833 e.Å ⁻³ | |

Table 56: Cyanobis[tris(trimethylsilyl)silyl]germane (**28**)

| | | |
|-----------------------------------|------------------------------------------------------------------|---------------------------------------------------|
| Empirical formula | C ₁₉ H ₅₅ GeN ₂ Si ₈ | |
| Formula weight | 594.95 | |
| Temperature | 100(2) K | |
| Wavelength | 0.71073 Å | |
| Crystal system, space group | monoclinic, P2(1) | |
| Unit cell dimensions | a = 9.616(2) Å, b = 31.089(7) Å, c = 12.743(3) Å, | α = 90 deg. β = 109.962(4) deg. γ = 90 deg. |
| Volume | 3580.7(15) Å ³ | |
| Z, Calculated density | 4, 1.104 Mg/m ³ | |
| Absorption coefficient | 1.132 mm ⁻¹ | |
| F(000) | 1280 | |
| Crystal size | 0.44 × 0.26 × 0.10 mm | |
| Theta range for data collection | 1.70 to 26.36 deg. | |
| Limiting indices | -12 ≤ h ≤ 11, -38 ≤ k ≤ 38, -15 ≤ l ≤ 15 | |
| Reflections collected / unique | 28432 / 14325 [R(int) = 0.0591] | |
| Completeness to θ = 26.36 | 99.9 % | |
| Absorption correction | SADABS | |
| Max. and min. transmission | 0.8952 and 0.6358 | |
| Refinement method | Full-matrix least-squares on F ² | |
| Data / restraints / parameters | 14325 / 3 / 566 | |
| Goodness-of-fit on F ² | 1.072 | |
| Final R indices [I > 2σ(I)] | R1 = 0.0675, wR2 = 0.1375 | |
| R indices (all data) | R1 = 0.0763, wR2 = 0.1416 | |
| Absolute structure parameter | 0.040(9) | |
| Largest diff. peak and hole | 2.835 and -1.210 e.Å ⁻³ | |

Table 57: Tris(trimethylsilyl)silylcyanide (**29**)

| | | |
|-----------------------------------|----------------------------------------------------------------|-------------------------------------------|
| Empirical formula | C ₁₀ H ₂₇ N Si ₄ | |
| Formula weight | 273.69 | |
| Temperature | 100(2) K | |
| Wavelength | 0.71073 Å | |
| Crystal system, space group | cubic, Pa-3 | |
| Unit cell dimensions | a = 15.4642(17) Å, b = 15.4642(17) Å, c = 15.4642(17) Å, | α = 90 deg. β = 90 deg. γ = 90 deg. |
| Volume | 3698.1(7) Å ³ | |
| Z, Calculated density | 8, 0.983 Mg/m ³ | |
| Absorption coefficient | 0.301 mm ⁻¹ | |
| F(000) | 1200 | |
| Crystal size | 0.30 × 0.26 × 0.24 mm | |
| Theta range for data collection | 2.28 to 26.35 deg. | |
| Limiting indices | -19 ≤ h ≤ 19, -19 ≤ k ≤ 19, -19 ≤ l ≤ 19 | |
| Reflections collected / unique | 27855 / 1265 [R(int) = 0.0298] | |
| Completeness to θ = 26.35 | 100.0 % | |
| Absorption correction | SADABS | |
| Max. and min. transmission | 0.9313 and 0.9151 | |
| Refinement method | Full-matrix least-squares on F ² | |
| Data / restraints / parameters | 1265 / 0 / 49 | |
| Goodness-of-fit on F ² | 1.181 | |
| Final R indices [I > 2σ(I)] | R1 = 0.0324, wR2 = 0.0817 | |
| R indices (all data) | R1 = 0.0329, wR2 = 0.0823 | |
| Largest diff. peak and hole | 0.330 and -0.112 e.Å ⁻³ | |

Table 58: 1-Germa-2,2,5,5-tetrakis(trimethylsilyl)-3,3,4,4-tetramethylcyclopentasilan-1-ylidene · PMe₃ (**30**)

| | | |
|-----------------------------------|----------------------------------------------------------|-------------------------------------------------|
| Empirical formula | C ₁₉ H ₅₇ Ge P Si ₈ | |
| Formula weight | 613.93 | |
| Temperature | 100(2) K | |
| Wavelength | 0.71073 Å | |
| Crystal system, space group | monoclinic, C2/c | |
| Unit cell dimensions | a = 15.514(3) Å, b = 21.002(4) Å, c = 22.116(4) Å, | α = 90 deg. β = 91.23(3) deg. γ = 90 deg. |
| Volume | 7204(2) Å ³ | |
| Z, Calculated density | 8, 1.132 Mg/m ³ | |
| Absorption coefficient | 1.169 mm ⁻¹ | |
| F(000) | 2640 | |
| Crystal size | 0.28 × 0.22 × 0.18 mm | |
| Theta range for data collection | 1.63 to 26.36 deg. | |
| Limiting indices | -19 ≤ h ≤ 19, -26 ≤ k ≤ 26, -27 ≤ l ≤ 27 | |
| Reflections collected / unique | 28394 / 7346 [R(int) = 0.0232] | |
| Completeness to θ = 26.36 | 99.8 % | |
| Absorption correction | SADABS | |
| Max. and min. transmission | 0.8172 and 0.7356 | |
| Refinement method | Full-matrix least-squares on F ² | |
| Data / restraints / parameters | 7346 / 0 / 281 | |
| Goodness-of-fit on F ² | 1.047 | |
| Final R indices [I > 2σ(I)] | R1 = 0.0220, wR2 = 0.0581 | |
| R indices (all data) | R1 = 0.0235, wR2 = 0.0588 | |
| Largest diff. peak and hole | 1.000 and -0.194 e.Å ⁻³ | |

Table 59: 1-Stanna-2,2,4,4-tetrakis(trimethylsilyl)-3,3-dimethylcyclobutasilan-1-ylidene · MeIiPr (**31**)

| | | |
|-----------------------------------|-----------------------------------------------------------------------------------|--------------------------------------------------|
| Empirical formula | C ₁₀₀ H ₂₄₈ N ₈ Si ₂₈ Sn ₄ | |
| Formula weight | 2824.34 | |
| Temperature | 100(2) K | |
| Wavelength | 0.71073 Å | |
| Crystal system, space group | monoclinic, P2(1)/c | |
| Unit cell dimensions | a = 10.002(2) Å, b = 22.662(4) Å, c = 18.148(4) Å, | α = 90 deg. β = 103.67(3) deg. γ = 90 deg. |
| Volume | 3997.0(14) Å ³ | |
| Z, Calculated density | 1, 1.173 Mg/m ³ | |
| Absorption coefficient | 0.865 mm ⁻¹ | |
| F(000) | 1496 | |
| Crystal size | 0.28 × 0.18 × 0.10 mm | |
| Theta range for data collection | 1.46 to 25.00 deg. | |
| Limiting indices | -11 ≤ h ≤ 11, -26 ≤ k ≤ 26, -21 ≤ l ≤ 21 | |
| Reflections collected / unique | 28161 / 7024 [R(int) = 0.1529] | |
| Completeness to θ = 25.00 | 99.9 % | |
| Absorption correction | SADABS | |
| Max. and min. transmission | 0.9185 and 0.7937 | |
| Refinement method | Full-matrix least-squares on F ² | |
| Data / restraints / parameters | 7024 / 60 / 416 | |
| Goodness-of-fit on F ² | 1.341 | |
| Final R indices [I > 2σ(I)] | R1 = 0.1294, wR2 = 0.2581 | |
| R indices (all data) | R1 = 0.1348, wR2 = 0.2611 | |
| Largest diff. peak and hole | 1.329 and -3.527 e.Å ⁻³ | |

Table 60: 1,5-Distanna-2,2,4,4,6,6,8,8-octakis(trimethylsilyl)bicyclo[3.3.0]hexasilaoct-1,5-ene (**32**)

| | | |
|-----------------------------------|----------------------------------------------------------|--------------------------------------------------|
| Empirical formula | C ₁₄ H ₄₂ Si ₇ Sn | |
| Formula weight | 525.80 | |
| Temperature | 100(2) K | |
| Wavelength | 0.71073 Å | |
| Crystal system, space group | monoclinic, P2(1)/n | |
| Unit cell dimensions | a = 13.155(3) Å, b = 12.804(3) Å, c = 17.581(4) Å, | α = 90 deg. β = 107.48(3) deg. γ = 90 deg. |
| Volume | 2824.5(10) Å ³ | |
| Z, Calculated density | 4, 1.236 Mg/m ³ | |
| Absorption coefficient | 1.199 mm ⁻¹ | |
| F(000) | 1096 | |
| Crystal size | 0.30 × 0.26 × 0.12 mm | |
| Theta range for data collection | 1.71 to 25.50 deg. | |
| Limiting indices | -15 ≤ h ≤ 15, -15 ≤ k ≤ 15, -21 ≤ l ≤ 21 | |
| Reflections collected / unique | 20788 / 5256 [R(int) = 0.0333] | |
| Completeness to θ = 25.50 | 99.9 % | |
| Absorption correction | SADABS | |
| Max. and min. transmission | 0.8695 and 0.7149 | |
| Refinement method | Full-matrix least-squares on F ² | |
| Data / restraints / parameters | 5256 / 0 / 232 | |
| Goodness-of-fit on F ² | 1.051 | |
| Final R indices [I > 2σ(I)] | R1 = 0.0989, wR2 = 0.2272 | |
| R indices (all data) | R1 = 0.1038, wR2 = 0.2309 | |
| Largest diff. peak and hole | 7.519 and -1.813 e.Å ⁻³ | |

Table 61: 1-Stanna-2,2,5,5-tetrakis(trimethylsilyl)-3,3,4,4-tetramethylcyclopentasilan-1-ylidene · IMe₄ (**33**)

| | | |
|-----------------------------------|-------------------------------------------------------------------|--------------------------------------------------|
| Empirical formula | C ₂₃ H ₆₀ N ₂ Si ₈ Sn | |
| Formula weight | 708.14 | |
| Temperature | 100(2) K | |
| Wavelength | 0.71073 Å | |
| Crystal system, space group | monoclinic, P2(1)/c | |
| Unit cell dimensions | a = 11.510(2) Å, b = 20.716(4) Å, c = 17.019(3) Å, | α = 90 deg. β = 106.55(3) deg. γ = 90 deg. |
| Volume | 3889.9(13) Å ³ | |
| Z, Calculated density | 4, 1.209 Mg/m ³ | |
| Absorption coefficient | 0.918 mm ⁻¹ | |
| F(000) | 1496 | |
| Crystal size | 0.26 × 0.22 × 0.12 mm | |
| Theta range for data collection | 1.59 to 26.36 deg. | |
| Limiting indices | -14 ≤ h ≤ 10, -24 ≤ k ≤ 25, -21 ≤ l ≤ 21 | |
| Reflections collected / unique | 24434 / 7892 [R(int) = 0.0426] | |
| Completeness to θ = 26.36 | 99.3 % | |
| Absorption correction | SADABS | |
| Max. and min. transmission | 0.8978 and 0.7962 | |
| Refinement method | Full-matrix least-squares on F ² | |
| Data / restraints / parameters | 7892 / 0 / 327 | |
| Goodness-of-fit on F ² | 0.945 | |
| Final R indices [I > 2σ(I)] | R1 = 0.0339, wR2 = 0.0745 | |
| R indices (all data) | R1 = 0.0453, wR2 = 0.0777 | |
| Largest diff. peak and hole | 0.858 and -0.414 e.Å ⁻³ | |

Table 62: Bis[tris(trimethylsilyl)silyl]stannylene · IMe₄ (**34**)

| | | |
|-----------------------------------|-------------------------------------------------------------------|-------------------------------------------------|
| Empirical formula | C ₂₅ H ₆₆ N ₂ Si ₈ Sn | |
| Formula weight | 738.21 | |
| Temperature | 100(2) K | |
| Wavelength | 0.71073 Å | |
| Crystal system, space group | monoclinic, P2(1)/n | |
| Unit cell dimensions | a = 15.945(3) Å, b = 17.060(3) Å, c = 17.474(4) Å, | α = 90 deg. β = 91.23(3) deg. γ = 90 deg. |
| Volume | 4752.2(16) Å ³ | |
| Z, Calculated density | 4, 1.032 Mg/m ³ | |
| Absorption coefficient | 0.754 mm ⁻¹ | |
| F(000) | 1568 | |
| Crystal size | 0.42 × 0.24 × 0.17 mm | |
| Theta range for data collection | 1.67 to 26.37 deg. | |
| Limiting indices | -19 ≤ h ≤ 19, -21 ≤ k ≤ 21, -21 ≤ l ≤ 21 | |
| Reflections collected / unique | 37316 / 9675 [R(int) = 0.0468] | |
| Completeness to θ = 26.37 | 99.6 % | |
| Absorption correction | SADABS | |
| Max. and min. transmission | 0.8825 and 0.7424 | |
| Refinement method | Full-matrix least-squares on F ² | |
| Data / restraints / parameters | 9675 / 0 / 347 | |
| Goodness-of-fit on F ² | 1.199 | |
| Final R indices [I > 2σ(I)] | R1 = 0.0502, wR2 = 0.1148 | |
| R indices (all data) | R1 = 0.0552, wR2 = 0.1173 | |
| Largest diff. peak and hole | 1.568 and -0.980 e.Å ⁻³ | |

Table 63: Bis[tris(trimethylsilyl)silyl]stannylene · PMe₃ (**35**)

| | | |
|-----------------------------------|----------------------------------------------------------|---------------------------------------------------|
| Empirical formula | C ₂₁ H ₆₃ P Si ₈ Sn | |
| Formula weight | 690.09 | |
| Temperature | 100(2) K | |
| Wavelength | 0.71073 Å | |
| Crystal system, space group | monoclinic, P2(1) | |
| Unit cell dimensions | a = 13.866(4) Å, b = 10.336(3) Å, c = 15.127(4) Å, | α = 90 deg. β = 112.467(4) deg. γ = 90 deg. |
| Volume | 2003.5(10) Å ³ | |
| Z, Calculated density | 2, 1.144 Mg/m ³ | |
| Absorption coefficient | 0.923 mm ⁻¹ | |
| F(000) | 732 | |
| Crystal size | 0.44 × 0.22 × 0.12 mm | |
| Theta range for data collection | 1.59 to 26.37 deg. | |
| Limiting indices | -17 ≤ h ≤ 17, -12 ≤ k ≤ 12, -18 ≤ l ≤ 18 | |
| Reflections collected / unique | 15834 / 8003 [R(int) = 0.0295] | |
| Completeness to θ = 26.37 | 99.4 % | |
| Absorption correction | SADABS | |
| Max. and min. transmission | 0.8963 and 0.6860 | |
| Refinement method | Full-matrix least-squares on F ² | |
| Data / restraints / parameters | 8003 / 11 / 404 | |
| Goodness-of-fit on F ² | 1.067 | |
| Final R indices [I > 2σ(I)] | R1 = 0.0568, wR2 = 0.1506 | |
| R indices (all data) | R1 = 0.0568, wR2 = 0.1506 | |
| Absolute structure parameter | 0.92(3) | |
| Largest diff. peak and hole | 2.798 and -0.540 e.Å ⁻³ | |

Table 64: 1,1-Bis[tris(trimethylsilyl)silyl]-2,3-diphenyl-1-germacyclopropene (**36**)

| | | |
|-----------------------------------|----------------------------------------------------------|--------------------------------------------------|
| Empirical formula | C ₃₂ H ₆₄ Ge Si ₈ | |
| Formula weight | 746.14 | |
| Temperature | 100(2) K | |
| Wavelength | 0.71073 Å | |
| Crystal system, space group | monoclinic, P2(1)/c | |
| Unit cell dimensions | a = 13.326(3) Å, b = 18.718(4) Å, c = 18.391(4) Å, | α = 90 deg. β = 102.16(3) deg. γ = 90 deg. |
| Volume | 4484.4(16) Å ³ | |
| Z, Calculated density | 4, 1.105 Mg/m ³ | |
| Absorption coefficient | 0.916 mm ⁻¹ | |
| F(000) | 1600 | |
| Crystal size | 0.30 × 0.18 × 0.12 mm | |
| Theta range for data collection | 1.56 to 26.36 deg. | |
| Limiting indices | -16 ≤ h ≤ 16, -23 ≤ k ≤ 23, -22 ≤ l ≤ 22 | |
| Reflections collected / unique | 35111 / 9152 [R(int) = 0.0444] | |
| Completeness to θ = 26.36 | 99.8 % | |
| Absorption correction | SADABS | |
| Max. and min. transmission | 0.8980 and 0.7707 | |
| Refinement method | Full-matrix least-squares on F ² | |
| Data / restraints / parameters | 9152 / 0 / 388 | |
| Goodness-of-fit on F ² | 1.037 | |
| Final R indices [I > 2σ(I)] | R1 = 0.0337, wR2 = 0.0786 | |
| R indices (all data) | R1 = 0.0426, wR2 = 0.0818 | |
| Largest diff. peak and hole | 0.669 and -0.243 e.Å ⁻³ | |

Table 65: [Z-1-Phenyl-2-(tris(trimethylsilyl)silyl)vinyl]tris(trimethylsilyl)silyl]germylene · PMe₃ (**37**)

| | | |
|-----------------------------------|------------------------------------------------------|-------------|
| Empirical formula | C ₂₉ H ₆₉ Ge P Si ₈ | |
| Formula weight | 746.12 | |
| Temperature | 100(2) K | |
| Wavelength | 0.71073 Å | |
| Crystal system, space group | orthorhombic, Pbca | |
| Unit cell dimensions | a = 25.174(5) Å, | α = 90 deg. |
| | b = 14.054(3) Å, | β = 90 deg. |
| | c = 25.198(5) Å, | γ = 90 deg. |
| Volume | 8915(3) Å ³ | |
| Z, Calculated density | 8, 1.112 Mg/m ³ | |
| Absorption coefficient | 0.955 mm ⁻¹ | |
| F(000) | 3216 | |
| Crystal size | 0.36 × 0.24 × 0.08 mm | |
| Theta range for data collection | 1.62 to 26.35 deg. | |
| Limiting indices | -30 ≤ h ≤ 31, -17 ≤ k ≤ 17, -31 ≤ l ≤ 31 | |
| Reflections collected / unique | 65992 / 9077 [R(int) = 0.0472] | |
| Completeness to θ = 26.35 | 99.8 % | |
| Absorption correction | SADABS | |
| Max. and min. transmission | 0.9275 and 0.7248 | |
| Refinement method | Full-matrix least-squares on F ² | |
| Data / restraints / parameters | 9077 / 0 / 373 | |
| Goodness-of-fit on F ² | 1.068 | |
| Final R indices [I > 2σ(I)] | R1 = 0.0395, wR2 = 0.0965 | |
| R indices (all data) | R1 = 0.0483, wR2 = 0.1004 | |
| Largest diff. peak and hole | 1.632 and -0.283 e.Å ⁻³ | |

Table 66: Bis[*Z*-1-phenyl-2-(tris(trimethylsilyl)silyl)vinyl]germylene · PMe₃ (**38**)

| | | |
|----------------------------------------------|---------------------------------------------------------|---------------------------------------------------------------|
| Empirical formula | C ₃₇ H ₇₅ Ge P Si ₈ | |
| Formula weight | 848.25 | |
| Temperature | 100(2) K | |
| Wavelength | 0.71073 Å | |
| Crystal system, space group | Triclinic, P-1 | |
| Unit cell dimensions | a = 9.809(2) Å, b = 14.698(3) Å, c = 20.257(4) Å, | α = 105.37(3) deg. β = 97.24(3) deg. γ = 109.32(3) deg. |
| Volume | 2583.3(9) Å ³ | |
| Z, Calculated density | 2, 1.090 Mg/m ³ | |
| Absorption coefficient | 0.832 mm ⁻¹ | |
| F(000) | 912 | |
| Crystal size | 0.45 × 0.34 × 0.24 mm | |
| Theta range for data collection | 1.55 to 26.37 deg. | |
| Limiting indices | -12 ≤ h ≤ 12, -18 ≤ k ≤ 18, -25 ≤ l ≤ 25 | |
| Reflections collected / unique | 20672 / 10411 [R(int) = 0.0281] | |
| Completeness to θ = 26.37 | 98.4 % | |
| Absorption correction | SADABS | |
| Max. and min. transmission | 0.8254 and 0.7060 | |
| Refinement method | Full-matrix least-squares on F ² | |
| Data / restraints / parameters | 10411 / 0 / 445 | |
| Goodness-of-fit on F ² | 1.040 | |
| Final R indices [<i>I</i> > 2σ(<i>I</i>)] | R1 = 0.0383, wR2 = 0.0909 | |
| R indices (all data) | R1 = 0.0455, wR2 = 0.0940 | |
| Largest diff. peak and hole | 0.773 and -0.299 e.Å ⁻³ | |

Table 67: (Z)-1-(2-(tris(trimethylsilyl)silyl)-1-phenylvinyl)-4-phenyl-1,2,2-tris(trimethylsilyl)-1,2-dihydro-1,2-silagermete (**39**)

| | | |
|-----------------------------------|----------------------------------------------------------|--------------------------------------------------|
| Empirical formula | C ₃₄ H ₆₆ GeSi ₈ | |
| Formula weight | 772.18 | |
| Temperature | 100(2) K | |
| Wavelength | 0.71073 Å | |
| Crystal system, space group | monoclinic, P2(1)/n | |
| Unit cell dimensions | a = 13.204(3) Å, b = 19.641(4) Å, c = 18.411(4) Å, | α = 90 deg. β = 109.70(3) deg. γ = 90 deg. |
| Volume | 4495.0(15) Å ³ | |
| Z, Calculated density | 4, 1.141 Mg/m ³ | |
| Absorption coefficient | 0.916 mm ⁻¹ | |
| F(000) | 1656 | |
| Crystal size | 0.40 × 0.22 × 0.14 mm | |
| Theta range for data collection | 1.57 to 26.38 deg. | |
| Limiting indices | -16 ≤ h ≤ 16, -24 ≤ k ≤ 24, -22 ≤ l ≤ 22 | |
| Reflections collected / unique | 34964 / 9187 [R(int) = 0.0434] | |
| Completeness to θ = 26.38 | 99.8 % | |
| Absorption correction | SADABS | |
| Max. and min. transmission | 0.8825 and 0.7108 | |
| Refinement method | Full-matrix least-squares on F ² | |
| Data / restraints / parameters | 9187 / 0 / 406 | |
| Goodness-of-fit on F ² | 1.097 | |
| Final R indices [I > 2σ(I)] | R1 = 0.0434, wR2 = 0.0924 | |
| R indices (all data) | R1 = 0.0517, wR2 = 0.0954 | |
| Largest diff. peak and hole | 0.795 and -0.372 e.Å ⁻³ | |

Table 68: Bis[*Z*-1-Phenyl-2-tris(trimethylsilyl)silylvinyl]germylene · IMe₄ (**40**)

| | | |
|----------------------------------------------|-------------------------------------------------------------------|-------------------------------------------------|
| Empirical formula | C ₄₁ H ₇₈ Ge N ₂ Si ₈ | |
| Formula weight | 896.36 | |
| Temperature | 100(2) K | |
| Wavelength | 0.71073 Å | |
| Crystal system, space group | monoclinic, P2(1)/c | |
| Unit cell dimensions | a = 16.640(3) Å, b = 24.909(5) Å, c = 12.786(3) Å, | α = 90 deg. β = 92.34(3) deg. γ = 90 deg. |
| Volume | 5295.4(18) Å ³ | |
| Z, Calculated density | 4, 1.124 Mg/m ³ | |
| Absorption coefficient | 0.787 mm ⁻¹ | |
| F(000) | 1928 | |
| Crystal size | 0.32 × 0.16 × 0.14 mm | |
| Theta range for data collection | 1.47 to 26.38 deg. | |
| Limiting indices | -20 ≤ h ≤ 20, -31 ≤ k ≤ 31, -15 ≤ l ≤ 15 | |
| Reflections collected / unique | 42092 / 10754 [R(int) = 0.0532] | |
| Completeness to θ = 26.38 | 99.4 % | |
| Absorption correction | SADABS | |
| Max. and min. transmission | 0.8978 and 0.7868 | |
| Refinement method | Full-matrix least-squares on F ² | |
| Data / restraints / parameters | 10754 / 0 / 491 | |
| Goodness-of-fit on F ² | 1.330 | |
| Final R indices [<i>I</i> > 2σ(<i>I</i>)] | R1 = 0.0764, wR2 = 0.1486 | |
| R indices (all data) | R1 = 0.0861, wR2 = 0.1523 | |
| Largest diff. peak and hole | 0.947 and -0.540 e.Å ⁻³ | |

Table 69: 1-[Tris(trimethylsilyl)silyl]-4-phenyl-1,2,2-tris(trimethylsilyl)-1,2-dihydro-1,2-silagermete (**41**)

| | | |
|-----------------------------------|-----------------------------------------------------------|-------------------------------------------------|
| Empirical formula | C ₂₆ H ₆₀ Ge Si ₈ | |
| Formula weight | 670.05 | |
| Temperature | 150(2) K | |
| Wavelength | 0.71073 Å | |
| Crystal system, space group | monoclinic, P2(1)/n | |
| Unit cell dimensions | a = 9.6420(19) Å, b = 18.886(4) Å, c = 22.043(4) Å, | α = 90 deg. β = 98.58(3) deg. γ = 90 deg. |
| Volume | 3969.1(14) Å ³ | |
| Z, Calculated density | 4, 1.121 Mg/m ³ | |
| Absorption coefficient | 1.028 mm ⁻¹ | |
| F(000) | 1440 | |
| Crystal size | 0.38 × 0.32 × 0.12 mm | |
| Theta range for data collection | 1.87 to 26.34 deg. | |
| Limiting indices | -12 ≤ h ≤ 12, -23 ≤ k ≤ 23, -27 ≤ l ≤ 27 | |
| Reflections collected / unique | 31171 / 8067 [R(int) = 0.0267] | |
| Completeness to θ = 26.34 | 99.8 % | |
| Absorption correction | SADABS | |
| Max. and min. transmission | 0.8866 and 0.6961 | |
| Refinement method | Full-matrix least-squares on F ² | |
| Data / restraints / parameters | 8067 / 0 / 334 | |
| Goodness-of-fit on F ² | 1.059 | |
| Final R indices [I > 2σ(I)] | R1 = 0.0286, wR2 = 0.0740 | |
| R indices (all data) | R1 = 0.0334, wR2 = 0.0764 | |
| Largest diff. peak and hole | 0.462 and -0.224 e.Å ⁻³ | |

Table 70: [Z-1-phenyl-2-tris(trimethylsilyl)silylvinyl]tris(trimethylsilyl)silylgermylene · IMe₄ (**42**)

| | | |
|-----------------------------------|-------------------------------------------------------------------|-------------------------------------------------|
| Empirical formula | C ₃₃ H ₇₂ Ge N ₂ Si ₈ | |
| Formula weight | 794.24 | |
| Temperature | 100(2) K | |
| Wavelength | 0.71073 Å | |
| Crystal system, space group | monoclinic, P2(1)/c | |
| Unit cell dimensions | a = 14.884(3) Å, b = 13.825(3) Å, c = 23.059(5) Å, | α = 90 deg. β = 96.53(3) deg. γ = 90 deg. |
| Volume | 4714.0(16) Å ³ | |
| Z, Calculated density | 4, 1.119 Mg/m ³ | |
| Absorption coefficient | 0.876 mm ⁻¹ | |
| F(000) | 1712 | |
| Crystal size | 0.27 × 0.18 × 0.12 mm | |
| Theta range for data collection | 1.55 to 26.38 deg. | |
| Limiting indices | -18 ≤ h ≤ 18, -17 ≤ k ≤ 17, -28 ≤ l ≤ 28 | |
| Reflections collected / unique | 37115 / 9634 [R(int) = 0.0701] | |
| Completeness to θ = 26.38 | 99.8 % | |
| Absorption correction | SADABS | |
| Max. and min. transmission | 0.9022 and 0.7979 | |
| Refinement method | Full-matrix least-squares on F ² | |
| Data / restraints / parameters | 9634 / 0 / 419 | |
| Goodness-of-fit on F ² | 1.047 | |
| Final R indices [I > 2σ(I)] | R1 = 0.0499, wR2 = 0.0995 | |
| R indices (all data) | R1 = 0.0685, wR2 = 0.1063 | |
| Largest diff. peak and hole | 0.618 and -0.325 e.Å ⁻³ | |

Table 71: [Z-1-Trimethylsilyl-2-(tris(trimethylsilyl)silyl)vinyl]tris(trimethylsilyl)silyl]germylene · IMe₄ (**44**)

| | | |
|-----------------------------------|-------------------------------------------------------------------|-------------|
| Empirical formula | C ₃₆ H ₈₂ Ge N ₂ Si ₉ | |
| Formula weight | 868.44 | |
| Temperature | 100(2) K | |
| Wavelength | 0.71073 Å | |
| Crystal system, space group | orthorhombic, P2(1)2(1)2(1) | |
| Unit cell dimensions | a = 9.2796(16) Å, | α = 90 deg. |
| | b = 10.6259(18) Å, | β = 90 deg. |
| | c = 51.214(9) Å, | γ = 90 deg. |
| Volume | 5049.9(15) Å ³ | |
| Z, Calculated density | 4, 1.142 Mg/m ³ | |
| Absorption coefficient | 0.846 mm ⁻¹ | |
| F(000) | 1880 | |
| Crystal size | 0.39 × 0.15 × 0.09 mm | |
| Theta range for data collection | 1.59 to 26.37 deg. | |
| Limiting indices | -11 ≤ h ≤ 11, -13 ≤ k ≤ 13, -63 ≤ l ≤ 63 | |
| Reflections collected / unique | 40615 / 10339 [R(int) = 0.0676] | |
| Completeness to θ = 26.37 | 99.9 % | |
| Absorption correction | SADABS | |
| Max. and min. transmission | 0.9278 and 0.7339 | |
| Refinement method | Full-matrix least-squares on F ² | |
| Data / restraints / parameters | 10339 / 0 / 459 | |
| Goodness-of-fit on F ² | 1.061 | |
| Final R indices [I > 2σ(I)] | R1 = 0.0439, wR2 = 0.0830 | |
| R indices (all data) | R1 = 0.0502, wR2 = 0.0848 | |
| Absolute structure parameter | 0.022(7) | |
| Largest diff. peak and hole | 0.679 and -0.407 e.Å ⁻³ | |

Table 72: [Z-1-Butyl-2-(tris(trimethylsilyl)silyl)vinyl]tris(trimethylsilyl)silylgermylene · PMe₃ (**48**)

| | | |
|-----------------------------------|------------------------------------------------------|-------------|
| Empirical formula | C ₂₇ H ₇₃ Ge P Si ₈ | |
| Formula weight | 726.13 | |
| Temperature | 100(2) K | |
| Wavelength | 0.71073 Å | |
| Crystal system, space group | orthorhombic, P2(1)2(1)2(1) | |
| Unit cell dimensions | a = 13.114(3) Å, | α = 90 deg. |
| | b = 18.322(4) Å, | β = 90 deg. |
| | c = 18.756(4) Å, | γ = 90 deg. |
| Volume | 4506.5(15) Å ³ | |
| Z, Calculated density | 4, 1.070 Mg/m ³ | |
| Absorption coefficient | 0.943 mm ⁻¹ | |
| F(000) | 1576 | |
| Crystal size | 0.37 × 0.31 × 0.20 mm | |
| Theta range for data collection | 1.55 to 26.28 deg. | |
| Limiting indices | -16 ≤ h ≤ 16, -22 ≤ k ≤ 22, -23 ≤ l ≤ 23 | |
| Reflections collected / unique | 35453 / 9047 [R(int) = 0.0672] | |
| Completeness to θ = 26.28 | 99.6 % | |
| Absorption correction | SADABS | |
| Max. and min. transmission | 0.8338 and 0.7217 | |
| Refinement method | Full-matrix least-squares on F ² | |
| Data / restraints / parameters | 9047 / 0 / 357 | |
| Goodness-of-fit on F ² | 1.003 | |
| Final R indices [I > 2σ(I)] | R1 = 0.0488, wR2 = 0.0943 | |
| R indices (all data) | R1 = 0.0612, wR2 = 0.0981 | |
| Absolute structure parameter | 0.032(9) | |
| Largest diff. peak and hole | 0.841 and -0.396 e.Å ⁻³ | |

Table 73: 5-Germa-1,3,3,6,8,8-hexakis(trimethylsilyl)-4,4,9,9-tetramethylspiro[4.4]-3,4,7,8-tetrasilanon-1,6-diene (**51**)

| | | |
|-----------------------------------|----------------------------------------------------------|-------------------------------------------|
| Empirical formula | C ₂₆ H ₆₈ Ge Si ₁₀ | |
| Formula weight | 734.29 | |
| Temperature | 100(2) K | |
| Wavelength | 0.71073 Å | |
| Crystal system, space group | orthorhombic, Fddd | |
| Unit cell dimensions | a = 18.093(4) Å, b = 30.534(6) Å, c = 32.837(7) Å, | α = 90 deg. β = 90 deg. γ = 90 deg. |
| Volume | 18141(6) Å ³ | |
| Z, Calculated density | 16, 1.075 Mg/m ³ | |
| Absorption coefficient | 0.954 mm ⁻¹ | |
| F(000) | 6336 | |
| Crystal size | 0.52 × 0.40 × 0.40 mm | |
| Theta range for data collection | 1.82 to 26.37 deg. | |
| Limiting indices | -22 ≤ h ≤ 22, -38 ≤ k ≤ 38, -40 ≤ l ≤ 40 | |
| Reflections collected / unique | 35050 / 4631 [R(int) = 0.0229] | |
| Completeness to θ = 26.37 | 99.7 % | |
| Absorption correction | SADABS | |
| Max. and min. transmission | 0.7014 and 0.6367 | |
| Refinement method | Full-matrix least-squares on F ² | |
| Data / restraints / parameters | 4631 / 0 / 179 | |
| Goodness-of-fit on F ² | 1.078 | |
| Final R indices [I > 2σ(I)] | R1 = 0.0220, wR2 = 0.0597 | |
| R indices (all data) | R1 = 0.0230, wR2 = 0.0602 | |
| Largest diff. peak and hole | 0.492 and -0.201 e.Å ⁻³ | |

Table 74: 4-germa-3,3,6,6-tetrakis(trimethylsilyl)-8,9-dimethyl-1,5-diphenylspiro[3.5]-3,7,8,9-tetrasilanon-1,5-diene (**53**)

| | | |
|-----------------------------------|-----------------------------------------------------------|-------------------------------------------------|
| Empirical formula | C ₃₂ H ₆₀ GeSi ₈ | |
| Formula weight | 742.11 | |
| Temperature | 100(2) K | |
| Wavelength | 0.71073 Å | |
| Crystal system, space group | monoclinic, P2(1)/n | |
| Unit cell dimensions | a = 9.7118(19) Å, b = 27.874(6) Å, c = 16.028(3) Å, | α = 90 deg. β = 98.49(3) deg. γ = 90 deg. |
| Volume | 4291.5(15) Å ³ | |
| Z, Calculated density | 4, 1.149 Mg/m ³ | |
| Absorption coefficient | 0.957 mm ⁻¹ | |
| F(000) | 1584 | |
| Crystal size | 0.30 × 0.15 × 0.10 mm | |
| Theta range for data collection | 1.46 to 26.37 deg. | |
| Limiting indices | -12 ≤ h ≤ 12, -34 ≤ k ≤ 34, -20 ≤ l ≤ 20 | |
| Reflections collected / unique | 34044 / 8740 [R(int) = 0.0543] | |
| Completeness to θ = 26.37 | 99.8 % | |
| Absorption correction | SADABS | |
| Max. and min. transmission | 0.9104 and 0.7623 | |
| Refinement method | Full-matrix least-squares on F ² | |
| Data / restraints / parameters | 8740 / 0 / 386 | |
| Goodness-of-fit on F ² | 1.394 | |
| Final R indices [I > 2σ(I)] | R1 = 0.0871, wR2 = 0.1525 | |
| R indices (all data) | R1 = 0.0933, wR2 = 0.1548 | |
| Largest diff. peak and hole | 0.798 and -0.766 e.Å ⁻³ | |

Table 75: 3,4,7-Trigermma-3,3,6,6-tetrakis(trimethylsilyl)-8,9-dimethyl-1,5-diphenyl-spiro[3.5]-8,9-disilanon-1,5-diene (**55**)

| | | |
|-----------------------------------|-----------------------------------------------------------------|-------------------------------------------------|
| Empirical formula | C ₃₂ H ₆₀ Ge ₃ Si ₆ | |
| Formula weight | 831.11 | |
| Temperature | 100(2) K | |
| Wavelength | 0.71073 Å | |
| Crystal system, space group | monoclinic, P2(1)/n | |
| Unit cell dimensions | a = 9.7468(19) Å, b = 27.980(6) Å, c = 16.054(3) Å, | α = 90 deg. β = 98.41(3) deg. γ = 90 deg. |
| Volume | 4331.2(15) Å ³ | |
| Z, Calculated density | 4, 1.275 Mg/m ³ | |
| Absorption coefficient | 2.254 mm ⁻¹ | |
| F(000) | 1728 | |
| Crystal size | 0.32 × 0.11 × 0.10 mm | |
| Theta range for data collection | 1.46 to 26.37 deg. | |
| Limiting indices | -12 ≤ h ≤ 12, -34 ≤ k ≤ 34, -20 ≤ l ≤ 20 | |
| Reflections collected / unique | 33865 / 8800 [R(int) = 0.0508] | |
| Completeness to θ = 26.37 | 99.5 % | |
| Absorption correction | SADABS | |
| Max. and min. transmission | 0.8060 and 0.5324 | |
| Refinement method | Full-matrix least-squares on F ² | |
| Data / restraints / parameters | 8800 / 0 / 386 | |
| Goodness-of-fit on F ² | 0.974 | |
| Final R indices [I > 2σ(I)] | R1 = 0.0423, wR2 = 0.0791 | |
| R indices (all data) | R1 = 0.0543, wR2 = 0.0826 | |
| Largest diff. peak and hole | 0.804 and -0.434 e.Å ⁻³ | |

Table 76: 3-Germa-4,4,7,7-tetrakis(trimethylsilyl)-5,5,6,6-tetramethyl-1,2-diphenyl-spiro[2.4]-4,5,6,7-tetrasilhept-1-ene (**56**)

| | | |
|-----------------------------------|----------------------------------------------------------|--------------------------------------------------|
| Empirical formula | C ₃₀ H ₅₈ Ge Si ₈ | |
| Formula weight | 716.07 | |
| Temperature | 200(2) K | |
| Wavelength | 0.71073 Å | |
| Crystal system, space group | monoclinic, C2/c | |
| Unit cell dimensions | a = 13.843(3) Å, b = 17.869(4) Å, c = 17.503(4) Å, | α = 90 deg. β = 101.50(3) deg. γ = 90 deg. |
| Volume | 4242.5(15) Å ³ | |
| Z, Calculated density | 4, 1.121 Mg/m ³ | |
| Absorption coefficient | 0.966 mm ⁻¹ | |
| F(000) | 1528 | |
| Crystal size | 0.36 × 0.26 × 0.20 mm | |
| Theta range for data collection | 1.88 to 26.37 deg. | |
| Limiting indices | -17 ≤ h ≤ 17, -21 ≤ k ≤ 22, -21 ≤ l ≤ 21 | |
| Reflections collected / unique | 14538 / 4326 [R(int) = 0.0618] | |
| Completeness to θ = 26.37 | 99.4 % | |
| Absorption correction | SADABS | |
| Max. and min. transmission | 0.8303 and 0.7225 | |
| Refinement method | Full-matrix least-squares on F ² | |
| Data / restraints / parameters | 4326 / 0 / 185 | |
| Goodness-of-fit on F ² | 0.984 | |
| Final R indices [I > 2σ(I)] | R1 = 0.0439, wR2 = 0.1023 | |
| R indices (all data) | R1 = 0.0557, wR2 = 0.1073 | |
| Largest diff. peak and hole | 0.701 and -0.303 e.Å ⁻³ | |

Table 77: 4-Germa-5,5,6,6-tetrakis(trimethylsilyl)-3,3,5,5-tetramethyl-1,2-diphenyl-spiro[3.3]-3,5,6,7-tetrasilhept-1-ene (**58**)

| | | |
|-----------------------------------|-----------------------------------------------------------|--------------------------------------------------|
| Empirical formula | C ₃₂ H ₅₈ GeSi ₈ | |
| Formula weight | 743.10 | |
| Temperature | 100(2) K | |
| Wavelength | 0.71073 Å | |
| Crystal system, space group | monoclinic, P2(1)/n | |
| Unit cell dimensions | a = 10.786(3) Å, b = 35.733(10) Å, c = 10.841(3) Å, | α = 90 deg. β = 96.252(5) deg. γ = 90 deg. |
| Volume | 4153(2) Å ³ | |
| Z, Calculated density | 4, 1.188 Mg/m ³ | |
| Absorption coefficient | 0.989 mm ⁻¹ | |
| F(000) | 1582 | |
| Crystal size | 0.34 × 0.22 × 0.15 mm | |
| Theta range for data collection | 1.97 to 26.57 deg. | |
| Limiting indices | -13 ≤ h ≤ 13, -44 ≤ k ≤ 44, -13 ≤ l ≤ 13 | |
| Reflections collected / unique | 32831 / 8603 [R(int) = 0.0620] | |
| Completeness to θ = 26.57 | 99.0 % | |
| Absorption correction | SADABS | |
| Max. and min. transmission | 0.8658 and 0.7298 | |
| Refinement method | Full-matrix least-squares on F ² | |
| Data / restraints / parameters | 8603 / 0 / 368 | |
| Goodness-of-fit on F ² | 1.096 | |
| Final R indices [I > 2σ(I)] | R1 = 0.0647, wR2 = 0.1444 | |
| R indices (all data) | R1 = 0.0785, wR2 = 0.1505 | |
| Largest diff. peak and hole | 2.256 and -0.457 e.Å ⁻³ | |

Table 78: 4,5,6-Trigirma-5,5,6,6-tetrakis(trimethylsilyl)-3,3,5,5-tetramethyl-1,2-diphenyl-spiro[3.3]-3,7-disilahept-1-ene (**59**)

| | | |
|-----------------------------------|-----------------------------------------------------------------|--------------------------------------------------|
| Empirical formula | C ₃₀ H ₅₈ Ge ₃ Si ₆ | |
| Formula weight | 805.07 | |
| Temperature | 100(2) K | |
| Wavelength | 0.71073 Å | |
| Crystal system, space group | Monoclinic, P2(1)/n | |
| Unit cell dimensions | a = 10.817(3) Å, b = 35.902(9) Å, c = 10.823(3) Å, | α = 90 deg. β = 96.083(5) deg. γ = 90 deg. |
| Volume | 4179.6(19) Å ³ | |
| Z, Calculated density | 4, 1.279 Mg/m ³ | |
| Absorption coefficient | 2.333 mm ⁻¹ | |
| F(000) | 1672 | |
| Crystal size | 0.22 × 0.08 × 0.04 mm | |
| Theta range for data collection | 1.98 to 26.38 deg. | |
| Limiting indices | -13 ≤ h ≤ 13, -44 ≤ k ≤ 44, -13 ≤ l ≤ 13 | |
| Reflections collected / unique | 33243 / 8542 [R(int) = 0.0948] | |
| Completeness to θ = 26.38 | 99.9 % | |
| Absorption correction | SADABS | |
| Max. and min. transmission | 0.9124 and 0.6278 | |
| Refinement method | Full-matrix least-squares on F ² | |
| Data / restraints / parameters | 8542 / 0 / 368 | |
| Goodness-of-fit on F ² | 1.182 | |
| Final R indices [I > 2σ(I)] | R1 = 0.0894, wR2 = 0.1834 | |
| R indices (all data) | R1 = 0.1116, wR2 = 0.1927 | |
| Largest diff. peak and hole | 2.037 and -0.995 e.Å ⁻³ | |

Table 79: 60

| | | |
|--------------------------------------|----------------------------------------------------------|-------------------------------------------------------------------------------------|
| Empirical formula | C ₂₆ H ₆₆ Ge Si ₁₀ | |
| Formula weight | 732.28 | |
| Temperature | 100(2) K | |
| Wavelength | 0.71073 Å | |
| Crystal system, space group | triclinic, P-1 | |
| Unit cell dimensions | a = 11.239(3) Å, b = 12.700(3) Å, c = 16.768(4) Å, | $\alpha = 95.387(4)$ deg. $\beta = 107.925(4)$ deg. $\gamma = 96.425(4)$ deg. |
| Volume | 2242.0(9) Å ³ | |
| Z, Calculated density | 2, 1.085 Mg/m ³ | |
| Absorption coefficient | 0.965 mm ⁻¹ | |
| F(000) | 788 | |
| Crystal size | 0.32 × 0.14 × 0.09 mm | |
| Theta range for data collection | 1.63 to 26.32 deg. | |
| Limiting indices | -13 ≤ h ≤ 14, -15 ≤ k ≤ 15, -20 ≤ l ≤ 20 | |
| Reflections collected / unique | 15527 / 8748 [R(int) = 0.0339] | |
| Completeness to $\theta = 26.32$ | 96.1 % | |
| Absorption correction | None | |
| Max. and min. transmission | 0.9182 and 0.7476 | |
| Refinement method | Full-matrix least-squares on F ² | |
| Data / restraints / parameters | 8748 / 0 / 356 | |
| Goodness-of-fit on F ² | 1.035 | |
| Final R indices [$I > 2\sigma(I)$] | R1 = 0.0417, wR2 = 0.1024 | |
| R indices (all data) | R1 = 0.0508, wR2 = 0.1063 | |
| Largest diff. peak and hole | 1.180 and -0.355 e.Å ⁻³ | |

Table 80: {Dichloro[tris(trimethylsilyl)silyl]germyl}[tris(trimethylsilyl)silyl]germylene · PMe₃ (**62**)

| | | |
|-----------------------------------|--------------------------------------------------------------------------------------------------|--------------------------------------------------------------|
| Empirical formula | C ₄₂ H ₁₂₆ Cl ₄ Ge ₄ P ₂ Si ₁₆ | |
| Formula weight | 1574.97 | |
| Temperature | 150(2) K | |
| Wavelength | 0.71073 Å | |
| Crystal system, space group | triclinic, P-1 | |
| Unit cell dimensions | a = 14.280(3) Å, b = 15.683(3) Å, c = 19.427(4) Å, | α = 90.32(3) deg. β = 103.57(3) deg. γ = 92.27(3) deg. |
| Volume | 4225.2(15) Å ³ | |
| Z, Calculated density | 2, 1.238 Mg/m ³ | |
| Absorption coefficient | 1.826 mm ⁻¹ | |
| F(000) | 1656 | |
| Crystal size | 0.25 × 0.23 × 0.08 mm | |
| Theta range for data collection | 1.08 to 25.00 deg. | |
| Limiting indices | -16 ≤ h ≤ 16, -18 ≤ k ≤ 18, -23 ≤ l ≤ 23 | |
| Reflections collected / unique | 29917 / 14683 [R(int) = 0.0715] | |
| Completeness to θ = 25.00 | 98.6 % | |
| Absorption correction | SADABS | |
| Max. and min. transmission | 0.8677 and 0.6582 | |
| Refinement method | Full-matrix least-squares on F ² | |
| Data / restraints / parameters | 14683 / 0 / 655 | |
| Goodness-of-fit on F ² | 1.054 | |
| Final R indices [I > 2σ(I)] | R1 = 0.1064, wR2 = 0.2597 | |
| R indices (all data) | R1 = 0.1524, wR2 = 0.2782 | |
| Largest diff. peak and hole | 1.721 and -1.196 e.Å ⁻³ | |

Table 81: Bis{dichloro[tris(trimethylsilyl)silyl]germyl}germylene · PMe₃ (**64**)

| | | |
|-----------------------------------|-----------------------------------------------------------------------------------|-------------------------------------------|
| Empirical formula | C ₂₅ H ₇₄ Cl ₄ Ge ₃ P Si ₈ | |
| Formula weight | 990.35 | |
| Temperature | 100(2) K | |
| Wavelength | 0.71073 Å | |
| Crystal system, space group | Orthorhombic, P2(1)2(1)2(1) | |
| Unit cell dimensions | a = 10.694(2) Å, b = 16.314(3) Å, c = 30.352(6) Å, | α = 90 deg. β = 90 deg. γ = 90 deg. |
| Volume | 5295.2(18) Å ³ | |
| Z, Calculated density | 4, 1.242 Mg/m ³ | |
| Absorption coefficient | 2.121 mm ⁻¹ | |
| F(000) | 2061 | |
| Crystal size | 0.35 × 0.22 × 0.16 mm | |
| Theta range for data collection | 1.34 to 26.39 deg. | |
| Limiting indices | -13 ≤ h ≤ 13, -20 ≤ k ≤ 20, -37 ≤ l ≤ 37 | |
| Reflections collected / unique | 42073 / 10817 [R(int) = 0.0777] | |
| Completeness to θ = 26.39 | 99.8 % | |
| Absorption correction | SADABS | |
| Max. and min. transmission | 0.7278 and 0.5240 | |
| Refinement method | Full-matrix least-squares on F ² | |
| Data / restraints / parameters | 10817 / 0 / 415 | |
| Goodness-of-fit on F ² | 1.022 | |
| Final R indices [I > 2σ(I)] | R1 = 0.0519, wR2 = 0.1090 | |
| R indices (all data) | R1 = 0.0649, wR2 = 0.1135 | |
| Absolute structure parameter | 0.980(10) | |
| Largest diff. peak and hole | 0.983 and -0.412 e.Å ⁻³ | |

Table 82: **65**

| | | |
|--------------------------------------|-----------------------------------------------------------------------------------|----------------------------------------------------------------------|
| Empirical formula | C ₂₂ H ₆₃ Cl ₂ Ge ₂ P Si ₈ | |
| Formula weight | 799.49 | |
| Temperature | 100(2) K | |
| Wavelength | 0.71073 Å | |
| Crystal system, space group | monoclinic, P2(1)/c | |
| Unit cell dimensions | a = 11.649(2) Å, b = 19.428(4) Å, c = 19.098(4) Å, | $\alpha = 90$ deg. $\beta = 102.65(3)$ deg. $\gamma = 90$ deg. |
| Volume | 4217.4(15) Å ³ | |
| Z, Calculated density | 4, 1.259 Mg/m ³ | |
| Absorption coefficient | 1.830 mm ⁻¹ | |
| F(000) | 1680 | |
| Crystal size | 0.38 × 0.14 × 0.12 mm | |
| Theta range for data collection | 1.51 to 26.37 deg. | |
| Limiting indices | -14 ≤ h ≤ 14, -24 ≤ k ≤ 23, -23 ≤ l ≤ 23 | |
| Reflections collected / unique | 33389 / 8608 [R(int) = 0.0572] | |
| Completeness to $\theta = 26.37$ | 99.9 % | |
| Absorption correction | SADABS | |
| Max. and min. transmission | 0.8103 and 0.5430 | |
| Refinement method | Full-matrix least-squares on F ² | |
| Data / restraints / parameters | 8608 / 0 / 335 | |
| Goodness-of-fit on F ² | 1.203 | |
| Final R indices [$I > 2\sigma(I)$] | R1 = 0.0784, wR2 = 0.1678 | |
| R indices (all data) | R1 = 0.0907, wR2 = 0.1737 | |
| Largest diff. peak and hole | 5.372 and -1.136 e.Å ⁻³ | |

Table 83: 2-Chloro-2-tris(trimethylsilyl)silyl-5,5-bis(trimethylsilyl)-3-phenyl-1,2-digerma-5-silacyclopent-3-en-1-ylidene · PMe₃ (**69**)

| | | |
|-----------------------------------|----------------------------------------------------------------------|-------------------------------------------|
| Empirical formula | C ₂₄ H ₆₀ Cl Ge ₂ P Si ₇ | |
| Formula weight | 756.95 | |
| Temperature | 273(2) K | |
| Wavelength | 0.71073 Å | |
| Crystal system, space group | orthorhombic, Pbca | |
| Unit cell dimensions | a = 20.615(5) Å, b = 12.857(3) Å, c = 31.315(7) Å, | α = 90 deg. β = 90 deg. γ = 90 deg. |
| Volume | 8300(3) Å ³ | |
| Z, Calculated density | 8, 1.211 Mg/m ³ | |
| Absorption coefficient | 1.767 mm ⁻¹ | |
| F(000) | 3184 | |
| Crystal size | 0.21 × 0.18 × 0.13 mm | |
| Theta range for data collection | 1.63 to 26.37 deg. | |
| Limiting indices | -25 ≤ h ≤ 25, -16 ≤ k ≤ 16, -39 ≤ l ≤ 36 | |
| Reflections collected / unique | 52700 / 8486 [R(int) = 0.0605] | |
| Completeness to θ = 26.37 | 100.0 % | |
| Absorption correction | SADABS | |
| Max. and min. transmission | 0.8028 and 0.7079 | |
| Refinement method | Full-matrix least-squares on F ² | |
| Data / restraints / parameters | 8486 / 0 / 352 | |
| Goodness-of-fit on F ² | 1.022 | |
| Final R indices [I > 2σ(I)] | R1 = 0.0378, wR2 = 0.0830 | |
| R indices (all data) | R1 = 0.0526, wR2 = 0.0886 | |
| Largest diff. peak and hole | 0.908 and -0.343 e.Å ⁻³ | |

Table 84: **70**

| | | |
|--------------------------------------|------------------------------------------------------------------------------------|------------------------------------------------------------------------|
| Empirical formula | C ₃₁ H ₈₃ Cl ₂ Ge ₂ P Si ₁₀ | |
| Formula weight | 983.92 | |
| Temperature | 100(2) K | |
| Wavelength | 0.71073 Å | |
| Crystal system, space group | monoclinic, P2(1)/c | |
| Unit cell dimensions | a = 12.424(3) Å, b = 27.226(6) Å, c = 18.602(3) Å, | $\alpha = 90$ deg. $\beta = 117.562(12)$ deg. $\gamma = 90$ deg. |
| Volume | 5578(2) Å ³ | |
| Z, Calculated density | 4, 1.172 Mg/m ³ | |
| Absorption coefficient | 1.437 mm ⁻¹ | |
| F(000) | 2088 | |
| Crystal size | 0.22 × 0.08 × 0.06 mm | |
| Theta range for data collection | 1.44 to 26.27 deg. | |
| Limiting indices | -15 ≤ h ≤ 11, -30 ≤ k ≤ 16, -23 ≤ l ≤ 22 | |
| Reflections collected / unique | 14662 / 10308 [R(int) = 0.0903] | |
| Completeness to $\theta = 26.27$ | 91.3 % | |
| Absorption correction | None | |
| Max. and min. transmission | 0.9188 and 0.7428 | |
| Refinement method | Full-matrix least-squares on F ² | |
| Data / restraints / parameters | 10308 / 6 / 473 | |
| Goodness-of-fit on F ² | 0.894 | |
| Final R indices [$I > 2\sigma(I)$] | R1 = 0.0901, wR2 = 0.1409 | |
| R indices (all data) | R1 = 0.1797, wR2 = 0.1671 | |
| Largest diff. peak and hole | 1.176 and -0.559 e.Å ⁻³ | |

Table 85: **71**

| | | |
|-----------------------------------|-----------------------------------------------------------------------------------|-------------|
| Empirical formula | C ₄₅ H ₈₁ Cl ₂ Ge ₂ P Si ₈ | |
| Formula weight | 1093.87 | |
| Temperature | 100(2) K | |
| Wavelength | 0.71073 Å | |
| Crystal system, space group | orthorhombic, Pccn | |
| Unit cell dimensions | a = 26.870(5) Å, | α = 90 deg. |
| | b = 36.690(7) Å, | β = 90 deg. |
| | c = 12.656(3) Å, | γ = 90 deg. |
| Volume | 12477(4) Å ³ | |
| Z, Calculated density | 8, 1.165 Mg/m ³ | |
| Absorption coefficient | 1.255 mm ⁻¹ | |
| F(000) | 4608 | |
| Crystal size | 0.48 × 0.10 × 0.10 mm | |
| Theta range for data collection | 0.94 to 26.37 deg. | |
| Limiting indices | -33 ≤ h ≤ 32, -40 ≤ k ≤ 44, -15 ≤ l ≤ 15 | |
| Reflections collected / unique | 74307 / 12615 [R(int) = 0.0791] | |
| Completeness to θ = 26.37 | 98.9 % | |
| Absorption correction | SADABS | |
| Max. and min. transmission | 0.8848 and 0.5841 | |
| Refinement method | Full-matrix least-squares on F ² | |
| Data / restraints / parameters | 12615 / 0 / 544 | |
| Goodness-of-fit on F ² | 1.043 | |
| Final R indices [I > 2σ(I)] | R1 = 0.0485, wR2 = 0.1086 | |
| R indices (all data) | R1 = 0.0679, wR2 = 0.1157 | |
| Largest diff. peak and hole | 1.955 and -0.580 e.Å ⁻³ | |

Table 86: Germanium dichloride · bis[*Z*-1-phenyl-2-tris(trimethylsilyl)silylvinyl]-germylene · IMe₄ (**72**)

| | | |
|----------------------------------------------|--------------------------------------------------------------------------------------------------|-------------------------------------------------|
| Empirical formula | C ₄₅ H ₈₆ Cl ₂ Ge ₂ N ₂ O Si ₈ | |
| Formula weight | 1111.96 | |
| Temperature | 100(2) K | |
| Wavelength | 0.71073 Å | |
| Crystal system, space group | monoclinic, P2(1)/c | |
| Unit cell dimensions | a = 20.953(4) Å, b = 11.089(2) Å, c = 26.753(5) Å, | α = 90 deg. β = 98.04(3) deg. γ = 90 deg. |
| Volume | 6155(2) Å ³ | |
| Z, Calculated density | 4, 1.200 Mg/m ³ | |
| Absorption coefficient | 1.250 mm ⁻¹ | |
| F(000) | 2352 | |
| Crystal size | 0.34 × 0.22 × 0.17 mm | |
| Theta range for data collection | 1.54 to 26.36 deg. | |
| Limiting indices | -26 ≤ h ≤ 26, -13 ≤ k ≤ 13, -33 ≤ l ≤ 33 | |
| Reflections collected / unique | 48128 / 12542 [R(int) = 0.0601] | |
| Completeness to θ = 26.36 | 99.8 % | |
| Absorption correction | SADABS | |
| Max. and min. transmission | 0.8156 and 0.6758 | |
| Refinement method | Full-matrix least-squares on F ² | |
| Data / restraints / parameters | 12542 / 0 / 563 | |
| Goodness-of-fit on F ² | 1.169 | |
| Final R indices [<i>I</i> > 2σ(<i>I</i>)] | R1 = 0.0721, wR2 = 0.1550 | |
| R indices (all data) | R1 = 0.0871, wR2 = 0.1622 | |
| Largest diff. peak and hole | 1.244 and -0.810 e.Å ⁻³ | |

Table 87: 1-Bromo-1-ethylgerma-2,2,5,5-tetrakis(trimethylsilyl)tetramethylcyclopentasilane (**73**)

| | | |
|-----------------------------------|-----------------------------------------------------------|--------------------------------------------------|
| Empirical formula | C ₁₈ H ₅₃ Br Ge Si ₈ | |
| Formula weight | 646.82 | |
| Temperature | 100(2) K | |
| Wavelength | 0.71073 Å | |
| Crystal system, space group | monoclinic, C2/c | |
| Unit cell dimensions | a = 17.463(4) Å, b = 9.3270(19) Å, c = 43.232(9) Å, | α = 90 deg. β = 100.79(3) deg. γ = 90 deg. |
| Volume | 6917(2) Å ³ | |
| Z, Calculated density | 8, 1.242 Mg/m ³ | |
| Absorption coefficient | 2.325 mm ⁻¹ | |
| F(000) | 2720 | |
| Crystal size | 0.20 × 0.12 × 0.09 mm | |
| Theta range for data collection | 1.92 to 26.37 deg. | |
| Limiting indices | -21 ≤ h ≤ 21, -11 ≤ k ≤ 11, -53 ≤ l ≤ 53 | |
| Reflections collected / unique | 26817 / 7076 [R(int) = 0.0712] | |
| Completeness to θ = 26.37 | 99.8 % | |
| Absorption correction | SADABS | |
| Max. and min. transmission | 0.8181 and 0.6535 | |
| Refinement method | Full-matrix least-squares on F ² | |
| Data / restraints / parameters | 7076 / 13 / 299 | |
| Goodness-of-fit on F ² | 1.117 | |
| Final R indices [I > 2σ(I)] | R1 = 0.0527, wR2 = 0.1058 | |
| R indices (all data) | R1 = 0.0710, wR2 = 0.1117 | |
| Largest diff. peak and hole | 1.030 and -0.495 e.Å ⁻³ | |

Table 88: 1-Hydroxy-1-germa-2,2,5,5-tetrakis(trimethylsilyl)-3,3,4,4-tetramethylcyclopentasilane (**74**)

| | | |
|-----------------------------------|-----------------------------------------------------------|--------------------------------------------------|
| Empirical formula | C ₁₆ H ₅₀ Ge O Si ₈ | |
| Formula weight | 555.87 | |
| Temperature | 100(2) K | |
| Wavelength | 0.71073 Å | |
| Crystal system, space group | monoclinic, P2/c | |
| Unit cell dimensions | a = 12.715(3) Å, b = 8.6713(17) Å, c = 16.752(6) Å, | α = 90 deg. β = 119.13(2) deg. γ = 90 deg. |
| Volume | 1613.4(8) Å ³ | |
| Z, Calculated density | 2, 1.144 Mg/m ³ | |
| Absorption coefficient | 1.253 mm ⁻¹ | |
| F(000) | 596 | |
| Crystal size | 0.45 × 0.30 × 0.22 mm | |
| Theta range for data collection | 1.83 to 26.23 deg. | |
| Limiting indices | -15 ≤ h ≤ 15, -10 ≤ k ≤ 10, -20 ≤ l ≤ 20 | |
| Reflections collected / unique | 12278 / 3250 [R(int) = 0.0329] | |
| Completeness to θ = 26.23 | 99.7 % | |
| Absorption correction | SADABS | |
| Max. and min. transmission | 0.7701 and 0.6025 | |
| Refinement method | Full-matrix least-squares on F ² | |
| Data / restraints / parameters | 3250 / 0 / 139 | |
| Goodness-of-fit on F ² | 1.094 | |
| Final R indices [I > 2σ(I)] | R1 = 0.0238, wR2 = 0.0639 | |
| R indices (all data) | R1 = 0.0251, wR2 = 0.0645 | |
| Largest diff. peak and hole | 0.595 and -0.186 e.Å ⁻³ | |

Table 89: Amino[tris(trimethylsilyl)silyl][bis(trimethylsilyl)silyl]germane (**76**)

| | | |
|-----------------------------------|-----------------------------------------------------------|---------------------------------------------------------------|
| Empirical formula | C ₁₅ H ₄₉ Ge N Si ₇ | |
| Formula weight | 512.77 | |
| Temperature | 100(2) K | |
| Wavelength | 0.71073 Å | |
| Crystal system, space group | triclinic, P-1 | |
| Unit cell dimensions | a = 9.1948(18) Å, b = 12.428(3) Å, c = 15.523(3) Å, | α = 106.91(3) deg. β = 94.28(3) deg. γ = 111.35(3) deg. |
| Volume | 1547.9(5) Å ³ | |
| Z, Calculated density | 2, 1.100 Mg/m ³ | |
| Absorption coefficient | 1.263 mm ⁻¹ | |
| F(000) | 552 | |
| Crystal size | 0.32 × 0.22 × 0.17 mm | |
| Theta range for data collection | 1.40 to 26.56 deg. | |
| Limiting indices | -11 ≤ h ≤ 11, -15 ≤ k ≤ 15, -19 ≤ l ≤ 19 | |
| Reflections collected / unique | 12133 / 6310 [R(int) = 0.0462] | |
| Completeness to θ = 26.56 | 97.5 % | |
| Absorption correction | SADABS | |
| Max. and min. transmission | 0.8140 and 0.6881 | |
| Refinement method | Full-matrix least-squares on F ² | |
| Data / restraints / parameters | 6310 / 2 / 240 | |
| Goodness-of-fit on F ² | 1.104 | |
| Final R indices [I > 2σ(I)] | R1 = 0.0802, wR2 = 0.1905 | |
| R indices (all data) | R1 = 0.0914, wR2 = 0.1970 | |
| Largest diff. peak and hole | 1.638 and -1.246 e.Å ⁻³ | |

Table 90: 5,7-Digerma-6,13-disulfo-1,1,4,4,8,8,11,11-octakis(trimethylsilyl)octa-methyl-dispiro[4.1.4.1]dodecasilane (**77**)

| | | |
|-----------------------------------|---------------------------------------------------------------------------------|-------------------------------------------------------------|
| Empirical formula | C ₃₈ H ₉₆ Ge ₂ S ₂ Si ₁₆ | |
| Formula weight | 1211.89 | |
| Temperature | 100(2) K | |
| Wavelength | 0.71073 Å | |
| Crystal system, space group | monoclinic, C2/c | |
| Unit cell dimensions | a = 24.864(8) Å, b = 9.994(2) Å, c = 29.604(6) Å, | α = 89.46(3) deg. β = 93.80(3) deg. γ = 90.60(3) deg. |
| Volume | 7339(3) Å ³ | |
| Z, Calculated density | 4, 1.097 Mg/m ³ | |
| Absorption coefficient | 1.160 mm ⁻¹ | |
| F(000) | 2576 | |
| Crystal size | 0.28 × 0.24 × 0.12 mm | |
| Theta range for data collection | 1.64 to 26.00 deg. | |
| Limiting indices | -30 ≤ h ≤ 30, -12 ≤ k ≤ 12, -36 ≤ l ≤ 36 | |
| Reflections collected / unique | 22180 / 7148 [R(int) = 0.3404] | |
| Completeness to θ = 26.00 | 98.1 % | |
| Absorption correction | SADABS | |
| Max. and min. transmission | 0.8734 and 0.7372 | |
| Refinement method | Full-matrix least-squares on F ² | |
| Data / restraints / parameters | 7148 / 0 / 289 | |
| Goodness-of-fit on F ² | 0.973 | |
| Final R indices [I > 2σ(I)] | R1 = 0.0871, wR2 = 0.1943 | |
| R indices (all data) | R1 = 0.2380, wR2 = 0.2400 | |
| Largest diff. peak and hole | 2.312 and -2.199 e.Å ⁻³ | |

Table 91: 1,2,2,5-Tetrakis(trimethylsilyl)-7,7-diphenyl-bicyclo[3.2.0]-7-carba-1-germa-6-oxa-heptasilane (**79**)

| | | |
|-----------------------------------|----------------------------------------------------------|-------------------------------------------|
| Empirical formula | C ₂₉ H ₅₈ Ge O Si ₈ | |
| Formula weight | 720.06 | |
| Temperature | 100(2) K | |
| Wavelength | 0.71073 Å | |
| Crystal system, space group | orthorhombic, Pbca | |
| Unit cell dimensions | a = 18.247(4) Å, b = 18.899(4) Å, c = 23.171(5) Å, | α = 90 deg. β = 90 deg. γ = 90 deg. |
| Volume | 7991(3) Å ³ | |
| Z, Calculated density | 8, 1.197 Mg/m ³ | |
| Absorption coefficient | 1.027 mm ⁻¹ | |
| F(000) | 3072 | |
| Crystal size | 0.34 × 0.34 × 0.14 mm | |
| Theta range for data collection | 1.76 to 26.38 deg. | |
| Limiting indices | -22 ≤ h ≤ 22, -23 ≤ k ≤ 23, -28 ≤ l ≤ 28 | |
| Reflections collected / unique | 60848 / 8171 [R(int) = 0.0518] | |
| Completeness to θ = 26.38 | 100.0 % | |
| Absorption correction | SADABS | |
| Max. and min. transmission | 0.8695 and 0.7214 | |
| Refinement method | Full-matrix least-squares on F ² | |
| Data / restraints / parameters | 8171 / 0 / 368 | |
| Goodness-of-fit on F ² | 1.089 | |
| Final R indices [I > 2σ(I)] | R1 = 0.0372, wR2 = 0.0850 | |
| R indices (all data) | R1 = 0.0470, wR2 = 0.0887 | |
| Largest diff. peak and hole | 1.258 and -0.225 e.Å ⁻³ | |

Table 92: 2,3,7,7,8,8-Hexamethyl-6,6,9,9-tetrakis[tris(trimethylsilylsilyl)-spiro[4.4]-5-germa-1,4-dioxa-6,7,8,9-tetrasilanon-2-ene (**81**)

| | | |
|-----------------------------------|-------------------------------------------------------------------|--------------------------------------------------------------|
| Empirical formula | C ₂₀ H ₅₄ Ge O ₂ Si ₈ | |
| Formula weight | 623.94 | |
| Temperature | 100(2) K | |
| Wavelength | 0.71073 Å | |
| Crystal system, space group | triclinic, P-1 | |
| Unit cell dimensions | a = 9.5187(19) Å, b = 11.025(2) Å, c = 17.622(4) Å, | α = 103.03(3) deg. β = 92.00(3) deg. γ = 99.13(3) deg. |
| Volume | 1774.1(6) Å ³ | |
| Z, Calculated density | 2, 1.168 Mg/m ³ | |
| Absorption coefficient | 1.149 mm ⁻¹ | |
| F(000) | 668 | |
| Crystal size | 0.16 × 0.10 × 0.08 mm | |
| Theta range for data collection | 1.92 to 26.30 deg. | |
| Limiting indices | -11 ≤ h ≤ 11, -13 ≤ k ≤ 13, -21 ≤ l ≤ 21 | |
| Reflections collected / unique | 14174 / 7080 [R(int) = 0.0723] | |
| Completeness to θ = 26.30 | 98.3 % | |
| Absorption correction | SADABS | |
| Max. and min. transmission | 0.9137 and 0.8376 | |
| Refinement method | Full-matrix least-squares on F ² | |
| Data / restraints / parameters | 7080 / 0 / 298 | |
| Goodness-of-fit on F ² | 1.139 | |
| Final R indices [I > 2σ(I)] | R1 = 0.0947, wR2 = 0.1724 | |
| R indices (all data) | R1 = 0.1283, wR2 = 0.1845 | |
| Largest diff. peak and hole | 1.197 and -0.978 e.Å ⁻³ | |

Table 93: 5,7-Digerma-6,13-diseleno-1,1,4,4,8,8,11,11-octakis(trimethylsilyl)octamethyldispiro[4.1.4.1]dodecasilane (**82**)

| | | |
|-----------------------------------|----------------------------------------------------------------------------------|--------------------------------------------------------------|
| Empirical formula | C ₃₂ H ₉₆ Ge ₂ Se ₂ Si ₁₆ | |
| Formula weight | 1233.63 | |
| Temperature | 100(2) K | |
| Wavelength | 0.71073 Å | |
| Crystal system, space group | triclinic, P-1 | |
| Unit cell dimensions | a = 9.870(2) Å, b = 14.612(3) Å, c = 23.672(5) Å, | α = 105.26(3) deg. β = 90.76(3) deg. γ = 99.54(3) deg. |
| Volume | 3242.1(11) Å ³ | |
| Z, Calculated density | 2, 1.264 Mg/m ³ | |
| Absorption coefficient | 2.367 mm ⁻¹ | |
| F(000) | 1288 | |
| Crystal size | 0.36 × 0.22 × 0.14 mm | |
| Theta range for data collection | 0.89 to 25.99 deg. | |
| Limiting indices | -12 ≤ h ≤ 12, -17 ≤ k ≤ 17, -29 ≤ l ≤ 28 | |
| Reflections collected / unique | 24227 / 12366 [R(int) = 0.0795] | |
| Completeness to θ = 25.99 | 97.2 % | |
| Absorption correction | SADABS | |
| Max. and min. transmission | 0.7329 and 0.4829 | |
| Refinement method | Full-matrix least-squares on F ² | |
| Data / restraints / parameters | 12366 / 6 / 501 | |
| Goodness-of-fit on F ² | 1.032 | |
| Final R indices [I > 2σ(I)] | R1 = 0.0915, wR2 = 0.2362 | |
| R indices (all data) | R1 = 0.1608, wR2 = 0.2586 | |
| Largest diff. peak and hole | 1.626 and -1.017 e.Å ⁻³ | |

Table 94: Trimethylsilyl[tris(trimethylsilyl)silyl]germylene–hafnocene · PMe₃ complex (**84**)

| | | |
|-----------------------------------|--------------------------------------------------------------------------------------------------|----------------------------------------------------------------|
| Empirical formula | C ₅₀ H ₁₁₀ Ge ₂ Hf ₂ P ₂ Si ₁₀ | |
| Formula weight | 1556.38 | |
| Temperature | 100(2) K | |
| Wavelength | 0.71073 Å | |
| Crystal system, space group | triclinic, P-1 | |
| Unit cell dimensions | a = 9.415(2) Å, b = 12.612(3) Å, c = 15.024(3) Å, | α = 79.078(3) deg. β = 87.697(3) deg. γ = 89.796(3) deg. |
| Volume | 1750.2(7) Å ³ | |
| Z, Calculated density | 1, 1.477 Mg/m ³ | |
| Absorption coefficient | 4.052 mm ⁻¹ | |
| F(000) | 788 | |
| Crystal size | 0.28 × 0.14 × 0.09 mm | |
| Theta range for data collection | 1.64 to 26.22 deg. | |
| Limiting indices | -11 ≤ h ≤ 11, -15 ≤ k ≤ 15, -18 ≤ l ≤ 18 | |
| Reflections collected / unique | 13707 / 6902 [R(int) = 0.0293] | |
| Completeness to θ = 26.22 | 97.8 % | |
| Absorption correction | SADABS | |
| Max. and min. transmission | 0.7118 and 0.3966 | |
| Refinement method | Full-matrix least-squares on F ² | |
| Data / restraints / parameters | 6902 / 0 / 313 | |
| Goodness-of-fit on F ² | 1.113 | |
| Final R indices [I > 2σ(I)] | R1 = 0.0454, wR2 = 0.1062 | |
| R indices (all data) | R1 = 0.0503, wR2 = 0.1082 | |
| Largest diff. peak and hole | 3.227 and -1.094 e.Å ⁻³ | |

Table 95: Cyano[bis(trimethylsilyl)]silyl{bis[tris(trimethylsilyl)silyl]germylene · IMe₄}-silver(I) · B(C₆F₅)₃ (**85**)

| | | |
|-----------------------------------|-----------------------------------------------------------------------------------------|--------------------------------------------------|
| Empirical formula | C ₅₀ H ₈₄ Ag B F ₁₅ Ge N ₃ Si ₁₁ | |
| Formula weight | 1512.46 | |
| Temperature | 100(2) K | |
| Wavelength | 0.71073 Å | |
| Crystal system, space group | monoclinic, P2(1)/c | |
| Unit cell dimensions | a = 21.491(4) Å, b = 15.045(3) Å, c = 25.250(5) Å, | α = 90 deg. β = 101.46(3) deg. γ = 90 deg. |
| Volume | 8001(3) Å ³ | |
| Z, Calculated density | 4, 1.256 Mg/m ³ | |
| Absorption coefficient | 0.851 mm ⁻¹ | |
| F(000) | 3112 | |
| Crystal size | 0.28 × 0.22 × 0.14 mm | |
| Theta range for data collection | 1.58 to 26.38 deg. | |
| Limiting indices | -26 ≤ h ≤ 26, -18 ≤ k ≤ 18, -31 ≤ l ≤ 31 | |
| Reflections collected / unique | 61932 / 16335 [R(int) = 0.0810] | |
| Completeness to θ = 26.38 | 99.7 % | |
| Absorption correction | SADABS | |
| Max. and min. transmission | 0.8902 and 0.7966 | |
| Refinement method | Full-matrix least-squares on F ² | |
| Data / restraints / parameters | 16335 / 0 / 767 | |
| Goodness-of-fit on F ² | 0.874 | |
| Final R indices [I > 2σ(I)] | R1 = 0.0433, wR2 = 0.0924 | |
| R indices (all data) | R1 = 0.0762, wR2 = 0.1006 | |
| Largest diff. peak and hole | 1.264 and -0.334 e.Å ⁻³ | |

Table 96: Tris(trimethylsilyl)silyl{bis[tris(trimethylsilyl)silyl]stannylene · IMe₄} gold(I) (**86**)

| | | |
|-----------------------------------|-----------------------------------------------------------------------|-------------------------------------------------------------|
| Empirical formula | C ₃₄ H ₉₃ Au N ₂ Si ₁₂ Sn | |
| Formula weight | 1182.84 | |
| Temperature | 100(2) K | |
| Wavelength | 0.71073 Å | |
| Crystal system, space group | triclinic, P-1 | |
| Unit cell dimensions | a = 12.976(3) Å, b = 13.772(3) Å, c = 18.980(4) Å, | α = 79.38(3) deg. β = 73.75(3) deg. γ = 67.67(3) deg. |
| Volume | 3000.5(11) Å ³ | |
| Z, Calculated density | 2, 1.309 Mg/m ³ | |
| Absorption coefficient | 3.121 mm ⁻¹ | |
| F(000) | 1216 | |
| Crystal size | 0.24 × 0.18 × 0.10 mm | |
| Theta range for data collection | 1.60 to 26.37 deg. | |
| Limiting indices | -16 ≤ h ≤ 16, -17 ≤ k ≤ 17, -23 ≤ l ≤ 23 | |
| Reflections collected / unique | 23897 / 12073 [R(int) = 0.0413] | |
| Completeness to θ = 26.37 | 98.4 % | |
| Absorption correction | SADABS | |
| Max. and min. transmission | 0.7455 and 0.5213 | |
| Refinement method | Full-matrix least-squares on F ² | |
| Data / restraints / parameters | 12073 / 51 / 600 | |
| Goodness-of-fit on F ² | 1.247 | |
| Final R indices [I > 2σ(I)] | R1 = 0.0734, wR2 = 0.1460 | |
| R indices (all data) | R1 = 0.0800, wR2 = 0.1488 | |
| Largest diff. peak and hole | 3.448 and -3.715 e.Å ⁻³ | |

Table 97: **87**

| | | |
|-----------------------------------|--------------------------------------------------------------------------------------------------|--------------------------------------------------------------|
| Empirical formula | C ₈₈ H ₂₂₄ Au ₂ N ₈ Si ₃₂ Sn ₄ | |
| Formula weight | 3162.32 | |
| Temperature | 100(2) K | |
| Wavelength | 0.71073 Å | |
| Crystal system, space group | triclinic, P-1 | |
| Unit cell dimensions | a = 16.853(3) Å, b = 22.261(5) Å, c = 24.201(5) Å, | α = 117.19(3) deg. β = 90.60(3) deg. γ = 99.63(3) deg. |
| Volume | 7923(3) Å ³ | |
| Z, Calculated density | 2, 1.325 Mg/m ³ | |
| Absorption coefficient | 2.743 mm ⁻¹ | |
| F(000) | 3228 | |
| Crystal size | 0.28 × 0.22 × 0.14 mm | |
| Theta range for data collection | 1.23 to 26.36 deg. | |
| Limiting indices | -20 ≤ h ≤ 21, -27 ≤ k ≤ 27, -30 ≤ l ≤ 30 | |
| Reflections collected / unique | 63787 / 31822 [R(int) = 0.0291] | |
| Completeness to θ = 26.36 | 98.4 % | |
| Absorption correction | SADABS | |
| Max. and min. transmission | 0.7000 and 0.5139 | |
| Refinement method | Full-matrix least-squares on F ² | |
| Data / restraints / parameters | 31822 / 0 / 1279 | |
| Goodness-of-fit on F ² | 0.982 | |
| Final R indices [I > 2σ(I)] | R1 = 0.0330, wR2 = 0.0719 | |
| R indices (all data) | R1 = 0.0425, wR2 = 0.0745 | |
| Largest diff. peak and hole | 1.417 and -0.719 e.Å ⁻³ | |

Table 98: **88**

| | | |
|--------------------------------------|-------------------------------------------------------------------|----------------------------------------------------------------------|
| Empirical formula | C ₂₄ H ₆₁ N ₃ Si ₈ Sn | |
| Formula weight | 735.17 | |
| Temperature | 100(2) K | |
| Wavelength | 0.71073 Å | |
| Crystal system, space group | monoclinic, P2(1)/c | |
| Unit cell dimensions | a = 12.745(3) Å, b = 25.615(5) Å, c = 12.832(3) Å, | $\alpha = 90$ deg. $\beta = 102.49(3)$ deg. $\gamma = 90$ deg. |
| Volume | 4090.0(14) Å ³ | |
| Z, Calculated density | 4, 1.194 Mg/m ³ | |
| Absorption coefficient | 0.877 mm ⁻¹ | |
| F(000) | 1552 | |
| Crystal size | 0.36 × 0.24 × 0.12 mm | |
| Theta range for data collection | 1.59 to 26.38 deg. | |
| Limiting indices | -15 ≤ h ≤ 15, -31 ≤ k ≤ 31, -15 ≤ l ≤ 16 | |
| Reflections collected / unique | 32304 / 8340 [R(int) = 0.0591] | |
| Completeness to $\theta = 26.38$ | 99.9 % | |
| Absorption correction | SADABS | |
| Max. and min. transmission | 0.9021 and 0.7432 | |
| Refinement method | Full-matrix least-squares on F ² | |
| Data / restraints / parameters | 8340 / 0 / 349 | |
| Goodness-of-fit on F ² | 1.003 | |
| Final R indices [$I > 2\sigma(I)$] | R1 = 0.0393, wR2 = 0.0862 | |
| R indices (all data) | R1 = 0.0564, wR2 = 0.0927 | |
| Largest diff. peak and hole | 1.069 and -0.349 e.Å ⁻³ | |

References

- [1] Y. Mizuhata, T. Sasamori, N. Tokitoh, *Chem. Rev.* **2009**, *109*, 3479–3511.
- [2] C. Marschner, *Eur. J. Inorg. Chem.* **2015**, *2015*, 3805–3820.
- [3] R. S. Ghadwal, H. W. Roesky, S. Merkel, J. Henn, D. Stalke, *Angew. Chem., Int. Ed.* **2009**, *48*, 5683–5686.
- [4] A. Jana, I. Objartel, H. W. Roesky, D. Stalke, *Inorg. Chem.* **2009**, *48*, 798–800.
- [5] W. P. Neumann, *Chem. Rev.* **1991**, *91*, 311–334.
- [6] P. Jutzi, A. Becker, C. Leue, H. G. Stammer, B. Neumann, M. B. Hursthouse, A. Karaulov, *Organometallics* **1991**, *10*, 3838–3842.
- [7] J. G. Winter, P. Portius, G. Kociok-Köhn, R. Steck, A. C. Filippou, *Organometallics* **1998**, *17*, 4176–4182.
- [8] O. Kühn, P. Lönnecke, J. Heinicke, *Polyhedron* **2001**, *20*, 2215 – 2222.
- [9] A. V. Zabula, F. E. Hahn, T. Pape, A. Hepp, *Organometallics* **2007**, *26*, 1972–1980.
- [10] F. E. Hahn, A. V. Zabula, T. Pape, A. Hepp, *Z. Anorg. Allg. Chem.* **2008**, *634*, 2397–2401.
- [11] L. Wang, S.-C. Rosca, V. Poirier, S. Sinbandhit, V. Dorcet, T. Roisnel, J.-F. Carpentier, Y. Sarazin, *Dalton Trans.* **2014**, *43*, 4268–4286.
- [12] V. Y. Lee, M. Kawai, A. Sekiguchi, H. Ranaivonjatovo, J. Escudié, *Organometallics* **2009**, *28*, 4262–4265.
- [13] M. Grenz, E. Hahn, W.-W. du Mont, J. Pickardt, *Angew. Chem., Int. Ed.* **1984**, *23*, 61–63.
- [14] P. Jutzi, W. Steiner, E. König, G. Huttner, A. Frank, U. Schubert, *Chem. Ber.* **1978**, *111*, 606.
- [15] K. Izod, E. R. Clark, W. Clegg, R. W. Harrington, *Organometallics* **2012**, *31*, 246–255.
- [16] B. D. Reken, T. M. Brown, J. C. Fettinger, H. M. Tuononen, P. P. Power, *J. Am. Chem. Soc.* **2012**, *134*, 6504–6507.
- [17] D. E. Goldberg, D. H. Harris, M. F. Lappert, K. M. Thomas, *J. Chem. Soc., Chem. Commun.* **1976**, 261–262.
- [18] P. J. Davidson, D. H. Harris, M. F. Lappert, *J. Chem. Soc., Dalton Trans.* **1976**, 2268–2274.

- [19] D. E. Goldberg, P. B. Hitchcock, M. F. Lappert, K. M. Thomas, A. J. Thorne, T. Fjeldberg, A. Haaland, B. E. R. Schilling, *J. Chem. Soc., Dalton Trans.* **1986**, 2387–2394.
- [20] P. Jutzi, A. Becker, H. G. Stammer, B. Neumann, *Organometallics* **1991**, *10*, 1647–1648.
- [21] M. Weidenbruch, M. Stürmann, H. Kilian, S. Pohl, W. Saak, *Chem. Ber.* **1997**, *130*, 735–738.
- [22] L. Lange, B. Meyer, W.-W. du Mont, *J. Organomet. Chem.* **1987**, *329*, C17 – C20.
- [23] P. Jutzi, H. Schmidt, B. Neumann, H.-G. Stammer, *Organometallics* **1996**, *15*, 741–746.
- [24] G. L. Wegner, R. J. F. Berger, A. Schier, H. Schmidbaur, *Organometallics* **2001**, *20*, 418–423.
- [25] R. S. Simons, L. Pu, M. M. Olmstead, P. P. Power, *Organometallics* **1997**, *16*, 1920–1925.
- [26] P. Wilfling, K. Schittelkopf, M. Flock, R. H. Herber, P. P. Power, R. C. Fischer, *Organometallics* **2015**, *34*, 2222–2232.
- [27] G. H. Spikes, Y. Peng, J. C. Fettinger, P. P. Power, *Z. Anorg. Allg. Chem.* **2006**, *632*, 1005–1010.
- [28] L. Li, T. Fukawa, T. Matsuo, D. Hashizume, H. Fueno, K. Tanaka, K. Tamao, *Nature Chem.* **2012**, *4*, 361–365.
- [29] J. M. Bender, M. M. Banaszak Holl, J. W. Kampf, *Organometallics* **1997**, *16*, 2743–2745.
- [30] N. Tokitoh, K. Manmaru, R. Okazaki, *Organometallics* **1994**, *13*, 167–171.
- [31] K. W. Klinkhammer, W. Schwarz, *Angew. Chem., Int. Ed.* **1995**, *34*, 1334–1336.
- [32] K. Klinkhammer, *Polyhedron* **2002**, *21*, 587 – 598.
- [33] N. Katir, D. Matioszek, S. Ladeira, J. Escudié, A. Castel, *Angew. Chem., Int. Ed.* **2011**, *50*, 5352–5355.
- [34] A. Heine, D. Stalke, *Angew. Chem., Int. Ed.* **1994**, *33*, 113–115.
- [35] K. W. Klinkhammer, *Organosilicon Chemistry III*, Wiley-VHC, Weinheim, Germany, **1998**, 82-85.
- [36] S. P. Mallela, S. Hill, R. A. Geanangel, *Inorg. Chem.* **1997**, *36*, 6247–6250.

- [37] J. Hlina, Ph.D. thesis, TUG, **2013**.
- [38] J. Hlina, J. Baumgartner, C. Marschner, L. Albers, T. Müller, *Organometallics* **2013**, *32*, 3404–3410.
- [39] X. Q. Xiao, H. Zhao, Z. Xu, G. Lai, X. L. He, Z. Li, *Chem. Commun.* **2013**, *49*, 2706–2708.
- [40] S. Ishida, T. Iwamoto, M. Kira, *Organometallics* **2009**, *28*, 919–921.
- [41] M. Kira, *Chem. Commun.* **2010**, *46*, 2893–2903.
- [42] A. D. Phillips, S. Hino, P. P. Power, *J. Am. Chem. Soc.* **2003**, *125*, 7520–7521.
- [43] H. Arp, J. Baumgartner, C. Marschner, T. Müller, *J. Am. Chem. Soc.* **2011**, *133*, 5632–5635.
- [44] J. Hlina, J. Baumgartner, C. Marschner, L. Albers, T. Müller, V. V. Jouikov, *Chem. Eur. J.* **2014**, *20*, 9357–9366.
- [45] E. A. Carter, A. W. Goddard III, *J. Phys. Chem.* **1986**, *90*, 998–1001.
- [46] R. S. Grev, H. F. Schaefer III, P. P. Gaspar, *J. Am. Chem. Soc.* **1991**, *113*, 5638–5643.
- [47] M. C. Holthausen, W. Koch, Y. Apeloig, *J. Am. Chem. Soc.* **1999**, *121*, 2623–2624.
- [48] P. P. Gaspar, A. M. Beatty, T. Chen, T. Haile, D. Lei, W. R. Winchester, J. Braddock-Wilking, N. P. Rath, W. T. Klooster, T. F. Koetzle, S. A. Mason, A. Albinati, *Organometallics* **1999**, *18*, 3921–3932.
- [49] A. Sekiguchi, T. Tanaka, M. Ichinohe, K. Akiyama, S. Tero-Kubota, *J. Am. Chem. Soc.* **2003**, *125*, 4962–4963.
- [50] B. E. Eichler, A. D. Phillips, P. P. Power, *Organometallics* **2003**, *22*, 5423–5426.
- [51] J. Fischer, Ph.D. thesis, TUG, **2005**.
- [52] Y. Cheng, Z. Duan, T. Li, Y. Wu, *Synlett* **2007**, *4*, 543–546.
- [53] P. A. Rupar, M. C. Jennings, P. J. Ragona, K. M. Baines, *Organometallics* **2007**, *26*, 4109–4111.
- [54] P. A. Rupar, V. N. Staroverov, P. J. Ragona, K. M. Baines, *J. Am. Chem. Soc.* **2007**, *129*, 15138–15139.
- [55] J. H. Konnert, D. Britton, Y. M. Chow, *Acta Crystallogr. Sect. B* **1972**, *28*, 180–187.
- [56] R. K. Siwatch, S. Nagendran, *Chem. Eur. J.* **2014**, *20*, 13551–13556.

- [57] Z. D. Brown, P. Vasko, J. C. Fettinger, H. M. Tuononen, P. P. Power, *J. Am. Chem. Soc.* **2012**, *134*, 4045–4048.
- [58] J. Belzner, H. Ihmels, M. Noltemeyer, *Tetrahedron Lett.* **1995**, *36*, 8187 – 8190.
- [59] P. Jutzi, D. Eikenberg, B. Neumann, H.-G. Stammler, *Organometallics* **1996**, *15*, 3659–3663.
- [60] H. Kobayashi, T. Iwamoto, M. Kira, *J. Am. Chem. Soc.* **2005**, *127*, 15376–15377.
- [61] J. Hlina, J. Baumgartner, C. Marschner, P. Zark, T. Müller, *Organometallics* **2013**, *32*, 3300–3308.
- [62] M. A. Chaubon, H. Ranaivonjatovo, J. Escudié, J. Satge, *Main Group Met. Chem.* **2011**, *19*, 145–160.
- [63] H. Arp, C. Marschner, J. Baumgartner, P. Zark, T. Müller, *J. Am. Chem. Soc.* **2013**, *135*, 7949–7959.
- [64] T. Fukawa, V. Y. Lee, M. Nakamoto, A. Sekiguchi, *J. Am. Chem. Soc.* **2004**, *126*, 11758–11759.
- [65] V. Y. Lee, T. Fukawa, M. Nakamoto, A. Sekiguchi, B. L. Tumanskii, M. Karni, Y. Apeloig, *J. Am. Chem. Soc.* **2006**, *128*, 11643–11651.
- [66] N. Kuhn, T. Kraty, *Synthesis* **1993**, 561–562.
- [67] A. J. Ruddy, P. A. Rugar, K. J. Bladek, C. J. Allan, J. C. Avery, K. M. Baines, *Organometallics* **2010**, *29*, 1362–1367.
- [68] W. Ando, H. Ohgaki, Y. Kabe, *Angew. Chem.* **1994**, *106*, 723–725.
- [69] A. H. Cowley, S. W. Hall, C. M. Nunn, J. M. Power, *J. Chem. Soc., Chem. Commun.* **1988**, 753–754.
- [70] H. Ohgaki, Y. Kabe, W. Ando, *Organometallics* **1995**, *14*, 2139–2141.
- [71] S. Freitag, J. Henning, H. Schubert, L. Wesemann, *Angew. Chem., Int. Ed.* **2013**, *52*, 5640–5643.
- [72] S. Freitag, K. M. Krebs, J. Henning, J. Hirdler, H. Schubert, L. Wesemann, *Organometallics* **2013**, *32*, 6785–6791.
- [73] C. Eisenhut, T. Szilvási, N. C. Breit, S. Inoue, *Chem. Eur. J.* **2014**, *21*, 1949–1954.
- [74] W. Ando, T. Ohtaki, Y. Kabe, *Organometallics* **1994**, *13*, 434–435.
- [75] T. Ohtaki, Y. Kabe, W. Ando, *Heteroat. Chem.* **1994**, *5*, 313–320.

- [76] T. Ohtaki, W. Ando, *Chem. Lett.* **1994**, *23*, 1061–1064.
- [77] R. D. Sweeder, F. A. Edwards, K. A. Miller, M. M. Banaszak Holl, J. W. Kampf, *Organometallics* **2002**, *21*, 457–459.
- [78] R. D. Sweeder, Z. T. Cygan, M. M. Banaszak Holl, J. W. Kampf, *Organometallics* **2003**, *22*, 4613–4615.
- [79] B. Valentin, A. Castel, P. Rivière, M. Mauzac, M. Onyszchuk, A. M. Lebuis, *Heteroat. Chem.* **1999**, *10*, 125–132.
- [80] V. Y. Lee, A. Sekiguchi, *Organometallic Compounds of Low-Coordinate Si, Ge, Sn and Pb: From Phantom Species to Stable Compounds*, John Wiley & Sons Ltd, **2010**, Chapter 4.
- [81] M. F. Lappert, S. J. Miles, J. L. Atwood, M. J. Zaworotko, A. J. Carty, *J. Organomet. Chem.* **1981**, *212*, C4 – C6.
- [82] K. A. Miller, T. W. Watson, Bender, M. M. Banaszak Holl, J. W. Kampf, *J. Am. Chem. Soc.* **2001**, *123*, 982–983.
- [83] R. D. Sweeder, K. A. Miller, F. A. Edwards, J. Wang, M. M. Banaszak Holl, J. W. Kampf, *Organometallics* **2003**, *22*, 5054–5062.
- [84] Y. Peng, J.-D. Guo, B. D. Ellis, Z. Zhu, J. C. Fettinger, S. Nagase, P. P. Power, *J. Am. Chem. Soc.* **2009**, *131*, 16272–16282.
- [85] S. M. I. Al-Rafia, M. R. Momeni, R. McDonald, M. J. Ferguson, A. Brown, E. Rivard, *Angew. Chem.* **2013**, *25*, 6518–6523.
- [86] F. Meiners, W. Saak, M. Weidenbruch, *Z. Anorg. Allg. Chem.* **2002**, *628*, 2821–2822.
- [87] J. Ohshita, N. Honda, K. Nada, T. Iida, T. Mihara, Y. Matsuo, A. Kunai, A. Naka, M. Ishikawa, *Organometallics* **2003**, *22*, 2436–2441.
- [88] N. Fukaya, M. Ichinohe, Y. Kabe, A. Sekiguchi, *Organometallics* **2001**, *20*, 3364–3366.
- [89] A. Sekiguchi, R. Izumi, S. Ihara, M. Ichinohe, V. Y. Lee, *Angew. Chem., Int. Ed.* **2002**, *41*, 1598–1600.
- [90] R. A. Moss, J. Tian, R. R. Sauers, R. S. Sheridan, A. Bhakta, P. S. Zuev, *Org. Lett.* **2005**, *7*, 4645–4648.
- [91] A. de Meijere, D. Faber, U. Heinecke, R. Walsh, T. Müller, Y. Apeloig, *Eur. J. Org. Chem.* **2001**, *2001*, 663–680.

- [92] A. V. Protchenko, M. P. Blake, A. D. Schwarz, C. Jones, P. Mountford, S. Aldridge, *Organometallics* **2015**, *34*, 2126–2129.
- [93] Z. Wang, J.-P. Pitteloud, L. Montes, M. Rapp, D. Derane, S. F. Wnuk, *Tetrahedron* **2008**, *64*, 5322 – 5327.
- [94] H.-M. Chen, J. P. Oliver, *J. Organomet. Chem.* **1986**, *316*, 255 – 260.
- [95] V. Y. Lee, M. Ichinohe, A. Sekiguchi, *J. Organomet. Chem.* **2001**, *636*, 41 – 48.
- [96] P. A. Rupar, M. C. Jennings, K. M. Baines, *Organometallics* **2008**, *27*, 5043–5051.
- [97] J. Fischer, J. Baumgartner, C. Marschner, *Organometallics* **2005**, *24*, 1263–1268.
- [98] C. Kayser, R. Fischer, J. Baumgartner, C. Marschner, *Organometallics* **2002**, *21*, 1023–1030.
- [99] J. Koecher, M. Lehnig, *Organometallics* **1984**, *3*, 937–939.
- [100] J. Koecher, M. Lehnig, W. P. Neumann, *Organometallics* **1988**, *7*, 1201–1207.
- [101] N. Tokitoh, T. Matsumoto, K. Manmaru, R. Okazaki, *J. Am. Chem. Soc.* **1993**, *115*, 8855–8856.
- [102] T. Matsumoto, N. Tokitoh, , R. Okazaki, *J. Am. Chem. Soc.* **1999**, *121*, 8811–8824.
- [103] S. M. I. Al-Rafia, P. A. Lummis, M. J. Ferguson, R. McDonald, E. Rivard, *Inorg. Chem.* **2010**, *49*, 9709–9717.
- [104] S. K. Liew, S. M. I. Al-Rafia, J. T. Goettel, P. A. Lummis, S. M. McDonald, L. J. Miedema, M. J. Ferguson, R. McDonald, E. Rivard, *Inorg. Chem.* **2012**, *51*, 5471–5480.
- [105] T. Sasamori, Y. Sugiyama, N. Takeda, N. Tokitoh, *Organometallics* **2005**, *24*, 3309–3314.
- [106] P. Bazinet, G. P. A. Yap, , D. S. Richeson, *J. Am. Chem. Soc.* **2001**, *123*, 11162–11167.
- [107] W.-P. Leung, C.-L. Wan, K.-W. Kan, T. C. W. Mak, *Organometallics* **2010**, *29*, 814–820.
- [108] K. M. Baines, J. A. Cooke, J. J. Vittal, *Heteroat. Chem.* **1994**, *5*, 293–303.
- [109] K. Hillner, W. P. Neumann, *Tetrahedron Lett.* **1986**, *27*, 5347 – 5350.
- [110] B. Flores-Chávez, J. G. Alvarado-Rodríguez, N. Andrade-López, V. García-Montalvo, E. Aquino-Torres, *Polyhedron* **2009**, *28*, 782 – 788.

- [111] J. Li, C. Schenk, C. Goedecke, G. Frenking, C. Jones, *J. Am. Chem. Soc.* **2011**, *133*, 18622–18625.
- [112] W.-P. Leung, C.-W. So, Z.-X. Wang, J.-Z. Wang, , T. C. W. Mak, *Organometallics* **2003**, *22*, 4305–4311.
- [113] M. Wojnowska, M. Noltemeyer, H.-J. Füllgrabe, A. Meller, *J. Organomet. Chem.* **1982**, *228*, 229 – 238.
- [114] H. Puff, K. Braun, S. Franken, T. R. Kök, W. Schuh, *J. Organomet. Chem.* **1987**, *335*, 167 – 178.
- [115] N. Tokitoh, T. Matsumoto, H. Ichida, R. Okazaki, *Tetrahedron Lett.* **1991**, *32*, 6877 – 6878.
- [116] M. Veith, M. Nötzel, L. Stahl, V. Huch, *Z. Anorg. Allg. Chem.* **1994**, *620*, 1264–1270.
- [117] A. Schäfer, M. Weidenbruch, S. Pohl, *J. Organomet. Chem.* **1985**, *282*, 305 – 313.
- [118] A. G. Brook, W. J. Chatterton, J. F. Sawyer, D. W. Hughes, K. Vorspohl, *Organometallics* **1987**, *6*, 1246–1256.
- [119] W.-P. Leung, K.-W. Kan, C.-W. So, , T. C. W. Mak, *Organometallics* **2007**, *26*, 3802–3806.
- [120] K. M. Baines, W. G. Stibbs, *Coord. Chem. Rev.* **1995**, *145*, 157 – 200.
- [121] A. Kawachi, Y. Tanaka, K. Tamao, *Chem. Lett.* **1999**, *28*, 21–22.
- [122] G.L.Wegner, A.Jockisch, A.Schier, H.Schmidbaur, *Z.Naturforsch.* **2000**, *55*, 347.
- [123] M. Unno, Y. Kawai, H. Shioyama, H. Matsumoto, *Organometallics* **1997**, *16*, 4428–4434.
- [124] T. J. Marks, *J. Am. Chem. Soc.* **1971**, *93*, 7090–7091.
- [125] M. F. Lappert, R. S. Rowe, *Coord. Chem. Rev.* **1990**, *100*, 267–292.
- [126] E. Negishi, F. E. Cederbaum, T. Takahashi, *Tetrahedron Lett.* **1986**, *27*, 2829 – 2832.
- [127] R. M. Whittal, G. Ferguson, J. F. Gallagher, W. E. Piers, *J. Am. Chem. Soc.* **1991**, *113*, 9867–9868.
- [128] W. E. Piers, R. M. Whittal, G. Ferguson, J. F. Gallagher, R. D. J. Froese, H. J. Stronks, P. H. Krygsman, *Organometallics* **1992**, *11*, 4015–4022.
- [129] J. Bareš, P. Richard, P. Meunier, N. Pirio, Z. Padělková, Z. Černošek, I. Císařová, A. Růžička, *Organometallics* **2009**, *28*, 3105–3108.

- [130] H. Arp, J. Baumgartner, C. Marschner, P. Zark, T. Müller, *J. Am. Chem. Soc.* **2012**, *134*, 10864–10875.
- [131] M. Zhang, X. Liu, C. Shi, C. Ren, Y. Ding, H. W. Roesky, *Z. Anorg. Allg. Chem.* **2008**, *634*, 1755–1758.
- [132] A. Fürstner, H. Krause, C. W. Lehmann, *Chem. Commun.* **2001**, 2372–2373.
- [133] W. Wang, S. Inoue, S. Enthaler, M. Driess, *Angew. Chem., Int. Ed.* **2012**, *51*, 6167–6171.
- [134] A. Brück, D. Gallego, W. Wang, E. Irran, M. Driess, J. F. Hartwig, *Angew. Chem., Int. Ed.* **2012**, *51*, 11478–11482.
- [135] D. Gallego, A. Brück, E. Irran, F. Meier, M. Kaupp, M. Driess, J. F. Hartwig, *J. Am. Chem. Soc.* **2013**, *135*, 15617–15626.
- [136] B. Blom, M. Stoelzel, M. Driess, *Chem. Eur. J.* **2013**, *19*, 40–62.
- [137] M. E. Fasulo, M. C. Lipke, T. D. Tilley, *Chem. Sci.* **2013**, *4*, 3882–3887.
- [138] P. B. Glaser, T. D. Tilley, *J. Am. Chem. Soc.* **2003**, *125*, 13640–13641.
- [139] R. Waterman, P. G. Hayes, T. D. Tilley, *Acc. Chem. Res.* **2007**, *40*, 712–719.
- [140] M. M. Kireenko, K. V. Zaitsev, Y. F. Oprunenko, A. V. Churakov, V. A. Tafeenko, S. S. Karlov, G. S. Zaitseva, *Dalton Trans.* **2013**, *42*, 7901–7912.
- [141] J. D. Cotton, P. J. Davidson, M. F. Lappert, *J. Chem. Soc., Dalton Trans.* **1976**, 2275–2286.
- [142] C. Pluta, K.-R. Pörschke, R. Mynott, P. Betz, C. Krüger, *Chem. Ber.* **1991**, *124*, 1321–1325.
- [143] C. Pluta, K.-R. Pörschke, B. Gabor, R. Mynott, *Chem. Ber.* **1994**, *127*, 489–500.
- [144] J. Krause, C. Pluta, K.-R. Pörschke, R. Goddard, *J. Chem. Soc., Chem. Commun.* **1993**, 1254–1256.
- [145] M. Weidenbruch, A. Stilter, K. Peters, H. G. V. Schnering, *Chem. Ber.* **1996**, *129*, 1565–1567.
- [146] C. Watanabe, Y. Inagawa, T. Iwamoto, M. Kira, *Dalton Trans.* **2010**, *39*, 9414–9420.
- [147] J. Hlina, H. Arp, M. Walewska, U. Flörke, K. Zangger, C. Marschner, J. Baumgartner, *Organometallics* **2014**, *33*, 7069–7077.
- [148] J. Klett, K. W. Klinkhammer, M. Niemeyer, *Chem. Eur. J.* **1999**, *5*, 2531–2536.

- [149] L. Kool, M. Rausch, H. Alt, M. Herberhold, U. Thewalt, B. Honold, *J. Organomet. Chem.* **1986**, *310*, 27 – 34.
- [150] M. Zirngast, M. Flock, J. Baumgartner, C. Marschner, *J. Am. Chem. Soc.* **2009**, *131*, 15952–15962.
- [151] J. Arnold, D. M. Roddick, T. D. Tilley, A. L. Rheingold, S. J. Geib, *Inorg. Chem.* **1988**, *27*, 3510–3514.
- [152] M. L. Cole, D. E. Hibbs, C. Jones, P. C. Junk, N. A. Smithies, *Inorg. Chim. Acta* **2005**, *358*, 102 – 108.
- [153] N. Zhao, J. Zhang, Y. Yang, G. Chen, H. Zhu, H. W. Roesky, *Organometallics* **2013**, *32*, 762–769.
- [154] M. J. Sgro, W. E. Piers, P. E. Romero, *Dalton Trans.* **2015**, *44*, 3817–3828.
- [155] Y. Inagawa, S. Ishida, T. Iwamoto, *Chem. Lett.* **2014**, *43*, 1665–1667.
- [156] J. A. Cabeza, J. M. Fernández-Colinas, P. García-Álvarez, D. Polo, *Inorg. Chem.* **2012**, *51*, 3896–3903.
- [157] B. Findeis, M. Contel, L. H. Gade, M. Laguna, M. C. Gimeno, I. J. Scowen, M. McPartlin, *Inorg. Chem.* **1997**, *36*, 2386–2390.
- [158] M. Joost, P. Gualco, S. Mallet-Ladeira, A. Amgoune, D. Bourissou, *Angew. Chem., Int. Ed.* **2013**, *52*, 7160–7163.
- [159] M. M. Oroz, A. Schier, H. Schmidbaur, *Z. Naturforsch.* **1999**, *54*, 26.
- [160] H. Piana, H. Wagner, H. Schubert, *Chem. Ber.* **1991**, *124*, 63.
- [161] M. Wilfling, K. Klinkhammer, *Angew. Chem., Int. Ed.* **2010**, *49*, 3219–3223.
- [162] J. Mayer, J. Willnecker, H. Schubert, *Chem. Ber.* **1989**, *122*, 223.
- [163] J. D. Farwell, P. B. Hitchcock, M. F. Lappert, A. V. Protchenko, *J. Organomet. Chem.* **2007**, *692*, 4953 – 4961.
- [164] R. G. Pearson, *J. Chem. Educ.* **1968**, *45*, 581.
- [165] A. B. Pangborn, M. A. Giardello, R. H. Grubbs, R. K. Rosen, F. J. Timmers, *Organometallics* **1996**, *15*, 1518–1520.
- [166] H. Gilman, C. L. Smith, *J. Organomet. Chem.* **1967**, *8*, 245–253.
- [167] C. Marschner, *Eur. J. Inorg. Chem.* **1998**, 221–226.

- [168] J. D. Farwell, M. F. Lappert, C. Marschner, C. Strissel, T. Tilley, *J. Organomet. Chem.* **2000**, *603*, 185–188.
- [169] M. A. Meshgi, J. Baumgartner, C. Marschner, *Organometallics* **2015**, *34*, 3721–3731.
- [170] D. Matioszek, N. Katir, S. Ladeira, A. Castel, *Organometallics* **2011**, *30*, 2230–2235.
- [171] C. Kayser, G. Kickelbick, C. Marschner, *Angew. Chem., Int. Ed.* **2002**, *41*, 989–992.
- [172] R. Fischer, D. Frank, W. Gaderbauer, C. Kayser, C. Mechtler, J. Baumgartner, C. Marschner, *Organometallics* **2003**, *22*, 3723–3731.
- [173] W. J. Leigh, C. R. Harrington, I. Vargas-Baca, *J. Am. Chem. Soc.* **2004**, *126*, 16105–16116.
- [174] C. D. Schaeffer, L. K. Myers, S. M. Coley, J. C. Otter, C. H. Yoder, *J. Chem. Educ.* **1990**, *67*, 347–349.
- [175] G. A. Morris, R. Freeman, *J. Am. Chem. Soc.* **1979**, *101*, 760–762.
- [176] B. J. Helmer, R. West, *Organometallics* **1982**, *1*, 877–879.
- [177] *SAINTPLUS: Software Reference Manual, Version 6.45*, Bruker-AXS: Madison, WI, **1997-2003**.
- [178] G. M. Sheldrick, *SADABS. Version 2.10*, Bruker AXS, Madison, WI, **2003**.
- [179] G. M. Sheldrick, *Acta Crystallogr. A* **2008**, *64*, 112–122.
- [180] M. Ballestri, C. Chatgililoglu, K. B. Clark, D. Griller, B. Giese, B. Kopping, *J. Org. Chem.* **1991**, *56*, 678–683.

Małgorzata Walewska

Education

- 1.11.2012–31.12.2015 PhD studies at the Institute of Inorganic Chemistry,
Graz University of Technology, Austria,
Supervisor: Prof. Christoph Marschner
- 2011.06.27 MSc degree from Warsaw University of Technology,
thesis title: “NHC – carbene complexes of cyclopentadienyl-
nickel – synthesis and properties”
Supervisor: Prof. Antoni Pietrzykowski
- 2005–2011 Studies at the Faculty of Chemistry,
Warsaw University of Technology (WUT), Warsaw, Poland
- 2002–2005 37th Secondary School of Jarosław Dąbrowski, Warsaw, Poland

Research experience

- 1.11.2012–31.12.2015 Project assistant at the Institute of Inorganic Chemistry,
Graz University of Technology, Austria
- 1.09.2011–29.02.2011 Laboratory practice at the Institute of Organic Chemistry,
Ruhr University Bochum (RUB), Germany
Subject: synthesis and functionalization of calixarenes
- 30.03.2011–26.04.2011 Laboratory practice at Military University of Technology,
Warsaw, Poland
Subject: synthesis of triphenylbismuth
- 01.12.2009–30.06.2010 Laboratory practice at Institute of Organic Chemistry
(Polish Academy of Sciences), Warsaw, Poland
Subject: optimization of the isomerisation reaction
of 4-allyloxy-2-azetidinones